STRUCTURED EDIBLE OIL: TOWARDS A NEW GENERATION OF FAT MIMETICS

EDITED BY: Miguel Cerqueira, Stephen Robert Euston and Luiz Henrique Fasolin
PUBLISHED IN: Frontiers in Sustainable Food Systems

frontiers Research Topics

frontiers

ISSN 1664-8714
ISBN 978-2-88966-814-4
DOI 10.3389/978-2-88966-814-4

About Frontiers

Frontiers is more than just an open-access publisher of scholarly articles: it is a pioneering approach to the world of academia, radically improving the way scholarly research is managed. The grand vision of Frontiers is a world where all people have an equal opportunity to seek, share and generate knowledge. Frontiers provides immediate and permanent online open access to all its publications, but this alone is not enough to realize our grand goals.

Frontiers Journal Series

The Frontiers Journal Series is a multi-tier and interdisciplinary set of open-access, online journals, promising a paradigm shift from the current review, selection and dissemination processes in academic publishing. All Frontiers journals are driven by researchers for researchers; therefore, they constitute a service to the scholarly community. At the same time, the Frontiers Journal Series operates on a revolutionary invention, the tiered publishing system, initially addressing specific communities of scholars, and gradually climbing up to broader public understanding, thus serving the interests of the lay society, too.

Dedication to Quality

Each Frontiers article is a landmark of the highest quality, thanks to genuinely collaborative interactions between authors and review editors, who include some of the world's best academicians. Research must be certified by peers before entering a stream of knowledge that may eventually reach the public - and shape society; therefore, Frontiers only applies the most rigorous and unbiased reviews.
Frontiers revolutionizes research publishing by freely delivering the most outstanding research, evaluated with no bias from both the academic and social point of view. By applying the most advanced information technologies, Frontiers is catapulting scholarly publishing into a new generation.

What are Frontiers Research Topics?

Frontiers Research Topics are very popular trademarks of the Frontiers Journals Series: they are collections of at least ten articles, all centered on a particular subject. With their unique mix of varied contributions from Original Research to Review Articles, Frontiers Research Topics unify the most influential researchers, the latest key findings and historical advances in a hot research area! Find out more on how to host your own Frontiers Research Topic or contribute to one as an author by contacting the Frontiers Editorial Office: frontiersin.org/about/contact

STRUCTURED EDIBLE OIL: TOWARDS A NEW GENERATION OF FAT MIMETICS

Topic Editors:
Miguel Cerqueira, International Iberian Nanotechnology Laboratory (INL), Portugal
Stephen Robert Euston, Heriot-Watt University, United Kingdom
Luiz Henrique Fasolin, Campinas State University, Brazil

Prof. Ashok Patel of Guangdong Technion-Israel Institute of Technology (GTIIT), who served as a Topic Editor for this Research Topic, sadly passed away on Sunday 17th May 2020. We want to acknowledge the important role he played in developing this Research Topic.

Citation: Cerqueira, M., Euston, S. R., Fasolin, L. H., eds. (2021). Structured Edible Oil: Towards a New Generation of Fat Mimetics. Lausanne: Frontiers Media SA. doi: 10.3389/978-2-88966-814-4

Table of Contents

frontiers in Sustainable Food Systems

EDITORIAL
published: 26 March 2021
doi: 10.3389/fsufs.2021.652644

Editorial: Structured Edible Oil: Towards a New Generation of Fat Mimetics

Miguel A. Cerqueira[1]*, *Luiz H. Fasolin*[2]* and *Stephen R. Euston*[3]*

[1] International Iberian Nanotechnology Laboratory, Braga, Portugal, [2] Department of Food Engineering, Faculty of Food Engineering, Campinas State University, Campinas, Brazil, [3] School of Engineering and Physical Sciences, Institute of Biological Chemistry, Biophysics and Bioengineering, Heriot-Watt University, Edinburgh, United Kingdom

Keywords: oleogel, organogel, oleofoam, emulsion, fat mimetic

Editorial on the Research Topic

Structured Edible Oil: Towards a New Generation of Fat Mimetics

Edited by:
Guillermo Raul Castro, Consejo Nacional de Investigaciones Científicas y Técnicas (CONICET), Argentina

Reviewed by:
Suzana Ferreira-Dias, Instituto Superior Agronomia Universidade de Lisboa, Portugal
Guadalupe Virginia Nevárez-Moorillón, Autonomous University of Chihuahua, Mexico

***Correspondence:**
Miguel A. Cerqueira
miguel.cerqueira@inl.int
Luiz H. Fasolin
lfasolin@unicamp.br
Stephen R. Euston
s.r.euston@hw.ac.uk

Specialty section:
This article was submitted to Sustainable Food Processing, a section of the journal Frontiers in Sustainable Food Systems

Received: *12 January 2021*
Accepted: *25 February 2021*
Published: *26 March 2021*

Citation:
Cerqueira MA, Fasolin LH and Euston SR (2021) Editorial: Structured Edible Oil: Towards a New Generation of Fat Mimetics. Front. Sustain. Food Syst. 5:652644. doi: 10.3389/fsufs.2021.652644

Saturated and trans (produced during partial hydrogenation of unsaturated oils) fatty acids in food are related to several comorbidities and mainly to the raise in blood cholesterol levels, which in turn is a risk factor for cardiovascular disease (CVD), and as such, hydrogenated fats have become one of the biggest health issues around processed foods in recent years. Not only does this contribute to increased morbidity but is also a major economic cost for national healthcare providers and governments. The European Heart Network in the European Cardiovascular Disease Statistics (Wilkins et al., 2017) put the total costs of CVD (healthcare and other—productivity loss, etc.) as £26Bn in 2015 alone. The cost of CVD to the UK is around €14.82Bn per year (Public Health England, 2017).

Some of the blame for dietary related health issues has been leveled at the food industry for producing high calorie, energy dense foods (Wilding, 2012). Wilding (2012) has described the food industry as "an unhealthy alliance of producers and marketers," which he says have "successfully promoted energy dense foods, many of which provide positive reinforcement that increases consumption, effectively producing a "cafeteria diet" for the whole human population—a well-proved way of causing obesity in experimental animals."

In their defense, manufacturers have tried introducing reduced calorie foods, where fats (or carbohydrates) have been removed and replaced with other ingredients to lower the energy density. Take up of these has been low, however, as their taste and texture are often considered inferior by the consumer (Hamilton et al., 2000; McEwan and Sharp, 2000). Poole et al. (2020) have pointed out that even the smallest change to texture and flavor of a food product can disenfranchise the consumer base, which is no incentive for manufacturers to reformulate their products. Clearly, if current strategies for fat replacement or low energy density foods production are not producing products of sufficient quality, then other strategies for the formulation of healthier foods should be researched. The challenges are mainly related to the physicochemical properties of fats and their influence on food structure and organoleptic properties. Therefore, the scientific community and the industry are looking for new ways to structure oils and replace the existing fats by healthier fats and obtain reduced low-fat content products while maintaining the organoleptic properties and convenience of the products, ensuring acceptance by consumers.

In this Research Topic *Structured Edible Oil: Towards a New Generation of Fat Mimetics* emerging methods for the replacement of fats in food systems are presented. These are focused on ways to structure polyunsaturated edible oils (so-called oleogelation) so they can be used in place of their saturated counterparts. A range of oleogelation mechanisms are explored. Avendaño-Vásquez et al., studied the well-known ability of alkyl ester waxes to self-associate in oils to form an oleogel,

demonstrating that it is possible to tune the melting properties of the gel by varying the relative chain lengths of the alkyl chains and through the addition of the monoacylglycerol 1-stearoyl-glycerol. In several of the studies, the use of non-lipophilic gelators is demonstrated. Bascuas et al. use the hydrocolloids hydroxymethyl cellulose and xanthan gum with the emulsion template method to produce oleogels with a high oxidative and physical stability. Gallegos Soto et al. have taken the use of hydrocolloids a step further and demonstrate that use chitosan in combination with anionic polysaccharides to replace 80% of the cocoa butter in dark chocolate with oleogelled oils. A third and novel type of oleogelator reported here by Whitby is the use of fumed silica particles. These are able to aggregate into branched fractal structures that form a network gel in the oil, with the structure and properties making them well-suited to encapsulation of bioactive ingredients in functional foods. The remaining papers review various aspects for oleogel structure and applications. Park and Maleky give a mini-review concentrating on food applications and in particular the nutritional, texture, and stability of various oleogels in real formulations. Fameau et al. report a very interesting study on oleofoams, oil systems where air bubble are trapped in an oleogelled network. They highlight the potential of using these to replace solid fat with liquid oils and air bubbles, and point to the very high stability of the air bubbles with adsorbed gelators as being a key attribute of these systems. Finally, Wijarnprecha et al. discuss the highly important topic of oleogel water-in-oil emulsions. Some oleogels, particularly those containing gelators that form hydrates, are highly unstable in the presence of even small amounts of water. Solving this is the key to opening up oleogel technology to a wide range of intermediate and high-water activity foods, including food emulsions.

Fat mimetics will be for sure a trend topic in the next 5–10 years, and it is clear from the papers published in this Research Topic the great possibilities of using oleogelation in this regard. The topics covered represent some of the infinite possibilities for research and innovation in this field. The work that is still ongoing foresees great endeavors in this area and it is expected that industry will adopt some of the new ideas for their products.

For this Research topic, it is important to highlight the important role of our friend and colleague Dr. Ashok Patel who served as a Topic Editor and who sadly passed away in May 2020.

AUTHOR CONTRIBUTIONS

All authors listed have made a substantial, direct and intellectual contribution to the work, and approved it for publication.

REFERENCES

Hamilton, J., Knox, B., Hill, D., and Parr, H. (2000). Reduced fat products—consumer perceptions and preferences. *Br. Food J.* 102, 494–506. doi: 10.1108/00070700010336454

McEwan, J. A., and Sharp, T. M. (2000). Technical, economic and consumer barriers to the consumption of reduced fat bakery products. *Nutr. Food Sci.* 30, 16–18. doi: 10.1108/00346650010304710

Poole, J., Bentley, J., Barraud, L., Samish, I., Dalkas, G., Matheson, A., et al. (2020). Rising to the challenges: Solution-based case studies highlighting innovation and evolution in reformulation. *Nutr. Bull.* 45, 332–340. doi: 10.1111/nbu.12456

Public Health England (2017). *Cardiovascular Disease Prevention Action Plan - 2017 to 2018*. Available online at: https://assets.publishing.service.gov.uk/government/uploads/system/uploads/attachment_data/file/648190/cardiovascular_disease_prevention_action_plan_2017_to_2018.pdf (accessed 11 January 2021).

Wilding, J. (2012). Are the causes of obesity primarily environmental? Yes. *BMJ* 354:e5843. doi: 10.1136/bmj.e5843

Wilkins, E., Wilson, L., Wickramasinghe, K., Bhatnagar, P., Leal, J., Luengo-Fernandez, R., et al. (2017). *European Cardiovascular Disease Statistics 2017*. Brussels: European Heart Network.

Conflict of Interest: The authors declare that the research was conducted in the absence of any commercial or financial relationships that could be construed as a potential conflict of interest.

frontiers in Sustainable Food Systems

ORIGINAL RESEARCH
published: 24 July 2020
doi: 10.3389/fsufs.2020.00111

Designing Hydrocolloid-Based Oleogels With High Physical, Chemical, and Structural Stability

Santiago Bascuas[1], *Ana Salvador*[2], *Isabel Hernando*[1]* *and Amparo Quiles*[1]

[1] *Department of Food Technology, Universitat Politècnica de València, Valencia, Spain,* [2] *Institute of Agrochemistry and Food Technology (IATA-CSIC), Valencia, Spain*

Numerous studies conducted have shown a direct relationship between the high consumption of saturated and *trans*-fats and the risk of suffering from cardiovascular diseases, diabetes, and different cancers. Oleogels, with a suitable lipid profile of mono-, poly-unsaturated fatty acids, and similar functionality to traditional solid fat, can be a healthy alternative in food formulation. The aim of this study is to develop edible oleogels with a healthy and stable lipid profile, using the emulsion-template approach and hydrocolloids as oleogelators. Oleogels were developed from sunflower oil and sunflower oil with a high content of monounsaturated acids, using hydroxypropylmethylcellulose (HPMC) and xanthan gum (XG) as oleogelators. The influence of two drying conditions (60°C for 24 h and 80°C for 10 h 30 min) along with the composition of the oil on the structural, physical, and oxidative stability of oleogels were studied. All oleogels presented a stable network and high physical stability with oil losses <14% after 35 days of storage. Rheological properties showed that oleogels displayed a low frequency dependent and $G' > 10^5$ Pa related to solid gel-like behavior. Oleogels made with sunflower oil rich in monounsaturated fatty acids resulted in higher oxidative stability, with those developed at drying temperatures of 80°C for 10 h 30 min having a greater structural and physical stability.

Keywords: oleogelation, HPMC, xanthan gum, sunflower oil, rheological properties, peroxide value, light microscopy

OPEN ACCESS

Edited by:
Luiz Henrique Fasolin, Campinas State University, Brazil

Reviewed by:
Yong Wang, Jinan University, China
Guadalupe Virginia Nevárez-Moorillón, Autonomous University of Chihuahua, Mexico

***Correspondence:**
Isabel Hernando
mihernan@tal.upv.es

Specialty section:
This article was submitted to Sustainable Food Processing, a section of the journal Frontiers in Sustainable Food Systems

Received: *15 April 2020*
Accepted: *17 June 2020*
Published: *24 July 2020*

Citation:
Bascuas S, Salvador A, Hernando I and Quiles A (2020) Designing Hydrocolloid-Based Oleogels With High Physical, Chemical, and Structural Stability. Front. Sustain. Food Syst. 4:111. doi: 10.3389/fsufs.2020.00111

INTRODUCTION

Food products such as chocolate, ice cream, meat, butters, margarine, and bakery products, are formulated with considerable amounts of solid fats, rich in saturated and/or *trans*-fatty acids. Solid fats have a key role in improving quality attributes such as mouthfeel and texture. Several studies have reported the relationship between the negative cardiovascular effects and the increased consumption of saturated and *trans*-fatty acids (Mozaffarian and Clarke, 2009; Morenga and Montez, 2017). Therefore, authorities have regulated or provided some suggestions to limit consumption of many food products formulated with a large amount of saturated and/or *trans*-fats (Health Canada, 2012; Food and Drug Administration (FDA), 2015; European Union (EU), 2019). Thus, the food industry and food scientists show great interest to find new strategies and product formulations with a better nutritional profile, *trans*-fat free, low content in saturated fatty acids, and a high content in unsaturated fats (Moghtadaei et al., 2018; Pehlivanoglu et al., 2018; Luo et al., 2019).

Oleogels have gained popularity for their potential application in cosmetic and pharmaceutical industries (Vintiloiu and Leroux, 2008; Bastiat and Leroux, 2009) and with food processing (Singh et al., 2017). Oleogelation allows structuring high concentration liquid oil (>90%) into a "gel-like" system with viscoelastic properties (Rogers et al., 2009).

In many of these oleogels, gelation is achieved by using low molecular weight organogelators (LWOG) such as hydroxylated fatty acids (Rogers et al., 2008), waxes (Lim et al., 2017; Martins et al., 2017), and lecithin (Bodennec et al., 2016). Besides LWOG, there are structured systems where liquid oil is organized into a polymer network. Within polymer gelation, cellulose derivative, ethylcellulose (EC) is a non-aqueous gelator with the ability to produce oleogels using a direct approach (Laredo et al., 2011; Zetzl et al., 2012; Giacintucci et al., 2018). The most common limitations of the EC oleogels are the poor oxidative stability because of the high temperatures (>135–140°C) required to induce the polymer EC gelation (Gravelle et al., 2012). Therefore, using hydrocolloid-based oleogelators including different sources of proteins (Patel et al., 2015; de Vries et al., 2017) and polysaccharides like celluloses ethers, methylcellulose (MC) (Patel et al., 2014a; Tanti et al., 2016a,b; Meng et al., 2018a), and hydroxypropylmethylcellulose (HPMC) (Patel et al., 2013; Oh and Lee, 2018; Oh et al., 2019; Bascuas et al., 2020), have attracted noticeable research attention. Hydrocolloids are widely used in food because of their commercial availability, large production, and low cost (Scholten, 2019; Abdolmaleki et al., 2020).

HPMC is a surface-active amphiphilic biopolymer and can be adsorbed to the oil droplet, protecting the oil droplets, thus, decreasing the amount of oil available for separation (Wollenweber et al., 2000; Li et al., 2013). Moreover, the addition of thickening agents, like XG, has shown an increase of the emulsion stability through bulk phase viscosity enhancement and interaction between the polysaccharides (Meng et al., 2018b; Encina-Zelada et al., 2019). Since HPMC and XG have a predominantly hydrophilic characteristic, their dispersibilities are limited in non-polar solvents. To overcome this problem, HPMC and XG must first be hydrated in an aqueous solution. Foam-template and emulsion-template are the most indirect methods used in structuring edible oils with hydrocolloids. In the foam-template approach, a water soluble cellulose derivative is foamed and freeze-dried to create a porous structure and has been shown to absorb a large amount of oil (Patel et al., 2013). However, freeze-drying is an expensive and time-consuming technique (do Vale Morais et al., 2016). The emulsion-template approach, first prepared by Romoscanu and Mezzenga (2006) using proteins, comprises an indirect multi-step process. In this method, first, an oil-in-water emulsion is produced as a template stabilized by a combination of water soluble biopolymers. Second, the water phase is removed to drive the structure formation; finally, the dried product is homogenized to obtain an oleogel. In both methods, as the oil binding is purely physical, it is necessary to shear the oil-sorbed polymer obtain a strong gel (Patel et al., 2013; Oh et al., 2019).

Sunflower oil is one of the most attractive vegetable oils used by food industry and is one of the most ingested worldwide, with a domestic consumption of 18.07 million metric tons during 2018–2019 (United States Department of Agriculture (USDA), 2020). Because of its low cost and high overall acceptability, sunflower oil has been used to produce oleogels (Yang et al., 2017; Jiang et al., 2018; Okuro et al., 2018; Tavernier et al., 2018). However, the predominant unsaturated fatty acids present in sunflower oils are susceptible to oxidation (Kozłowska and Gruczynska, 2018). Patel et al. (2014b) structured sunflower oil using MC and XG into solid-like oleogels using the emulsion-template approach; the drying of the emulsion in the oven (80°C for 32 h) gave oleogels with a poor oxidative stability. Developing strategies to improve the oil oxidative stability without influencing its nutritional and sensory properties, while maintaining the feasibility of use by food industry, represents an important advance in the quality of the oleogels made with hydrocolloids. Therefore, to improve the oxidative stability of oleogels, different strategies could optimize the processing conditions and the oil composition of the oleogel, favoring monounsaturated fatty acids (MUFA) with a longer oxidation induction period (Lee et al., 2007). It would be interesting to investigate the impact of using high MUFA oils and different processing conditions not only on the chemical stability, but also on the structural properties of oleogels based on water-soluble food polymers.

The objective of this work is to structure sunflower oil and sunflower oil with a high monounsaturated fatty acid content using the emulsion-template method, with HPMC and XG as oleogelators, to achieve oleogels with high structural, physical, and oxidative stability. For this, the influence of processing conditions and oil composition on the structure, physical, and chemical properties of oleogel will be compared and analyzed.

MATERIALS AND METHODS

Ingredients

Hydroxypropylmethylcellulose (HPMC "K4M"; 4000 cP) was provided by Dow Chemical Company (Midland, MI, United States) and xanthan gum (XG; Satiaxine CX 931) by Cargill R & D (Vilvoorde, Belgium). Water (Bezoya, Segovia, Spain, with a calcium content 6.32 mg L^{-1}), refined sunflower oil (fatty acids composition: SFA: 13, MUFA: 23, PUFA: 64, Consum, España), and high oleic sunflower oil (fatty acids composition: SFA: 10, MUFA: 65, PUFA: 25, Carrefour, España) were purchased in local supermarkets.

Oleogels Preparation

Based on the procedures described by Patel et al. (2014a) with some modifications, we prepared oleogels using emulsion-template method, HPMC (1 g) was dispersed in 38.4 g cold water and mixed using a stirrer (Heildolph RZR 1, Schwabach, Germany) at 1,010 rpm for 30 min, the resulting aqueous solution was stored at 8°C overnight. Subsequently, 0.6 g of XG was added to the HPMC solution and stirred (Heildolph RZR 1, Schwabach, Germany) for 5 min at 1,010 rpm, 60 g of oil was then added and homogenized (Ultraturrax T18, IKA, Germany) at 13,000 rpm for 6 min. The emulsions were spread on aluminum foil and dried in an oven (KB115, BINDER, Germany) using two different drying conditions: 80°C for 10 h 30 min, and 60°C for

24 h. These were the minimum times needed to reach constant dry weight (moisture: 2.31 ± 0.532% at 60°C; 1.59 ± 0.112% at 80°C) at the indicated conditions. The dried products were ground in a grinder (Moulinex A320R1, Paris, France) for 4 s to produce the oleogels. Four oleogels S60 (sunflower oil and drying at 60°C), SH60 (high oleic sunflower oil and drying at 60°C), S80 (sunflower oil and drying at 80°C), and SH80 (high oleic sunflower oil and drying at 80°C) were prepared in triplicate.

Microstructure of the Oleogels

The microstructure of oleogels was studied by optical microscopy with a Nikon Eclipse 80i optical microscope (Nikon Co., Ltd., Tokyo, Japan) and incorporated camera (ExwaveHAD, model No. DXC-190, Sony Electronics Inc., Park Ridge, New Jersey, USA. UU.). The oleogels were cut with a cryostat (CM 1950, Leica) to obtain 20 μm thick sections that were placed on a glass slide. These sections were visualized by polarized light and by clear field microscopy using 2% Sudan as a staining agent to study the lipid fraction. The images were captured and stored at 1,280 × 1,024 pixels using the microscope software (NIS-Elements M, Version 4.0, Nikon, Tokyo, Japan).

Oil Loss of Oleogels

Determination was made by measuring the percentage of oil migration over 35 days at 20°C, using the method of Doan et al. (2016) with modifications. The weight of released oil was measured at intervals of 1, 7, 14, 21, 28, and 35 days. A funnel and filter paper was positioned above an Erlenmeyer flask collecting the dripping liquid oil from the oleogels. The weight of the funnel, the filter paper, and the Erlenmeyer flask were measured (M1). Then 10 g of oleogel was weighed (M3) and set into the funnel. Samples were removed at each time interval with a flat, small spatula. The weight of the funnel, the filter paper, and the flask with the liquid oil released was measured again (M2). The results were expressed as g oil loss per 100 g oleogel, calculated using Equation 1 and were measured in triplicate for each sample.

$$\text{Oil loss} = \frac{\text{M2} - \text{M1}}{\text{M3}} \times 100\ \% \quad (1)$$

The experimental data were fitted to a first-order equation using Solver software (Microsoft Excel):

$$\text{OL} = \text{OL max}\ (1 - e^{-kt}) \quad (2)$$

where OLmax is the value of OL (oil loss) at sufficiently long (infinite) time, k is the kinetic constant, and t is the chosen time.

Oxidative Stability of Oleogels

Peroxide values (PV) and specific absorption in the visible ultraviolet (k_{232} and k_{270}) were used to study the oxidative stability of the oleogels during storage. The PV was analyzed using the acetic acid/chloroform solution method, according to Cho and Lee (2015), and k_{232} and k_{270} were determined according to ISO 3656:2011 (ISO, 2011), using a UV-VIS spectrophotometer (UV-VIS spectrophotometer, 1000, CECIL, UK). All the samples were stored at 20°C for 35 days and were evaluated every 7 days.

Rheological Properties of Oleogels

The rheological behavior of oleogels was evaluated using small amplitude oscillatory shear in a controlled stress rheometer [AR-G2, TA Instruments (Crawley, England)] with a Peltier heating system. A 20 mm diameter plate-plate sensor geometry with a serrated surface and a 1.5 mm gap was used. The oleogels rested for a 10 min equilibration time after reaching the measurement position.

Stress sweeps were conducted at a frequency of 1 Hz to measure the extent of the linear viscoelastic response. Frequency sweeps from 0.1 to 10 Hz at a stress wave amplitude (100 Pa) inside the linear region were performed. Storage modulus (G′), loss modulus (G″), and tan δ (G″/G′) values were recorded. The testing temperature was always 20°C.

Statistical Analysis

Results were statistically analyzed using analysis of variance (ANOVA) with the least significant differences (LSD) calculated at a level of significance $p < 0.05$. Statistical analyses were conducted using XLStat 2019 (Addinsoft, Barcelona, España).

RESULTS AND DISCUSSION

Oleogel Microstructure

Figure 1 shows that the oleogel S60 constitutes a polymeric network that extends, forming branches that compartmentalize and trap fat globules (**Figure 1A**). However, accumulations of free and unstructured fat can also be seen (**Figure 1E**). This may be because of a coalescence phenomenon between fat globules, likely because the network formed by the structuring agents has not resisted the drying process and has not physically trapped all the fat globules (**Figure 1E**). Camino et al. (2009) and Wollenweber et al. (2000) studied the role of HPMC as a fat structuring agent; they found that this hydrocolloid could adsorb at the surface of fat globules, forming a viscoelastic multilayer structure because of a train loop tail conformation. In contrast, Patel et al. (2014a) studied the role of XG on the structure of oleogels, finding that XG can increase the viscosity of the emulsion by improving its stability in combination with MC during the drying process. In fact, they observed oil leakage on emulsions stabilized by using only cellulose derivates. Here, in the S80 oleogel, the hydrocolloids form a homogeneous network where most of the fat globules remain trapped (**Figure 1F**). In this oleogel structuring agents have a more homogeneous distribution and more structured fat (**Figure 1B**) than in the oil of S60 (**Figure 1E**) is observed. In oleogel SH60 the polymeric network formed by hydrocolloids is observed distributed throughout the oleogel (**Figures 1C,G**), surrounding the fat globules (**Figure 1G**). However, unstructured fat and coalescence phenomena can also be observed. In oleogel SH80 hydrocolloids show a uniform and homogeneous network (**Figure 1D**) that surrounds and traps fat globules (**Figure 1H**). In SH80 the fat appears more structured than in the other oleogels, probably because the hydrocolloid network has a greater stability. Comparing the same type of oil oleogels undergone drying at 80°C, more stable polymeric networks exist, capable of retaining fat globules than those dried at 60°C. Probably, drying

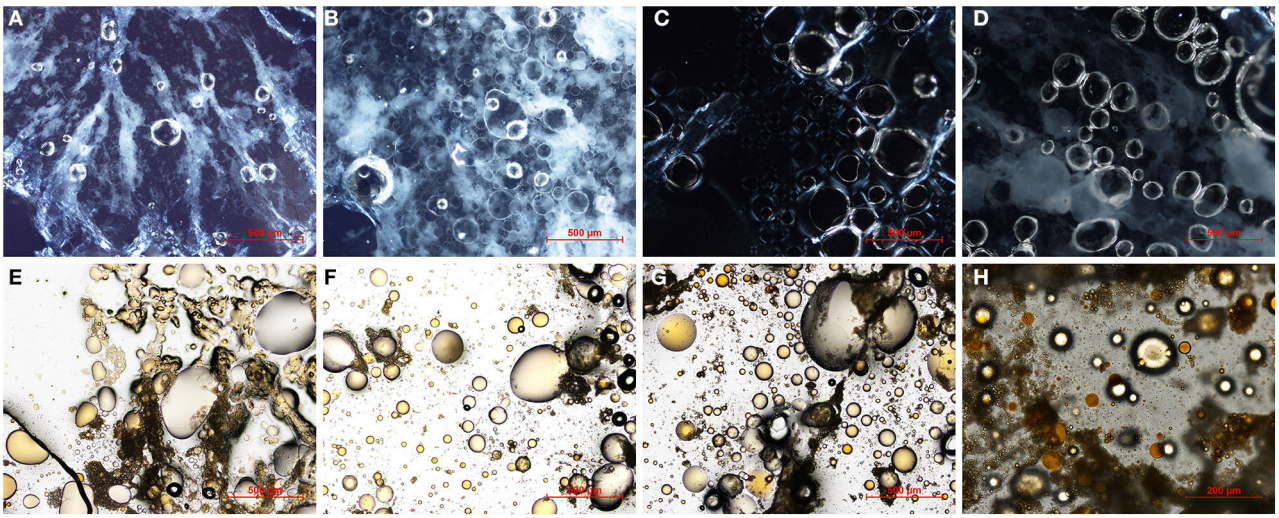

FIGURE 1 | Optical microscopy micrographs of oleogels prepared with sunflower (S) and high oleic sunflower oil (SH), and developed by conventional drying at 60°C (S60, SH60) and 80°C (S80, SH80), under **(A–D)** polarized light, **(E–H)** bright field with Sudan 2%.

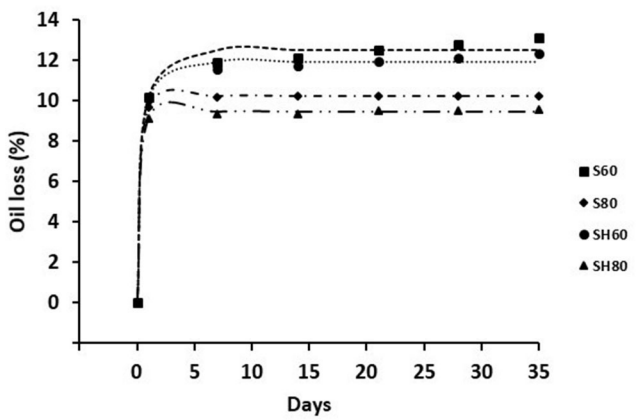

FIGURE 2 | Oil loss curves for oleogels prepared with sunflower (S) and high oleic sunflower oil (SH), and developed by conventional drying at 60°C (S60, SH60) and 80°C (S80, SH80).

TABLE 1 | Kinetics parameters of the oil loss.

	S60	S80	SH60	SH80
OLmax (%)	12.49 ± 0.43^{B}	10.24 ± 0.19^{A}	11.94 ± 0.63^{B}	9.44 ± 0.42^{A}
K ($days^{-1}$)	1.70 ± 0.05^{A}	2.91 ± 0.03^{B}	1.88 ± 0.47^{A}	3.41 ± 0.23^{B}
R^2	0.99	1.00	0.99	1.00

Oleogels prepared with sunflower (S) and high oleic sunflower oil (SH), developed by drying at 60°C (S60 and SH60) and 80°C (S80 and SH80). Values with different capital letters (A, B, … Z) within the same row are significantly different ($p < 0.05$) according to the LSD multiple range test.

the emulsion at 60°C, which is slower than at 80°C, favors the attractive interactions between the xanthan gum helix (XG-XG), and weakens HPMC-XG interactions. This would lead to the formation of a weaker network when drying is carried out at 60°C if compared to 80°C (Carnali, 1992; Lapasin and Pricl, 1995). Monounsaturated sunflower oil seems to be retained more in the polymeric network than sunflower oil.

Physical Stability of Oleogels

The physical stability of oleogels is related to their ability to retain oil during storage. **Figure 2** shows the proportion of oil loss at 1, 7, 14, 21, 28, and 35 days of storage at 20°C of all oleogels developed in this study. The experimental data were fitted to a first-order equation. Exponential decay kinetic model presented a R^2 more than 0.99 for all cases (**Table 1**), evidencing the excellent fit between the formula and the experimental data.

Freshly made oleogels showed no oil losses, however the greatest loss of oil took place in all the oleogels studied during the first 24 h of storage. k values were significantly lower ($p < 0.05$) for S60 and SH60, indicating a slower loss of oil for these samples within the first 24 h. However, OLmax values indicated that oleogels S80 and SH80 presented significantly lower ($p < 0.05$) amount of oil exuded over the whole storage, while S60 and SH60 oleogels had the highest values, without significant differences ($p < 0.05$) between them. Other authors (Meng et al., 2018c) also developed stable oleogels with soybean oil using the emulsion-template method, varying HPMC concentration (0.2–1%) and constant XG concentration (0.3%); however, the stability during storage was not studied. They suggested that the formation of semi-crystalline structure due to the hydrogen bonding within the chains of the polysaccharides, resulted in oleogels with high physical stability, especially from oleogel made with highest HPMC concentration. As explained before, a stronger network would be obtained when drying at higher temperature; the strength of the network would be helping to prevent the oil release from the oleogel.

Oxidative Stability

Table 2 shows the peroxide values (PV) of the oleogels stored for 35 days at 20°C. The upper limit for the PV of fresh oils is <15–20 meq kg^{-1} (Codex Alimentarius, 2001; Gómez-Alonso et al., 2004). PV > 20 correspond to very poor-quality fats and oils, which normally would have significant off flavors (O'Keefe and Pike, 2010). The PV of sunflower and high oleic sunflower oils used in this study were 3.24 ± 0.07 and 6.27 ± 0.29 meq kg^{-1}, respectively. These values indicate that both oils are suitable.

The oleogels S60, S80, SH60, and SH80 had initial PV of 12.86 ± 0.51, 16.22 ± 0.68, 7.78 ± 0.76, and 7.69 ± 0.07, respectively (**Table 2**). The process of making oleogels causes oxidative degradation of the oil, mainly in those formulated with sunflower oil. However, all the oleogels studied showed adequate initial PV, while oleogels made with high oleic sunflower oil (SH60 and SH80) presented significantly lower PV ($p < 0.05$) throughout storage, but with no significant differences ($p < 0.05$) between them. The oleogels made with sunflower oil (S60 and S80) had the highest PV, with S60 showing the highest PV throughout storage.

Regarding the behavior of each oleogel, those made with sunflower oil (S60 and S80) showed a significant increase ($p < 0.05$) in PV throughout the entire storage, reaching values >40 meq kg^{-1} at the end of the storage period. The oleogel made with high oleic sunflower oil (SH60), showed significant increases ($p < 0.05$) of PV on storage days 14 and 28 and SH80 on days 14, 21, and 35, with both oleogels reaching PV around 15 meq kg^{-1} at the end of the storage period.

The specific UV extinction coefficient (k) at 232 and 270 nm is an estimator of fat deterioration. The k_{232} is normally considered an indicator of primary oxidation products, such as hydroperoxides and conjugated dienes. While k_{270} measures conjugated trienes (as secondary oxidation products), ketones, aldehydes, and primary oxidation products of linolenic acid (Maskan and Bagci, 2003; Tavakoli et al., 2017). The specific absorption values in the visible ultraviolet (k_{232} and k_{270}) of the oils used in the production of oleogels were 3.40 ± 0.28 and 3.51 ± 0.14 for sunflower oil, and 2.15 ± 0.02 and 0.78 ± 0.04 for high oleic sunflower. These values agree with Albi et al. (1997), who reported a k_{232} and k_{270} value for fresh sunflower oil of 4.70 and 3.15, and 2.32 and 0.83 for high oleic sunflower.

The oleogels S60, S80, SH60, and SH80 had initial values of k_{232} and k_{270} of 3.92 ± 0.50, 2.86 ± 0.01; 4.50 ± 0.23, 5.33 ± 0.15; 2.51 ± 0.05, 0.80 ± 0.08; and 2.20 ± 0.09, 0.86 ± 0.06; respectively (**Table 3**). The SH60 and SH80 oleogels showed significantly lower values of k_{232} and k_{270} ($p < 0.05$) throughout the storage period, without significant differences ($p < 0.05$) between them. While the S60 and S80 oleogels presented the highest values, with S60 showing the highest k_{232} values, and the lowest k_{270} values. In oleogels made with sunflower oil (S60 and S80) a significant increase ($p < 0.05$) of k_{232} values was observed throughout storage, while the k_{270} values remained stable while increasing at the end of storage, specifically on day 28.

In oleogels made with oleic-rich sunflower oil (SH60 and SH80), a significant increase in k_{232} values was observed every 14 days of storage, but from day 28 these values remained stable. The values of k_{270} remained stable in oleogel SH60 until day 7 of storage and after increased, mainly on day 14. In oleogel SH80 the values of k_{270} remained stable until day 21; on day 28 there was a significant increase ($p < 0.05$), but remained stable until day 35. The oleogels made with oleic-rich sunflower oil were more stable to oxidation than the oleogels made with sunflower oil. The high content in MUFA in SH60 and SH80 oleogels would

TABLE 2 | Peroxide value (meq kg^{-1}) during storage at 20°C.

Storage (days)	S60	S80	SH60	SH80
0	12.86 ± 0.51^{aB}	16.22 ± 0.68^{aC}	7.78 ± 0.76^{aA}	7.69 ± 0.07^{aA}
7	19.62 ± 1.64^{bB}	18.27 ± 0.42^{bB}	8.47 ± 0.62^{aA}	9.00 ± 0.52^{aA}
14	27.07 ± 0.56^{cC}	21.68 ± 0.62^{cB}	11.08 ± 0.17^{bA}	10.58 ± 0.18^{bA}
21	32.69 ± 1.43^{dC}	30.60 ± 0.96^{dB}	11.90 ± 0.14^{bA}	12.13 ± 1.26^{cA}
28	39.35 ± 0.95^{eC}	34.71 ± 0.94^{eB}	14.63 ± 0.32^{cA}	13.39 ± 1.29^{cdA}
35	46.81 ± 1.70^{fC}	44.22 ± 1.27^{fB}	15.49 ± 1.13^{cA}	14.66 ± 0.39^{dA}

Oleogels prepared with sunflower (S) and high oleic sunflower oil (SH), developed by drying at 60°C (S60 and SH60) and 80°C (S80 and SH80). Values with different lowercase letters (a, b, … z) within the same column are significantly different ($p < 0.05$) according to the LSD multiple range test. Values with different capital letters (A, B, … Z) within the same row are significantly different ($p < 0.05$) according to the LSD multiple range test.

TABLE 3 | Oxidation spectrophotometric parameters k_{232} and k_{270} during storage at 20°C.

Storage (days)	S60		S80		SH60		SH80	
	232 nm	270 nm	232 nm	270 nm	232 nm	270 nm	232 nm	270 nm
0	3.92 ± 0.50^{aC}	2.86 ± 0.01^{aB}	4.50 ± 0.23^{aB}	5.33 ± 0.15^{aC}	2.51 ± 0.05^{Aa}	0.80 ± 0.08^{aA}	2.20 ± 0.09^{Aa}	0.86 ± 0.06^{aA}
7	4.74 ± 0.78^{bB}	2.69 ± 0.19^{aB}	4.65 ± 0.34^{abB}	5.52 ± 0.34^{aC}	2.63 ± 0.16^{aA}	0.83 ± 0.11^{abA}	2.29 ± 0.14^{aA}	1.00 ± 0.12^{abA}
14	5.48 ± 0.74^{bcB}	3.06 ± 0.17^{abB}	5.06 ± 0.09^{bB}	5.50 ± 0.19^{aC}	3.20 ± 0.04^{bA}	1.29 ± 0.12^{dA}	2.74 ± 0.15^{bA}	0.90 ± 0.099^{aA}
21	5.77 ± 0.57^{cB}	3.05 ± 0.47^{abB}	5.55 ± 0.40^{Cb}	5.62 ± 0.19^{aC}	3.20 ± 0.22^{bA}	1.23 ± 0.16^{cdA}	3.01 ± 0.32^{bA}	0.97 ± 0.24^{aA}
28	6.67 ± 0.06^{dC}	3.46 ± 0.17^{bB}	5.90 ± 0.15^{cdB}	6.72 ± 0.50^{bC}	3.71 ± 0.24^{cA}	1.06 ± 0.12^{cA}	3.36 ± 0.08^{cA}	1.20 ± 0.09^{bA}
35	6.88 ± 0.28^{eC}	2.92 ± 0.15^{aB}	6.19 ± 0.12^{dB}	7.16 ± 0.62^{bC}	3.67 ± 0.40^{cA}	1.04 ± 0.16^{bcA}	3.37 ± 0.21^{cA}	1.22 ± 0.003^{bA}

Oleogels prepared with sunflower (S) and high oleic sunflower oil (SH), developed by drying at 60°C (S60 and SH60) and 80°C (S80 and SH80). Values with different lowercase letters (a, b, … z) within the same column are significantly different ($p < 0.05$) according to the LSD multiple range test. Values with different capital letters (A, B, … Z) within the same row are significantly different ($p < 0.05$) according to the LSD multiple range test.

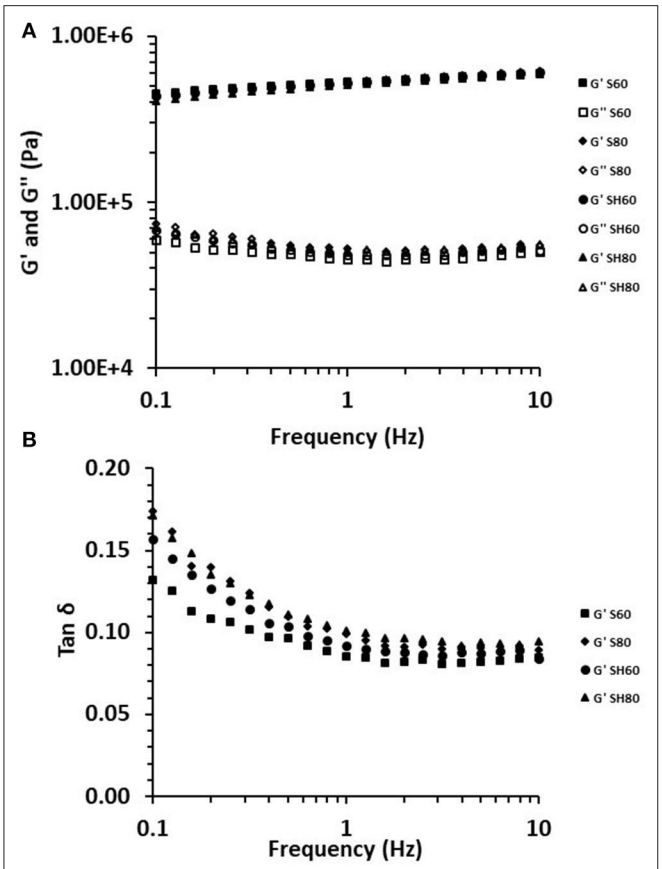

FIGURE 3 | Frequency sweep **(A)**, and tan δ as a function of frequency **(B)** for oleogels prepared with sunflower (S) and high oleic sunflower oil (SH), and developed by conventional drying at 60°C (S60, SH60) and 80°C (S80, SH80).

be helping to delay oxidation, as MUFA have longer induction periods than PUFA, which are major components in S60 and S80 oleogels.

Rheology

To better understand the structural changes, the dynamic mechanical spectra were studied. The viscoelastic properties of the samples are shown in **Figure 3**. Over the entire frequency range studied (0.1–10 Hz) (**Figure 3A**), a low G′ and G″ dependence with frequency was observed, suggesting and all oleogels presented an elastic modulus (G′) higher than viscous modulus (G″), indicating a typical behavior of solid gels (Guenet, 2016). Luo et al. (2019) obtained comparable low frequency dependent results from camellia-oil based oleogels structured with tea polyphenol-palmitate and varying citrus pectin concentration. Meng et al. (2018c) dried soybean emulsions in a vacuum drying oven at 90°C and analyzed the frequency sweep of oleogels formulated with 0.2–1% of HPMC (400 and 1500 cP) and 0.3% XG, showing similar dependency on frequency, but a lower value of G′, which may be for the viscosity of HPMC (4000 cP) and the higher XG concentration (0.6%) used in our study. The loss tangent (tan δ = G″/G′) of oleogels, showed a similar trend, with a tan $\delta \approx 0.1$, confirming the existence of a strong internal network (**Figure 3B**). These results were corroborated analyzing statistical differences at 1 Hz (**Table 4**) with no significant differences between oleogels for the dynamic modulus (G′ and G″) and tan δ values higher for the S80 and SH80 oleogels, indicating that these samples had lower viscoelastic behavior.

TABLE 4 | Viscoelastic rheological parameters (at 1 Hz) of oleogels.

	G′ (Pa)	G″ (Pa)	tan δ
S60	513,040 ± 25,686^{a}	48,291 ± 6,085^{a}	0.094 ± 0.010^{ab}
S80	604,043 ± 81,836^{a}	64,035 ± 15,816^{a}	0.105 ± 0.012^{b}
SH60	559,315 ± 37,206^{a}	48,100 ± 1,884^{a}	0.086 ± 0.005^{a}
SH80	545,941 ± 32,973^{a}	55,753 ± 3,706^{a}	0.102 ± 0.001^{b}

Oleogels prepared with sunflower (S) and high oleic sunflower oil (SH), developed by drying at 60°C (S60 and SH60) and 80°C (S80 and SH80). Values with different lowercase letters (a, b, … z) within the same column are significantly different ($p < 0.05$) according to the LSD multiple range test.

CONCLUSIONS

It is possible to develop physically, chemically, and structurally stable oleogels using sunflower oil and sunflower oil with a high content monounsaturated fatty acids, using HPMC and XG as structuring agents with the emulsion-template method and the drying conditions 60°C for 24 h and 80°C for 10 h 30 min). The stability of oleogels during storage is influenced by the composition of the oil and the drying conditions of the oleogel process. However, oleogels made with sunflower oil high in monounsaturated fatty acids show better oxidative stability during storage than those made with sunflower oil, regardless of the drying conditions used. Furthermore, drying at 80°C for 10 h 30 min generates oleogels with greater structural and physical stability than drying at 60°C for 24 h, regardless of the oil composition of the oleogel. Therefore, the oxidative stability of the oleogel is greatly influenced by the type of oil, improving when the oil has a high content of monounsaturated fatty acids, still, the drying conditions (time and temperature) have a marked influence on the structural and physical stability.

DATA AVAILABILITY STATEMENT

The raw data supporting the conclusions of this article will be made available by the authors, without undue reservation.

AUTHOR CONTRIBUTIONS

SB: experimental work and writing the draft manuscript. AS: investigation and methodology. IH: writing–review and editing and funding acquisition. AQ: supervision and funding

acquisition. All authors contributed to the article and have approved the final manuscript.

FUNDING

The authors would like to thank Universitat Politècnica de València by FPI-UPV 2017 grant and the project RTI2018-099738-B-C22 from the Ministerio de Ciencia, Innovacion y Universidades.

ACKNOWLEDGMENTS

Special thanks goes to Phillip John Bentley for assistance in correcting the English manuscript.

REFERENCES

Abdolmaleki, K., Alizadeh, L., Nayebzadeh, K., Hosseini, S. M., and Shahin, R. (2020). Oleogel production based on binary and ternary mixtures of sodium caseinate, xanthan gum, and guar gum: optimization of hydrocolloids concentration and drying method. *J. Texture Stud.* 51, 290–299. doi: 10.1111/jtxs.12469

Albi, T., Lanzón, A., Guinda, A., Pérez-Camino, M. C., and León, M. (1997). Microwave and conventional heating effects on some chemical parameters of edible fats. *Agric. Food Chem.* 45, 3000–3003. doi: 10.1021/jf970168c

Bascuas, S., Hernando, I., Moraga, G., and Quiles, A. (2020). Structure and stability of edible oleogels prepared with different unsaturated oils and hydrocolloids. *Int. J. Food Sci. Technol.* 55, 1458–1467. doi: 10.1111/ijfs.14469

Bastiat, G., and Leroux, J. C. (2009). Pharmaceutical organogels prepared from aromatic amino acid derivatives. *J. Mater. Chem.* 19, 3867–3877. doi: 10.1039/b822657a

Bodennec, M., Guo, Q., and Rousseau, D. (2016). Molecular and microstructural characterization of lecithin-based oleogels made with vegetable oil. *RSC Adv.* 6, 47373–47381. doi: 10.1039/C6RA04324K

Camino, N. A., Pérez, O. E., Sanchez, C. C., Rodriguez Patino, J. M., and Pilosof, A. M. R. (2009). Hydroxypropylmethylcellulose surface activity at equilibrium and adsorption dynamics at the air-water and oil-water interfaces. *Food Hydrocoll.* 23, 2359–2368. doi: 10.1016/j.foodhyd.2009.06.013

Carnali, J. O. (1992). Gelation in physically associating biopolymer systems. *Rheol. Acta* 31, 399–412. doi: 10.1007/BF00701120

Cho, Y. J., and Lee, S. (2015). Extraction of rutin from Tartary buckwheat milling fractions and evaluation of its thermal stability in an instant fried noodle system. *Food Chem.* 176, 40–44. doi: 10.1016/j.foodchem.2014.12.020

Codex Alimentarius (2001). *Codex Standard for Named Vegetable Oils*. Codex Alimentarius CX-STAN 210-1999, Vol. 8. Rome: Secretariat of the Joint FAO/WHO Food Standards Programme; FAO, 11–25.

de Vries, A., Gomez, Y. L., Van der Linden, E., and Scholten, E. (2017). The effect of oil type on network formation by protein aggregates into oleogels. *RSC Adv.* 7, 11803–11812. doi: 10.1039/C7RA00396J

do Vale Morais, A. R., Alencar, É. D. N., Júnior, F. H. V., de Oliveira, C. M., Marcelino, H. R., Barratt, G., et al. (2016). Freeze-drying of emulsified systems: a review. *Int. J. Pharm.* 503, 102–114. doi: 10.1016/j.ijpharm.2016.02.047

Doan, C. D., Patel, A. R., Tavernier, I., De Clercq, N., Van Raemdonck, K., de Walle, D. V., et al. (2016). The feasibility of wax-based oleogel as a potential co-structurant with palm oil in low-saturated fat confectionery fillings. *Eur. J. Lipid Sci. Technol.* 118, 1903–1914. doi: 10.1002/ejlt.201500172

Encina-Zelada, C. R., Cadavez, V., and Teixeira, J. A. (2019). Optimization of quality properties of gluten-free bread by a mixture design of Xanthan, Guar, and Hydroxypropyl Methyl cellulose gums. *Foods* 8:156. doi: 10.3390/foods8050156

European Union (EU) (2019). Commission Regulation (EU) 2019/649 of 24 April 2019 amending Annex III to Regulation (EC) No 1925/2006 of the European Parliament and of the Council as regards trans-fat, other than trans-fat naturally occurring in fat of animal origin. *J. Euro. Union.* 2019, 17–20.

Food and Drug Administration (FDA) (2015). *Final Determination Regarding Partially Hydrogenated Oils (Removing Trans-Fat)*. Available online at: (March 9, 2020).

Giacintucci, V., Di Mattia, C. D., Sacchetti, G., Flamminii, F., Gravelle, A. J., Baylis, B., et al. (2018). Ethylcellulose oleogels with extra virgin olive oil: the role of oil minor components on microstructure and mechanical strength. *Food Hydrocoll.* 84, 508–514. doi: 10.1016/j.foodhyd.2018.05.030

Gómez-Alonso, S., Mancebo-Campos, V., Salvador, M. D., and Fregapane, G. (2004). Oxidation kinetics in olive oil triacylglycerols under accelerated shelf-life testing (25–75°C). *Eur. J. Lipid Sci. Technol.* 106, 369–375. doi: 10.1002/ejlt.200300921

Gravelle, A. J., Barbut, S., and Marangoni, A. G. (2012). Ethylcellulose oleogels: manufacturing considerations and effects of oil oxidation. *Food Res. Int.* 48, 578–583. doi: 10.1016/j.foodres.2012.05.020

Guenet, J. M. (2016). Organogels: Thermodynamics, Structure, Solvent Role, and Properties. Cham: Springer International Publishing.

Health Canada (2012). *It's Your Health-Fats: The Good The Bad and The Ugly*. Available online at: https://www.hc-sc.gc.ca/hl-vs/alt_formats/pdf/iyh-vsv/med/fats-gras-eng.pdf (accessed March 9, 2020).

ISO (2011). Animal and Vegetable Fats and Oils. Determination of Ultraviolet Absorbance Expressed as Specific UV Extinction. Geneva: International Organization for Standardization.

Jiang, Y., Liu, L., Wang, B., Sui, X., Zhong, Y., Zhang, L., et al. (2018). Cellulose-rich oleogels prepared with an emulsion-templated approach. *Food Hydrocoll.* 77, 460–464. doi: 10.1016/j.foodhyd.2017.10.023

Kozłowska, M., and Gruczynska, E. (2018). Comparison of the oxidative stability of soybean and sunflower oils enriched with herbal plant extracts. *Chem. Pap.* 72, 2607–2615. doi: 10.1007/s11696-018-0516-5

Lapasin, R., and Pricl, S., (eds). (1995). "Rheology of polysaccharide systems," in *Rheology of Industrial Polysaccharides: Theory and Applications* (Boston, MA: Springer) 250–494. doi: 10.1007/978-1-4615-2185-3

Laredo, T., Barbut, S., and Marangoni, A. G. (2011). Molecular interactions of polymer oleogelation. *Soft Matter* 7, 2734–2743. doi: 10.1039/c0sm00885k

Lee, J., Lee, Y., and Choe, E. (2007). Temperature dependence of the autoxidation and antioxidants of soybean, sunflower, and olive oil. *Eur. Food Res. Technol.* 226, 239–246. doi: 10.1007/s00217-006-0532-5

Li, X., Al-Assaf, S., Fang, Y., and Phillips, G. O. (2013). Competitive adsorption between sugar beet pectin (SBP) and hydroxypropyl methylcellulose (HPMC) at the oil/water interface. *Carbohydr. Polym.* 91, 573–580. doi: 10.1016/j.carbpol.2012.08.075

Lim, J., Jeong, S., Oh, I. K., and Lee, S. (2017). Evaluation of soybean oil-carnauba wax oleogels as an alternative to high saturated fat frying media for instant fried noodles. *LWT Food Sci. Technol.* 84, 788–794. doi: 10.1016/j.lwt.2017.06.054

Luo, S. Z., Hu, X. F., Jia, Y. J., Pan, L. H., Zheng, Z., Zhao, Y. Y., et al. (2019). Camellia oil-based oleogels structuring with tea polyphenol-palmitate particles and citrus pectin by emulsion-templated method: preparation, characterization, and potential application. *Food Hydrocoll.* 95, 76–87. doi: 10.1016/j.foodhyd.2019.04.016

Martins, A. J., Cerqueira, M. A., Cunha, R. L., and Vicente, A. A. (2017). Fortified beeswax oleogels: effect of β-carotene on the gel structure and oxidative stability. *Food Funct.* 8, 4241–4250. doi: 10.1039/C7FO00953D

Maskan, M., and Bagci, H. I. (2003). The recovery of used sunflower seed oil utilized in repeated deep-fat frying process. *Eur. Food Res. Technol.* 218, 26–31. doi: 10.1007/s00217-003-0794-0

Meng, Z., Qi, K., Guo, Y., Wang, Y., and Liu, Y. (2018a). Physical properties, microstructure, intermolecular forces, and oxidation stability of soybean oil oleogels structured by different cellulose ethers. *Eur. Food Res. Technol.* 120:1700287. doi: 10.1002/ejlt.201700287

Meng, Z., Qi, K., Guo, Y., Wang, Y., and Liu, Y. (2018b). Effects of thickening agents on the formation and properties of edible oleogels based on hydroxypropyl methyl cellulose. *Food Chem.* 246, 137–149. doi: 10.1016/j.foodchem.2017.10.154

Meng, Z., Qi, K., Guo, Y., Wang, Y., and Liu, Y. (2018c). Macro-microstructure characterization and molecular properties of emulsion-templated polysaccharide oleogels. *Food Hydrocoll.* 77, 17–29. doi: 10.1016/j.foodhyd.2017.09.006

Moghtadaei, M., Soltanizadeh, N., and Goli, S. A. H. (2018). Production of sesame oil oleogels based on beeswax and application as partial substitutes of animal fat in beef burger. *Food Res. Int*. 108, 368–377. doi: 10.1016/j.foodres.2018.03.051

Morenga, L. T., and Montez, J. M. (2017). Health effects of saturated and *trans*-fatty acid intake in children and adolescents: systematic review and meta-analysis. *PLoS ONE* 12:e0186672. doi: 10.1371/journal.pone.0186672

Mozaffarian, D., and Clarke, R. (2009). Quantitative effects on cardiovascular risk factors and coronary heart disease risk of replacing partially hydrogenated vegetable oils with other fats and oils. *Eur. J. Clin. Nutr.* 63, S22–S33. doi: 10.1038/sj.ejcn.1602976

Oh, I., Lee, J. H., Lee, H. G., and Lee, S. (2019). Feasibility of hydroxypropyl methylcellulose oleogel as an animal fat replacer for meat patties. *Food Res. Int.* 122, 566–572. doi: 10.1016/j.foodres.2019.01.012

Oh, I. K., and Lee, S. (2018). Utilization of foam structured hydroxypropyl methylcellulose for oleogels and their application as a solid fat replacer in muffins. *Food Hydrocoll.* 77, 796–802. doi: 10.1016/j.foodhyd.2017.11.022

O'Keefe, S. F., and Pike, O. A. (2010). "Fat characterization," in *Food Analysis*, ed S. S. Nielsen (New York, NY: Springer), 239–260. doi: 10.1007/978-1-4419-1478-1_14

Okuro, P. K., Tavernier, I., Bin Sintang, M. D., Skirtach, A. G., Vicente, A. A., Dewettinck, K., et al. (2018). Synergistic interactions between lecithin and fruit wax in oleogel formation. *Food Funct.* 9, 1755–1767. doi: 10.1039/C7FO01775H

Patel, A. R., Cludts, N., Bin Sintang, M. D., Lesaffer, A., and Dewettinck, K. (2014b). Edible oleogels based on water soluble food polymers: preparation, characterization, and potential application. *Food Funct.* 5, 2833–2841. doi: 10.1039/C4FO00624K

Patel, A. R., Cludts, N., Bin Sintang, M. D., Lewille, B., Lesaffer, A., and Dewettinck, K. (2014a). Polysaccharide-based oleogels prepared with an emulsion-templated approach. *ChemPhysChem* 15, 3435–3439. doi: 10.1002/cphc.201402473

Patel, A. R., Rajarethinem, P. S., Cludts, N., Lewille, B., De Vos, W. H., Lesaffer, A., et al. (2015). Biopolymer-based structuring of liquid oil into soft solids and oleogels using water-continuous emulsions as templates. *Langmuir* 31, 2065–2073. doi: 10.1021/la502829u

Patel, A. R., Schatteman, D., Lesaffer, A., and Dewettinck, K. (2013). A foam-templated approach for fabricating organogels using a water-soluble polymer. *RSC Adv.* 3, 22900–22903. doi: 10.1039/C3RA44763D

Pehlivanoglu, H., Demirci, M., Toker, O. S., Konar, N., Karasu, S., and Sagdic, O. (2018). Oleogels, a promising structured oil for decreasing saturated fatty acid concentrations: production and food-based applications. *Crit. Rev. Food Sci. Nutr.* 58, 1330–1341. doi: 10.1080/10408398.2016.1256866

Rogers, M. A., Wrigh, A. J., and Marangoni, A. G. (2008). Engineering the oil binding capacity and crystallinity of self-assembled fibrillar networks of 12-hydroxystearic acid in edible oils. *Soft Matter* 4, 1483–1490. doi: 10.1039/b803299h

Rogers, M. A., Wright, A. J., and Marangoni, A. G. (2009). Oil organogels: the fat of the future? *Soft Matter* 5, 1594–1596. doi: 10.1039/b822008p

Romoscanu, A. I., and Mezzenga, R. (2006). Emulsion-templated fully reversible protein-in-oil gels. *Langmuir* 22, 7812–7818. doi: 10.1021/la060878p

Scholten, E. (2019). Edible oleogels: how suitable are proteins as a structurant? *Curr. Opin. Food Sci.* 27, 36–42. doi: 10.1016/j.cofs.2019.05.001

Singh, A., Auzanneau, F. I., and Rogers, M. A. (2017). Advances in edible oleogel technologies - a decade in review. *Food Res. Int.* 97, 307–317. doi: 10.1016/j.foodres.2017.04.022

Tanti, R., Barbut, S., and Marangoni, A. G. (2016a). Hydroxypropyl methylcellulose and methylcellulose structured oil as a replacement for shortening in sandwich cookie creams. *Food Hydrocoll.* 61, 329–337. doi: 10.1016/j.foodhyd.2016.05.032

Tanti, R., Barbut, S., and Marangoni, A. G. (2016b). Oil stabilization of natural peanut butter using food grade polymers. *Food Hydrocoll.* 61, 399–408. doi: 10.1016/j.foodhyd.2016.05.034

Tavakoli, A., Sahari, M. A., and Barzegar, M. (2017). Antioxidant activity of Berberis integerrima seed oil as a natural antioxidant on the oxidative stability of soybean oil. *Int. J. Food Prop.* 20, S2914–S2925. doi: 10.1080/10942912.2017.1382509

Tavernier, I., Doan, C. D., Van der Meeren, P., Heyman, B., and Dewettinck, K. (2018). The potential of waxes to alter the microstructural properties of emulsion-templated oleogels. *Eur. J. Lipid Sci. Technol.* 120:1700393. doi: 10.1002/ejlt.201700393

United States Department of Agriculture (USDA) (2020). *Consumption of Vegetable Oils Worldwide from 20135/2014 to 2019/2020, by Oil Type (in Million Metric Tons)*. Available online at: https://www.statista.com/statistics/263937/vegetable-oils-global-consumption/ (accessed March 28, 2020).

Vintiloiu, A., and Leroux, J. C. (2008). Organogels and their use in drug delivery - a review. *J. Control. Release* 125, 179–192. doi: 10.1016/j.jconrel.2007.09.014

Wollenweber, C., Makievski, A. V., Miller, R., and Daniels, R. (2000). Adsorption of hydroxypropyl methylcellulose at the liquid/liquid interface and the effect on emulsion stability. *Colloids Surf. A: Physicochem. Eng. Asp.* 172, 91–101. doi: 10.1016/S0927-7757(00)00569-0

Yang, S., Li, G., Saleh, A. S. M., Yang, H., Wang, N., Wang, P., et al. (2017). Functional characteristics of oleogel prepared from sunflower oil with β-sitosterol and stearic acid. *J. Am. Oil Chem. Soc.* 94, 1153–1164. doi: 10.1007/s11746-017-3026-7

Zetzl, A. K., Marangoni, A. G., and Barbut, S. (2012). Mechanical properties of ethylcellulose oleogels and their potential for saturated fat reduction in frankfurters. *Food Funct*. 3, 327–337. doi: 10.1039/c2fo10202a

Conflict of Interest: The authors declare that the research was conducted in the absence of any commercial or financial relationships that could be construed as a potential conflict of interest.

frontiers in Sustainable Food Systems

MINI REVIEW
published: 06 August 2020
doi: 10.3389/fsufs.2020.00110

Recent Advances in Understanding and Use of Oleofoams

Anne-Laure Fameau[1]* *and Arnaud Saint-Jalmes*[2]

[1] L'Oréal R&I, Saint-Ouen, France, [2] Univ Rennes, CNRS, IPR (Institut de Physique de Rennes) - UMR 6251, Rennes, France

This review aims at presenting recent advancements on the understanding of oleofoams for food applications. Edible oleofoams are currently based on heating a vegetable oil solution containing a high-melting point component, which crystallize upon cooling. After aeration (mostly by whipping), crystals adsorb to air bubble surfaces. The remaining crystals in excess in the continuous phase form an oleogel. Due to both the presence of crystals at the interface and in the bulk, the resulting oleofoams exhibits high stability to drainage, coalescence, and disproportionation. The mechanisms leading to the high foam stability are still under investigations to understand and to discriminate between bulk and interfacial rheology effects. The research on edible oleofoams are still scarce in comparison to aqueous food foams even if they present promising applications. In the area of molecular gastronomy, oleofoams are already produced. Oleofoams are a great opportunity for food technologists to develop healthier food products with a low fat content associated to new sensorial properties. However, it is important to better understand these systems in order to help food technologists to use oleofoams and it will contribute to expand this new promising area in food science.

Keywords: oleofoams, oleogel, organogel, whipped oil, crystalline particles, pickering stabilization, interfacial rheology, contact angle

OPEN ACCESS

Edited by:
Luiz Henrique Fasolin, Campinas State University, Brazil

Reviewed by:
Bernard Paul Binks, University of Hull, United Kingdom
Björn Braunschweig, University of Münster, Germany

***Correspondence:**
Anne-Laure Fameau
anne-laure.fameau@rd.loreal.com

Specialty section:
This article was submitted to Sustainable Food Processing, a section of the journal Frontiers in Sustainable Food Systems

Received: *03 May 2020*
Accepted: *17 June 2020*
Published: *06 August 2020*

Citation:
Fameau A-L and Saint-Jalmes A (2020) Recent Advances in Understanding and Use of Oleofoams. Front. Sustain. Food Syst. 4:110. doi: 10.3389/fsufs.2020.00110

INTRODUCTION

Liquid foams are complex colloidal systems based on gas bubbles dispersed in a liquid continuous phase containing surface-active components giving rise to the foam formation and stabilization (Cantat et al., 2013). Liquid foams are widely applied in many industries, especially in the food industry. Two different categories of liquid foams exist: aqueous or non-aqueous (Friberg, 2010). Non-aqueous foams based on edible oils represent a new promising emerging field for edible applications, and are commonly called oleofoams (Heymans et al., 2017; Dickinson, 2020). These systems are more difficult to obtain in comparison to aqueous foams due to the lower surface-activity of most edible emulsifiers at the oil-air interface in comparison to air-water interface (Fameau and Saint-Jalmes, 2017). Nevertheless, the fundamental research in this area is tremendously growing since 2015, and the industrial potential of oleofoams is high as novel structuring materials to substitute solid fats (Heymans et al., 2017).

Indeed, in the last few decades, both governmental institutions and consumers asked the food industry to improve the nutritional quality of food products. The food industry need to replace saturated fat by unsaturated fat or by lowering fat content in order to improve nutritional aspects of food products (Patel and Dewettinck, 2016). However, it is impossible to simply replace solid fats by edible oils since it leads to a loss of texture, structure, and mouthfeel, which are provided by the presence of solid fats. Oleofoams could be used by food technologists to create food products with

reduced fat content in combination with new textures and sensorial properties (Gunes et al., 2017; Chisholm et al., 2018; Gehin-Delval et al., 2019a).

In the area of molecular gastronomy, the production of edible oil foams started even well before the increased interest of researchers for these systems the incorporation of air bubbles in the vegetable oils provides a different mouthfeel and appearance to oil products, which are important attributes for molecular gastronomy. The advantages of oleofoams for food technologists are not only based on the texture and reduced fat content, but also on the fact that oleofoams exhibit very long term stability even above room temperature, and they can be obtained with few or even without any additives (Binks and Marinopoulos, 2017). The enhancement of food shelf-life is mandatory to reduce food waste and to keep food products quality during storage. Oleofoams are based on oil without water, which drastically reduced microbial spoilage and therefore less or no preservatives are needed (Heymans et al., 2017). All these advantages are also very important regarding the increasing trend in developing "clean label" in food industry (Heymans et al., 2017).

This mini-review describe the recent studies and patents on edible oleofoams and summarizes the current state of knowledge concerning the stabilization mechanisms.

OLEOFOAMS: FORMATION, STRUCTURE, AND APPLICATIONS

Oleofoams are made of gas bubbles in a continuous oil phase (**Figure 1**). The first discovery of oil foams was done in the 1970s (Sanders, 1970). These systems regained interest more than 30 years later with the studies by Shrestha et al. (2006, 2008, 2010). However, it is only in the last 5 years that this field began to grow tremendously for edible applications (Heymans et al., 2017). Edible oil foams are obtained in two steps. In the first step, an edible vegetable oil containing a high-melting edible component are heated above the solubility boundary of the mixture (**Figure 1**) (Fameau, 2018). By cooling the mixture below the solubility boundary, the high-melting edible component crystallizes. In the second step, the mixture is whipped to introduce air bubbles leading to oleofoams. The whipping can take place during or after the cooling process (Fameau and Saint-Jalmes, 2017). Whatever the foaming process, foam formation is only possible when crystals are present in solution that is to say below the solubility boundary (Fameau and Saint-Jalmes, 2017). Crystalline particles from various systems have been used to obtain oil foams. The first systems described in the literature for food applications were based on mono and/or diglycerides (Shrestha et al., 2006, 2008, 2010). Then, it is only 10 years later that three new fatty components have also been shown to give oil foams: fatty alcohols (Fameau et al., 2015), fatty acids (Binks et al., 2016), and triglycerides (Mishima et al., 2016). Last year, the mixture of phytosterols and monoglycerides have been demonstrated also to form oleofoams (Truong et al., 2019). Another approach to produce oleofoams is to use oil/fat containing a high proportion of saturated medium-length fatty acid chains in order to have additive-free edible oleofoams as described in 2017 after the first study on oleofoams based on triglycerides (Binks and Marinopoulos, 2017). By controlling the temperature, the triglycerides with high melting point crystallize and other triglycerides with low melting point remain in a liquid state. Coconut oil, shea butter and cocoa butter are naturally composed of crystalline particles dispersed inside a continuous oil liquid phase giving rise to oil foams (Binks and Marinopoulos, 2017).

The gas bubbles are generally covered by a dense layer of adsorbed crystals that considerably reduces disproportionation and coalescence (Binks et al., 2016). The role of the crystals on the stabilization is described sections Crystal Properties for the Design of Oleofoams and Stabilization Mechanisms. The fraction of non-adsorbed crystals, which increases with crystals concentration, serve to strengthen the gel network in the continuous oil phase (Co and Marangoni, 2012; Mishra et al., 2020). When the excess of crystalline particles in the continuous oil phase is high enough (i.e., above the gel point depending on the temperature), the particles form a network because of short-range (van der Waals) attractive forces between crystals. An oleogel is created which impends buoyancy-driven creaming of air bubbles within the foam. Therefore, oleofoams exhibit high stability against drainage, coalescence and disproportionation. Some oleofoam systems are stable during months (Fameau et al., 2015; Binks et al., 2016). The presence of crystalline particles is the key parameter to produce oleofoams (see sections Crystal Properties for the Design of Oleofoams and Stabilization Mechanisms). Each foam bubble is covered by adsorbed crystalline particles, which prevent the relaxation of the bubble to a spherical shape. In oleofoams, most of the bubbles are non-spherical and possess textured surfaces (Binks et al., 2016).

The resulting rheological properties of oleofoams is still debated, but appears to be both due to contribution of the crystals coating the bubbles and to the rheology of the gelled continuous phase in which the bubbles are dispersed (Gunes et al., 2017; Mishra et al., 2020; Saha et al., 2020) (see section Stabilization Mechanisms). Gunes et al. determined that the elastic modulus of oleofoams are two orders of magnitude higher than the modulus of a broken (=highly sheared) oleogel at the same concentration of monoglycerides in the oil, but still lower that the initial unbroken network at rest (Gunes et al., 2017). The whipping/mixing process, by modifying the bulk network probably plays a crucial role, by both setting the morphology of the crystals and the actual rheological properties of the oleofoam continuous phase (Gunes et al., 2017). At low frequencies, some oleofoams tends to behave as viscous liquids (Fameau et al., 2015). Therefore, the oleofoams have a good flowability without collapsing due to their rheological properties (Gunes et al., 2017; Heymans et al., 2018). This is a key parameter for the food industry that need easy-to-handle product that could be pumped through pipes and easy mixed with other components (Heymans et al., 2018). However, the flowable character strongly depends on the amount of incorporated gas, and of the size of the gas pockets. It is important to keep in mind that to produce oleofoams from oleogels, they need to behave as viscous dispersions once the whipping or mixing process starts in order to allow air

FIGURE 1 | By whipping an oleogel containing crystals inside a liquid oil, oleofoams are obtained. Crystals stabilize the oleofoam due to their presence in bulk and at the interface as observed by optical microscopy.

incorporation, implying specific rheological properties (such as yielding) of these oleogels (Mishra et al., 2020). The gas incorporation process is crucial: it sets the size of the bubbles, the amount of gas, the rheology of the continuous phase and the morphology of the crystals. All these intermediate-scales parameters then control the macroscopic stability and rheology of the produced oleofoam.

In the last 2 years, oleofoams were described in several patents to partially replace fat in food products (Chisholm et al., 2018; Gunes et al., 2018). For example, sponge cakes, biscuits and laminated pastry can be obtained from olefoams by replacing part of the butter (Chisholm et al., 2018; Gehin-Delval et al., 2019a). The oleofoams were based on 10 wt.% of cacao butter improver (CBI) in high oleic sunflower oil (Chisholm et al., 2018). At 60°C, CBI is soluble in the high oleic sunflower oil. All the food products obtained with oleofoams were very similar to the references based on butter by technical testing. However, the food products with oleofoams contained less fat by volume (Chisholm et al., 2018).

CRYSTAL PROPERTIES FOR THE DESIGN OF OLEOFOAMS

The key criterion for crystals to adsorb at the air/oil interface is to exhibit a suitable contact angle below 90° (Binks et al., 2016; Fameau and Saint-Jalmes, 2017). To understand the arrangement of triacylglycerols crystals around the air bubbles of an oleofoam based on salad oil, Mishima and coworkers used synchrotron radiation microbeam X-ray diffraction (Mishima et al., 2016). They demonstrated that the lamellar planes of the crystals near the air-oil surface are arranged almost parallel to the surface (Mishima et al., 2016). It means that the lamellar planes composed of methyl end groups are facing the air phase, whereas the lateral planes composed of glycerol groups are connected to each other through the crystals adsorbed at the air-oil surface (Mishima et al., 2016). We can suppose that the same type of arrangement occurs for the other crystalline particles based on fatty acids and fatty alcohols.

For aqueous foams stabilized by particles called Pickering foams, both the foamability and foam stability depend on the size, shape and concentration of solid particles (Lam et al., 2014). These parameters are also important for oleofoams as highlighted by the first studies (Shrestha et al., 2010; Fameau et al., 2015; Binks et al., 2016; Gunes et al., 2017). Needle-like and platelet-like shapes lead to adsorption, whereas spherulitic shapes do not allow contact line pinning and hence do not favor adsorption (Gunes et al., 2017; Mishra et al., 2020). To change the size and shape of the crystalline particles, Mishima et al. changed the crystallization and tempering process for a system based on long-chain triglycerides dispersed in salad oil (Mishima et al., 2016). The quantity of foam then varied as a function of the process and resulting polymorphs showing the influence of crystals size and morphology. In this study, the best foaming agent was tiny β-fat crystals (Mishima et al., 2016). Another study from Heymans et al. confirmed the effect of tempering on the foaming properties (Heymans et al., 2018), whereas other authors did not observe a link between foam quantity and crystalline polymorphs (Gunes et al., 2017). Such attempts to correlate crystals size, morphology, and polymorphs with the oleofam properties need to be done with precautions; for instance, tempering also affect the solid fat content and the bulk rheological properties, which have a strong impact on the oleofams (Mishra et al., 2020).

It is also suggested that the size and shape of the particles could be the main parameter governing the bubbles size and not the bulk rheology (Gunes et al., 2017). Gunes et al. showed that to decrease the bubbles size in oleofoams, the size of the crystals need to be decreased. Whipping induced the breakage of the crystals. On the opposite, Mishra et al. showed that the size of the bubbles actually depends on the rheology of the continuous phase: they evidence correlations between the imposed shear rate, the morphology and sizes of the crystals, the yield stress of the solution and the final bubbles size. In particular, the highest bulk yield stresses gave the smallest bubbles. Such apparently different results tend to show that there are still missing parameters, most likely linked to the gas incorporation process that need to be taken into account to identify the real correlations. Indeed, no data exist on the size of the crystals inside the oil foams in comparison to the size of the crystals initially contained in the oleogel. Scattering techniques such as Ultra Small Angle Scattering X-rays (USAXS) and neutrons (USANS) could be helpful to determine the crystals size inside the oleofoams as a function of the whipping process (Peyronel et al., 2014; Mikhailovskaya et al., 2017; Marangoni et al., 2020). Moreover, the structure at the interface, the thickness of the interfacial layer, and the resulting interfacial rheological properties are still unknown. The use of neutron and X-ray reflectivity combined with interfacial rheology could help to obtain new insights on

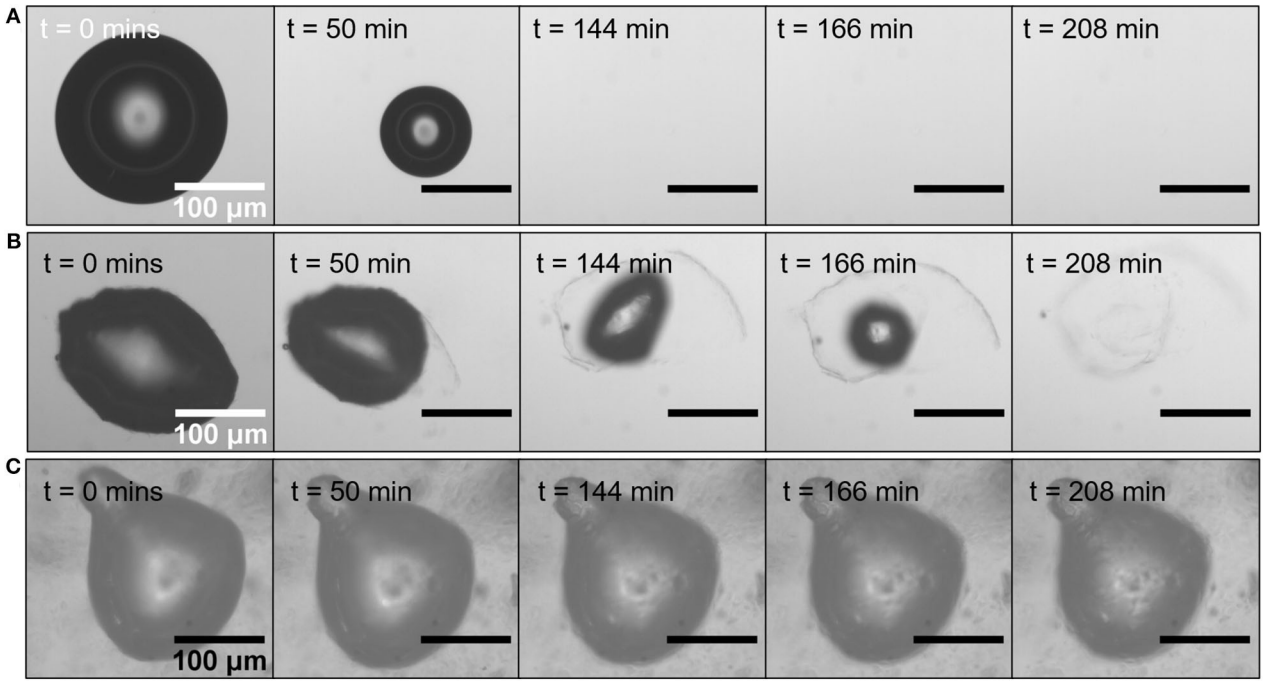

FIGURE 2 | Image sequences of evolution of air bubbles at 25°C. **(A)** A bare bubble quickly dissolve in sunflower oil. **(B)** Bubble coated by synthetic waxes in sunflower oil. The solid interfacial layer unfold leading to bubble dissolution. **(C)** Bubble inside an oleofoam remains stable over the same timescale. Reproduced from reference (Saha et al., 2020) with permission from Springer.

the interfacial properties depending on the nature of the fatty components (Fameau and Salonen, 2014).

STABILIZATION MECHANISMS

In oleofoams, the long-term stability result from both bulk and interfacial contributions (Gunes et al., 2017; Saha et al., 2020). Various destabilizing phenomena tends to destroy such gas dispersions. It is therefore important to associate the interfacial and bulk properties only to the destabilization mechanism that they actually hinder. The presence of the crystals layer at the bubble surface has a first stabilizing effect by reducing the surface tension, but they act mostly through the occurrence of a packed elastic layer (Shrestha et al., 2006; Saha et al., 2020). The main goal of such a layer is to prevent coalescence and disproportionation (or ripening). By diluting oleofoams with oil, only single bubbles can be observed (Gunes et al., 2017; Saha et al., 2020). The crystals remained attached to the bubbles and the non-spherical shape remained during few minutes to hours depending on the oleofoam systems and process (**Figure 2B**) (Gunes et al., 2017; Saha et al., 2020). That is to say many orders of magnitude longer that the relaxation timescales of the bare bubble in oil (**Figure 2A**). However, when crystals coating bubbles are diluted in a high quantity of oil, it was also observed that the gas bubbles dissolve, whereas no dissolution was observed for bubbles in the oleofoam (**Figures 2B,C**) (Gunes et al., 2017). These first results were confirmed this year by Saha et al., who demonstrated that the crystals were able to leave slowly the interface under a bubble dissolution driving force leading to the disappearance of the bubbles as illustrated in **Figure 2** (Saha et al., 2020). The behavior of a bubble embedded in an oleofoam that is to say surrounded by crystals in the bulk is not the same than a bubble surrounded only by liquid oil. Bubbles in an oleofoam owe their stability to both bulk and interfacial rheology, whereas bubbles coated by crystals but surrounded by liquid oil are only stabilized due to the interfacial dilatational rheology of the crystal layer. This is not sufficient to avoid bubbles dissolution. Crystals both at the interface and in the bulk are needed to confer long-term stability and avoid Oswald ripening and bubbles dissolution. Thus, the usual Pickering mechanism of stabilization, found for aqueous foams, is here insufficient to arrest bubble dissolution (Saha et al., 2020). Additional effects coming from the crystals in the continuous phase and the closely packed crystals in foam films can also arise to reduce Oswald ripening (Gunes et al., 2017).

Since the first studies in 2015, it was highlighted that the bulk rheological properties are also very important for foam stabilization; here mostly for acting against the gravitational drainage and the coalescence. However, this year it was demonstrated that for yield stresses higher than gravitational ones, no phase separation occurs, as well as no flow within films separating bubbles (Mishra et al., 2020). Oppositely, for very weak gel, a high rate of coalescence with the free surface during whipping is observed, which prevents to wrap bubbles with crystals (Gunes et al., 2017). Without a sufficient contribution of the bulk, the foam stabilization against destabilization mechanism is impossible (Mishra et al., 2020). The interfacial

contribution on the foam stability is a key parameter, but to obtain stable oleofoams over long timescales, films and bulk contributions are also required. The main problems to date to draw clear conclusions on the stabilization mechanisms come from the fact that in each study the fatty component to stabilize the oil foams was different (waxes, fatty alcohol, fatty acids, mono-glyceride, di-glyceride, and tri-glycerides), as well as their purity, and also the process to produce the foam varied. More fundamental studies on the same systems are needed by combining techniques at different length scales as it was done in the past for aqueous foams (Fameau and Salonen, 2014). The readers need also to keep in mind that the crystallization mechanisms in bulk and at the interface depends on the nature of the fatty components, which are linked to their chemical structure, the nature of the edible liquid phase and the process applied to the systems (cooling rate, shearing rate, etc.).

NEW EDIBLE OIL SYSTEM BASED ON OLEOFOAMS

A novel application of oleofoams is the creation of air-in-oil-in-water (A/O/W) systems, in order to design new food products (Brun et al., 2015; Gehin-Delval et al., 2019b; Goibier et al., 2019). In a first step, an oleofoam is produced. In a second step, the oleofoams is emulsified in a continuous phase containing a food grade emulsifier to stabilize the oil droplets and a food grade thickener to protect against creaming of the droplets. Two examples of A/O/W are described in the literature and highlighted the parameters to take into account to produce A/O/W systems (Brun et al., 2015; Goibier et al., 2019). The solid fat content of the oleogel used to produce the initial oleofoams is one of the crucial parameter. The crystals quantity needs to be high enough to stabilize efficiently the air bubbles, but not too high, otherwise it is impossible to maintain a fluid-like oil phase fluid during the emulsification step. The imposed shear rate is also an important parameter to produce A/O/W. Too low shear rates could not cause droplets break-up inside the aqueous phase, but too high shear rates induced release of the air bubbles. These A/O/W system based on oleofoams are already described in a recent patent, in which a standard mayonnaise recipe was prepared by replacing the oil phase of the mayonnaise by the oleofoam (10 wt.% of CBI inside high oleic sunflower oil) (Gehin-Delval et al., 2019b). The resulting mayonnaise based on oleofams was less greasy and had a lower density than the standard mayonnaise based only on high oleic sunflower oil. As consumers, generally add mayonnaise to their meal by volume and not by weight, the mayonnaise based on oleofam enable to reduce the fat consumed and to deduce the consumption of saturated fat.

CONCLUDING REMARKS

Oleofoams are very promising for the food industry since the benefits include long-term stability above room temperature, healthier food products with a low fat content, and new sensorial properties. In the recent years, the main building blocks explaining the oleofoams stability have been identified, allowing us to draw of first picture based on contributions from interfaces and bulk. The crystals govern the entire foam stability. However, a deeper understanding on the stabilization mechanisms is still required to help food industry to design new food products based on oleofoams. In the future, it will be important to continue the recent works to establish the detailed link between the rheological properties of the oleogel and the ones of the resulting oleofoams, and the crystal concentration, their size and shape, through the foaming process (Mishra et al., 2020). It is important also to separate bulk and interfacial effects. A better understanding of oleofoams could be obtained by using techniques and modifying some technical approaches developed to study Pickering aqueous foams and emulsions, but also oleogels and lipid crystallization such as: interfacial rheology, NMR, microscopy techniques, neutron, and X-ray scattering techniques (Fameau and Salonen, 2014; Mikhailovskaya et al., 2017; Marangoni and Garti, 2018; Low et al., 2020; Metilli et al., 2020). New fundamental insights will offer the possibility to design new food products, but also oil foams for cosmetic and pharmaceutical applications.

AUTHOR CONTRIBUTIONS

A-LF was the main author of the manuscript. AS-J contributed in the manuscript writing and assisting the main author. All authors contributed to the article and approved the submitted version.

REFERENCES

Binks, B. P., Garvey, E. J., and Vieira, J. (2016). Whipped oil stabilised by surfactant crystals. *Chem. Sci.* 7, 2621–2632. doi: 10.1039/C6SC00046K

Binks, B. P., and Marinopoulos, I. (2017). Ultra-stable self-foaming oils. *Food Res. Int.* 95, 28–37. doi: 10.1016/j.foodres.2017.02.020

Brun, M., Delample, M., Harte, E., Lecomte, S., and Leal-Calderon, F. (2015). Stabilization of air bubbles in oil by surfactant crystals: a route to produce air-in-oil foams and air-in-oil-in-water emulsions. *Food Res. Int.* 67, 366–375. doi: 10.1016/j.foodres.2014.11.044

Cantat, I., Cohen-Addad, S., Elias, F., Graner, F., Höhler, R., Pitois, O., et al. (2013). *Foams: Structure and Dynamics*. Oxford: OUP. doi: 10.1093/acprof:oso/9780199662890.001.0001

Chisholm, H., Gunes, Z. D., Gehin-Delval, C., Nouzille, C. A., Garvey, E., Destribats, M. J., et al. (2018). *Aerated Confectionery Material.* Patent No. US 2018 / 0064127 A1, Vervey.

Co, E. D., and Marangoni, A. G. (2012). Organogels: an alternative edible oil-structuring method. *J. Am. Oil Chem. Soc.* 89, 749–780. doi: 10.1007/s11746-012-2049-3

Dickinson, E. (2020). Advances in food emulsions and foams: reflections on research in the neo-Pickering era. *Curr. Opin. Food Sci.* 33, 52–60. doi: 10.1016/j.cofs.2019.12.009

Fameau, A.-L. (2018). "Chapter 13: non-aqueous foams based on edible oils," in *Edible Oil Structuring: Concepts, Methods and Applications,* ed A. R. Patel (London: The Royal Society of Chemistry), 275–307. doi: 10.1039/9781788010184-00275

Fameau, A.-L., Lam, S., Arnould, A., Gaillard, C., Velev, O. D., and Saint-Jalmes, A. (2015). Smart nonaqueous foams from lipid-based oleogel. *Langmuir* 31, 13501–13510. doi: 10.1021/acs.langmuir.5b03660

Fameau, A.-L., and Saint-Jalmes, A. (2017). Non-aqueous foams: Current understanding on the formation and stability mechanisms. *Adv. Colloid Interface Sci.* 247, 454–464. doi: 10.1016/j.cis.2017.02.007

Fameau, A.-L., and Salonen, A. (2014). Effect of particles and aggregated structures on the foam stability and aging. *Comptes Rendus Phys.* 15, 748–760. doi: 10.1016/j.crhy.2014.09.009

Friberg, S. E. (2010). Foams from non-aqueous systems. *Curr. Opin. Colloid Interface Sci.* 15, 359–364. doi: 10.1016/j.cocis.2010.05.011

Gehin-Delval, C., Chisholm, H., Chung, W., Deyber, H., Destribats, M. J., Gunes, Z. D., et al. (2019a). *Method for Forming a Laminated Pastry*. Patent No. US 2019/0200625 A1, Vervey.

Gehin-Delval, C., Chisholm, H., Gunes, Z. D., Deyber, H., Pelloux, C., Schafer, O., et al. (2019b). *Food Composition Comprising Gas Bubbles*. Patent No. US 10, 383, 352 B2, Vervey.

Goibier, L., Pillement, C., Monteil, J., Faure, C., and Leal-Calderon, F. (2019). Emulsification of non-aqueous foams stabilized by fat crystals: Towards novel air-in-oil-in-water food colloids. *Food Chem.* 293, 49–56. doi: 10.1016/j.foodchem.2019.04.080

Gunes, D. Z., Murith, M., Godefroid, J., Pelloux, C., Deyber, H., Schafer, O., et al. (2017). Oleofoams: properties of crystal-coated bubbles from whipped oleogels-evidence for pickering stabilization. *Langmuir* 33, 1563–1575. doi: 10.1021/acs.langmuir.6b04141

Gunes, Z. D., Schafer, O., Chisholm, H., Deyber, H., Pelloux, C., and Binks, B. P. (2018). *Lipid Based Foam*. Patent No.WO 2016/150978, Vervey.

Heymans, R., Tavernier, I., Danthine, S., Rimaux, T., Van der Meeren, P., and Dewettinck, K. (2018). Food-grade monoglyceride oil foams: the effect of tempering on foamability, foam stability and rheological properties. *Food Funct.* 9, 3143–3154. doi: 10.1039/C8FO00536B

Heymans, R., Tavernier, I., Dewettinck, K., and Van der Meeren, P. (2017). Crystal stabilization of edible oil foams. *Trends food Sci. Technol.* 69, 13–24. doi: 10.1016/j.tifs.2017.08.015

Lam, S., Velikov, K. P., and Velev, O. D. (2014). Pickering stabilization of foams and emulsions with particles of biological origin. *Curr. Opin. Colloid Interface Sci.* 19, 490–500. doi: 10.1016/j.cocis.2014.07.003

Low, L. E., Siva, S. P., Ho, Y. K., Chan, E. S., and Tey, B. T. (2020). Recent advances of characterization techniques for the formation, physical properties and stability of Pickering emulsion. *Adv. Colloid Interface Sci.* 277:102117. doi: 10.1016/j.cis.2020.102117

Marangoni, A. G., and Garti, N. (eds.). (2018). *Edible Oleogels: Structure and Health Implications*. San Diego, CA: AOC Press.

Marangoni, A. G., Van Duynhoven, J. P. M., Acevedo, N. C., Nicholson, R. A., and Patel, A. R. (2020). Advances in our understanding of the structure and functionality of edible fats and fat mimetics. *Soft Matter* 16, 289–306. doi: 10.1039/C9SM01704F

Metilli, L., Francis, M., Povey, M., Lazidis, A., Marty-Terrade, S., Ray, J., et al. (2020). Latest advances in imaging techniques for characterizing soft, multiphasic food materials. *Adv. Colloid Interface Sci.* 279:102154. doi: 10.1016/j.cis.2020.102154

Mikhailovskaya, A., Zhang, L., Cousin, F., Boue, F., Yazhgur, P., Muller, F., et al. (2017). Probing foam with neutrons. *Adv. Colloid Interface Sci.* 247, 444–453. doi: 10.1016/j.cis.2017.07.024

Mishima, S., Suzuki, A., Sato, K., and Ueno, S. (2016). Formation and microstructures of whipped oils composed of vegetable oils and high-melting fat crystals. *J. Am. Oil Chem. Soc.* 93, 1453–1466. doi: 10.1007/s11746-016-2888-4

Mishra, K., Dufour, D., and Windhab, E. J. (2020). Yield stress dependent foaming of edible crystal-melt suspensions. *Cryst. Growth Des*. 20, 1292–1301. doi: 10.1021/acs.cgd.9b01558

Patel, A. R., and Dewettinck, K. (2016). Edible oil structuring: an overview and recent updates. *Food Funct.* 7, 20–29. doi: 10.1039/C5FO01006C

Peyronel, F., Pink, D. A., and Marangoni, A. G. (2014). Triglyceride nanocrystal aggregation into polycrystalline colloidal networks: Ultra-small angle X-ray scattering, models and computer simulation. *Curr. Opin. Colloid Interface Sci.* 19, 459–470. doi: 10.1016/j.cocis.2014.07.001

Saha, S., Saint-Michel, B., Leynes, V., Binks, B. P., and Garbin, V. (2020). Stability of bubbles in wax-based oleofoams: decoupling the effects of bulk oleogel rheology and interfacial rheology. *Rheol. Acta* 59, 255–266. doi: 10.1007/s00397-020-01192-x

Sanders, P. A. (1970). Stabilization of aerosol emulsions and foams. *J. Soc. Cosmet. Chem.* 21, 377–391.

Shrestha, L. K., Aramaki, K., Kato, H., Takase, Y., and Kunieda, H. (2006). Foaming properties of monoglycerol fatty acid esters in nonpolar oil systems. *Langmuir* 22, 8337–8345. doi: 10.1021/la061204h

Shrestha, L. K., Shrestha, R. G., Sharma, S. C., and Aramaki, K. (2008). Stabilization of nonaqueous foam with lamellar liquid crystal particles in diglycerol monolaurate/olive oil system. *J. Colloid Interface Sci.* 328, 172–179. doi: 10.1016/j.jcis.2008.08.051

Shrestha, R. G., Shrestha, L. K., Solans, C., Gonzalez, C., and Aramaki, K. (2010). Nonaqueous foam with outstanding stability in diglycerol monomyristate/olive oil system. *Colloids Surfaces A Physicochem. Eng. Asp.* 353, 157–165. doi: 10.1016/j.colsurfa.2009.11.007

Truong, T., Prakash, S., and Bhandari, B. (2019). Effects of crystallisation of native phytosterols and monoacylglycerols on foaming properties of whipped oleogels. *Food Chem.* 285, 86–93. doi: 10.1016/j.foodchem.2019.01.134

Conflict of Interest: The authors declare that the research was conducted in the absence of any commercial or financial relationships that could be construed as a potential conflict of interest.

frontiers in Sustainable Food Systems

ORIGINAL RESEARCH
published: 11 September 2020
doi: 10.3389/fsufs.2020.00132

Self-Assembly of Symmetrical and Asymmetrical Alkyl Esters in the Neat State and in Oleogels

*Gilda Avendaño-Vásquez, Anaid De la Peña-Gil, Maria E. Charó-Alvarado, Miriam A. Charó-Alonso and Jorge F. Toro-Vazquez**

Facultad de Ciencias Químicas-CIEP, Universidad Autónoma de San Luis Potosí, San Luis Potosí, Mexico

Saturated alkyl esters play an important role in determining the functional properties of the vegetable waxes used in the formulations of natural cosmetics and edible oleogels. We studied the relationship between the thermo-mechanical properties and crystal microstructure developed by saturated symmetrical (SE: 14:14, 16:16, 18:18, 20:20, and 22:22) and asymmetrical (AE: 18:14, 18:16, 18:20, 18:22) esters in the neat state and in oleogels. Additionally, we evaluated the effect of 1-stearoyl-glycerol (MSG; 0.5 and 1%) in the development of SE and AE oleogels. The X-ray and microscopy analysis in the neat state showed that SE self-assembled developing plate-like crystals, while AE developed acicular-like crystals. Microscopy analysis indicated that AE and SE followed similar crystallization behavior in the oleogels. The AE oleogels had higher elasticity (G') than the SE oleogels. In both types of oleogels as the ester carbon number increased the oleogels' G' decreased and crystal size increased. The addition of just 0.5% MSG, particularly in the AE oleogels, limited the decrease in G' as the ester carbon number increased, mainly because MSG decreased crystal size. The calorimetry results suggested that during cooling the MSG and the alkyl esters developed a co-crystal. Nevertheless, part of the MSG did not interact with the ester molecules and crystallized independently. These MSG crystals acted as active fillers of the microstructure formed by the co-crystals. The overall effect was that in comparison with the alkyl ester oleogels the alkyl ester oleogels with 0.5 and 1% MSG had higher G' with frequency independent rheological behavior. This rheological behavior was particularly evident with the AE oleogels. Therefore, ester composition and molecular structure (i.e., symmetry or asymmetry) greatly influence its molecular self-assembly and subsequently the oleogels' thermo-mechanical properties. Studies using molecular mechanics modeling are underway to establish the mechanism for AE and SE self-assembly with and without MSG. The overall goal is to understand and control the crystallization of vegetable waxes for the development of functional edible oleogels.

Keywords: oleogels, alkyl esters, monoglycerides, vegetable wax, cosmetics, co-crystals

OPEN ACCESS

Edited by:
Miguel Cerqueira, International Iberian Nanotechnology Laboratory (INL), Portugal

Reviewed by:
Vânia Regina Nicoletti, São Paulo State University, Brazil
Fabio Valoppi, University of Helsinki, Finland

****Correspondence:***
Jorge F. Toro-Vazquez
toro@uaslp.mx

Specialty section:
This article was submitted to Sustainable Food Processing, a section of the journal Frontiers in Sustainable Food Systems

Received: *09 April 2020*
Accepted: *24 July 2020*
Published: *11 September 2020*

Citation:
Avendaño-Vásquez G, De la Peña-Gil A, Charó-Alvarado ME, Charó-Alonso MA and Toro-Vazquez JF (2020) Self-Assembly of Symmetrical and Asymmetrical Alkyl Esters in the Neat State and in Oleogels. Front. Sustain. Food Syst. 4:132. doi: 10.3389/fsufs.2020.00132

INTRODUCTION

Several molecules of low molecular weight (<3,000 Da) at temperatures below their solubility limit in an organic solvent (i.e., vegetable oil), have the capability of self-assembly. Through this process lipophilic or amphiphilic molecules like phytosterols (Bot and Agterof, 2006; Bot et al., 2008, 2009), lecithin (Han et al., 2014; Martínez-Ávila et al., 2019), monoglycerides (Chen et al., 2009; López-Martínez et al., 2014), (R)-12-hydroxystearic acid (Rogers and Marangoni, 2008; Lam and Rogers, 2011; Abraham et al., 2012; Co and Marangoni, 2013), *n*-alkanes, long chain alkyl esters, fatty acids and fatty alcohols (Gandolfo et al., 2004; Morales-Rueda et al., 2009; Lam and Rogers, 2011; Co and Marangoni, 2013; Sagiri et al., 2015) form three-dimensional crystal structures that physically trap vegetable oils providing them with viscoelastic and thermoreversible properties (Toro-Vazquez and Pérez-Martínez, 2018).

Several studies have shown that this process (i.e., organogelation) is a useful and novel alternative to structure vegetable oils for food systems without the use of *trans* and/or saturated fats (Dassanayake et al., 2011; Marangoni and Garti, 2011; Co and Marangoni, 2012; Rogers et al., 2014). Nowadays, the food industry faces the need to develop thermodynamically stable systems with functional properties accepted by the consumers without the use of *trans* and saturated fatty acids. This is due to the well-documented negative effect of the saturated and *trans* fats on cardiovascular health. One of the most promising alternatives for the development of edible gelled systems (i.e., oleogels) is the use of natural vegetable waxes (Blake et al., 2018). Additionally, the major cosmetic companies are moving away from animal-based (e.g., tallow) and petroleum derived materials (e.g., petroleum jelly), looking now for renewable and functional vegetable-based materials. We can also develop vegetable waxes-based oleogels with useful and novel functional properties for the cosmetics' industry (Ferrari and Mondet, 2003; Morales et al., 2010; Perez-Nowak, 2012). The use of vegetable waxes is the current natural trend for the development of natural cosmetics, e.g., organic cosmetics (Cosmetic Lab, 2016; Fórmula Botánica, 2019).

Most of the vegetable waxes already in the commercial market are characterized by their high content of long chain saturated alkyl esters (i.e., >60%). In other waxes a different lipid-like compound is the major component (i.e., *n*-alkanes) and the alkyl esters is a minor but still a significant component fraction (between 6 and 16%) (Blake et al., 2018). In any case, the alkyl esters in the vegetable waxes are essentially constituted by saturated long chain fatty acids between 16 and 32 carbon atoms (Doan et al., 2017), which provide the waxes with a solid texture at room temperature. Exception to this is the liquid wax obtained from jojoba (*Simmondsia chinensis*) seeds composed by nearly 97% of esters constituted by heneicosanoic acid (21:0), behenic acid (22:0), and particularly 13, 16-docosadienoic acid (22:2), and fatty alcohols of 20, 22 and 24 carbons with one double bond (*cis*-11-eicosenol, *cis*-13-docosenol, and *cis*-15-tetracosenol) (Busson-Breysse et al., 1994; Ghamdi et al., 2017). Thus, the alkyl ester content is often used to explain the crystallization and melting behavior of the vegetable waxes in the neat state and in the development of oleogels. Within this context, rice bran and sunflower waxes are considered chemically homogeneous given their high alkyl ester content (92–100%) and low compositional heterogeneity (i.e., less than 6% of free alkyl acids and free alkyl alcohols) (Doan et al., 2017). These two vegetable waxes crystallize as one single narrow exotherm, developing large needle-like crystals with high melting entropy values. In contrast, carnauba and candelilla wax with lower concentration of their main component (i.e., carnauba wax with 62–85% of alkyl esters and candelilla wax with 45–65% of *n*-alkanes) have higher heterogeneous composition. In consequence, the carnauba and the candelilla wax crystallize showing broader exotherms with multiple peaks developing small dendritic crystals or microplatelets, respectively, with lower melting entropy. This is particularly evident with candelilla wax that shows the higher compositional heterogeneity with just 6–16% of alkyl esters (Alvarez-Mitre et al., 2012; Blake et al., 2014; Doan et al., 2017).

From the above, it is evident that the alkyl esters play an important role in the physical properties showed by vegetable waxes. Nevertheless, there is limited information about their physical properties either in the pure state or in oleogels. Within this context the main objective of this study was to investigate the relationship between the thermomechanical properties and crystal microstructure developed by saturated alkyl esters in the neat state and in oleogels. This, using pure alkyl esters constituted by saturated fatty acids and fatty alcohols with the same number of carbons [symmetrical esters; myristyl myristate (14:14), palmityl palmitate (16:16), stearyl stearate (18:18), arachidyl arachidate (20:20) and behenyl behenate (22:22)] and with different number of carbon [asymmetrical esters; stearyl myristate (18:14), stearyl palmitate (18:16), stearyl arachidate (18:20), and stearyl behenate (18:22)].

On the other hand, studies done by different research groups had shown that the crystallization behavior of vegetable waxes (i.e., crystal size and shape) and further development of the crystal network are affected by other components, naturally present in the wax or intentionally added (Toro-Vazquez et al., 2007; Dassanayake et al., 2009; Morales-Rueda et al., 2009; Chopin-Doroteo et al., 2011; Blake et al., 2014; Hwang et al., 2014; Rocha-Amador et al., 2014). Monoglycerides are a minor component commonly present in refined vegetable oils at low concentrations commonly between 0.05 and 0.2% (Gunstone, 2002). Because their amphiphilic character and capability of developing hydrogen bonds when added to vegetable oils the monoglycerides are able to develop emulsions and oleogels (Ojijo et al., 2004; Chen et al., 2009; López-Martínez et al., 2014; Marangoni and Garti, 2018). Therefore, monoglycerides play an important role in the development and stability of organogelled emulsions (Toro-Vazquez et al., 2013a). In these systems the monoglycerides might affect the self-assembly of alkyl esters present in vegetable waxes. Thus, a second objective of this study was to investigate the effect of intentionally added monoglycerides (0.5 and 1%) in the self-assembly of alkyl esters during the formation of oleogels.

MATERIALS AND METHODS

Materials

Refined, bleached and deodorized high oleic safflower oil was obtained from a local distributor (Coral International, San Luis Potosi, Mexico). The high oleic safflower oil was used as the liquid phase in the development of oleogels. As previously determined by HPLC the major triacylglyceride in the vegetable oil was OOO (65.65 ± 0.15%), followed by LOO (16.26% ± 0.04), and POO (8.58% ± 0.04), and minor concentrations of StOO (2.64 ± 0.01%), LLO (2.25 ± 0.02%), POL (1.70% + 0.11), StLL (0.87 ± 0.05%), and LLL (0.46 ± 0.01%) (O = oleic acid; L = linoleic acid; St = stearic acid; P = palmitic acid) (Alvarez-Mitre et al., 2012). Analytical grade 1-stearoyl-*rac*-glycerol (MSG) with a purity >99% was obtained from Sigma Aldrich (St. Louis, MO, USA). The linear alkyl esters with a purity > 99% were obtained from Nu-Check Prep, Inc. (Elysian, MN, USA) and were constituted by saturated fatty acids and saturated fatty alcohols with the same number of carbons (i.e., symmetrical esters, SE) or with different number of carbon (i.e., asymmetrical esters, AE). The SE were: tetradecyl tetradecanoate (myristyl myristate; 14:14), hexadecyl hexadecanoate (palmityl palmitate; 16:16), octadecyl octadecanoate (stearyl stearate; 18:18), eicosyl eicosanoate (arachidyl arachidate; 20:20), and docosanyl docosanoate (behenyl behenate; 22:22), and the AE were: octadecyl tetradecanoate (stearyl myristate; 18:14), octadecyl hexadecanoate (stearyl palmitate; 18:16), octadecyl eicosanoate (stearyl arachidate; 18:20), and octadecyl docosanoate (stearyl behenate; 18:22). The MSG and alkyl esters were stored under desiccant conditions (phosphorus pentoxide) at -20°C.

X-Ray Measurements

Neat alkyl esters were initially heated at 160°C for 20 min, after that the samples were allowed to cool at room temperature followed by 24 h storage at −5°C. After this time the samples X-ray pattern, in a silicon crystal sample holder, were recorded at 5°C with a Bruker D8 Advance diffractometer (CuKα-irradiation λ = 1.5406, high-rate detector Lynx Eye) equipped with a parallel beam geometry. Angular scans were obtained from 1° to 40° using a step size of 0.01° and a scan speed of 0.32°/s. Data processing and analyses were performed using DIFFRAC.EVA software (V 5.1, Bruker, Karlsruhe, Germany).

Crystallization and Melting Behavior of Alkyl Esters

Differential Scanning Calorimetry of Neat Alkyl Esters

The crystallization and melting profile of the neat alkyl esters (SE and AE) were determined by differential scanning calorimetry (Q2000, TA Instruments; New Castle, DL, USA). The corresponding sample (≈5–7 mg) was sealed in aluminum pans, heated at 160°C for 20 min and then cooled to 10°C/min until achieving −5°C. After 2 min at this temperature the system was heated at 5°C/min until achieving 160°C. The use of this time-temperature condition assured the full melting of all the alkyl esters studied, particularly those with the highest number of carbons (i.e., 20:20, 22:22). The crystallization and heating thermograms were determined with the equipment software by plotting the heat flux of the sample as a function of the temperature. Using the first derivative of the heat flux from the cooling thermogram we determined the temperature at the beginning of the crystallization exotherm (T_{Cr}), and the area below the corresponding exotherm (i.e., heat of crystallization; ΔH_{Cr}). From the heating thermogram we determined the temperature at the maximum of the heat flow of the endotherm (T_M), and the heat of melting (ΔH_M). For each alkyl ester we obtained two independent cooling and heating thermograms ($n = 2$).

Fitting of the Hildebrand Equation

We evaluated the ideal crystallization/melting behavior of the SE and AE through the Hildebrand equation (Hildebrand and Robert-Lane, 1950),

$$\ln(x) = \frac{\Delta H_M}{R\left(\frac{1}{T_S} - \frac{1}{T_E}\right)} \quad (1)$$

$$\frac{1}{T_S} = \frac{1}{T_E} + \frac{R[\ln(X)]}{\Delta H_M} \quad (2)$$

where ΔH_M is the enthalpy of fusion per mole of the corresponding neat alky ester, T_E and Ts are the melting temperature of the neat alky ester and in the oil solutions (i.e., $T_S = T_M$; see previous section), respectively, X is the mole fraction of the alkyl ester in the vegetable oil, and R is the universal gas constant. For this we prepared 500 mg of 0.5–5% alkyl esters solutions in safflower oil solutions in glass vials (12 mm × 35 mm). To solubilize the alkyl esters the vials were placed in an oven set to 100°C and heated during 15 min with intermittent 1 min gently mixing periods using a vortex mixer. The crystallization and heating thermograms for the alkyl esters solutions in safflower oil as described in previous section. However, in this case the sample was heated at 100°C for 20 min and then cooled to 10°C/min until achieving −5°C. After 2 min at this temperature the system was heated at 5°C/min until achieving 100°C. The corresponding thermal parameters were fitted to the Hildebrand equation determining the linear regression of $\ln(X)$ on $1/T_S$ and comparing the ΔH_M for neat alkyl esters calculated with the fitting equation with the corresponding ΔH_M value determined experimentally. For each alkyl ester concentration of the SE and AE we did at least three independent determinations ($n \geq 3$).

Effect of MSG in the Thermal Behavior of Alkyl Esters Solutions in the Vegetable Oil

To evaluate the MSG effect in the crystallization/melting behavior of the alkyl esters, we prepared 3% alkyl esters-MSG solutions containing 0, 0.5, or 1% (wt/wt) of MSG. For this we prepared the corresponding 3% alkyl ester solution as indicated in the previous section, adding the corresponding proportion of MSG once the alkyl esters solution achieved 80–85°C. Afterwards, the alkyl ester and alkyl ester-MSG solutions were stored at 5°C until their use. The crystallization and melting profile of the 3% alkyl esters-MSG solution were determined by differential scanning calorimetry. To evaluate the MSG effect in the crystallization and

melting profile of the alkyl ester-MSG system, we determined also the cooling and heating thermograms for the 0.5 and 1% MSG solutions in safflower oil. For each of the alkyl esters-MSG systems studied we obtained two independent cooling and heating thermograms ($n = 2$).

Rheological Measurements in the Oleogels

The storage (G') and loss (G'') modulus of the alkyl ester-MSG systems were measured with an Anton Paar MCR301 rheometer (Paar Physica MCR 301, Stuttgart, Germany) using a steel truncated cone plate geometry (CP25-1TG). A sample of a pre-heated (≈100°C) alkyl ester-MSG system was applied on the base of the rheometer geometry previously set at 100°C, and the cone was set using the true-gap function of the software. After 20 min at 100°C, the system was cooled at 10°C/min until achieving −5°C. After 2 min at this temperature we applied a strain sweep between 0.001 and 100% using a frequency (ω) of 1 Hz. The G' and G'' of the alkyl ester-MSG system were obtained from the linear viscoelastic region (strain between 0.002 and 0.03%). In a parallel experiment we determined the phase shift angle (δ) as a function of ω (−5°C; 100 and 0.1 Hz) using a strain within the linear viscoelastic region. The sample temperature was controlled with a Peltier temperature control located on the base of the geometry and with a Peltier-controlled hood (H-PTD 200). The control of the equipment was made through the software Start Rheoplus US200/32 version 2.65 (Anton Paar, Graz, Austria). For each alkyl ester-MSG system we did two independent rheological measurements ($n = 2$).

Polarized Light Microscopy

Polarized light microphotographs (PLM) of the oleogels were obtained using a polarizing light microscope (Olympus BX51; Olympus Optical Co., Ltd., Tokyo, Japan) equipped with a color video camera (KP-D50; Hitachi Digital, Tokyo, Japan) and a heating/cooling stage (TP94; Linkam Scientific Instruments, Ltd., Surrey, England) connected to a temperature control station (LTS 350; Linkam Scientific Instruments, Ltd.) and a liquid nitrogen tank. A drop of the alkyl ester-MSG solution was applied on a glass slide and then set in the heating/cooling stage of the microscope. We applied the same time-temperature program as described in section 2.3, but here after arriving at a temperature 10°C above the corresponding T_{Cr} the sample was smear on the slide surface using another pre-heated glass slide at a 45° angle. Then, the stage was closed and the cooling continued until achieving −5°C. PLM of the corresponding microstructure were obtained after 2 min at this temperature.

Statistical Analysis

The treatment conditions studied (i.e., type of alkyl ester, concentration of MSG) were analyzed by ANOVA and contrast between the treatment means. The corresponding thermal parameters were fitted to the Hildebrand equation by linear regression. In all cases the software used was STATISTICA V 12 (StatSoft Inc., Tulsa, OK).

RESULTS AND DISCUSSION

X-Ray Diffraction and Thermal Behavior of Neat Alkyl Esters

The corresponding lattice spacings (d, Å) and calculated extended molecular lengths (L, Å) for the neat SE and AE are summarized in **Table 1**. As stated in the Materials and Methods section, the SE and AE oleogels studied were developed and characterized at −5°C while the X-ray analysis of the neat alkyl esters was done at 5°C. Unfortunately the diffractometer could not control the temperature below 5°C. However, as determined by DSC, the melting of the neat alkyl esters occurred at temperatures well above 5°C (see further discussion associated to **Figure 3B**). Within this context, we assumed that the alkyl esters' crystal polymorph present at 5°C was the same that at −5°C. The X-ray diffractograms (WAXS and SAXS) for the neat SE and AE are shown in the **Figures 1SM−5SM** of the Supplementary Material. The d value determined in the SAXS region (**Table 1**) was associated with the length of the repetition structural unit formed by the alkyl ester molecules in the crystal. In both type of esters the d values were shorter than the thicknesses of a lamellar structure resulting from two stacked alkyl chain molecules and larger than a single molecule. Unfortunately, we could not find reports in the literature about the molecular organization of neat alkyl esters in the solid state. Within this context, we propose that the SAXS d value resulted of structural units formed by parallel interdigitated alkyl chain molecules, possible with an inclination angle. This organization would allow the stabilization of the structure along the parallel hydrocarbon chains through van der Waals forces and, allegedly through hydrogen bonds developed between the oxygen of the carbonyl group and an alpha hydrogen of the parallel alkyl ester molecule. Preliminary results obtained by our group through molecular mechanics simulations showed that, in addition to intermolecular dispersion forces, the formation of hydrogen bonds between parallel interdigitated alkyl ester molecules might occur between the parallel hydrocarbon chains. Within this framework, the length of the repetition unit determined by X-ray diffraction for the SE showed values of 44.64 Å, 52.02 Å, 62.80 Å, 71.83 Å, and 82.28 Å for the 14:14, 16:16, 18:18, 20:20, and 22:22, respectively; and for the AE of 67.28 Å, 67.28 Å, and 65.21 Å for 18:16, 18:20, and 18:22, respectively (**Table 1**). It was interesting to note that for the SE the length of the repetition unit showed a significant linear relationship with the number of carbons of the alkyl ester ($R^2 = 0.997$, $P < 0.001$). In contrast, for the AE the 18:16, 18:20, and 18:22 had a similar repetition unit length, this despite the increase in the carbon number from 34 (18:16) to 40 (18:22). This behavior was not observed by the 18:14 ester. The 18:14 was the only alkyl ester that showed two short-angle spacings at 43.49 Å and 52.34 Å, indicating that neat 18:14 crystallized in two different polymorphs. We also observed these two 18:14 polymorphs in the corresponding melting thermogram (results show later in **Figure 6SM** panel B). Thus, the polymorphism might be associated with the different behavior of the 18:14 unit length when compared with the mean unit length's observed by 18:16, 18:20, and 18:22 (66.59 Å ± 1.19 Å). On the other hand, the d values showed by

TABLE 1 | Lattice spacing (*d*) determined by X-ray diffraction (SAXS and WAXS region) and calculated extended molecular length (*L*) for the alkyl esters studied in neat powder.

	Alkyl ester	*d* (Å)		*L*[a] (Å)	Proposed packing arrangement	Predominant crystal shape
		SAXS region	WAXS region			
Symmetric	14:14	44.64	12.43, 4.54, 4.39, 4.30, 4.20, 4.09, 3.80	36.93	Monoclinic	Platelet
	16:16	52.02	14,15, 4.60, 4.29, 4.21, 4.11, 3.80	42.21	Monoclinic	Platelet
	18:18	62.80	16.01, 4.34, 4.27, 4.21, 4.12, 3.80	47.48	Monoclinic	Platelet
	20:20	71.83	17.79, 4.15, 3.73	52.76	Orthorhombic	Platelet
	22:22	82.28	19.78, 4.23, 3.78	58.03	Orthorhombic	Platelet
Asymmetric	18:14	52.34, 43.49	4.22, 3.80	42.21	Orthorhombic	Acicular
	18:16	67.28	16.97, 4.24, 3.82	44.84	Orthorhombic	Acicular
	18:20	67.28	17.04, 4.23, 3.81	50.16	Orthorhombic	Acicular
	18.22	65.21	16.67, 4.23, 3.77	52.76	Orthorhombic	Acicular

[a] *The corresponding alkyl ester molecule was obtained using Chemdraw Ultra software (V. 12.0.2.1076; Cambridge Soft Corporation, USA), and then measured using Chem3D software (V. 17.1). In order to obtain the theoretical carbon-carbon length, in all cases we preserved the extended molecular configuration of the alkyl ester.*

the alkyl esters in the WAXS region corresponded to higher order diffractions in the progression shown by a lamella packing arrangement. Thus, the diffractograms for the AE and for 20:20 and 22:22 showed the characteristic *d* values for an orthorhombic subcell with WAXS diffraction peaks at approximately 3.8 Å and 4.2 Å (**Table 1**). In contrast, 14:14, 16:16, and 18:18 did not show a diffraction pattern that supported their assignation to a particular subcell structure (**Table 1**). Nevertheless, similar to neat *n*-alkanes that crystallize in the monoclinic subcell structure, the major diffraction peak for these alkyl esters appeared at 4.2 Å. Thus, the neat 14:14, 16:16, and 18:18 were tentatively associated to a monoclinic subcell structure. We also observed that except 16:16, the relative intensity of the SE diffractograms was weaker in the SAXS region than in the WAXS region (**Figures 1SM−3SM**; Supplementary Material). This difference in the diffraction intensity was higher the longer the alkyl chains of the SE. These results showed that the molecular interactions within the lamellar planes (i.e., interplanar short spacings) of SE crystals occurred more frequently than those between the parallel interdigitated alkyl chain molecules. The parallel interdigitated chain molecules were aligned along the axis vertical to the interplanar plane (i.e., long spacings). The overall result was that, except 16:16, the neat SE crystals had a lower growth along the axis perpendicular to the lamellar plane in comparison with the interplanar growth. Consequently, we might expect that neat SE crystallized developing mainly plate-like crystals. In contrast, the AE diffractograms showed a lower diffraction signal in the WAXS region than in the SAXS region (**Figures 4SM, 5SM**; Supplementary Material). Therefore, the neat AE crystallized along the axis vertical to the interplanar plane, thus developing mainly acicular-like crystals. Unfortunately, PLM photographs of neat alkyl esters were very difficult to obtain. This, mainly because under the experimental conditions neat esters crystallized very fast overcrowding the field and making impossibly to distinguish crystals' shape and size. Within this context we decided to evaluate the crystal shape developed by the alkyl esters using concentrated vegetable oil solutions (60% wt/wt). We assumed that at this high concentration the effect of minor components or the triacylglycerides of the vegetable oil did not affect the crystallization habit of the alkyl esters of that occurring in the neat state. The PLM for the 60% solutions for some AE (i.e., 18:14 and 18:20) and SE (i.e., 16:16 and 20:20) are shown in **Figures 1**, **2**. In the 60% ester solutions the 18:14 and 18:20 developed fibrillar crystals while the 16:16 and 20:20 formed plate crystals. These results showed that the symmetry or asymmetry of the alkyl ester had an effect in the crystal shape.

The crystallization and melting thermograms for the neat AE and SE are shown in **Figure 6SM** (Supplementary Material), and the T_{Cr}, T_M, ΔH_{Cr}, and ΔH_M behavior as a function of the ester's carbon number are shown in **Figures 3**, **4**. Using low molecular weight gelators in the neat state and in vegetable oil solution, our group established that the gelator's molecular structure is associated with the onset of their molecular self-assembly (i.e., T_{Cr}) (Toro-Vazquez et al., 2013b). In the same way we established that the gelator's solubility temperature in the vegetable oil is indirectly associated with T_{Cr}, while T_M and the heats of melting (ΔH_M) and crystallization (ΔH_{Cr}) are associated with the energies of the molecular interactions that stabilize the crystal structure in the neat state and in the oleogel (Toro-Vazquez et al., 2013b). Within this context, independent of the type of alkyl ester (i.e., SE or AE), T_{Cr} and T_M of the neat alkyl esters had a direct linear relationship with the carbon number ($P < 0.005$; **Figure 3**). The linear equations reported in **Figures 3A,B** indicated that the increase of just one carbon in the alkyl chain of SE and AE resulted in a T_{Cr} and T_M increment of about 2°C. In other words, independent of the type of ester, the longer the ester hydrocarbon chain the higher the onset temperature for its molecular self-assembly (i.e., higher T_{Cr}). In the same way, the longer the alkyl ester the higher the temperature to achieve the complete breakup of the non-covalent interactions stabilizing the alkyl ester crystals (i.e., higher T_M). Similar results for T_M have been reported for neat *n*-alkanes with even and odd carbon number between 7 and 32 (Boese et al., 1999; McGann and Lacks, 1999). These results showed that T_{Cr} and T_M of the alkyl esters in the neat state depend essentially on the carbon number. Consequently, the longer the alkyl esters chain the higher the onset temperature

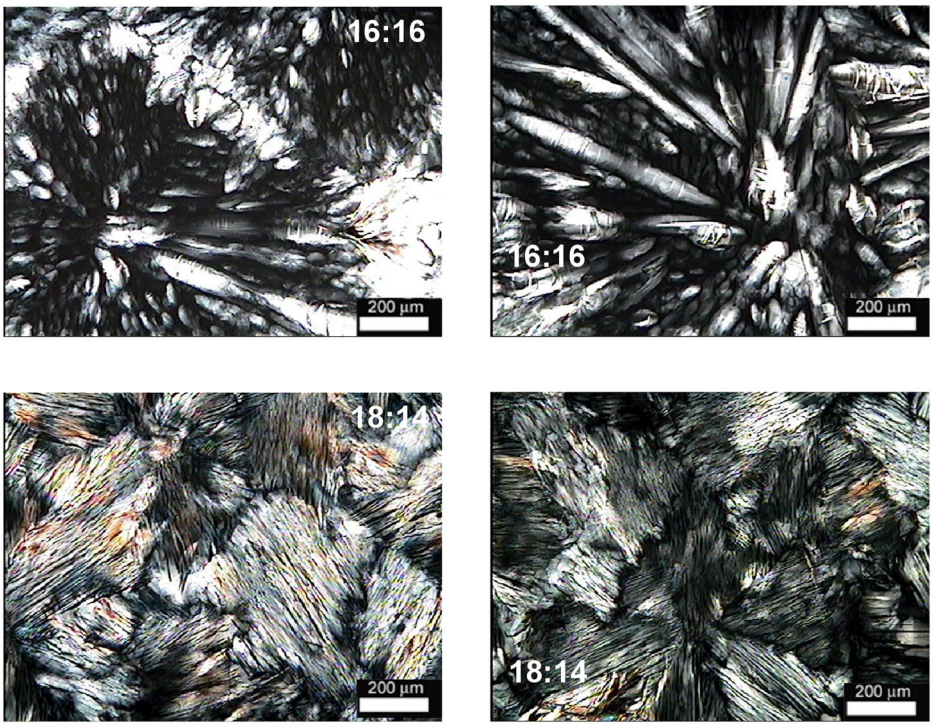

FIGURE 1 | Polarized light microscopy for 60% (wt/wt) solutions in high oleic safflower oil of the symmetric (16:16) and asymmetric (18:14) alkyl esters. The same ester solution is presented for two preparation slides at the same level of magnification.

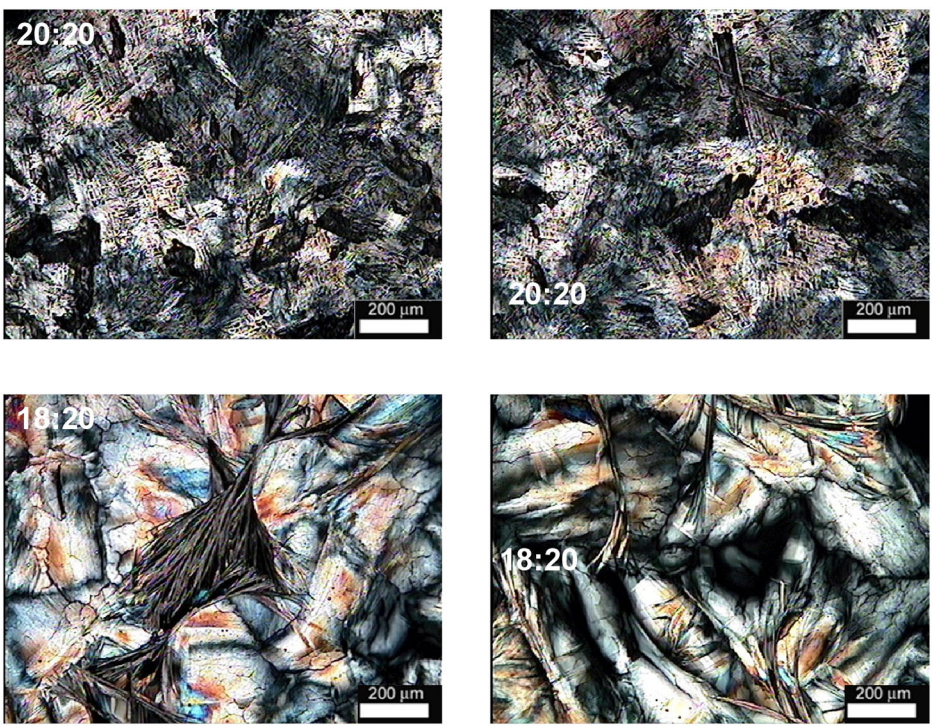

FIGURE 2 | Polarized light microscopy for 60% (wt/wt) solutions in high oleic safflower oil of the symmetric (20:20) and asymmetric (18:20) alkyl esters. The same ester solution is presented for two preparation slides at the same magnification.

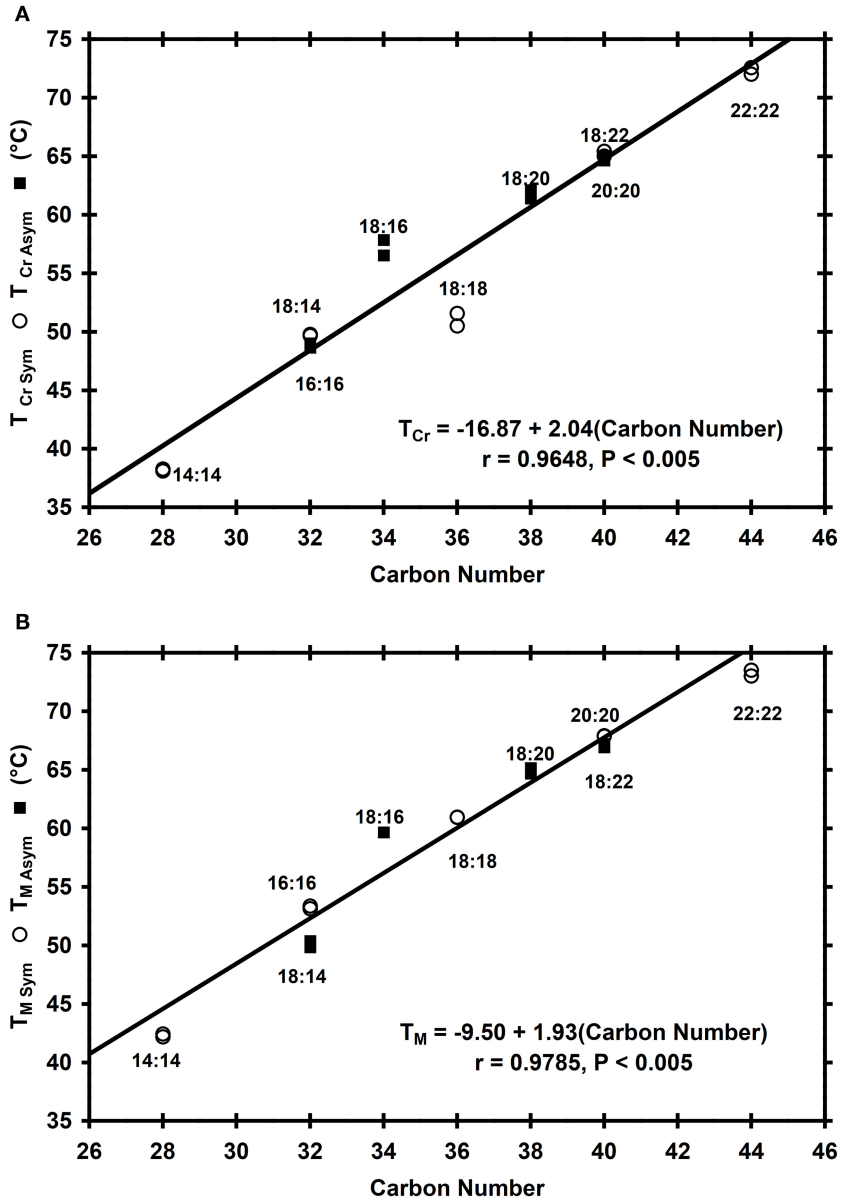

FIGURE 3 | Crystallization (T_{Cr}) and melting (T_M) temperatures for the neat symmetric and asymmetric neat esters as a function of the carbon number of the alkyl esters. The equations show the linear regression of T_{Cr} **(A)** and T_M **(B)** as a function of the alkyl esters carbon number, the corresponding regression coefficient (r) and statistical significance (P).

for the molecular self-assembly (i.e., T_{Cr}) and more significant the van der Waals forces became for molecular self-assembly and crystal structure stabilization (i.e., higher T_M). The results shown in **Figure 3** showed that the symmetry or asymmetry of the alkyl esters studied did not affect the T_{Cr} and T_M behavior as a function of the carbon number.

On the other hand, in comparison with T_{Cr} and T_M the ΔH_{Cr} and ΔH_M of the neat alkyl esters showed a different behavior as a function of the carbon number (**Figure 4**). Thus, ΔH_{Cr} and ΔH_M for the SE observed a quadratic increase as a function of the carbon number ($R^2 > 0.89$; $P < 0.001$). In contrast, for the AE the 18:16, 18:20, and 18:22 showed statistically the same ΔH_{Cr} and ΔH_M with mean values of 141.5 kJ/mol (± 7.4 kJ/mol) and 138.0 kJ/mol (± 7.7 kJ/mol), respectively. However, of all AE studied 18:14 showed the lower ΔH_{Cr} (109.7 ± 4.2 kJ/mol) and ΔH_M (107.2 ± 6.3 kJ/mol) values, a behavior surely associated with its polymorphic behavior as established previously by X-ray analysis (**Figure 4SM** panel A; Supportive Information). The 18:14 polymorphic behavior was also observed in the corresponding melting thermogram as one minor endotherm around 38°C followed by a major endotherm around 49°C (**Figure 6SM** panel B). The ΔH_M plotted for 18:14 in **Figure 4B**

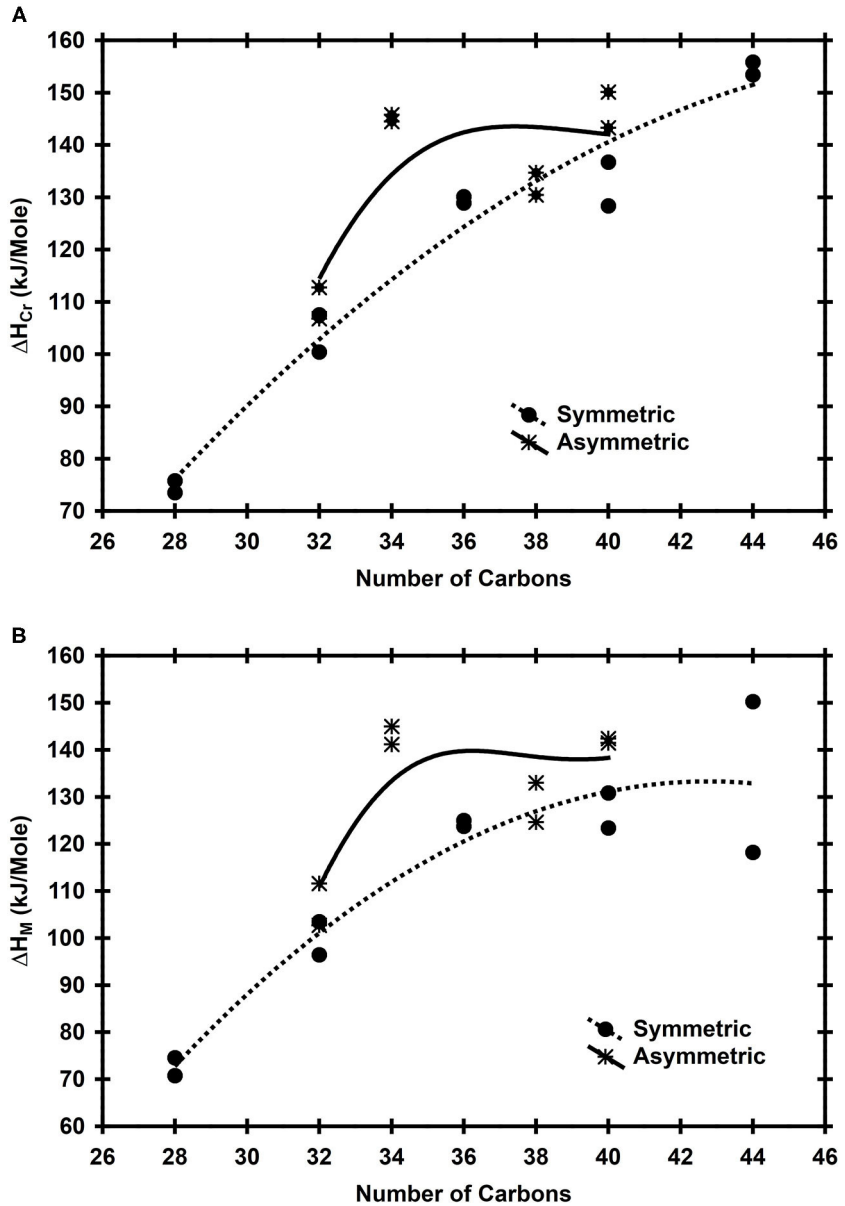

FIGURE 4 | Heat of crystallization [ΔH_{Cr}; **(A)**] and melting [ΔH_M; **(B)**] for the neat symmetric and asymmetric esters as a function of the alkyl esters carbon number.

was just for the major exotherm. Thus, the lower ΔH_{Cr}, ΔH_M, and shorter length of the repetition unit of 18:14 (**Table 1**; **Figure 4**) were the result of its polymorphism. Thus, ΔH_{Cr} and ΔH_M for the AE followed a similar trend as the repetition unit length previously discussed, i.e., 18:16, 18:20, and 18:22 had the same repetition unit length (66.59 Å ± 1.19 Å) while 18:14 showed two short-angle spacings at 43.49 Å and 52.34 Å. These results along with the X-ray diffractograms (**Figures 1SM−5SM**) and PLM (**Figures 1**, **2**) observations showed that the symmetry or asymmetry of the ester molecules had a significant effect in the crystallization of neat esters. We also observed an additional difference in the crystallization behavior between SE and AE. It is well established that supercooling, i.e., the difference between the melting and the crystallization temperature of a compound, provides the thermodynamic drive for the molecular self-assembly of gelator molecules. Thus, from the corresponding thermograms of each ester we calculated the difference between the temperature at the end of melting (T_{M-End}) and the onset temperature for crystallization (T_{Cr-O}). Within this context, the difference T_{M-End} - T_{Cr-O} for the ester solutions was considered as a relative measurement of the supercooling required to achieve the alkyl ester crystallization. The **Figure 7SM** showed that the relative supercooling required to achieve the molecular self-assembly of AE increased linearly ($R^2 = 0.78$; $P < 0.10$) as

a function of the carbon number while for SE decreased ($R^2 = 0.80$; $P < 0.05$). Thus, as the carbon number increased the molecular self-assembly of the AE was harder to achieve than for the SE (**Figure 7SM**). However, the energy required for melting (ΔH_M) of the orthorhombic crystals developed by 18:16, 18:20, and 18:22 was statistically the same (**Figure 4B**). This, in spite of the increase in the carbon number for these AE. In contrast, the energy required for melting of the SE crystals increased quadratically as a function of the carbon number (**Figure 4B**), achieving a plateau above 40 carbons (20:20). Above a carbon number of 40 the SE crystallized in the orthorhombic phase while below 40 carbons (i.e., 14:14, 16:16, and 18:18) as monoclinic (**Table 1**). Based on the supercooling behavior show in **Figure 7SM**, the crystal shape and polymorph developed by alkyl esters would depend on their symmetry or asymmetry and in their length.

Behavior of the Asymmetric and Symmetric Esters in Vegetable Oil Solution

We used the Hildebrand equation (Equation 1) to fit the corresponding thermal parameters obtained with the 0.5–5% (wt/wt) ester oil solutions. With the cooling program used 14:14 solutions below 3% did not achieve full crystallization. Therefore, to have enough experimental data just for the 14:14 ester we included the 6% ester concentration. The results showed that for all ester solutions the Hildebrand equation (Equation 2) fitted the change of T_s (i.e., melting temperature of the alkyl ester in the oil solution, T_M) as a function of the ester molar fraction with a determination coefficient (R^2) above 0.90 ($P < 0.01$). The Hildebrand equation parameters for the AE and SE solutions in vegetable oil and corresponding statistical significance of the linear regression are reported in **Table 1SM** of the Supplementary Material. These results showed that within the concentration interval used for the AE and SE solutions (**Table 1SM**), the alkyl esters behave as ideal solutes in the vegetable oil, i.e., the melting temperature of the AE and SE in the vegetable oil was a direct function of the alkyl ester concentration.

Within the previous context we used the corresponding Hildebrand equation (**Table 1SM** of the Supplementary Material) to estimate the ΔH_M and T_M values for the neat AE and SE assuming an X value of 1 (i.e., ΔH_M and T_M were the estimated values for the neat esters). Subsequently, we determined the percentage of absolute error when these values where used as predictors of the corresponding experimental ΔH_M and T_M values. The results showed that, independent of the type of ester, the predicted T_M had an absolute error lower than 9%. In contrast, the predicted ΔH_M for the neat SE had an absolute error between 15 and 51%. On the other hand, except the equation for 18:14 that provided an absolute error of 18%, the predicted ΔH_M for the neat AE had an absolute error lower than 9%. Evidently, the SE developed a different crystal organization (i.e., polymorph) crystallizing from the vegetable oil solution than from the melt, and from there the large differences observed between the predicted and the experimental ΔH_M value. In contrast, except 18:14, the AE in vegetable oil solutions and from the melt crystallized developing the same polymorph (i.e., orthorhombic; **Table 1**). As already discussed, 18:14 was the only ester that showed the development of two polymorphs, a phenomenon probably associated to the low predictive capacity of the estimated ΔH_M value. Unfortunately, we could not corroborate these conclusions with experimental measurements since at the ester concentration used in the vegetable oil (i.e., lower than 6%), the X-ray signal of our equipment was low and did not provide reliable diffractograms.

Relationship Between the Rheology and Microstructure of the Asymmetric and Symmetric Esters Oleogels

The development of an oleogel requires the formation of a self-supporting structure by the gelator's molecules that physically trap the organic solvent. The minimal gelling concentration of a gelator (i.e., vegetable wax, alkyl ester), also known as the critical gelling concentration, is associated to the minimal mass of crystals that develops the self-supporting structure in a giving solvent (i.e., vegetable oil). This gelling parameter is function of the gelator solubility in the solvent as affected by time-temperature conditions (i.e., gel setting temperature, cooling rate) (Toro-Vazquez and Pérez-Martínez, 2018). Thus, the minimal gelator concentration for vegetable waxes with significant concentration of alkyl esters (e.g., carnauba wax, rice hull wax, safflower wax) has been reported between 1 and 5% by different authors (Dassanayake et al., 2009; Blake et al., 2014; Patel et al., 2015). However, there are not minimal or critical gelator concentration data reported in the literature for neat alkyl esters in vegetable oil or any other solvent. Unfortunately, because limited availability of pure esters, we could not experimentally determine their minimal gelator concentration. Working with *n*-alkanes with 24, 28, 32, and 36 carbons and several organic solvents, Abdallah and Weiss (2000) reported critical gelator concentrations >5.1%, >2.1%, 2.3%, and 1.3%, respectively. In the same way, using silicon oil, mineral oil and decane as solvents Pal et al. (2013) reported critical gelator concentrations between 0.6 and 3.8% for a series of positional isomers of keto octadecanoic acid (i.e., carboxylic acids with a carbonyl group inserted in different positions). However, none of these studies used vegetable oil as solvent. Thus, we established a 3% (wt/wt) ester concentration to compare the thermo-mechanical properties of AE and SE oleogels with and without MSG. As already mentioned, the monoglycerides are minor native components present in vegetable oils. However, once intentionally added to the vegetable oil to develop emulsions or organogelled emulsions, their amphiphilic character and capability of developing hydrogen bonds might favor or hinder the self-assembly of the alkyl esters.

The G', measured at $-5°C$, as a function of the carbon number for the 3% AE and SE oleogels with 0, 0.5, and 1% of MSG are shown in **Figure 5**. As established by DSC, at $-5°C$ we assured the complete crystallization of the alkyl ester and MSG present in the vegetable oil solutions. The PLM photographs for the corresponding SE oleogels with 0, 0.5, and 1% MSG are shown in **Figures 6–8** and for the AE oleogels in **Figures 9–11**. Independent of the MSG concentration we achieved the highest

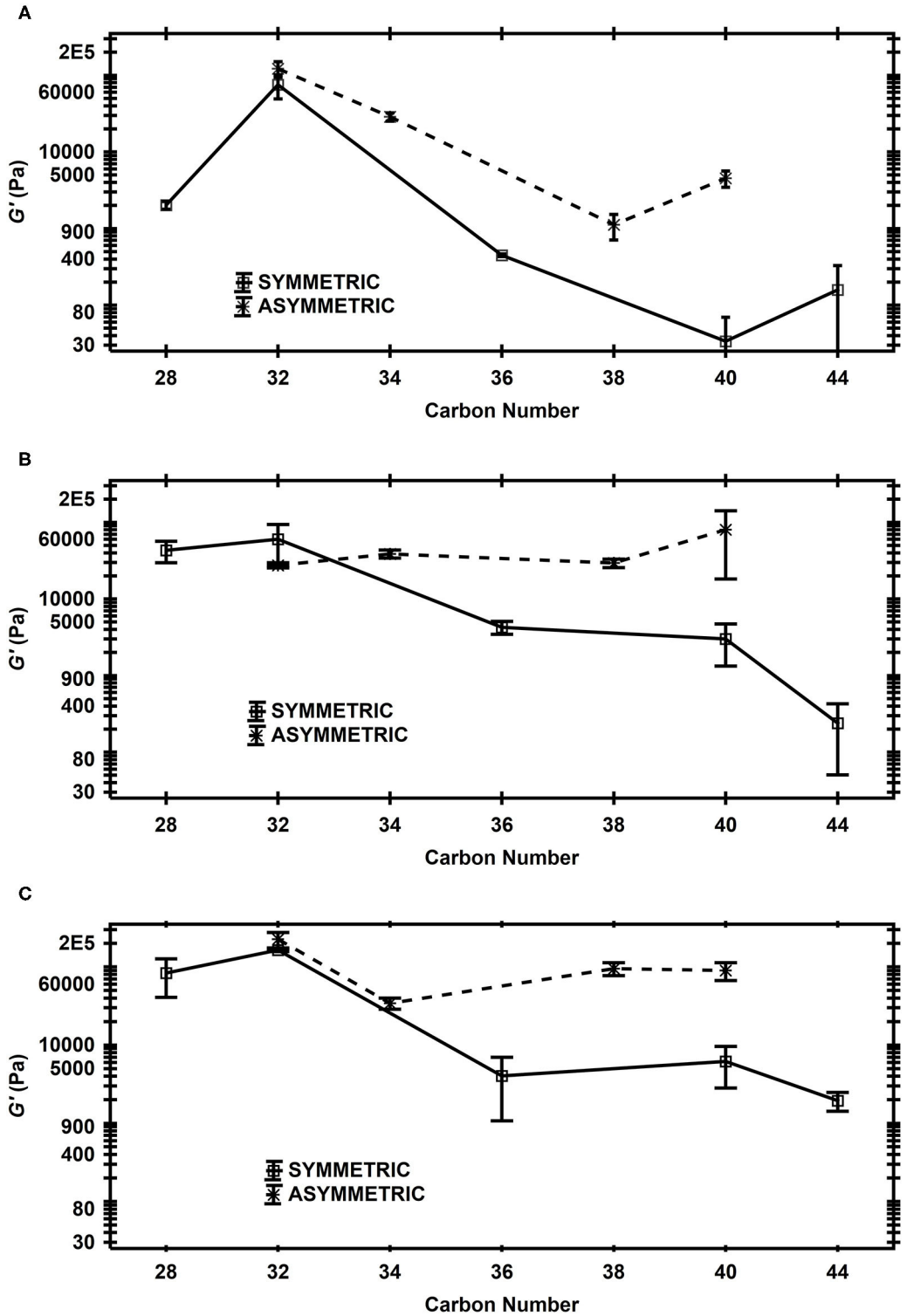

FIGURE 5 | Elastic modulus (G'; −5°C) for the 3% (wt/wt) oleogels formulated with symmetric and asymmetric alkyl esters as a function of the carbon number of the esters. **(A)** 0% MSG; **(B)** 0.5% MSG; **(C)** 1% MSG (wt/wt).

oleogel's elasticity in the AE and SE oleogels developed with the 32 carbons esters (i.e., 16:16 and 18:14; $P < 0.05$) (**Figure 5**). Above 32 carbons, independent of the MSG concentration, the elasticity of the SE oleogels showed a decreasing trend as the carbon number increased (**Figure 5**). The AE oleogels with 0% MSG also showed a similar G' decreasing behavior (**Figure 5A**).

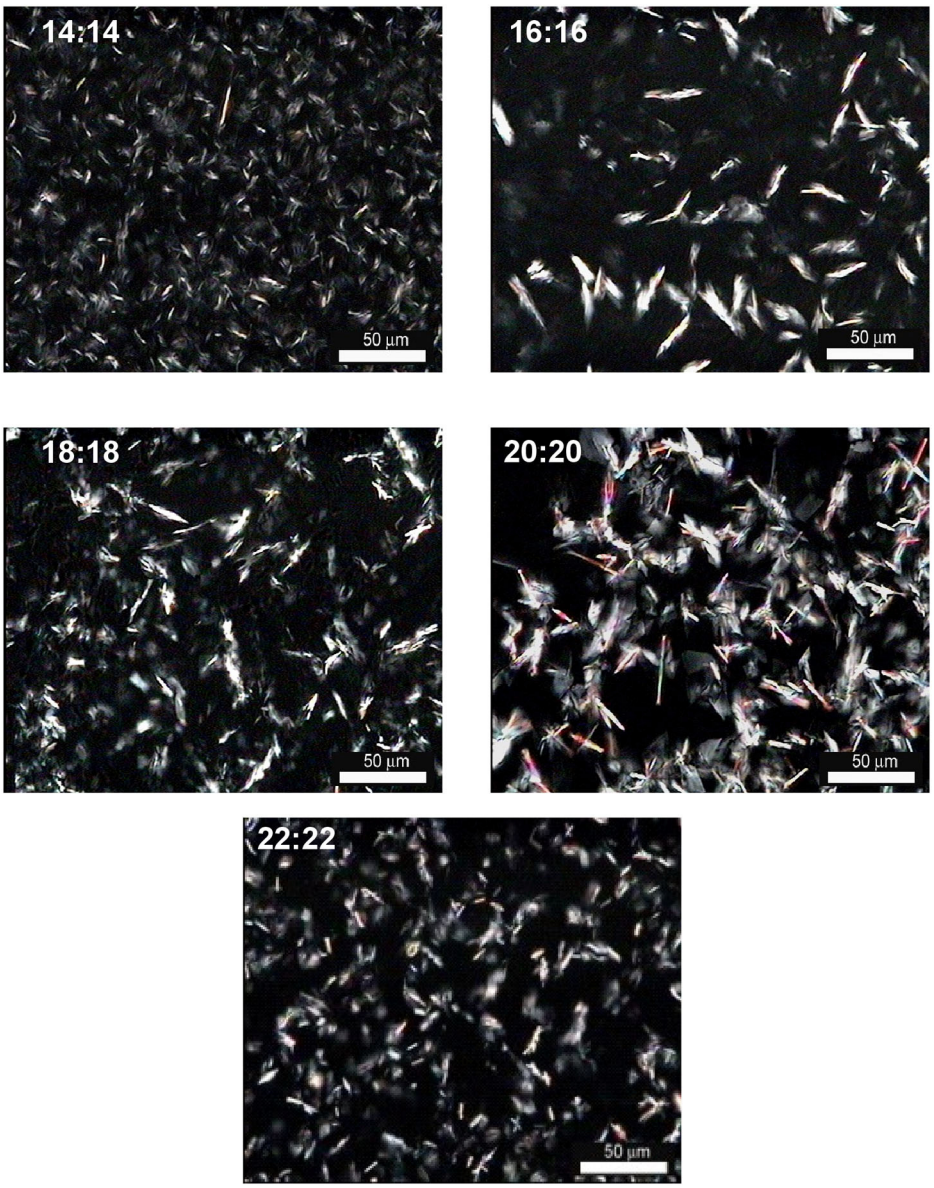

FIGURE 6 | Polarized light microscopy (−5°C) for the 3% (wt/wt) oleogels in high oleic safflower oil formulated with the symmetric alkyl esters indicated and 0% MSG.

Nevertheless, in all cases the AE oleogels had higher G' than the SE oleogels, particularly in the presence of MSG (**Figures 5B,C**). Hwang et al. (2012) reported that wax esters with longer alkyl chains esters required lower quantity to achieve gelation that waxes with shorter alkyl chains. The results in **Figure 5A** showed that the esters' gelation capability in vegetable oils depends not only on the alkyl chain length, but also on the symmetry or asymmetry of the alkyl chains respect to the ester bond. However, it is important to note that, in contrast with the study of Hwang et al. (2012) that used native waxes (i.e., mixtures of wax esters) containing other additional minor components, the present study used pure saturated alkyl esters. The PLM for the oleogels with 0% MSG showed that, overall, the AE crystals were larger (**Figure 9**) than those developed by the SE (**Figure 6**). Additionally, the AE crystallized in acicular shaped crystals while the SE crystallized mainly as plate-like shaped crystals. This was evident when comparing the PLM of oleogels developed by esters with the same carbon number, i.e., 18:14 and 16:16, and particularly the 18:22 and 20:20 esters (**Figures 6**, **9**). These observations agreed with the microestructure developed by the alkyl esters in the 60% ester solutions previously discussed (**Figures 1**, **2**). For the SE oleogels with 0% MSG the crystals' size increased from the ester with 28 carbons (i.e., 14:14) up to 40 carbons ester (i.e., 20:20). The increase in crystal size resulted in lower extent of crystal-crystal interaction, and therefore in the crystal network's strength. The overall effect was a reduction in

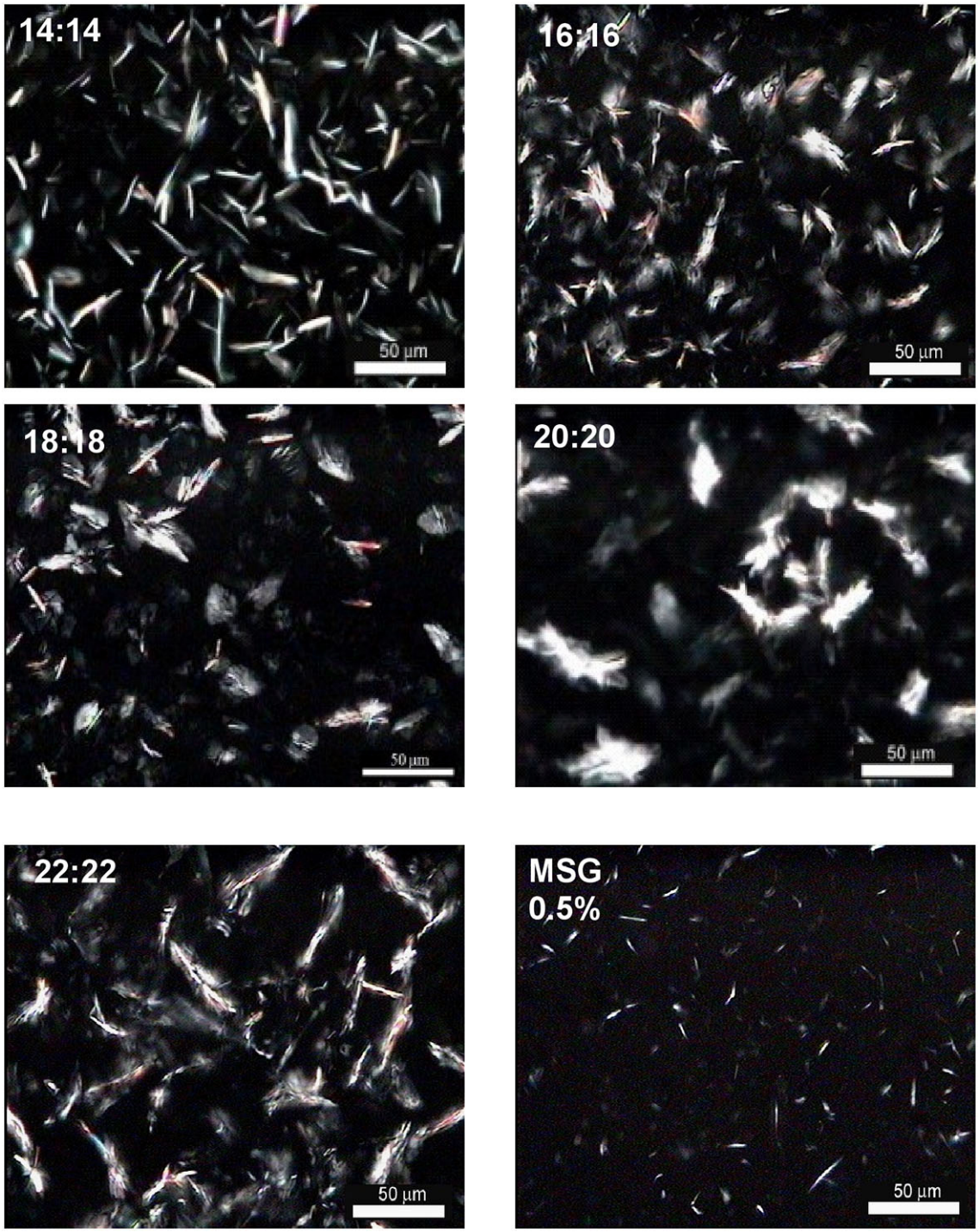

FIGURE 7 | Polarized light microscopy (−5°C) for the 3% (wt/wt) oleogels in high oleic safflower oil formulated with the symmetric alkyl esters indicated and 0.5% MSG.

the elasticity of the SE oleogels as the carbon number increased from 32 (16:16) up to 40 (20:20) (**Figures 5A**, **6**). In contrast, the 22:22 oleogel was structured by smaller crystals (**Figure 6**) that resulted in an increase in G'. However, the increase in G' was not statistically different from the elasticity provided by the 20:20 oleogels (**Figures 5A**, **6**). The AE oleogels with 0% MSG also showed an increase in crystal size as the carbon number increased, a behavior associated with the decrease in

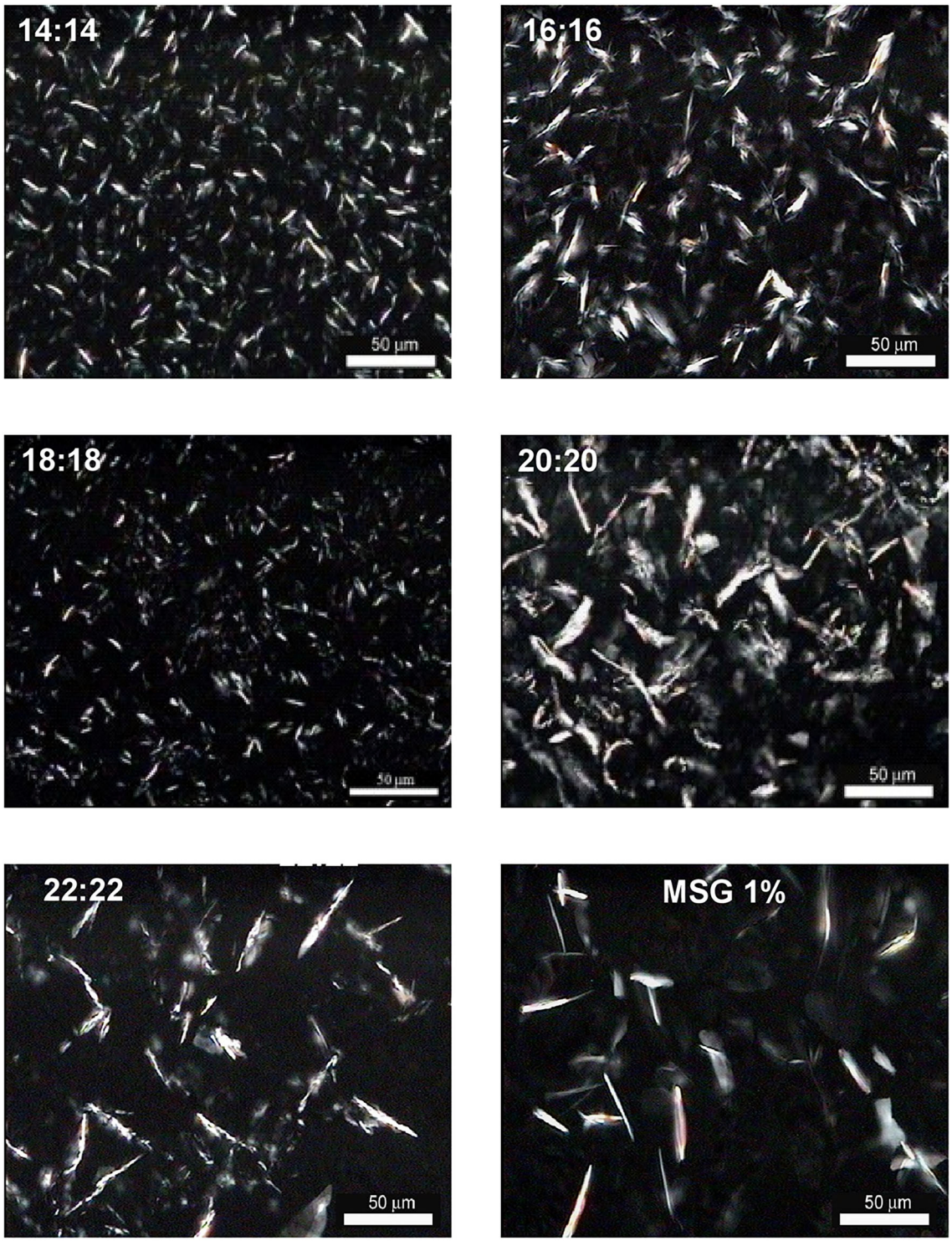

FIGURE 8 | Polarized light microscopy (−5°C) for the 3% (wt/wt) oleogels in high oleic safflower oil formulated with the symmetric alkyl esters indicated and 1% MSG.

the oleogels' elasticity (**Figures 5A**, **9**). The results showed in **Figures 5A**, **6**, **9** indicated that the AE oleogels structured by large acicular crystals (18:14, 18:16, 18:20, and 18:22, **Figure 9**) resulted in gels with higher G' when compared with the SE oleogels structured by smaller plate-like crystals (16:16, 18:18, 20:20, and 22:22, **Figure 6**). Thus, crystal shape in addition to

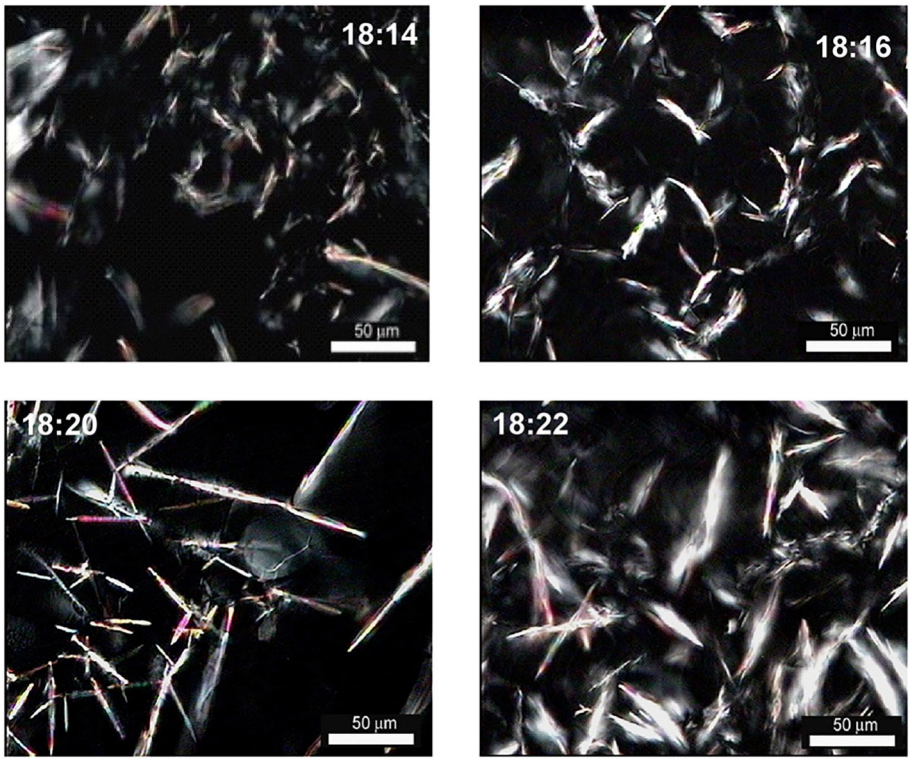

FIGURE 9 | Polarized light microscopy (−5°C) for the 3% (wt/wt) oleogels in high oleic safflower oil formulated with the asymmetric alkyl esters indicated and 0% MSG.

size determined the oleogels rheology. These results agreed with those obtained previously with low molecular weight gelators in the neat state and in oleogels (Toro-Vazquez et al., 2013b). In particular, the 18:22 oleogel was structured by bundles of large fibers (**Figure 9**) that would increase the crystal-crystal interaction resulting in higher oleogel elasticity than the one achieved by the 20:20 oleogel (**Figures 5A**, **6**). It is important to note that cooling thermograms of the vegetable oil showed that its crystallization onset (i.e., development of a solid phase) occurred between −15°C and −20°C. Additionally, rheological measurements of the vegetable oil under the time-temperature conditions to develop and measure the AE and SE oleogels, showed that G'' was always greater of G'. These results showed that vegetable oil remained liquid at −5°C and therefore its contribution to the oleogels' elasticity was negligible.

Regarding the effect of MSG we noted that the addition of MSG increased the oleogels' elasticity independent of the type of ester and the ester carbon number (**Figure 5**). However, the MSG effect was higher in the AE oleogels than in the SE oleogels (**Figures 5B,C**). In particular, the addition of just 0.5% of MSG limited the decrease in G' observed in the oleogels without MSG as the carbon number increased (**Figure 5**). The addition of MSG had a dramatic effect in the ester's crystal size and shape (**Figures 7**, **8** for SE; **Figures 10**, **11** for the AE). This effect was particularly evident in the AE oleogels (compare the photographs of **Figure 9** with those in **Figures 10**, **11**). Thus, in comparison with the microstructure of the AE oleogels with 0% MSG (**Figure 9**), the addition of just 0.5% MSG to AE oleogels modified the crystal shape and, particularly, decreased the crystal size (**Figure 10**). However, based on the microphotographs of the oleogels we considered that higher MSG concentrations (i.e., 1% MSG) had no additional effect in the crystal shape and size of the AE (**Figure 11**). It is important to note that, in comparison with the oleogels with 0% MSG, the addition of MSG ought to result in approximately 0.5 or 1% increase in the oleogels' solid content. Rheological measurements of 0.5 and 1% MSG vegetable oil solutions at −5°C provided G' values of just around 40 Pa or lower, i.e., the solid phase developed by the MSG was not sufficient to form an oleogel. Nevertheless, the increase in the crystal mass (i.e., solid content) and decrease in the crystal size associated with the addition of MSG would result in higher crystal-crystal interaction, and subsequently in higher oleogels' elasticity, particularly in the AE with 38 and 40 carbons (**Figure 5**).

We did a more detailed rheological analysis of the oleogels by plotting, for the SE and AE oleogels at the different MSG concentrations, the phase angle (δ) as a function of ω (**Figures 12**, **13**). The δ parameter, defined as $\tan^{-1}(G''/G')$, is used to evaluate in a sensitive way the viscoelastic changes occurring in complex systems. Thus, in pure viscous systems, like the vegetable oil, $\delta = 90°$ since G'' completely dominates G'. In contrast, $\delta = 0°$ in fully structured systems with ideal elastic behavior since G' completely dominates G''. When the viscous and elastic behavior are exactly balanced $G' = G''$ and, therefore, $\delta = 45°$

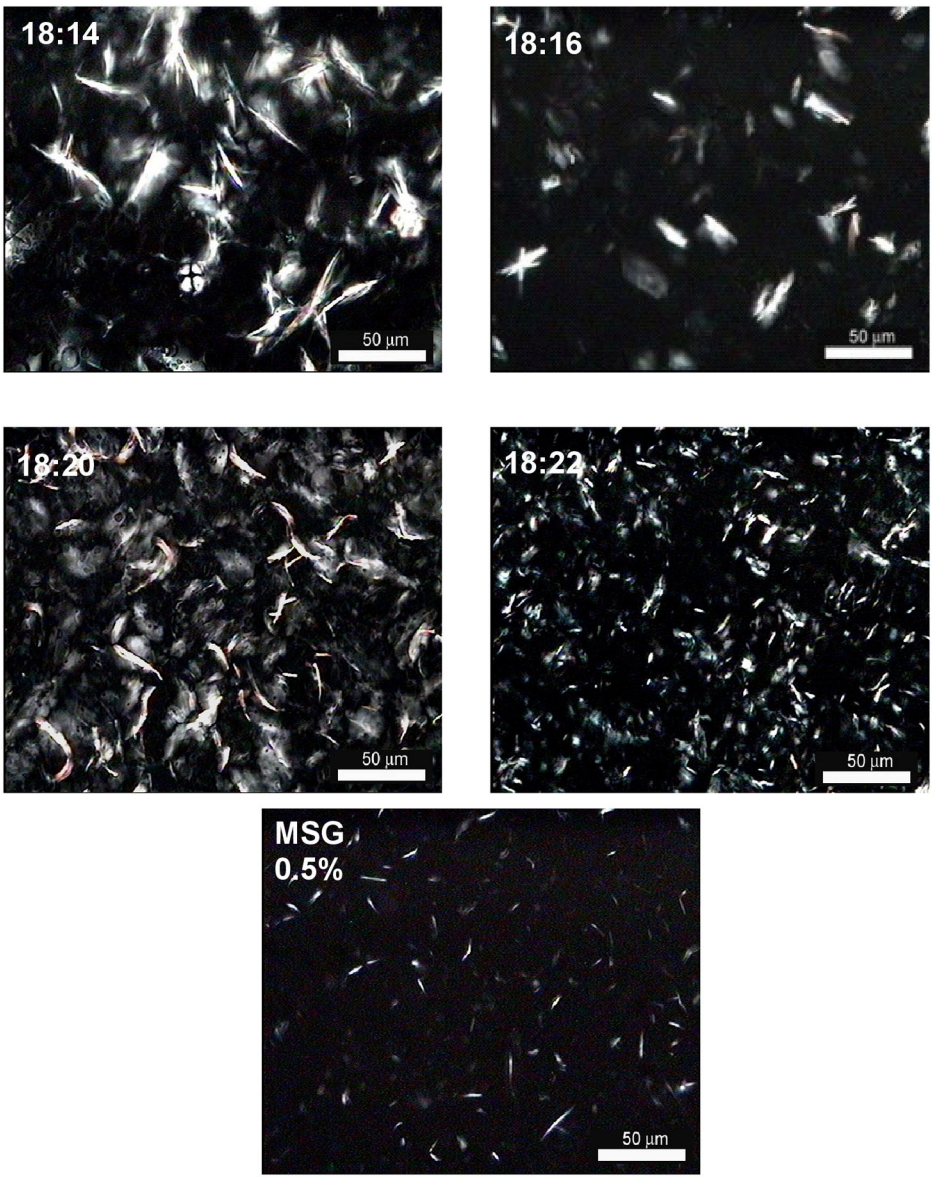

FIGURE 10 | Polarized light microscopy (−5°C) for the 3% (wt/wt) oleogels in high oleic safflower oil formulated with the asymmetric alkyl esters indicated and 0.5% MSG.

(Mezger, 2014). Consequently, in gelled systems (i.e., oleogels) where $G' > G''$ the δ values would be lower than 45° and the smaller the δ value the larger the gel's elasticity. The use of δ sweeps as a function of ω was particularly useful because allows the study of viscoelastic changes occurring as a function of a timescale in complex systems like crystallization of triglycerides or phosphatidylcholine in vegetable or mineral oil (Toro-Vazquez et al., 2005; Martínez-Ávila et al., 2019). Within this context, in solid-like materials δ would have values lower than 45° with a rheological behavior nearly independent of δ (i.e., true gels). In contrast, the more δ behaves ω dependent showing values above 45° the more fluid like is the material (i.e., a sol or a gel-like material). Thus, except the 16:16 oleogel, the ω sweeps of the SE oleogels with 0% MSG showed δ values above 20°. In particular, the 14:14 and 18:18 oleogels with 0% MSG observed a frequency independent rheological behavior at a $\omega < 15$ Hz with δ values between 30° and 40°. However, at higher ω the δ values increased up to values between 75° and 80° (**Figure 12A**). In contrast, below 1.5 Hz the 20:20 oleogel with 0% MSG showed δ values that varied between 20° and 50°, while the 22:22 oleogel had δ values between 20° and 35°. Thus, below 1.5 Hz the 20:20 and 22:22 oleogels with 0% MSG showed frequency dependent rheological behavior that further continued at higher ω until δ achieved values around 50° to 55°. These results showed that the 14:14, 18:18, 20:20 and the 22:22 oleogels with 0% MSG were weak gels that would go through phase separation

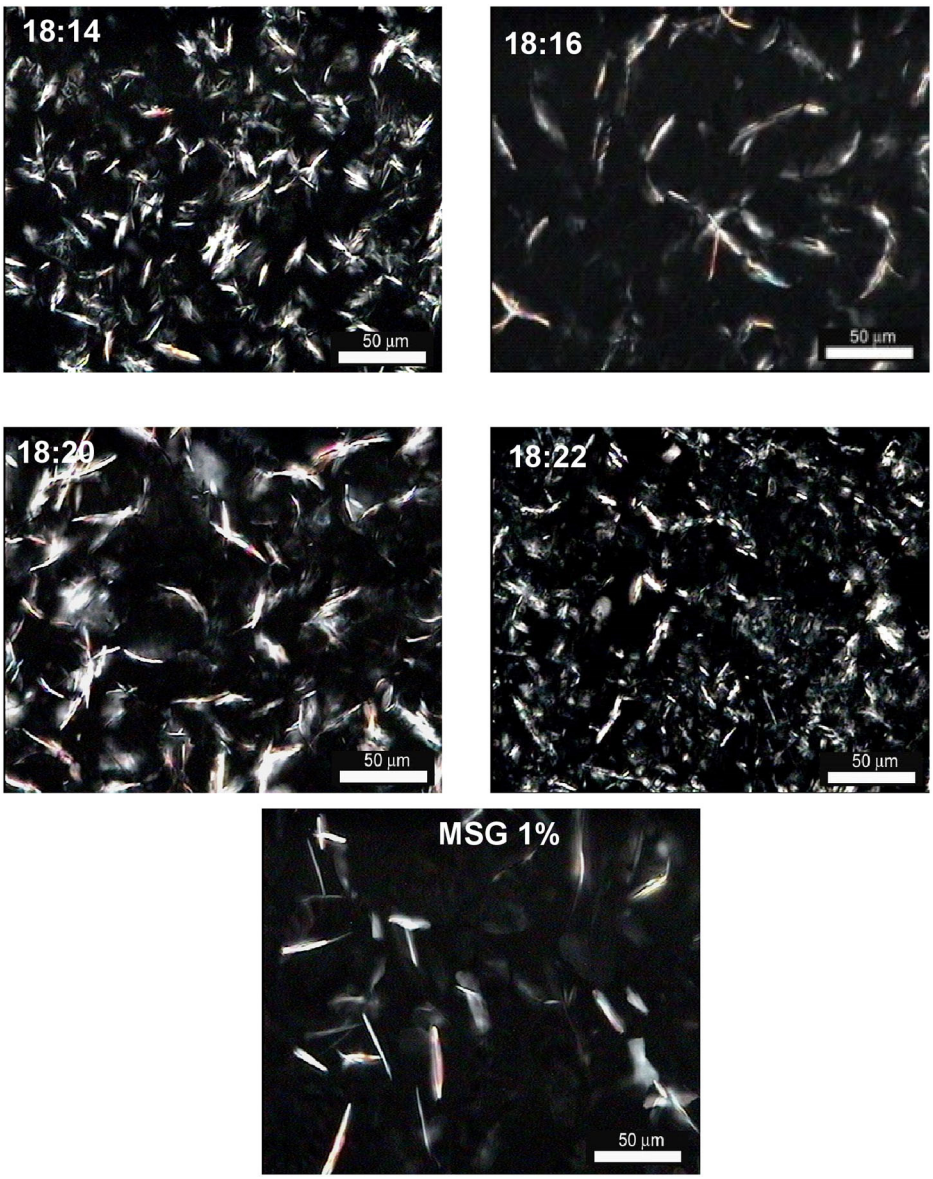

FIGURE 11 | Polarized light microscopy (−5°C) for the 3% (wt/wt) oleogels in high oleic safflower oil formulated with the asymmetric alkyl esters indicated and 1% MSG.

during storage. In fact these oleogels showed some visual phase separation after about four to six weeks of storage at −5°C. The exception to this behavior was the 16:16 oleogel with 0% MSG. This oleogel showed essentially a frequency independent rheological behavior in most of the ω interval, providing δ values around 16° (**Figure 12A**). Thus, the 16:16 oleogels with 0% MSG showed the rheological behavior of a true gel. However, the 16:16 oleogels' rheological behavior could not be explained considering just the oleogels' microstructure (**Figure 6**). In contrast, the AE oleogels with 0% MSG had δ values well below 35° showing essentially a frequency independent rheological behavior. At ω higher than 0.3 Hz the AE oleogels with 0% MSG had a tendency of achieving lower δ values (i.e., higher elasticity) as the carbon number decreased from 18:22 (δ ≈ 20° to 29°) to 18:14 (δ ≈ 6° to 10°) (**Figure 13A**). Thus, in contrast with the SE oleogels with 0% MSG all the AE oleogels with 0% MSG showed the rheological behavior of a true gel. Within this context it is important to point out that for the same carbon number, the AE oleogels (i.e., 18:14, 18:22) had significantly lower δ values (i.e., higher elasticity) than the corresponding SE oleogels (i.e., 16:16, 20:20) (**Figures 12A**, **13A**). The difference in rheological behavior between the SE and AE oleogels with 0% MSG was explained considering the oleogels microstructure previously discussed (**Figures 6**, **9**) and its effect in the crystal-crystal interaction and therefore in the oleogels elasticity. Nevertheless, as previously indicated, the 16:16 oleogel with 0% MSG was the only SE that showed a ω independent

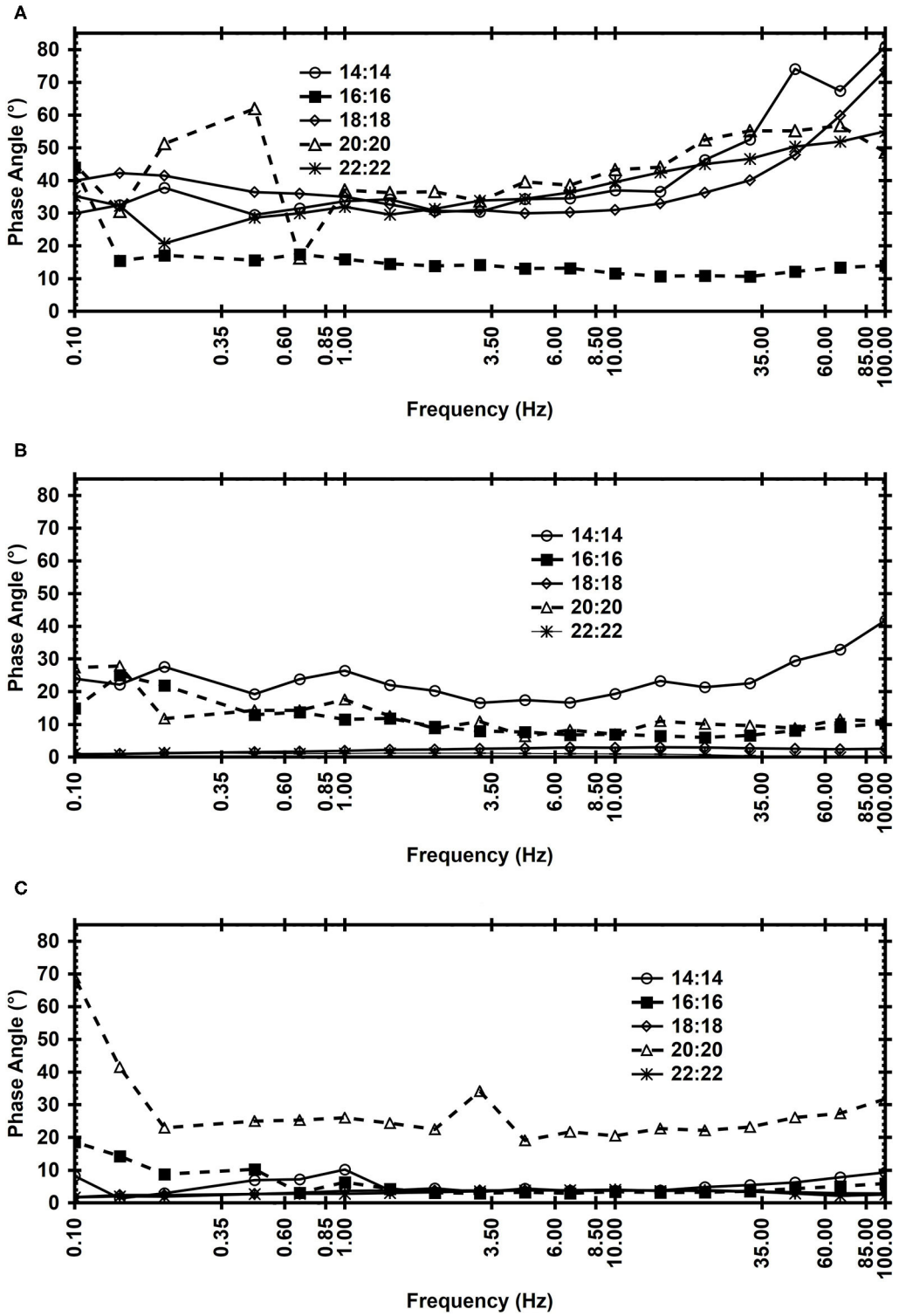

FIGURE 12 | Frequency sweeps (−5°C) for the 3% (wt/wt) oleogels in high oleic safflower oil formulated with the symmetric alkyl esters indicated and: 0% MSG **(A)**, 0.5% MSG **(B)**, and 1% MSG **(C)**.

rheological behavior as the AE oleogels (**Figures 12A**, **13A**). The 16:16 oleogel had a microstructure closer to that developed by the AE oleogels (**Figures 6**, **9**), and possible this was the reason the 16:16 oleogel showed similar ω independent rheological behavior as the AE oleogels. Within this context, as previously noted, the neat 16:16 was the only SE that showed a similar X-ray diffraction

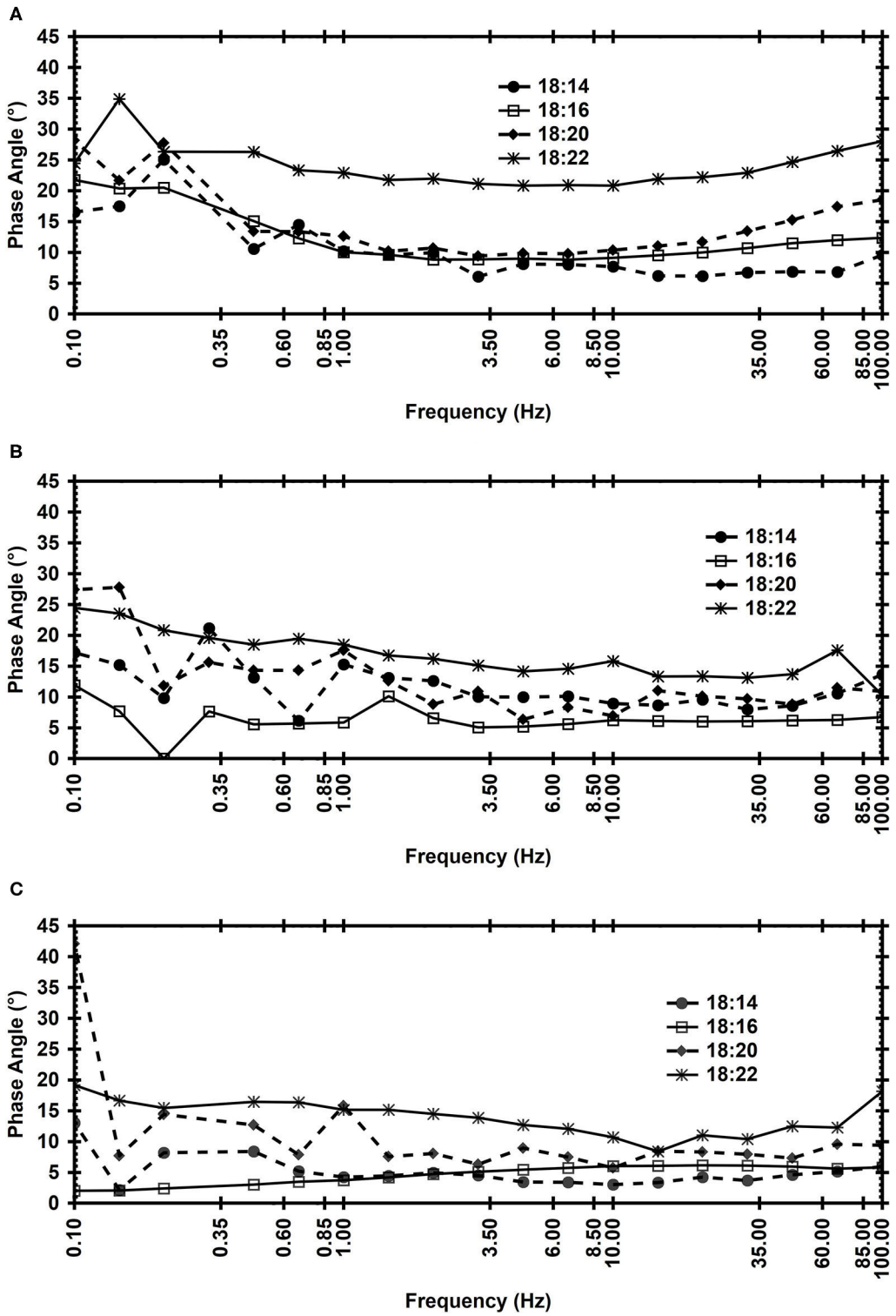

FIGURE 13 | Frequency sweeps (−5°C) for the 3% (wt/wt) oleogels in high oleic safflower oil formulated with the asymmetric alkyl esters indicated and: 0% MSG **(A)**, 0.5% MSG **(B)**, and 1% MSG **(C)**.

pattern to neat AE. Thus, like the neat AE the X-ray diffraction for 16:16 showed a lower diffraction signal in the WAXS region than in the SAXS region. Unfortunately, we could not find the reasons why the particular crystallization and rheological behavior of the 16:16 ester in the neat state and the oleogel. We did not consider that the rheological behavior showed by the AE

and SE oleogels with 0% MSG was associated with differences in the oleogels' solid content. As already discussed, at the gel setting temperature used for rheological measurements (−5°C), we assured the complete crystallization of all the alkyl esters (i.e., 3%). Thus, cooling thermograms of the 3% alkyl esters solutions in the vegetable oil showed that the corresponding crystallization exotherm ended at a temperature well above the gel setting temperature (from −1.7°C for the 14:14 oleogel up to 37.2°C for the 22:22 oleogel). Unfortunately, due to the limited amount of pure esters available we could not determine the oleogels' solid content. Therefore, the rheological behavior of the SE and AE oleogels with 0% MSG was mainly associated with the microestructural organization of the alkyl esters in the oleogels (**Figures 6**, **9**).

On the other hand, independent of the type of ester, the addition of 0.5% MSG and particularly 1% MSG resulted in gels that provided lower δ values (**Figures 12B,C**, **13B,C**) and, therefore, better structured than the oleogels with 0% MSG (**Figures 12A**, **13A**). Except the δ behavior observed by the 18:20 and 20:20 oleogels with 1% MSG at ω lower than 0.30 Hz (**Figures 12C**, **13C**), and the 14:14 oleogel with 0.5% MSG at ω above 50 Hz (**Figure 12B**), all the AE and SE oleogels with 0.5% or 1% MSG showed δ values lower than 30° with ω independent rheological behavior (**Figures 12B,C**, **13B,C**). In contrast with the oleogels with 0% MSG, we considered that the rheological behaviors of the SE and AE oleogels with 0.5% and 1% MSG were associated with the microestructural organization of the oleogels previously discussed (**Figures 7**, **8** for the SE, and **Figures 10**, **11** for the AE), but also with the higher solid content associated with the MSG crystallization. Other studies had shown that the presence of minor components of vegetable oils (i.e., tripalmitin) have a profound effect in the gelation capability and the molecular self-assembly mechanism of the hentriacontane (i.e., *n*-alkane with 31 carbons) present in candelilla wax (Morales-Rueda et al., 2009; Chopin-Doroteo et al., 2011). As previously discussed, we observed that a small amount of MSG modified the crystal habit of neat alkyl esters (**Figures 7**, **8**), developing oleogels with higher elasticity than the ester oleogels (**Figures 5B,C**). As examples, the **Figures 8SM, 9SM** of the Supplementary Material show cooling and heating thermograms for a symmetrical (i.e., 18:18) and asymmetrical (i.e., 18:16) oleogels with 0.5 and 1% MSG, in comparison with the corresponding independent systems, i.e., the 3% alkyl ester oleogel and the corresponding 0.5 and 1% MSG solution in the vegetable oil. The photographs for these oleogels obtained at −5°C through PLM are included in the **Figures 8SM, 9SM**. We noted than the crystallization and further melting of the MSG in the corresponding 0.5 and 1% solutions were modified when occurred in the alkyl ester-MSG oleogels. Thus, during cooling and further melting of the independent systems the 3% alkyl esters, the 0.5 and 1% MSG showed exotherms and endotherms of different shapes, T_{Cr} and T_M. However, during cooling of the alkyl ester-0.5% MSG and alkyl ester-1% MSG systems both gelators crystallized showing just one exotherm. Upon heating the oleogels melted showing just one exotherm that, except the 18:18 and 18:22 alkyl esters, had a T_M statistically equal to the T_M of the corresponding 3% alkyl ester-0% MSG oleogel (see **Table 2SM** of the Supplementary Material). Within this context, the DSC results of alkyl esters-MSG oleogels suggested that the alkyl ester and the MSG crystallized as one entity, i.e., a co-crystal. It is important to point out that during melting of some of the alkyl ester-MSG oleogels we observed a small shoulder of the major melting endotherm (see arrow in the heating thermogram for the 3%18:18-1% MSG oleogel, **Figure 8SM** panel D). We associated this thermal behavior with the melting of MSG that apparently did not co-crystallize with the alkyl ester during cooling. This might be the reason why the 18:18 and 18:22 alkyl esters oleogels with 0.5 and 1% MSG showed an endotherm with a higher T_M than the corresponding alkyl esters oleogels with 0% MSG ($P < 0.05$; **Table 2SM** of the Supplementary Material).

The tentative alkyl esters-MSG co-crystals might develop through van deer Walls forces established between the hydrocarbon chain of the stearic acid esterified to the MSG and the alkyl chains of the AE or SE. This would result in a modification of the original ester self-assembly and, subsequently, in the crystal size and shape. The calorimetry results also showed that in alkyl ester-MSG oleogels, particularly developed with 1% MSG, part of the MSG did not interact with the ester molecules and crystallized independently of the co-crystals. These MSG crystals might act as active fillers of the major microstructure developed by the alkyl ester-MSG co-crystals. The overall effect was that the alkyl ester-MSG oleogels had higher G' with a δ frequency independent rheological behavior in comparison with the alkyl ester oleogels with 0% (**Figures 5**, **12**, **13**).

The results of this study showed that alkyl ester composition and structure (i.e., symmetry or asymmetry) greatly influences its molecular self-assembly, with the consequent effect in the oleogel's thermo-mechanical properties. Additionally, MSG commonly used in the development of organogelled emulsions (Toro-Vazquez et al., 2013a), affected the alkyl ester crystallization resulting in oleogels with higher elastic properties with frequency independent rheological behavior. The rheological properties of the alkyl esters-MSG oleogels were associated with the development of co-crystals between the ester and the monoglyceride. Additionally, part of the MSG that did not interact with the ester molecules and crystallized independently, acted as an active filler of the three-dimensional microstructure formed by the co-crystals. The relevance of these results resides in the major role that alkyl esters play in establishing the functional properties of vegetable wax's oleogels used in food systems and cosmetics. Ongoing studies using molecular mechanics modeling are underway to establish the mechanism for AE and SE self-assembly with and without MSG.

DATA AVAILABILITY STATEMENT

The raw data supporting the conclusions of this article will be made available by the authors, without undue reservation.

AUTHOR CONTRIBUTIONS

GA-V is currently a Ph. D. student and these results are part of her thesis research. GA-V was closely involved in the DSC, rheological measurements and implementing the microscopy technique to evaluate the crystallization of the esters in the neat state and in the oleogels. AD and MEC-A were mainly involved in doing the X-ray analysis and their diffractograms interpretation within the context of the symmetrical and asymmetrical ester molecular self-assembly. MAC-A and JT-V established the experimental conditions used in this study, integrated and analyzed all data. AD, MAC-A, and JT-V obtained and analyze the data associated with the Hildebrand equation applied to the crystallization and melting behavior of the ester in vegetable oil solutions. JT-V was the project and research group leader, also acting as GA-V's thesis advisor. All authors contributed to the article and approved the submitted version.

ACKNOWLEDGMENTS

The present research was supported by Consejo Nacional de Ciencia y Tecnología (CONACYT) through the Grant No. CB-280981-2018. GA-V greatly appreciates the scholarship provided by CONACYT to conclude her Ph.D. program. The technical support from Marisol Davila Martínez is greatly appreciated.

SUPPLEMENTARY MATERIAL

The Supplementary Material for this article can be found online at: https://www.frontiersin.org/articles/10.3389/fsufs.2020.00132/full#supplementary-material

REFERENCES

Abdallah, D. J., and Weiss, R. G. (2000). n-Alkanes gel n-alkanes (and many other organic liquids). *Langmuir* 16, 352–355. doi: 10.1021/la990795r

Abraham, S., Lan, Y., Lam, R. S. H., Grahame, D. A. S., Kim, J. J. H., Weiss, R. G., et al. (2012). Influence of positional isomers on the macroscale and nanoscale architectures of aggregates of racemic hydroxyoctadecanoic acids in their molecular gel, dispersion, and solid states. *Langmuir* 28, 4955–4964. doi: 10.1021/la204412t

Alvarez-Mitre, F. M., Morales-Rueda, J. A., Dibildox-Alvarado, E., Charó-Alonso, M. A., and Toro-Vazquez, J. F. (2012). Shearing as a variable to engineer the rheology of candelilla wax organogels. *Food Res. Intern.* 49, 580–587. doi: 10.1016/j.foodres.2012.08.025

Blake, A. I., Co, E., and Marangoni, A. G. (2014). Structure and physical properties of plant wax crystal networks and their relationship to oil binding capacity. *J. Am. Oil Chem. Soc.* 91, 885–903. doi: 10.1007/s11746-014-2435-0

Blake, A. I., Toro-Vazquez, J. F., and Hwang, H.-S. (2018). "Wax oleogels," in *Edible Oleogels. Structure and Health Implications,* eds G. Alejandro, M. Nissim Garti (San Diego, CA: AOCS Press),133–171. doi: 10.1016/B978-0-12-814270-7.00006-X

Boese, R., Weiss, H. C., and Bläser, D. (1999). The melting point alternation in the short-chain n-alkanes: Single-crystal X-ray analyses of propane at 30 K and of n-butane to n-nonane at 90 K. *Angew. Chem. Intern. Edn.* 38, 988–992.

Bot, A., and Agterof, W. G. M. (2006). Structuring of edible oils by mixtures of γ-oryzanol with β-sitosterol or related phytosterols. *J. Am. Oil Chem. Soc.* 83, 513–521. doi: 10.1007/s11746-006-1234-7

Bot, A., Den Adel, R., and Roijers, E. C. (2008). Fibrils of γ-oryzanol + β-sitosterol in edible oil organogels. *J. Am. Oil Chem. Soc.* 85, 1127–1134. doi: 10.1007/s11746-008-1298-7

Bot, A., den Adel, R., Roijers, E. C., and Regkos, C. (2009). Effect of sterol type on structure of tubules in sterol + γ-oryzanol-based organogels. *Food Biophys.* 4, 266–272. doi: 10.1007/s11483-009-9124-9

Busson-Breysse, J., Farines, M., and Soulier, J. (1994). Jojoba wax: its esters and some of its minor components. *J. Am. Oil Chem. Soc.* 71, 999–1002. doi: 10.1007/BF02542268

Chen, C. H., Damme, I. V., and Terentjev, E. M. (2009). Phase behavior of C18 monoglyceride in hydrophobic solutions. 432–439. doi: 10.1039/B813216J

Chopin-Doroteo, M., Morales-Rueda, J. A., Dibildox-Alvarado, E., Charó-Alonso, M. A., de la Peña-Gil, A., Jorge, F., et al. (2011). The effect of shearing in the thermo-mechanical properties of candelilla wax and candelilla wax-tripalmitin organogels. *Food Biophys.* 6, 359–376. doi: 10.1007/s11483-011-9212-5

Co, E., and Marangoni, A. G. (2012). Organogels: An alternative edible oil-structuring method. J. Am. Oil Chem. Soc. 89, 749–780. doi: 10.1007/s11746-012-2049-3

Co, E., and Marangoni, A. G. (2013). The formation of a 12-hydroxystearic acid/vegetable oil organogel under shear and thermal fields. *J. Am. Oil Chem. Soc.* 90, 529–544. doi: 10.1007/s11746-012-2196-6

Cosmetic Lab, S. C. (2016). *9 Most Important Natural Waxes For Cosmetics (Part Ii)*. Available online at: https://skinchakra.eu/blog/archives/411-9-most-important-natural-waxes-for-cosmetics-Part-II.html (accessed February 20 2019).

Dassanayake, L. S. K., Kodali, D. R., and Ueno, S. (2011). Formation of oleogels based on edible lipid materials. *Curr. Opin. Coll. Interf. Sci.* 16, 432–439. doi: 10.1016/j.cocis.2011.05.005

Dassanayake, L. S. K., Kodali, D. R., Ueno, S., and Sato, K. (2009). Physical properties of rice bran wax in bulk and organogels. *J. Am. Oil Chem. Soc.* 86, 1163–1173. doi: 10.1007/s11746-009-1464-6

Doan, C. D., To, C. M., De Vrieze, M., Lynen, F., Danthine, S., Brown, A., et al. (2017). Chemical profiling of the major components in natural waxes to elucidate their role in liquid oil structuring. *Food Chem.* 214, 717–725. doi: 10.1016/j.foodchem.2016.07.123

Ferrari, V., and Mondet, J. (2003). *Inventor; L'Oreal S. A., assignee. Care and/or Make-Up Cosmetic Composition Structured with Silicone Polymers and Organogelling Agents, in Rigid Form.* International WO/2003/105788. Available online at: https://patentscope.wipo.int/search/en/detail.jsf?docId=WO2003105788

Fórmula Botánica (2019). *6 Vegan Waxes for Organic Cosmetic Formulations*. Available online at: https://formulabotanica.com/6-vegan-waxes/ (accessed February 20 2019)

Gandolfo, F. G., Bot, A., and Flöter, E. (2004). Structuring of edible oils by long-chain fa, fatty alcohols, and their mixtures. *J. Am. Oil Chem. Soc.* 81, 1–6. doi: 10.1007/s11746-004-0851-5

Ghamdi, A. K., Al, E.lkholy, T. A., Abuhelal, S., Alabbadi, H., Qahwaji, D., Sobhy, H., et al. (2017). Study of Jojoba (Simmondsia chinensis) oil by gas chromatography. *Nat. Prod. Chem. Res.* 05:283. doi: 10.4172/2329-6836.1000283

Gunstone, F. D. (2002). *Vegetable Oils in Food Technology: Composition, Properties, and Uses*. Copenhagen: Blackwell Publishing Ltd.

Han, L., Li, L., Li, B., Zhao, L., Liu, G. Q., Liu, X., et al. (2014). Structure and physical properties of organogels developed by sitosterol and lecithin with sunflower oil. *J. Am. Oil Chem. Soc.* 91, 1783–1792. doi: 10.1007/s11746-014-2526-y

Hildebrand, J. H., and Robert-Lane, S. (1950). *The Solubility of Nonelectrolytes (3rd edn)*. New York, N.Y. : Reinhold.

Hwang, H. S., Sanghoon, K., Mukti, S., Jill, K. W. M., and Liu, S. X. (2012). Organogel formation of soybean oil with waxes. *J. Am. Oil Chem. Soc.* 89, 639–647. doi: 10.1007/s11746-011-1953-2

Hwang, H. S., Singh, M., Winkler-Moser, J. K., Bakota, E. L., and Liu, S. X. (2014). Preparation of margarines from organogels of sunflower wax and vegetable oils. *J. Food Sci.* 79, C1926–C1932. doi: 10.1111/1750-3841.12596

Lam, R. S. H., and Rogers, M. A. (2011). Activation energy of crystallization for trihydroxystearin, stearic acid, and 12-hydroxystearic acid under nonisothermal cooling conditions. *Crystal Growth Design* 11, 3593–3599. doi: 10.1021/cg200553t

López-Martínez, A., Morales-Rueda, J. A., Dibildox-Alvarado, E., Charó-Alonso, M. A., Marangoni, A. G., and Toro-Vazquez, J. F. (2014). Comparing the crystallization and rheological behavior of organogels developed by pure and commercial monoglycerides in vegetable oil. *Food Research Intern.* 64, 946–957. doi: 10.1016/j.foodres.2014.08.029

Marangoni, A. G., and Garti, N. (2011). *Edible Oleogels Structure and Health Implications*. Indiana, IL: AOCS Press.

Marangoni, A. G., and Garti, N. (2018). *Edible Oleogels Structure and Health Implications. 2nd Edn*. Indiana, IL: AOCS Press.

Martínez-Ávila, M., De la Peña-Gil, A., Álvarez-Mitre, F. M., Charó-Alonso, M. A., and Toro-Vazquez, J. F. (2019). Self-assembly of saturated and unsaturated phosphatidylcholine in mineral and vegetable oils. *J. Am. Oil Chem. Soc*. 96, 273–289. doi: 10.1002/aocs.12188

McGann, M. R., and Lacks, D. J. (1999). Chain length effects on the thermodynamic properties of n-alkane crystals. *J. Phys. Chem. B* 103, 2796–2802. doi: 10.1021/jp983932m

Mezger, T. G. (2014). *The Rheology Handbook: For Users of Rotational and Oscillatory Rheometers (4th edn)*. Hanover: Vincentz Network.

Morales, M., Gallardo, V., Clarés, B., García, M., and Ruiz, M. (2010). Study and description of hydrogels and organogels as vehicles for cosmetic active ingredients. *J. Cosm. Sci*. 60, 627–636. doi: 10.1111/j.1468-2494.2010.00580_4.x

Morales-Rueda, J. A., Dibildox-Alvarado, E., Charó-Alonso, M. A., Weiss, R. G., and Toro-Vazquez, J. F. (2009). Thermo-mechanical properties of candelilla wax and dotriacontane organogels in safflower oil. *Eur. J. Lipid Sci. Technol*. 111, 207–215. doi: 10.1002/ejlt.200810174

Ojijo, N. K. O., Neeman, I., Eger, S., and Shimoni, E. (2004). Effects of monoglyceride content, cooling rate and shear on the rheological properties of olive oil/monoglyceride gel networks. *J. Sci. Food Agric*. 84, 1585–1593. doi: 10.1002/jsfa.1831

Pal, A., Shibu, A., Michael, A. R., Joykrishna, D., and Richard, G. W. (2013). Comparison of dipolar, H-bonding, and dispersive interactions on gelation efficiency of positional isomers of keto and hydroxy substituted octadecanoic acids. *Langmuir* 29, 6467–6475. doi: 10.1021/la400664q

Patel, A. R., Babaahmadi, M., Lesaffer, A., and Dewettinck, K. (2015). Rheological profiling of organogels prepared at critical gelling concentrations of natural waxes in a triacylglycerol solvent. *J. Agric. Food Chem*. 63, 4862–4869. doi: 10.1021/acs.jafc.5b01548

Perez-Nowak, V. (2012). *Inventor; L'Oreal, S. A., Assignee. Fluid Cosmetic Composition, Useful for Making Up and/or Caring the Skin and/or Lips, Comprises Polyester, Non-Volatile Silicone Oil, Organogelling Agent Comprising N-Acylglutamides e.g. N-Lauroylglutamic Acid Dibutylamide, and Wax*. France patent FR2975296A1 (2012). Available online at: https://patents.google.com/patent/FR2975296A1/en?oq=FR+Patent+2975296+A1

Rocha-Amador, O. G., Gallegos-Infante, J. A., Huang, Q., Rocha-Guzman, N. E., Rociomoreno-Jimenez, M., and Gonzalez-Laredo, R. F. (2014). Influence of commercial saturated monoglyceride, mono-/diglycerides mixtures, vegetable oil, stirring speed, and temperature on the physical properties of organogels. *Intern. J. Food Sci*. 1–8. doi: 10.1155/2014/513641

Rogers, M. A., and Marangoni, A. G. (2008). Non-isothermal nucleation and crystallization of 12-hydroxystearic acid in vegetable oils. *Crys. Growth Design* 8, 4596–4601. doi: 10.1021/cg8008927

Rogers, M. A., Strober, T., Bot, A., Toro-Vazquez, J. F., Stortz, T., and Marangoni, A. G. (2014). Edible oleogels in molecular gastronomy. *Intern. J. Gastron. Food Sci*. 2, 22–31. doi: 10.1016/j.ijgfs.2014.05.001

Sagiri, S. S., Singh, V. K., Pal, K., Banerjee, I., and Basak, P. (2015). Stearic acid based oleogels: A study on the molecular, thermal and mechanical properties. *Mater. Sci. Eng. C* 48, 688–699. doi: 10.1016/j.msec.2014.12.018

Toro-Vazquez, J. F., Mauricio-Pérez, R., González-Chávez, M. M., Sánchez-Becerril, M., Ornelas-Paz, J., de, J., et al. (2013a). Physical properties of organogels and water in oil emulsions structured by mixtures of candelilla wax and monoglycerides. *Food Res. Intern*. 54, 1360–1368. doi: 10.1016/j.foodres.2013.09.046

Toro-Vazquez, J. F., Morales-Rueda, J., Torres-Martínez, A., Charó-Alonso, M. A., Mallia, V. A., and Weiss, R. G. (2013b). Cooling rate effects on the microstructure, solid content, and rheological properties of organogels of amides derived from stearic and (R)-12- hydroxystearic acid in vegetable oil. *Langmuir* 29, 7642–7654. doi: 10.1021/la400809a

Toro-Vazquez, J. F., Morales-Rueda, J. A., Dibildox-Alvarado, E., Charó-Alonso, M. A., Alonzo-Macias, M., and González-Chávez, M. M. (2007). Thermal and textural properties of organogels developed by candelilla wax in safflower oil. *J. Am. Oil Chem. Soc*. 84, 989–1000. doi: 10.1007/s11746-007-1139-0

Toro-Vazquez, J. F., and Pérez-Martínez, J. D. (2018). "Thermodynamic aspects of molecular gels," in *Monographs in Supramolecular Chemistry*, ed R. G. Weiss (London: Royal Society of Chemistry), 57–87. doi: 10.1039/9781788013147-00057

Toro-Vazquez, J. F., Rangel-Vargas, E., Dibildox-Alvarado, E., and and. Charó-Alonso, M. A. (2005). Crystallization of cocoa butter with and without polar lipids evaluated by rheometry, calorimetry and polarized light microscopy. *Eur. J. Lipid Sci. Technol*. 107, 641–55. doi: 10.1002/ejlt.200501163

Conflict of Interest: The authors declare that the research was conducted in the absence of any commercial or financial relationships that could be construed as a potential conflict of interest.

frontiers in Sustainable Food Systems

MINI REVIEW
published: 15 September 2020
doi: 10.3389/fsufs.2020.00139

A Critical Review of the Last 10 Years of Oleogels in Food

*Clifford Park and Farnaz Maleky**

Department of Food Science and Technology, The Ohio State University, Columbus, OH, United States

The field of oleogel research has been active in recent decades, generating numerous oleogels with desirable properties like thermal resistance, texture, and structural stability. Moreover, several food matrices have been formulated with oleogels. In some cases, oleogels in these food products have been shown to resemble textural attributes of products made with conventional hardstock fat, to enhance dietary nutrition, to demonstrate high physical and oxidative stability, and to exhibit a high oil binding capacity. These innovations clearly illustrate the potential of the field of oleogels, but certain drawbacks and a lack of in-depth information in various aspects have delayed its commercialization in the food industry. This review aims to update the current status of the oleogel field and to cover some areas that need to be addressed to make oleogel foods a reality in the near future.

Keywords: oleogel, food grade gelators, trans-fat replacer, oleogel's physical properties, oleogel's oxidation

OPEN ACCESS

Edited by:
Stephen Robert Euston, Heriot-Watt University, United Kingdom

Reviewed by:
Khakhanang Wijarnprecha, Ryerson University, Canada
Lilia Ahrné, University of Copenhagen, Denmark

****Correspondence:***
Farnaz Maleky
maleky.1@osu.edu

Specialty section:
This article was submitted to Sustainable Food Processing, a section of the journal Frontiers in Sustainable Food Systems

Received: *14 May 2020*
Accepted: *03 August 2020*
Published: *15 September 2020*

Citation:
Park C and Maleky F (2020) A Critical Review of the Last 10 Years of Oleogels in Food. Front. Sustain. Food Syst. 4:139. doi: 10.3389/fsufs.2020.00139

INTRODUCTION

In response to nutritionists' recommendations and governmental legislations for replacing saturated and trans fats in food, the field of oil structuring has been extensively investigated in recent decades (Hughes et al., 2009; Astrup et al., 2019). In particular, oleogels have emerged as a promising potential means of replacing hardstock fats in food systems. Oleogels can be characterized as semisolid systems in which continuous liquid phases are physically immobilized by self-assembled networks of gelators (Hughes et al., 2009; Rogers et al., 2014). Under the premise of improving nutrition and the well-being of consumers, oleogels are often structured with healthy liquids oils while exhibiting acceptable solid-like behavior. Despite the recent exponential growth in the oleogel field, the use of oleogels is still in the early stages of development due to a number of challenges. These challenges include the food regulations that not only require food grade gelators, but also impose restrictions on gelator concentrations in food products. So far, various oleogels with different classes of gelators have been formulated, but not all of them are food grade. Other limitations include the lack of knowledge of and uncertainties about their interaction with other food ingredients, how they behave under different processing conditions for different food products, and the need for inexpensive and easily-accessible food grade gelators. This review will evaluate the progress in the field of oleogel and discuss other key shortcomings that need to be addressed in future work.

EDIBLE OLEOGEL APPLICATIONS IN FOOD

Due to a growing surge in enthusiasm for the development of oleogels with desirable physical characteristics, recently various forms of oleogels have been produced with different combinations of gelators and vegetable oils.

As listed in **Table 1**, many food products including meat products, dairy, spreads, confectionaries, and pastries have been formulated with oleogels. Detailed information about gelators utilized in edible oleogels as well as oleogelation mechanisms can be found in the references listed in **Table 1** and other studies in the field. Although the substitution of saturated fat seems to be the major objective for oleogel application, these studies documented that oleogels can also offer other functionalities such as texture, thermal-reversible properties, oil binding capacity, and delivery of bioactive compounds. For instance, Patel et al. (2014a) formulated cakes with methylcellulose (MC) oleogels and documented similar hardness and chewiness to those made with shortening. In another study, emulsion-based shellac oleogels were shown to crystallize emulsion phases and water-oil interfaces, stabilizing the emulsion for 4 months (Patel et al., 2014b). In addition, cookies made with wax oleogels showed oil binding capacity above 93% with a minimum oil loss for 30 days (Fayaz et al., 2017). Stortz and Marangoni (2011) produced a heat resistant chocolate made with ethylcellulose (EC) oleogel, resisting melting up to 86°C. Lastly, O'Sullivan et al. (2017) incorporated β-carotene in EC oleogels and demonstrated that the oleogelation reduced the degradation of β-carotene compared to β-carotene in just oil, thus elevating its bioaccessibility. These examples serve as a library of possible beneficial oleogel properties suitable for food applications. However, it is important to remember that not all oleogels offer the aforementioned functionalities.

The appropriate selection of oils and oleogels is very important in providing successful products. For instance, Huang et al. (2018), who structured high oleic acid soybean oil into processed cheese products, reported that in a comparison of rice bran wax (RBW) and sunflower wax (SW), only RBW oleogels were able to mimic hardness of a milk fat control. This was shown to be related to chemical compositions of SW and RBW gelators. In particular, RBW consists of about 100% wax ester compared to sunflower (77% wax ester), which significantly affected physical properties of the cheese products (Huang et al., 2018). Yilmaz and Ögütcü (2015a) showed different hardness for SW oleogels

TABLE 1 | Examples of oleogel applications in food product formulation.

Food products	Liquid oil type	Organogelator type	References
MEAT PRODUCTS			
Frankfurter	Soybean; canola; sunflower	Rice bran wax; ethylcellulose; γ-oryzanol and phytosterol	Zetzl et al., 2012; Panagiotopoulou et al., 2016; Wolfer et al., 2018
Meat patties	Linseed; sesame	Oryzanol and β-sitosterol; beeswax	Moghtadaei et al., 2018; Martins et al., 2019
DAIRY PRODUCTS			
Cream cheese and processed cheese products	High oleic soybean; soybean;	Rice bran wax; ethycellulose and sunflower wax	Bemer et al., 2016; Huang et al., 2018; Park et al., 2018
Ice cream	High oleic sunflower; sunflower	Rice bran wax; γ-oryzanol and phytosterols	Zulim Botega et al., 2013; Moriano and Alamprese, 2017
SPREADS			
Margarine	Soybean	Sunflower wax, rice bran wax, and candelilla wax	Hwang et al., 2013
Spread	Sunflower; virgin olive and hazelnut	Shellac wax; beeswax and sunflower wax	Patel et al., 2014b; Yilmaz and Ögütcü, 2015a
CONFECTIONARIES			
Chocolate paste	Sunflower; pomegranate seed and palm	Shellac wax; monoglyceride, beeswax, and propolis wax	Patel et al., 2014b; Fayaz et al., 2017
Chocolate	Sunflower; hydrogenated palm kernel	γ-oryzanol and β-sitosterol; ethycellulose	Stortz and Marangoni, 2013; Wendt et al., 2017
Filling	Rice bran and palm; canola	Beeswax; hydroxypropyl methylcellulose and methylcellulose	Doan et al., 2016; Tanti et al., 2016a
PASTRIES			
Cookie	Refined hazelnut; canola; rice bran oil	Beeswax and sunflower wax; candelilla wax; bleached rice bran wax	Jang et al., 2015; Yilmaz and Ögütcü, 2015b; Pandolsook and Kupongsak, 2017
Cake	Sunflower; cotton and high oleic sunflower	Beeswax, candelilla wax, and rice bran wax; carnauba wax	Oh et al., 2017; Pehlivanoglu et al., 2018
OTHER APPLICATIONS			
Oleogels as carriers of bioactive compounds	High oleic sunflower; canola	Beeswax with β-carotene; ethylcellulose with β-carotene	Martins et al., 2017; O'Sullivan et al., 2017

made with hazelnut vs. virgin olive oils. **Figure 1** shows network comparisons of oleogel cream cheese products developed by Bemer et al. (2016) who replaced the milk fat with EC or RBW oleogels. Although the authors demonstrated the similarity of the morphology and distribution of the fat globules in oleogel cream cheeses (either made with EC or RBW) to the control product, it seems EC and RBW had different effects on the protein networks. The EC oleogel networks contained small lipid globules dispersed throughout a continuous protein matrix, while the RBW oleogel created a denser protein network compared to the EC samples. Overall, these examples show that while the combinations of oils and gelators are important for food production, their interactions with other food ingredients need careful evaluations.

NUTRITIONAL FUNCTIONALITIES OF OLEOGELS

Clearly, one major aim of oleogel development is to improve the health benefits of fatty food products. As expected, certain oleogel-based food products have been shown to contain healthier nutritional profiles compared to those made with conventional hardstock fats. For example, Bemer et al. (2016) incorporated RBW oleogels in cream cheese products and showed that replacing milkfat led to a 120% increase in unsaturated fat content and about a 90% reduction in saturated fat content. Bologna-type sausages formulated with oleogels replacing pork back fats showed about a 6% reduction in total saturated fat content and up to 21.15% increase in oleic acid levels (da Silva et al., 2019). A similar trend was observed in meat patties made with hydroxypropyl methylcellulose (HPMC) oleogels (Oh et al., 2019). These results clearly illustrate oleogels' capability for enhancing food nutrition; however, the digestibility of these products and their consumption for people with different diets is still not studied.

Some oleogels, particularly those made with EC and some waxes, have high melting points (70 ∼ 135°C) that may impact the meltability of lipid networks in human body temperature. Moreover, oleogels with low meltability may retard the release of the lipid matrix, hence possibly influencing the overall metabolism of oleogel food. To better validate oleogel usage in food, clinical trials with human subjects are necessary. As a

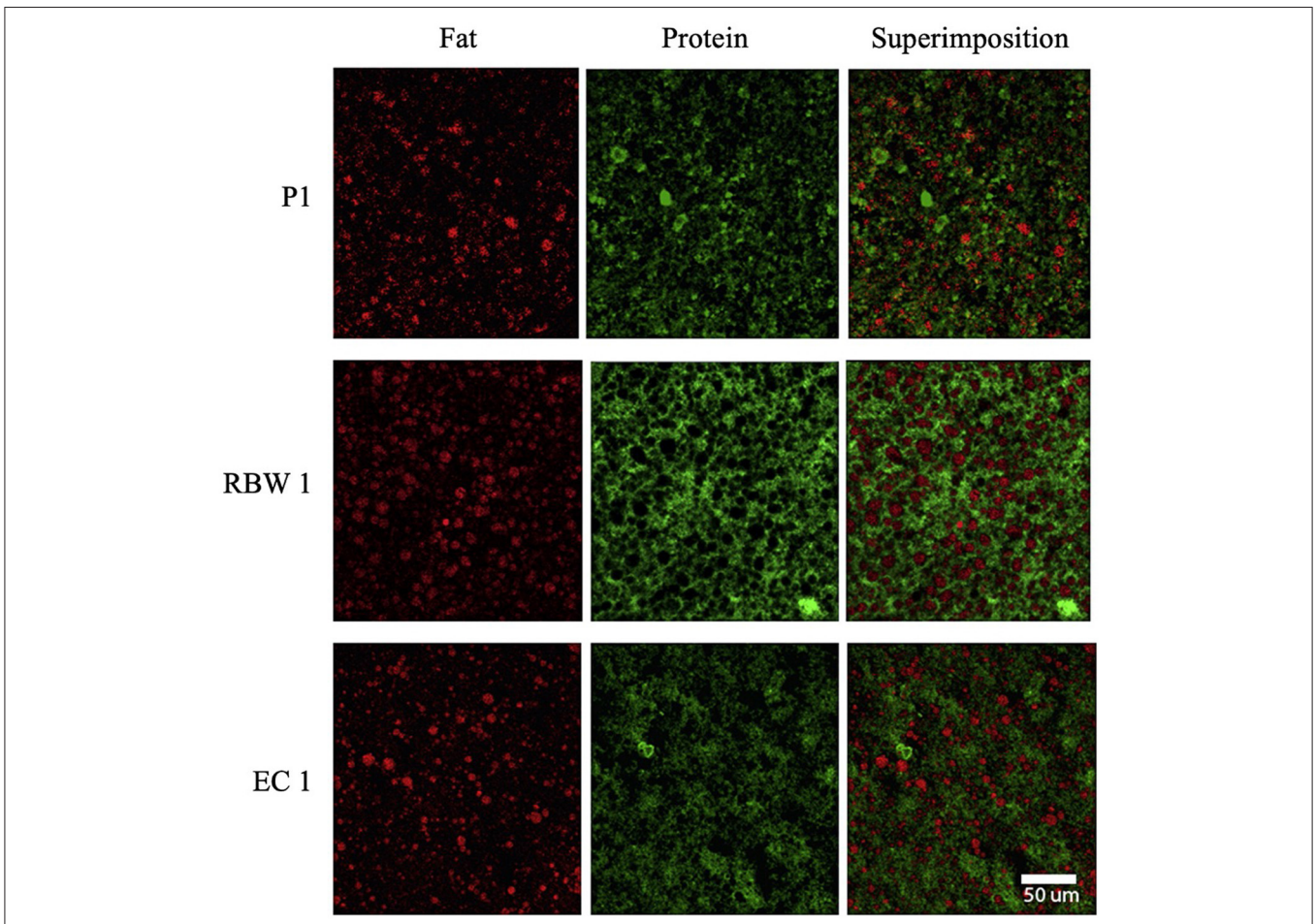

FIGURE 1 | Microstructure of commercial cream cheese (P1) and rice bran wax (RBW 1) and ethylcellulose (EC 1) oleogel cream cheese products. Lipids and proteins shown in red and green, respectively. Adopted from Bemer et al. (2016) with permission from Elsevier.

response to this need, some studies monitored the metabolism of oleogel food products. For example, Stortz et al. (2012) showed that mean serum triacylglycerol and free fatty acid levels from 12 young individuals consuming meals containing oleogels (2% 12-hydroxystearic acid and canola oil) were significantly lower compared to those who had meals with butter and margarine. Another study by Tan et al. (2017) reported higher blood triglycerides levels in 16 participants who consumed a meal with coconut oil compared to those consumed coconut oleogel gelled with 11% w/w EC. Such findings highlighted the effects of oleogelation on the digestion of fats and suggested that structural properties of oleogels may either restrict the absorption of dietary lipids or require a longer interval for lipids to be digested. Similarly, O'Sullivan et al. (2017), who studied the bioaccessibility of EC oleogels through *in vitro* digestion, noted that the lipid lipolysis percentage of EC oleogels was significantly lower than that of canola oil. The authors linked this finding with greater mechanical properties of the EC oleogels compared to the oil. Specifically, the former was more resistant to the mechanical breakdown, impeding the release of oil from the gel matrix and subsequently lowering the lipid lipolysis rate. These results may also be attributed to the high melting points of EC oleogels (135°C) and its meltability in the human body (Davidovich-Pinhas et al., 2015). Using human trials, Marangoni et al. (2007) noted that unlike liquid oil, a consumption of monoglyceride structured emulsion oleogel lowered serum triglyceride and insulin levels. This result suggested that oleogel matrices could be engineered in a way that they can modulate physiological responses of nutrient metabolism and provide healthier nutrition for consumers. However, Wright et al. (2014) observed that when this monoglyceride emulsion oleogel was baked in cookies and cakes, both serum triglyceride and insulin levels of human panelists were comparable to those who consumed ungelled oleogels.

All of these studies clearly document the complexity in the metabolism of oleogels and oleogel-formulated food products. It is also important to consider that not only the structure and composition of oleogels, but also the food formulations and their network formations can influence the digestion of oleogel food. Considering the high melting points of oleogels and the thermal processing required for their engineering, possible thermal degradation of final products needs investigations, as well. Oils and other micronutrients are prone to the oxidation that causes nutritional degradations and development of off-flavors. The review of studies on oil oxidation in some oleogel food products is provided in the stability section of this paper. However, no data was found on the effects of oleogelation on the nutritional properties of non-oil compounds. Robust clinical trials on oleogel food products evaluating how the structural and processing parameters required for oleogelation influence metabolism would help define values of oleogels for food applications. Considering a greater number of participants in different spectrums of age groups could also result in more conclusive findings.

TEXTURAL PROPERTIES OF OLEOGELS FOR FOOD APPLICATIONS

In addition to nutritional improvements, one of the main objectives of oleogel use is mimicking textural functionality of trans and hardstock fats. Although some studies reported acceptable consistency and appearance for oleogel products, not all of them demonstrated satisfying textural attributes compared to saturated fat controls. Frankfurters made with EC oleogels showed similar hardness and chewiness values compared to the beef fat controls, and the authors connected these results to the samples' similar microstructure (Zetzl et al., 2012). The authors' finding regarding the role of oleogel microstructure on the texture of oleogel food may be seen better in the comparison of the effects of different gelators on vegetable oil structuring, shown in **Figure 2**. Oleogels made with monoglycerides (**Figure 2A**) show large plate-like shapes of crystals (López-Martínez et al., 2014) while fibrous oleogel microstructures are obtained from phytosterols (**Figure 2B**) (Sawalha et al., 2013). **Figure 2C** shows thin fibrillar crystals with a branching out pattern in oleogels structured with 12-hydroxystearic acid (Co and Marangoni, 2013). Interestingly, ethylcellulose gelators are shown to create polymer-like oleogel networks with numerous pockets or holes between polymers as illustrated in **Figure 2D** (Zetzl et al., 2014). As expected, oleogels made with different waxes exhibit considerably different matrices. For instance, **Figure 2E** shows small linear crystal particles of candelilla wax oleogels (Patel et al., 2015) while thin needle-like crystal morphologies are reported for sunflower wax oleogels (**Figure 2F**) (Yilmaz and Ögütcü, 2014). These examples clearly indicate that oleogels structured with various gelator types generate different microstructural properties that may subsequently affect physical properties of the oleogels and the food made of them. It is also important to remember that processing parameters (cooling rate, gelator concentrations, oil-gelator combinations, etc.) can influence the oleogel formations (Blake and Marangoni, 2015). Patel et al. (2014a) documented the effects of oleogelation on minimizing crosslinking of the gluten network in MC oleogel cakes. In that study, the hardness and chewiness of cakes made with just sunflower oil considerably increased (due to the crosslinking of gluten) over time while those of the MC oleogel cakes changed considerably less. This was due to the MC oleogel acting as a physical barrier that helped reduce the movement of gluten networks (Patel et al., 2014a). The successful applications of oleogels on hardness, spreadability, and stickiness in cream cheese and processed cheese products are also reported by the Maleky group (Bemer et al., 2016; Huang et al., 2018). As mentioned before, the authors linked their observation to the similarity in the solid fat network between the oleogels and controlled products.

As anticipated, not all oleogel systems can provide mechanical properties comparable to the solid fat products, thus requiring investigations on various gelator concentrations or liquid oil compositions. For instance, Huang et al. (2018) structured processed cheese products with RBW or SW oleogels at wax concentrations of 0.5 or 1% and reported that SW oleogels

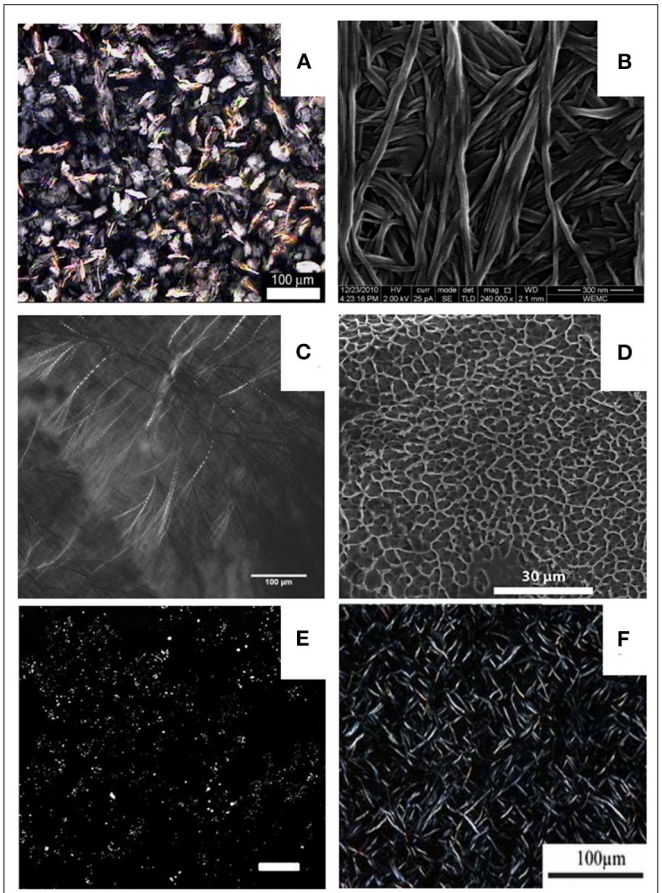

FIGURE 2 | Microstructures of oleogels structured with **(A)** monoglycerides in high oleic safflower oil (adopted from López-Martínez et al., 2014 with permission from Elsevier), **(B)** phytosterol tubules in sunflower oil (adopted from Sawalha et al., 2013 with permission from Wiley-VCH), **(C)** 12-hydroxystearic acid in canola oil (adopted from Co and Marangoni, 2013 with permission from Wiley-VCH), **(D)** ethylcellulose in canola oil (adopted from Zetzl et al., 2014 with permission from Elsevier), **(E)** candelilla wax in high oleic sunflower oil with a scale bar of 50 µm (adopted from Patel et al., 2015 with permission from ACS Publications), and **(F)** sunflower wax in olive oil (adopted from Yilmaz and Ögütcü, 2014 with permission from Wiley-VCH).

were not able to mimic hardness of the control cheese product. Specifically, only 1% RBW oleogel showed comparable hardness to the control. As previously stated, this could be due to the higher wax ester content of RBW compared to SW, however further analysis is required to clarify the observed discrapany. In a comparison of oleogel cookies with those made with shortening, Yilmaz and Ögütcü (2015b) reported lower hardness and higher fracturability for cookies made of hazelnut oil and 5% beeswax or sunflower wax. Interestingly, the same group reported comparable texture and acceptability for the oleogel and control cookies based on hedonic tests performed with 200 participants (Yilmaz and Ögütcü, 2015b). The observed discrepancy in the textural assessment of those cookies between panelists and a texture analyzer instrument clearly shows challenges of accurately assessing texture of oleogels and oleogel food using just instrumental analyses. Another example of unsuccessful oleogel application in texture mimicking is shown in meat patties made with various concentrations of HPMC oleogels (Oh et al., 2019). Oh et al. reported different tenderness and juiciness in oleogel samples due to their inherently different solid fat content, hardness, and storage modulus values; 30 panelists confirmed the samples' discrepancies.

These findings highlight that although certain oleogel matrices are able to mimic textural properties of hardstock fats, predicting how consumers will perceive the final physical properties of oleogel-formulated food remains challenging. So far, there are numerous studies describing textural attributes of oleogels and/or oleogel food, but not so many sensory evaluations have been conducted (Rogers et al., 2014). This lack of sensory evaluation may be attributed to challenges of designing sensory testing, requiring safe protocols (e.g., types and concentrations of gelators), and ensuring that oleogel food products are safe for consumption. Another limitation could be possible off-flavors and odors that oleogel foods may generate. Previously, Bemer et al. (2016) showed that panelists detected off-flavor and bitterness from the RBW oleogel cream cheese products, suggesting an area of the oleogel field that needs to be investigated. Although the aforementioned challenge in oleogel cream cheese remains untouched, similar analysis and information on other products may help identify optimal oleogels for specific food applications. This type of analysis is needed to increase the consumer acceptance of oleogel food.

OLEOGEL STABILITY IN FOOD SYSTEMS

Oil binding capacity, which refers to how strongly oil is bound in a given network, is a challenging phenomenon for many food producers. Food products with a low oil binding capacity release oil and undergo oil migration, which negatively affects their textural and sensory attributes. Considering the relatively low solid fat content of many oleogels and their high liquid oil content, appropriate processing and storage conditions are necessary for optimal oil retention. Several studies developed oleogels with different gelators and showed a linear relationship between mechanical strength of gels and oil binding capacity, suggesting that oleogels could minimize the oil loss when designed with greater mechanical strength and tightly arranged networks (Fayaz et al., 2017; da Silva et al., 2018; Meng et al., 2018). Blake and Marangoni (2015) illustrated that the oil binding capacity of wax oleogels can be improved by increasing wax concentrations and/or fast cooling, last of which forms a homogenous distribution of small fat crystals and subsequently small areas of pore space. Currently, limited information is available on the oil binding capacity of oleogel-formulated food. Processed cheese products made with 0.5% RBW showed a marginal oil loss of 0.53% after 24 h of storage at 20°C (Huang et al., 2018). In that study, increasing RBW concentration to 1% led to a lower oil loss around 0.34%. A study by Tanti et al. (2016b) also demonstrated that no oil loss was observed for peanut butters when stabilized with 2.2% of freeze-dried HPMC and MC. These results are promising, but oil loss

may be problematic for an industrial scale shearing process. It is also important to consider food regulations limiting high concentrations of gelators (e.g., FDA approves up to 3% of RBW in food). Additionally, dramatic changes in processing and crystallization temperature may influence other functional characteristics of the final products including polymorphic, microstructural, and physical properties. Clearly, more work is needed to examine how well other forms of oleogels preserve their physical entities and prevent the oil leakage and mass transfer in various food networks.

Another factor associated with oil stability is its oxidation and thermal degradation. As mentioned earlier, thermal processing required for oleogelation can induce lipid oxidation (Rogers et al., 2014). Studies reported peroxide values increased in oleogels post-processing as well as during storage (Gravelle et al., 2012; Yilmaz and Ögütcü, 2014; Park et al., 2018). Although, the reported peroxide values were under 10 mEq/kg, the value that is considered as rancid oil (Sebastian et al., 2014), further analysis on peroxide degradation and secondary oxidation during the oleogelation processing is not provided for many oleogel food products. Interestingly, some studies showed a reduction in the oil oxidation during the storage and post-processing of oleogels and oleogel food products. For example, Pandolsook and Kupongsak (2019) showed that RBW oleogels and water-in-oil emulsions made with RBW oleogels stored at 4 and 30 °C exhibited a higher oxidative stability compared to their controls (rice bran oil and emulsion, respectively) at both temperatures. Certain studies even documented further stability of the oils when oleogel networks were incorporated in food matrices. For example, Park et al. (2018) reported a lower aldehyde content in RBW oleogel cream cheeses compared to the oleogel itself while documenting no change in aldehyde content for 2 weeks. Oleogelation also significantly reduced the oxidation in bologna-type sausages and fish oil oleogels compared to control sausages made with pork back fat and fish oil, respectively (Hwang et al., 2018; da Silva et al., 2019). Low temperature storage (4°C) of frankfurters structured with sunflower oil and γ-oryzanol and phytosterol showed similar aldehyde content compared to controls for 30 days (Panagiotopoulou et al., 2016). Although these findings suggest that the oleogelations with carefully designed formulations, processing, and post-processing conditions may reduce the oxidation, not all oleogel systems exhibited good oxidative stability. Martins et al. (2017) reported a significantly greater amount of aldehyde formation over 20 days of storage in beeswax oleogels. Frankfurter-type sausages constructed with 10% RBW oleogels also generated significantly higher amounts of aldehyde compared to those made with pork fat (Wolfer et al., 2018). Meat patties structured with HPMC oleogels also showed a significantly lower oxidative stability compared to patties made with beef tallow (Oh et al., 2019). To overcome this issue, the authors suggest increasing the gelator concentrations for a greater oxidative stability. This increase may not be a good solution for many products considering the legislations on gelator concentrations and the effects of gelator concentrations on other physical properties of the product.

Hence, the assessment of oxidative stability of oleogels in food products needs further investigation. Performing multiple tests (e.g., both primary and secondary oxidation analyses) may address the lack of information regarding the oxidative stability of oleogel-formulated food. It would be also beneficial if future studies monitor the effects of the incorporation of lipid soluble antioxidants to the liquid oils on the minimization of the lipid oxidation of oleogel food.

CONCLUSION

The field of oleogels has grown extensively in the last decade, generating various food products with oleogels. However, to fulfill its potential usage in food products, there is a need for further investigations on various dimensions. In order to validate the oleogel applications in food to replace hardstock fats, the overall impact of oleogel digestion/metabolism must be clearly understood. In addition, acquiring detailed information regarding physical and oxidative stability of oleogels and their behavior in the presence of other ingredients and food matrices may advance oleogels utilization in many food products. Flavor development, textural qualities, and physical properties of oleogels and oleogel-formulated food must be also evaluated by sensory panels. Doing so may play a key role on the consumer acceptance of oleogel food products. While there are great potentials for oleogel applications in food products, more information is needed before the widespread use. Bridging the aforementioned knowledge gaps may play key roles on the future success of the oleogel field and increase the consumer acceptance of oleogel food products.

AUTHOR CONTRIBUTIONS

All authors listed have made a substantial, direct and intellectual contribution to the work, and approved it for publication.

REFERENCES

Astrup, A., Bertram, H. C. S., Bonjour, J. P., de Groot, L. C. P., Otto, M. C. D. O., Feeney, E. L., et al. (2019). WHO draft guidelines on dietary saturated and trans fatty acids: time for a new approach? *BMJ* 366, 1–6. doi: 10.1136/bmj.l4137

Bemer, H. L., Limbaugh, M., Cramer, E. D., Harper, W. J., and Maleky, F. (2016). Vegetable organogels incorporation in cream cheese products. *Food Res. Int.* 85, 67–75. doi: 10.1016/j.foodres.2016.04.016

Blake, A. I., and Marangoni, A. G. (2015). The use of cooling rate to engineer the microstructure and oil binding capacity of wax crystal networks. *Food Biophys.* 10, 456–465. doi: 10.1007/s11483-015-9409-0

Co, E., and Marangoni, A. G. (2013). The formation of a 12-hydroxystearic acid/vegetable oil organogel under shear and thermal fields. *J. Am. Oil Chem. Soc.* 90, 529–544. doi: 10.1007/s11746-012-2196-6

da Silva, S. L., Amaral, J. T., Ribeiro, M., Sebastiao, E. E., Vargas, C., de Lima Franze, F., et al. (2019). Fat replacement by oleogel rich in oleic acid and its impact on the technological, nutritional, oxidative, and sensory properties of Bologna-type sausages. *Meat Sci.* 149, 141–148. doi: 10.1016/j.meatsci.2018.11.020

da Silva, T. L. T., Arellano, D. B., and Martini, S. (2018). Physical properties of candelilla wax, monoacylglycerols, and fully hydrogenated oil oleogels. *J. Am. Oil Chem. Soc*. 95, 797–811. doi: 10.1002/aocs.12096

Davidovich-Pinhas, M., Barbut, S., and Maraongoni, A. G. (2015). The gelation of oil using ethyl cellulose. *Carbohydr. Polym*. 117, 869–878. doi: 10.1016/j.carbpol.2014.10.035

Doan, C. D., Patel, A. R., Tavernier, I., De Clercq, N., Van Raemdonck, K., Van de Walle, D., et al. (2016). The feasibility of wax-based oleogel as a potential co-structurant with palm oil in low-saturated fat confectionery fillings. *Eur. J. Lipid Sci. Tech*. 118, 1903–1914. doi: 10.1002/ejlt.201500172

Fayaz, G., Goli, S. A. H., Kadivar, M., Valoppi, F., Barba, L., Calligaris, S., et al. (2017). Potential application of pomegranate seed oil oleogels based on monoglycerides, beeswax and propolis wax as partial substitutes of palm oil in functional chocolate spread. *LWT* 86, 523–529. doi: 10.1016/j.lwt.2017.08.036

Gravelle, A. J., Barbut, S., and Marangoni, A. G. (2012). Ethylcellulose oleogels: manufacturing considerations and effects of oil oxidation. *Food Res. Int.* 48, 578–583. doi: 10.1016/j.foodres.2012.05.020

Huang, H., Hallinan, R., and Maleky, F. (2018). Comparison of different olegels in processed cheese products formulation. *Int. J. Food Sci*. 53, 2525–2534. doi: 10.1111/ijfs.13846

Hughes, N. E., Marangoni, A. G., Wright, A. J., Rogers, M. A., and Rush, J. W. E. (2009). Potential food applications of edible oil organogels. *Trends Food Sci. Technol*. 20, 470–480. doi: 10.1016/j.tifs.2009.06.002

Hwang, H. S., Fhaner, M., Winkler-Moser, J. K., and Liu, S. X. (2018). Oxidation of fish oil oleogels formed by natural waxes in comparison with bulk oil. *Eur. J. Lipid Sci. Tech*. 120:1700378. doi: 10.1002/ejlt.201700378

Hwang, H. S., Singh, M., Winkler-Moser, J. K., Bakota, E. L., and Liu, S. X. (2013). Margarine from oranogels of plant wax and soybean oil. *J. Am. Oil Chem. Soc*. 90, C1926–1932. doi: 10.1007/s11746-013-2315-z

Jang, A., Bae, W., Hwang, H. S., Lee, H. G., and Lee., S. (2015). Evaluation of canola oil oleogels with candelilla wax as an alternative to shortening in baked goods. *Food Chem*. 187, 525–529. doi: 10.1016/j.foodchem.2015.04.110

López-Martínez, A., Morales-Rueda, J. A., Dibildox-Alvarado, E., Charó-Alonso, M. A., Marangoni, A. G., and Toro-Vazquez, J. F. (2014). Comparing the crystallization and rheological behavior of organogels developed by pure and commercial monoglycerides in vegetable oil. *Food Res. Int*. 64, 946–957. doi: 10.1016/j.foodres.2014.08.029

Marangoni, A. G., Idziak, S. H. J., Vega, C., Batte, H., Ollivon, M., Jantiz, P. S., et al. (2007). Encapsulation-structuring of edible oil attenuates acute elevation of blood lipids and insulin in humans. *Soft Matter*. 3, 183–187. doi: 10.1039/B611985A

Martins, A. J., Cerqueira, M. A., Cunha, R. L., and Vincente, A. A. (2017). Fortified beeswax oleogels: effect of β-carotene on the gel structure and oxidative stability. *Food Funct*. 8, 4241–4250. doi: 10.1039/C7FO00953D

Martins, A. J., Lorenzo, J. M., Franco, D., Vincente, A. A., Cunha, R. L., Pastrana, L. M., et al. (2019). Omega-3 and polyunsaturated fatty acids-enriched hamburgers using sterol-based oleogels. *Eur. J. Lipid Sci. Tech*. 121:1900111. doi: 10.1002/ejlt.201900111

Meng, Z., Qi, K., Guo, Y., Wang, Y., and Liu, Y. (2018). Effects of thickening agents on the formation and properties of edible oleogels based on hydroxypropyl methyl cellulose. *Food Chem*. 246, 137–149. doi: 10.1016/j.foodchem.2017.10.154

Moghtadaei, M., Soltanizadeh, N., and Goli, S. A. H. (2018). Production of sesame oil oleogels based on beeswax and application as partial substitutes of animal fat in beef burger. *Food Res. Int*. 108, 368–377. doi: 10.1016/j.foodres.2018.03.051

Moriano, M. E., and Alamprese, C. (2017). Organogels as novel ingredients for low saturated fat ice creams. *LWT* 86, 371–376. doi: 10.1016/j.lwt.2017.07.034

Oh, I., Lee, J., Lee, H. G., and Lee, S. (2019). Feasibility of hydroxypropyl methylcellulose oleogel as an animal fat replacer for meat patties. *Food Res. Int*. 122, 566–572. doi: 10.1016/j.foodres.2019.01.012

Oh, I. K., Amoah, C., Lim, J., Jeong, S., and Lee, S. (2017). Assessing the effectiveness of wax-based sunflower oil oleogels in cakes as a shortening replacer. *LWT* 86, 430–437. doi: 10.1016/j.lwt.2017.08.021

O′Sullivan, C. M., Davidovich-Pinhas, M., Wright, A. J., Barbut, S., and Marangoni, A. G. (2017). Ethylcellulose oleogels for lipophilic bioactive delivery – effect of oleogelation on in vitro bioaccessibility and stability of beta-carotene. *Food Funct*. 8, 1438–1451. doi: 10.1039/C6FO01805J

Panagiotopoulou, E., Moschakis, T., and Katsanidis, E. (2016). Sunflower oil organogels and organogel-in-water emulsions (part II): implementation in frankfurter sausages. *LWT* 73, 351–356. doi: 10.1016/j.lwt.2016.06.006

Pandolsook, S., and Kupongsak, S. (2017). Influence of bleached rice bran wax on the physiochemical properties of organogels and water-in-oil emulsions. *J. Food Eng*. 214, 182–192. doi: 10.1016/j.jfoodeng.2017.06.030

Pandolsook, S., and Kupongsak, S. (2019). Storage stability of bleached rice bran wax oranogels and water-in-oil emulsions. *J. Food Meas Charact*. 13, 431–443. doi: 10.1007/s11694-018-9957-3

Park, C., Bemer, H. L., and Maleky, F. (2018). Oxidative stability of rice bran wax oleogels and an oleogel cream cheese product. *J. Am. Oil Chem. Soc*. 95, 1267–1275. doi: 10.1002/aocs.12095

Patel, A. R., Babaahmadi, M., Lesaffer, A., and Dewettinck, K. (2015). Rheological profiling of organogels prepared at critical gelling concentrations of natural waxes in a triacylglycerol solvent. *J. Agric. Food Chem*. 63, 4862–4869. doi: 10.1021/acs.jafc.5b01548

Patel, A. R., Cludts, N., Sintang, M. D. B., Lesaffer, A., and Dewettinck, K. (2014a). Edible oleogels based on water soluble food polymers: preparation, characterization and potential application. *Food Funct*. 5, 2833–2841. doi: 10.1039/C4FO00624K

Patel, A. R., Rajarethinem, P. S., Gredowska, A., Turhan, O., Lesaffer, A., De Vos, W. H., et al. (2014b). Edible applications of shellac oleogels: spreads, chocolate paste and cakes. *Food Funct*. 5, 645–652. doi: 10.1039/C4FO00034J

Pehlivanoglu, H., Ozulku, G., Yildirim, R. M., Demirci, M., Toker, O. S., and Sagdic, O. (2018). Investigating the usage of unsaturated fatty acid-rich and low-calorie oleogels as a shortening mimetics in cake. *J. Food Process Pres*. 42:e13621. doi: 10.1111/jfpp.13621

Rogers, M. A., Strober, T., Bot, A., Toro-Vazquez, J. F., Stortz, T., and Marangoni, A. (2014). Edible olegels in molecular gastronomy. *Int. J. Gastron. Food Sci*. 2, 22–31. doi: 10.1016/j.ijgfs.2014.05.001

Sawalha, H., Margry, G., den Adel, R., Venema, P., Bot, A., Flöter, E., et al. (2013). The influence of the type of oil phase on the self-assembly process of γ oryzanol + β-sitosterol tubules in organogel systems. *Eur. J. Lipid Sci. Tech*. 115, 295–300. doi: 10.1002/ejlt.201100395

Sebastian, A., Ghazani, S. M., and Marangoni, A. G. (2014). Quality and safety of frying oils used in restaurants. *Food Res. Int*. 64, 420–423. doi: 10.1016/j.foodres.2014.07.033

Stortz, T. A., and Marangoni, A. G. (2011). Heat resistant chocolate. *Trends Food Sci. Technol*. 22, 201–214. doi: 10.1016/j.tifs.2011.02.001

Stortz, T. A., and Marangoni, A. G. (2013). Ethylcellulose solvent substitution method of preparing heat resistant chocolate. *Food Res. Int*. 51, 797–803. doi: 10.1016/j.foodres.2013.01.059

Stortz, T. A., Zetzl, A. K., Barbut, S., Cattaruzza, A., and Marangoni, A. G. (2012). Edible oleogels in food products to help maximize health benefits and improve nutritional profiles. *Lipid Technol*. 24, 151–154. doi: 10.1002/lite.201200205

Tan, S. Y., Peh, E. W. Y., Marangoni, A. G., and Henry, C. J. (2017). Effects of liquid oil vs. oleogel co-ingested with a carbohydrate-rich meal on human blood triglycerides, glucose, insulin, and appetite. *Food Funct*. 8, 241–249. doi: 10.1039/C6FO01274D

Tanti, R., Barbut, S., and Marangoni, A. G. (2016a). Hydroxypropyl methylcellulose and methylcellulose structured oil as a replacement for shortening in sandwich cookie creams. *Food Hydrocoll*. 61, 329–337. doi: 10.1016/j.foodhyd.2016.05.032

Tanti, R., Barbut, S., and Marangoni, A. G. (2016b). Oil stabilization of natural peanut butter using food grade polymers. *Food Hydrocoll*. 61, 399–408. doi: 10.1016/j.foodhyd.2016.05.034

Wendt, A., Abraham, K., Wernecke, C., Pfeiffer, J., and Flöter, E. (2017). Application of β-sitosterol + γ-oryzanol-structured organogel as migration barrier in filled chocolate products. *J. Am. Oil Chem. Soc*. 94, 1131–1140. doi: 10.1007/s11746-017-3024-9

Wolfer, T. L., Acevedo, N. C., Prusa, K. J., Sebranek, J. G., and Tart,é, R. (2018). Replacement of pork fat in frankfurter-type sausages by soybean oil oleogels structured with rice bran wax. *Meat Sci*. 145, 352–362. doi: 10.1016/j.meatsci.2018.07.012

Wright, A., Pinto, C., Tulk, H., McCluskey, J., Goldstein, A., Huschka, B., et al. (2014). Monoacylglycerol gel offers improved lipid profiles in high and low moisture baked products but does not influence postprandial lipid and glucose responses. *Food Funct*. 5, 882–893. doi: 10.1039/C3FO60596E

Yilmaz, E., and Ögütcü, M. (2014). Comparative analysis of olive oil organogels containing beeswax and sunflower wax with breakfast margarine. *J. Food Sci.* 79, E1732–1738. doi: 10.1111/1750-3841.12561

Yilmaz, E., and Ögütcü, M. (2015a). Oleogels as spreadable fat and butter alternatives: sensory description and consumer perception. *RSC Adv*. 5, 50259–50267. doi: 10.1039/C5RA06689A

Yilmaz, E., and Ögütcü, M. (2015b). The texture, sensory properties and stability of cookies prepared with wax oleogels. *Food Funct*. 6, 1194–1204. doi: 10.1039/C5FO00019J

Zetzl, A. K., Gravelle, A. J., Kurylowicz, M., Dutcher, J., Barbut, S., and Marangoni, A. G. (2014). Microstructure of ethylcellulose oleogels and its relationship to mechanical properties. *Food Struct*. 2, 27–40. doi: 10.1016/j.foostr.2014.07.002

Zetzl, A. K., Marangoni, A. G., and Barbut, S. (2012). Mechanical properties of ethylcellulose oleogels and their potential for saturated fat reduction in frankfurters. *Food Funct*. 3, 327–337. doi: 10.1039/c2fo10202a

Zulim Botega, D. C., Marangoni, A. G., Smith, A. K., and Goff, H. D. (2013). The potential application of bran wax oleogel to replace solid fat and enhance unsaturated fat content in ice cream. *J Food Sci*. 78, C1334–1339. doi: 10.1111/1750-3841.12175

Conflict of Interest: The authors declare that the research was conducted in the absence of any commercial or financial relationships that could be construed as a potential conflict of interest.

frontiers in Sustainable Food Systems

MINI REVIEW
published: 22 October 2020
doi: 10.3389/fsufs.2020.585160

Structuring Edible Oils With Fumed Silica Particles

Catherine P. Whitby [1,2]*

[1] School of Fundamental Sciences, Massey University, Palmerston North, New Zealand, [2] MacDiarmid Institute for Advanced Material and Nanotechnology, Victoria University of Wellington, Wellington, New Zealand

Organogels are often made from solutions of proteins, polymers or fatty acids in oil. The macromolecular species crystallize, or assemble, into mesh structures that inhibit oil flow. This review focuses on using fumed silica nanoparticles as an alternative structuring agent. Fumed silica particles have a unique, branched morphology that means the particles aggregate into three-dimensional, interconnected networks. Two key aspects for formulating edible oleogels are addressed. Advances in our understanding of fumed silica particle aggregation in oil that point toward strategies for tuning the rheological properties of oleogels are examined. Secondly, the factors likely to affect the lipolysis of oils structured used fumed silica particles, and hence the bioavailability of ingredients loaded into the gels, are discussed. The next challenge for these promising materials is to target suitable applications for their use as fat replacement in foods.

Keywords: fumed silica aggregation, fumed silica gel rheology, oleogel, silica-lipid hybrid, fused silica

OPEN ACCESS

Edited by:
Luiz Henrique Fasolin, Campinas State University, Brazil

Reviewed by:
Zhao-Yan Sun, Chinese Academy of Sciences, China
Vesna Radovanović, Environmental Consulting Agency, Serbia

***Correspondence:**
Catherine P. Whitby
c.p.whitby@massey.ac.nz

Specialty section:
This article was submitted to Sustainable Food Processing, a section of the journal Frontiers in Sustainable Food Systems

Received: *19 July 2020*
Accepted: *28 September 2020*
Published: *22 October 2020*

Citation:
Whitby CP (2020) Structuring Edible Oils With Fumed Silica Particles. Front. Sustain. Food Syst. 4:585160. doi: 10.3389/fsufs.2020.585160

INTRODUCTION

Gels made from edible oils are potential replacements for the fat in a range of food products (Martins et al., 2018; Puşcaş et al., 2020). The challenge in reducing the fat content in a food is finding an alternative that performs similar functions (Marangoni et al., 2020). Trans- and saturated fats influence food texture. Fats are structured by triglyceride molecules that crystallize into a space-filling network of colloidal crystals (Tang and Marangoni, 2006; Lupi et al., 2016). The presence of the network imparts an elastic structure, and hence a desirable mouthfeel (Sato and Ueno, 2014; Macias-Rodriguez and Marangoni, 2018). The structure of a food also affects its digestibility and the bioavailability of nutrients (Michalski et al., 2013). This can be due to lipid being trapped within the network, or to the network components interfering with digestion (McClements, 2018). Thus, the choice of gelling agent remains critical (Marangoni and Edmund, 2012; Rogers, 2018). This mini review will examine the strategy of using fumed silica to structure edible oils.

Fumed silica nanoparticles aggregate in vegetable oils and assemble into a three-dimensional network. The presence of the network immobilizes the oil into a solid-like material that holds its shape and does not leak. The focus of the mini review is on how the surface chemistry of fumed silica particles can be manipulated to optimize their effectiveness as structuring agents. The review is divided into three parts. Firstly, the colloid chemistry of fumed silica particles is summarized. Secondly, the relationship between the structure of the networks and the organogel rheology is described. Finally, the impact of the particles on the rate of lipid digestion and release of encapsulated ingredients is considered.

COLLOID CHEMISTRY OF FUMED SILICA

Fumed silica nanoparticles have a unique shape and surface chemistry that is central to their ability to form structural frameworks in solvents. The shape of the particles is due to them being synthesized by flame hydrolysis of $SiCl_4$ at temperatures higher than 1,000°C (Hurd and Flower, 1988; Pratsinis, 1998). Chlorosilane reacts with hydrogen and oxygen to produce molten spheres of silica (called primary particles) with sizes between 5 and 30 nm. The primary particles collide together and fuse into chains of particles. The fused clusters are between 100 and 1,000 nm in length and have branched shapes, as shown in **Figure 1a**. Light scattering studies of the growth of fused clusters revealed that they have a fractal dimension of 1.5 ± 0.2 (Hurd and Flower, 1988; Pratsinis, 1998). Fumed silica powders are made of clusters entangled together into porous networks that extend up to 250 micrometers in size. The powders have specific surface areas that range between 50 and 400 $m^2\ g^{-1}$.

The large surface area of fumed silica powders means that their surface chemistry is critical to how the powders function when dispersed in solvents (Iler and Iler, 1979; Legrand, 1998). The primary particles are composed of SiO_4 tetrahedra. The atoms exposed on the particle surfaces are oxygen atoms that are part of siloxane groups (Si-O-Si), or silicon atoms that are part of silanol (Si-OH) groups (Vansant et al., 1995). The silanol groups are formed during particle synthesis, or by rehydroxylation of siloxane groups due to dissociative water adsorption. The surface reactivity of a powder depends on the number and distribution of silanol groups. Approximately every second silicon atom on a fumed silica surface bears a silanol group (Mathias and Wannemacher, 1988; Barthel, 1995). The groups are randomly distributed across the surface (Zaborski et al., 1989). Pristine fumed silica is hydrophilic and has a high surface energy due to their presence. Deactivation of the surface silanol groups by reaction with alkyl trichlorosilanes, or alkyl trialkoxysilanes, reduces the surface energy of the powder and the particle surfaces become hydrophobic (Gun'ko et al., 2000; Wang et al., 2000; Jiang et al., 2018).

The surface chemistry of fumed silica powders is modified by adsorption of lipid species when the powders are wetted by edible oils. The silanol groups on the particle surfaces are sites for molecular adsorption of species capable of forming hydrogen bonds, or of undergoing donor–acceptor interactions (Zhuravlev, 2000). The triglycerides in vegetable oils adsorb onto silica surfaces due to hydrogen bonding between the silanol groups and the ester carbonyl groups (Adhikari et al., 1994; Proctor et al., 1996). This reduces the proportion of silanol groups available to form hydrogen bonds.

Fumed silica tends to aggregate when dispersed in organic solvents (like edible oils). The interactions between colloidal particles are traditionally explained using DLVO theory. This approach approximates the total potential energy of interaction between two colloidal particles as the sum of their van der Waals interactions and the energy due to the overlap of their electrical double layers (Israelachvili, 2015). Double layer forces are weak in non-aqueous solvents (Christenson and Horn, 1985). Raghavan et al. (2000b) proposed that fumed silica particles aggregate due to van der Waals and hydrogen bonding interactions between silanol groups on adjacent hydrophilic fumed silica particles. The hydrogen bonding interactions enhance particle aggregation in solvents that interact only weakly with the particle surfaces (Raghavan et al., 2000b). In the case of silanised powders, they argued that a mismatch between the chemical nature of the solvent and the alkyl chains coating the silica surfaces leads to attractive interactions due to the negative free energy of mixing between the alkyl chains (Raghavan et al., 2000a). Thus, the interactions governing the aggregation of fumed silica particles are thought to be dispersion, solvation and hydrogen bonding forces.

There is evidence from measurements of the forces between silica surfaces in non-aqueous solvents to support these hypotheses. McNamee et al. (2004) found that electrostatic interactions between hydrophilic silica surfaces in dodecane were weak and long-ranged. No electrostatic repulsive forces were measurable between hydrophobic silica surfaces in dodecane (McNamee et al., 2004). Gee and Israelachvili (1990) measured attractive interactions between silica surfaces coated with hexadecyl hydrocarbon chains in tetradecane that could not be described by van der Waals forces alone. They proposed that the additional attractive interaction was due to entropic interactions between the hydrocarbon chains and the solvent molecules. Roke et al. (2005) probed the molecular structure of the interface between hydrophobic silica particles and hexadecane and observed that an ordered (frozen) interfacial layer formed as the temperature was lowered. They argued that this layer generates a short-range attraction between the particles. Although alkanes were used in these studies, it is likely that the findings can be generalized to dispersions of fumed silica in edible oils.

The attractive interactions between fumed silica particles cause them to assemble into three-dimensional networks in organic solvents. Electron microscopy imaging of frozen samples of fumed silica dispersions in sunflower oil by Patel et al. (2015b) confirmed the presence of fractal-like clusters of particles on the nanometre-scale. The kinetics of the aggregation between the clusters were followed indirectly using scattering techniques (Smith and Zukoski, 2006a,b; Nordström et al., 2012). Confocal microscopy imaging of fumed silica particle aggregates in olive oil showed that the clusters assemble into irregular, linear aggregate structures up to 20 μm in length (Whitby et al., 2018). The linear aggregates overlap and entangle together in a ramified manner on the microscopic scale, as shown in **Figure 1b**. Analysis of the spatial correlations between the particle aggregates revealed that the networks have a characteristic pore size. The sizes of the pore spaces depend on the fraction of silanol groups available to form hydrogen bonds between neighboring aggregates (Whitby et al., 2018). The hierarchy of fumed silica networks in edible oils resembles the different levels of structuring found in fat crystal networks (Tang and Marangoni, 2006).

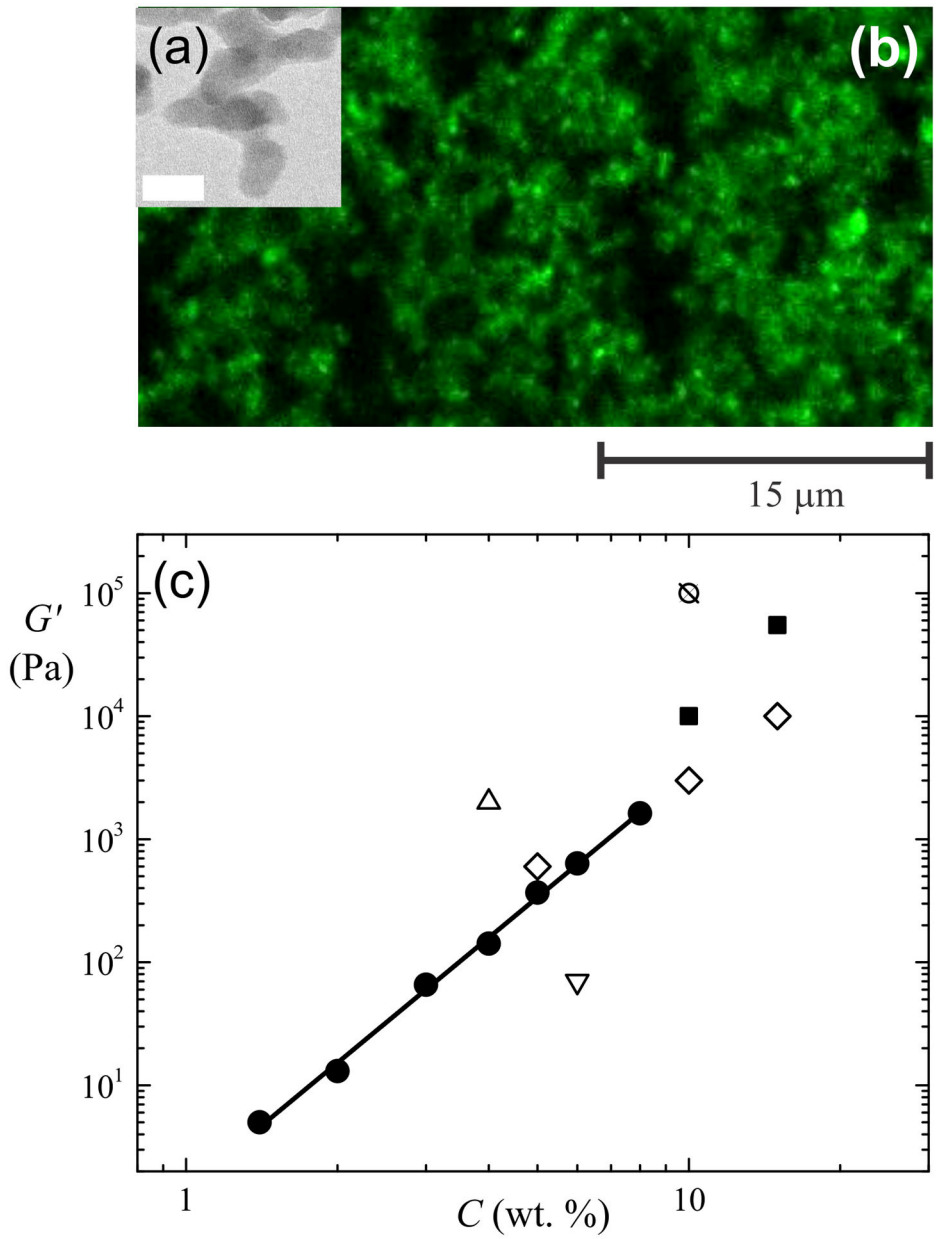

FIGURE 1 | (a) Electron microscope image of primary particles fused together into a chain-like cluster of fumed silica. The white bar corresponds to 20 nm. **(b)** Confocal fluorescence image of the entangled aggregates in a gel of 5 wt. % fumed silica particles in olive oil. **(c)** Particle concentration (*C*) dependence of the elasticity (*G'*) of gels of fumed silica in olive oil (•) (Whitby et al., 2018) and sunflower oil (■) (Patel et al., 2015b). The line is a power-law fit of the data for the olive oil gels with a scaling exponent, $n = 3.5$. For comparison, the elasticity of gels of glyceryl monostearate in a medium chain triglyceride oil (◊) (Cerqueira et al., 2017), ethyl cellulose in soybean oil (⊗) (Zetzl et al., 2014), berry wax in sunflower oil (▽) (Patel et al., 2015a) and carnauba wax in sunflower oil (△) (Patel et al., 2015a) is also shown.

RHEOLOGY OF FUMED SILICA OLEOGELS

Network formation by fumed silica particles in organic solvents causes the liquid to thicken. Increasing the particle concentration in the oil transforms the viscous liquid into a gel, a self-supporting material (Kosinski and Caruthers, 1986; Khan and Zoeller, 1993; Chen et al., 2005; Sugino and Kawaguchi, 2017). The viscoelastic character of the gels resembles the rheology of fat crystal networks (Macias-Rodriguez and Marangoni, 2018). Using oleogels as replacements for solid fat in food requires being able to characterize their mechanical properties, and to alter these properties to match the desired texture of the food product.

The rheology of oil dispersions of fumed silica is quantified by measuring their response to oscillatory stress. Gelled dispersions

of hydrophilic fumed silica in olive oil resist flowing and behave like viscoelastic solids, when small perturbations are applied (Whitby et al., 2018). This means that the connections between the overlapping silica aggregates are strong enough for the network to withstand the weight of the solvent trapped in the pores, and to store elastic strain. The solid-like behavior is characterized by the elastic storage modulus, G'. Larger perturbations cause a solid-liquid transition, due to energy being dissipated as the network of fractal clusters is broken apart (Whitby et al., 2018). The elastic structure of fumed silica organogels can be recovered once the applied stress is released (Patel et al., 2015b).

The rheological properties of fumed silica organogels are linked to the unique (fractal) shape and size of the aggregates formed by the particles. The elastic storage moduli of olive oil gels of hydrophilic fumed silica scale with the particle concentration (C) as $G' = aC^n$, where the scaling exponent $n \sim 3.5$, as shown in **Figure 1c** (Whitby et al., 2018). This is consistent with predictions made by physical models of the gels as space-filling networks of fractal clusters formed by diffusion limited aggregation between the clusters (Buscall et al., 1988). Similar behavior was observed for gels of fumed silica in mineral (Khan and Zoeller, 1993) and paraffin oils (Yziquel et al., 1999). The magnitude of the elasticity of the network structures in triglyceride solvents is, however, lower at a given particle concentration (Whitby et al., 2018). This is likely due to the impact of lipid adsorption on the hydrogen bonding capacity of the particle clusters and hence the strength of the links between the clusters in the network. Thus, the rheological properties of these systems are also linked to the interactions between the oil and the particles. **Figure 1c** shows that the elasticity of the gels is comparable in magnitude to that of oleogels formed using natural waxes, biopolymers and fatty acid crystals.

There is significant evidence that fumed silica gel rheology can be tuned by altering the interactions between the particles and hence the network morphology. Dispersions of methylated particles in olive oil tend to yield and flow even under small applied stresses (Whitby et al., 2018). Replacing some of the silanol groups on the particle surfaces with methyl groups reduces the hydrogen bonding capability of the particle aggregates. This was shown to lead to the formation of more tenuous networks with a larger average pore size (Whitby et al., 2018). Raghavan et al. (2000a) tuned the surface chemistry of fumed silica powders by reacting them with silanes of different chain length. They observed a correlation between the measured elastic moduli of dispersions of silanised fumed silica in polyethylene glycol and the calculated mismatch in solubility between the functional groups on the particle surfaces and the solvent. Patel et al. (2015b) found that the rheology of fumed silica dispersions in sunflower oil could be altered by thermal treatments. Wu and co-workers argued that heating fumed silica organogels affects the strength of hydrogen bonding interactions between the particles (Wu et al., 2012a,b).

Adding small amounts of a second solvent may also alter the interactions in fumed silica organogels. Providing the second solvent is not miscible in the edible oil, it may form liquid bridges between particles, and hence generate attractive capillary interactions between the particles (Koos and Willenbacher, 2011, 2012). This has not been investigated in edible oils gelled with fumed silica. But there is evidence in the literature that it is likely to enhance network formation. For example, the viscosity of suspensions of other food grade particles (cocoa and starch particles) in sunflower oil was manipulated by adding small volumes of water (Hoffmann et al., 2014).

LIPOLYSIS OF MIXTURES OF FUMED SILICA AND EDIBLE OILS

Given the potential applications for organogels in foods, it is important to consider how the digestion of edible oils will be impacted by gelation with fumed silica. Digestion involves the hydrolysis of triglycerides by lipase enzymes (Friedman and Nylund, 1980; Wilde and Chu, 2011; Singh et al., 2015; Maldonado-Valderrama, 2019). The enzymes break the triglycerides down into fatty acids and glycerols that are adsorbed into the bloodstream. Lipases are surface active proteins that catalyze reactions at the interface between aqueous and oil phases (Carey et al., 1983; Schmid and Verger, 1998; Mu and Høy, 2004). This means that the edible oil must be emulsified for the enzyme to be effective. The reaction kinetics are affected by the size of the oil droplets formed during emulsification, and hence the interfacial area, as well as the composition of the interface (Armand et al., 1999; Reis et al., 2009; Malaki Nik et al., 2011; Guo et al., 2017; Raikos and Ranawana, 2017). A network of fumed silica particles within the edible oil will presumably hinder emulsification of the oil and slow the release of any active ingredients (like drugs) dissolved in the oil.

Lipid digestion from fumed silica organgels has yet to be investigated. But we can glean insights from studies of digestion of edible oils gelled with fatty acids (Iwanaga et al., 2010, 2012; Lupi et al., 2013, 2018) and ethylcellulose (O'Sullivan et al., 2017). For example, Iwanaga et al. (2010) investigated the rate of release of ibuprofen from soybean oil gelled using 12-hydroxystearic acid. They observed that the ibuprofen released more slowly into simulated intestinal fluids from gels than from solutions of the drug in soybean oil. Lupi et al. (2013) studied the release of ferulic acid from olive oil gelled with policosanol (a fatty acid) in gastro-intestinal simulating fluids. They observed two stages in the release process. Lupi et al. (2013) found they could manipulate the release rate in the first stage by altering the concentration of the policosanol, and hence the gel viscosity. They proposed that release was controlled by diffusion of the drug molecules through the gel during this stage. The second stage was characterized by a faster release rate (Lupi et al., 2013, 2018; Pereira Camelo et al., 2016). The rate exceeded predictions by models for the release of drugs from polymer matrices due to diffusion alone (Siepmann and Siepmann, 2008; Fredenberg et al., 2011). Lupi et al. (2013) proposed that disruption of the network of fatty acid crystals enhanced the rate of drug diffusion by increasing the lipid-water interfacial area. O'Sullivan et al. (2017) investigated the release of β-carotene from canola oil gelled with ethylcellulose. They found that the lipids in gels

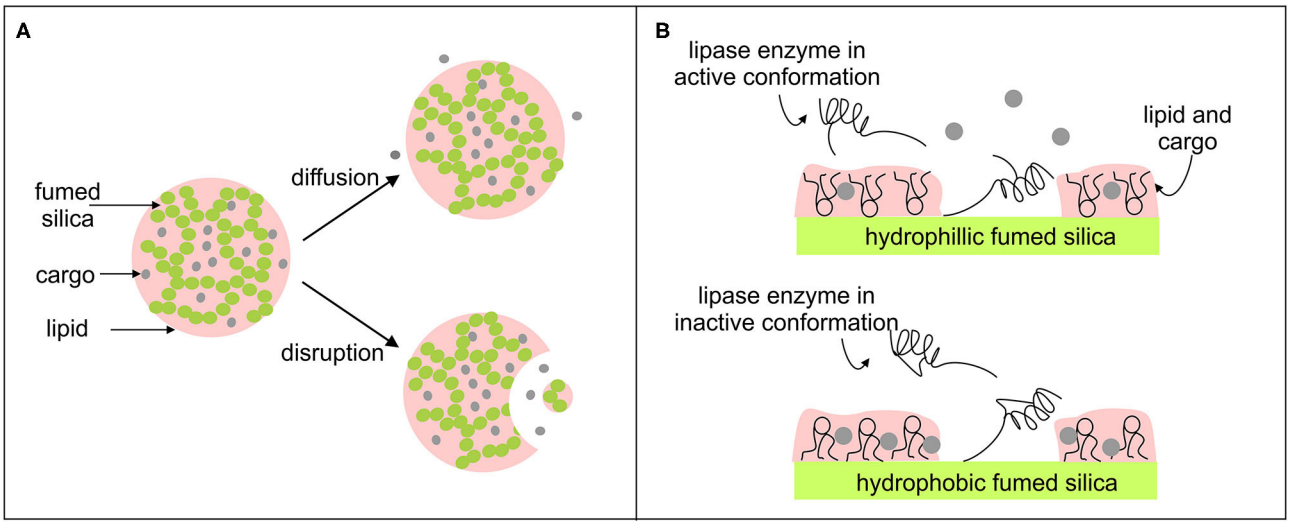

FIGURE 2 | (A) Schematic of the release of encapsulated ingredients (cargo) from fumed silica organogels during digestion by diffusion through the thickened oil and disruption of the particle network. **(B)** Schematic of how the interplay between the surface chemistry of the fumed silica and the conformation of the enzyme and lipid molecules on the silica surface may affect cargo release.

with weak mechanical properties were digested in simulated duodenal fluid at a similar rate to lipids in oil solutions of β-carotene. In contrast, the rate of lipid hydrolysis was slower from gels that were stiff enough to be cut up into pieces. O'Sullivan et al. (2017) argued that the canola oil was released more slowly from the stronger cellulose networks because they were harder to break apart. They observed variations in the rate of lipolysis in gels of similar strength and argued that the thickness of the walls in the cellulose networks must also affect their disruption.

It is likely that similar behavior will be observed for edible oils gelled using fumed silica. The release of the encapsulated cargo during digestion will occur by a combination of two mechanisms, as illustrated in **Figure 2A**. One is diffusion through the thickened solvent. The rate of diffusion will depend on the concentration of fumed silica particles. The other mechanism involves disruption (sometimes called degradation, or erosion) of the silica particle network. This will increase the surface area of the lipid exposed to digestive fluids. The rate of lipid digestion will therefore depend on the influence of the fumed silica particles on the interactions between the lipase enzymes and the lipid-water interface. Although this has yet to be investigated for fumed silica gels, Prestidge and co-workers have studied the digestion of mixtures of edible oils and inorganic particles, including fumed silica (Joyce et al., 2016c, 2018). Their findings provide insights into how the porous shape of fused silica could be used to manipulate the size of the lipid-water interfacial area available for lipase adsorption.

Tan et al. (2010) found that dispersing hydrophilic fumed silica particles in droplets of a medium chain triglyceride oil (Miglyol 812) reduced the rate of lipolysis. They argued that the presence of the particles limited access of the lipase enzymes to the lipid interface. On the other hand, Tan et al. (2010) observed that lipid digestion from hybrid particles made from fumed silica and oil droplets was faster than digestion from the oil drops alone. Electron microscopy imaging of the hybrid materials showed that they were micrometers in size and made of a "sponge-like" network of the silica particles. The pores in the network were up to 200 nm in size, which was comparable to the average diameter of the oil droplets (~172 nm). The network remained intact for at least 1 h during lipolysis (Simovic et al., 2009). Confocal fluorescence microscopy imaging revealed that the oil was spread throughout the porous network (Tan et al., 2012). Joyce et al. (2014) demonstrated that the rate and extent of lipid digestion depended on the relative proportions of silica and oil. They found that that lipid digestion was enhanced from hybrids containing insufficient oil to coat the available pore space (Joyce et al., 2014). The rate of digestion decreased as the amount of oil increased. Lipid digestion from hybrid particles containing enough oil to exceed monolayer coverage of their pores was slower than digestion from oil droplets alone.

The surface chemistry of fumed silica also has a critical effect on the interactions between lipase and the lipid-water interface. The rate of lipid hydrolysis is faster from hybrids made of hydrophilic fumed silica, rather than hydrophobic fumed silica (Joyce et al., 2016b). Reis et al. (2006) found that lipases adsorbed on hydrophilic silica surfaces catalyzed hydrolysis reactions. Lipases bound to hydrophobic silica favored esterification of triglycerides instead. They argued that lipase enzymes adsorbed on hydrophilic silica adopt conformations that expose the active hydrophobic sites which catalyze lipid hydrolysis (Reis et al., 2006). Joyce et al. (2016a) used mass spectrometry to find evidence for differences in the orientation of lipase enzymes adsorbed on silica surfaces of different

wettability. Evidence was also found for differences between the conformation of adsorbed lipids molecules on hydrophobic and hydrophilic silica (Joyce et al., 2015). Thus, the wettability of the silica surface may affect the orientation of lipid molecules and lipase enzymes adsorbed on the surface and hence the bioavailability of encapsulated ingredients, as illustrated in **Figure 2B**. The charge on the silica particles can also affect lipase action. Digestion products displace lipase enzymes from the lipid-water interface (Reis et al., 2008). Since hydrophilic surfaces are negatively charged, it is thought that electrostatic repulsions between the fatty acids and the silica network in the hybrids encourage removal of the digestion products, thus freeing up sites at the lipid-water interface for lipase adsorption (Joyce et al., 2014).

FUTURE OUTLOOK

Based on the evidence in the literature, using fumed silica to structure edible oils has advantages. The inorganic particles assemble into three dimensional, anisotropic networks which have similar structural and mechanical properties to networks of fat colloids. They could enhance the nutritional profiles of edible organogels by modulating the rate of lipid digestion and release of active ingredients encapsulated within the networks. The next step is to transform these structures into materials that mimic the texture and stability of fat and can be readily incorporated into food formulations.

Thus far, fumed silica oleogels have been incorporated into a limited number of composite materials for use in food products (Skelhon et al., 2012; Patel et al., 2015b; Chauhan et al., 2017a,b). For example, Skelhon et al. (2012) lowered the fat content of chocolate by replacing some of the cocoa butter with drops of fruit juice stabilized by a network of fumed silica in the remaining cocoa butter. They found that the chocolate emulsion formulations retained the crystalline fat structure needed for the chocolate to melt with the desired texture when eaten. Chauhan et al. (2017a,b) investigated the properties of composite networks of fumed silica and tripalmitin fat crystals used to gel soybean oil. They found that the composite networks retained the melting and rheological properties of full-fat networks. These results confirm the potential for creating healthier foods using hybrid mixtures of fumed silica organogels and solid fats.

AUTHOR CONTRIBUTIONS

CW review the literature, drafted and edited the manuscript text, and prepared the figures for the manuscript.

FUNDING

This work was supported by the Massey University Research Fund and the MacDiarmid Institute for Advanced Materials and Nanotechnology.

REFERENCES

Adhikari, C., Proctor, A., and Blyholder, G. D. (1994). Diffuse-reflectance fourier-transform infrared spectroscopy of vegetable oil triglyceride adsorption on silicic acid. *J. Am. Oil Chem. Soc.* 71, 589–594. doi: 10.1007/BF02540584

Armand, M., Pasquier, B., André, M., Borel, P., Senft, M., Peyrot, J., et al. (1999). Digestion and absorption of 2 fat emulsions with different droplet sizes in the human digestive tract. *Am. J. Clin. Nutr.* 70, 1096–1106. doi: 10.1093/ajcn/70.6.1096

Barthel, H. (1995). Surface interactions of dimethylsiloxy group-modified fumed silica. *Colloids Surf. A* 101, 217–226. doi: 10.1016/0927-7757(95)03179-H

Buscall, R., Mills, P. D. A., Goodwin, J. W., and Lawson, D. W. (1988). Scaling behaviour of the rheology of aggregate networks formed from colloidal particles. *J. Chem. Soc. Fara. Trans.* 84, 4249–4260. doi: 10.1039/f19888404249

Carey, M. C., Small, D. M., and Bliss, C. M. (1983). Lipid digestion and absorption. *Ann. Rev. Physiol.* 45, 651–677. doi: 10.1146/annurev.ph.45.030183.003251

Cerqueira, M. A., Fasolin, L. H., Picone, C. S. F., Pastrana, L. M., Cunha, R. L., and Vicente, A. A. (2017). Structural and mechanical properties of organogels: role of oil and gelator molecular structure. *Food Res. Int.* 96, 161–170. doi: 10.1016/j.foodres.2017.03.021

Chauhan, R. R., Dullens, R. P. A., Velikov, K. P., and Aarts, D. G. A. L. (2017a). The effect of colloidal aggregates on fat crystal networks. *Food Funct.* 8, 352–359. doi: 10.1039/C6FO01622G

Chauhan, R. R., Dullens, R. P. A., Velikov, K. P., and Aarts, D. G. A. L. (2017b). Exploring concentration, surface area and surface chemistry effects of colloidal aggregates on fat crystal networks. *RSC Adv.* 7, 28780–28787. doi: 10.1039/C7RA01803G

Chen, S., Øye, G., and Sjöblom, J. (2005). Rheological properties of silica particle suspensions in mineral oil. *J. Dispersion Sci. Tech.* 26, 791–798. doi: 10.1081/DIS-200063119

Christenson, H., and Horn, R. (1985). Non-aqueous liquids. *Chem. Scripta* 25, 37–41.

Fredenberg, S., Wahlgren, M., Reslow, M., and Axelsson, A. (2011). The mechanisms of drug release in poly(lactic-co-glycolic acid)-based drug delivery systems-a review. *Int. J. Pharma.* 415, 34–52. doi: 10.1016/j.ijpharm.2011.05.049

Friedman, H. I., and Nylund, B. (1980). Intestinal fat digestion, absorption, and transport. a review. *Am. J. Clin. Nutr.* 33, 1108–1139. doi: 10.1093/ajcn/33.5.1108

Gee, M. L., and Israelachvili, J. N. (1990). Interactions of surfactant monolayers across hydrocarbon liquids. *J. Chem. Soc. Fara. Trans.* 86, 4049–4058. doi: 10.1039/ft9908604049

Gun'ko, V. M., Vedamuthu, M. S., Henderson, G. L., and Blitz, J. P. (2000). Mechanism and kinetics of hexamethyldisilazane reaction with a fumed silica surface. *J. Colloid Interface Sci.* 228, 157–170. doi: 10.1006/jcis.2000.6934

Guo, Q., Ye, A., Bellissimo, N., Singh, H., and Rousseau, D. (2017). Modulating fat digestion through food structure design. *Prog. Lipid Res.* 68, 109–118. doi: 10.1016/j.plipres.2017.10.001

Hoffmann, S., Koos, E., and Willenbacher, N. (2014). Using capillary bridges to tune stability and flow behavior of food suspensions. *Food Hydrocoll.* 40, 44–52. doi: 10.1016/j.foodhyd.2014.01.027

Hurd, A. J., and Flower, W. L. (1988). In situ growth and structure of fractal silica aggregates in a flame. *J. Colloid Interface Sci.* 122, 178–192. doi: 10.1016/0021-9797(88)90301-3

Iler, R. K., and Iler, R. (1979). The chemistry of silica: solubility, polymerization, colloid and surface properties, and biochemistry. *Angew. Chem.* 92:328.

Israelachvili, J. N. (2015). *Intermolecular and Surface Forces*. London: Academic press.

Iwanaga, K., Kawai, M., Miyazaki, M., and Kakemi, M. (2012). Application of organogels as oral controlled release formulations of hydrophilic drugs. *Int. J. Pharma.* 436, 869–872. doi: 10.1016/j.ijpharm.2012.06.041

Iwanaga, K., Sumizawa, T., Miyazaki, M., and Kakemi, M. (2010). Characterization of organogel as a novel oral controlled release formulation for lipophilic

compounds. *Int. J. Pharma.* 388, 123–128. doi: 10.1016/j.ijpharm.2009.12.045

Jiang, J., Cao, J., Wang, W., and Xue, J. (2018). How silanization influences aggregation and moisture sorption behaviours of silanized silica: analysis of porosity and multilayer moisture adsorption. *Roy. Soc. Open Sci.* 5:180206. doi: 10.1098/rsos.180206

Joyce, P., Gustafsson, H., and Prestidge, C. A. (2018). Engineering intelligent particle-lipid composites that control lipase-mediated digestion. *Adv. Colloid Interface Sci.* 260, 1–23. doi: 10.1016/j.cis.2018.08.001

Joyce, P., Kempson, I., and Prestidge, C. A. (2015). QCM-D and ToF-SIMS investigation to deconvolute the relationship between lipid adsorption and orientation on lipase activity. *Langmuir* 31, 10198–10207. doi: 10.1021/acs.langmuir.5b02476

Joyce, P., Kempson, I., and Prestidge, C. A. (2016a). Orientating lipase molecules through surface chemical control for enhanced activity: a QCM-D and ToF-SIMS investigation. *Colloids Surf. B* 142, 173–181. doi: 10.1016/j.colsurfb.2016.02.059

Joyce, P., Tan, A., Whitby, C. P., and Prestidge, C. A. (2014). The role of porous nanostructure in controlling lipase-mediated digestion of lipid loaded into silica particles. *Langmuir* 30, 2779–2788. doi: 10.1021/la500094b

Joyce, P., Whitby, C. P., and Prestidge, C. A. (2016b). Interfacial processes that modulate the kinetics of lipase-mediated catalysis using porous silica host particles. *RSC Adv.* 6, 43802–43813. doi: 10.1039/C6RA08934H

Joyce, P., Whitby, C. P., and Prestidge, C. A. (2016c). Nanostructuring biomaterials with specific activities towards digestive enzymes for controlled gastrointestinal absorption of lipophilic bioactive molecules. *Adv. Colloid Interface Sci.* 237, 52–75. doi: 10.1016/j.cis.2016.10.003

Khan, S. A., and Zoeller, N. J. (1993). Dynamic rheological behavior of flocculated fumed silica suspensions. *J. Rheol.* 37, 1225–1235. doi: 10.1122/1.550378

Koos, E., and Willenbacher, N. (2011). Capillary forces in suspension rheology. *Science* 331, 897–900. doi: 10.1126/science.1199243

Koos, E., and Willenbacher, N. (2012). Particle configurations and gelation in capillary suspensions. *Soft Matter* 8, 3988–3994. doi: 10.1039/c2sm07347a

Kosinski, L. E., and Caruthers, J. M. (1986). The effect of particle concentration on the rheology of polydimethylsiloxane filled with fumed silica. *J. App. Polym. Sci.* 32, 3393–3406. doi: 10.1002/app.1986.070320203

Legrand, A. P. (1998). *The Surface Properties of Silicas*. Chichester: Wiley.

Lupi, F., Mancina, V., Baldino, N., Parisi, O., Scrivano, L., and Gabriele, D. (2018). Effect of the monostearate/monopalmitate ratio on the oral release of active agents from monoacylglycerol organogels. *Food Funct.* 9, 3278–3290. doi: 10.1039/C8FO00594J

Lupi, F. R., Gabriele, D., Baldino, N., Mijovic, P., Parisi, O. I., and Puoci, F. (2013). Olive oil/policosanol organogels for nutraceutical and drug delivery purposes. *Food Funct.* 4, 1512–1520. doi: 10.1039/c3fo60259a

Lupi, G. V., Baldino, N., de Cindio, B., Fischer, P., and Gabriele, D. (2016). The effects of intermolecular interactions on the physical properties of organogels in edible oils. *J. Colloid Interface Sci.* 483, 154–164. doi: 10.1016/j.jcis.2016.08.009

Macias-Rodriguez, B. A., and Marangoni, A. A. (2018). Linear and nonlinear rheological behavior of fat crystal networks. *Cri. Rev. Food Sci. Nutr.* 58, 2398–2415. doi: 10.1080/10408398.2017.1325835

Malaki Nik, A., Wright, A. J., and Corredig, M. (2011). Impact of interfacial composition on emulsion digestion and rate of lipid hydrolysis using different *in vitro* digestion models. *Colloids Surf. B* 83, 321–330. doi: 10.1016/j.colsurfb.2010.12.001

Maldonado-Valderrama, J. (2019). Probing *in vitro* digestion at oil-water interfaces. *Curr. Opin. Colloid Interf. Sci.* 39, 51–60. doi: 10.1016/j.cocis.2019.01.004

Marangoni, A. G., and Edmund, D. C. (2012). Organogels: an alternative edible oil-structuring method. *J. Am. Oil Chem. Soc.* 89, 749–780. doi: 10.1007/s11746-012-2049-3

Marangoni, A. G., van Duynhoven, J. P. M., Acevedo, N. C., Nicholson, R. A., and Patel, A. R. (2020). Advances in our understanding of the structure and functionality of edible fats and fat mimetics. *Soft Matter* 16, 289–306. doi: 10.1039/C9SM01704F

Martins, A. J., Vicente, A. A., Cunha, R. L., and Cerqueira, M. A. (2018). Edible oleogels: an opportunity for fat replacement in foods. *Food Funct.* 9, 758–773. doi: 10.1039/C7FO01641G

Mathias, J., and Wannemacher, G. (1988). Basic characteristics and applications of aerosil: 30. The chemistry and physics of the aerosil surface. *J. Colloid Interface Sci.* 125, 61–68. doi: 10.1016/0021-9797(88)90054-9

McClements, D. J. (2018). The biophysics of digestion: lipids. *Curr. Opin. Food Sci.* 21, 1–6. doi: 10.1016/j.cofs.2018.03.009

McNamee, C. E., Tsujii, Y., and Matsumoto, M. (2004). Interaction forces between two silica surfaces in an apolar solvent containing an anionic surfactant. *Langmuir* 20, 1791–1798. doi: 10.1021/la035730+

Michalski, M. C., Genot, C., Gayet, C., Lopez, C., Fine, F., Joffre, F., et al. (2013). Multiscale structures of lipids in foods as parameters affecting fatty acid bioavailability and lipid metabolism. *Prog. Lipid Res.* 52, 354–373. doi: 10.1016/j.plipres.2013.04.004

Mu, H., and Høy, C.-E. (2004). The digestion of dietary triacylglycerols. *Prog. Lipid Res.* 43, 105–133. doi: 10.1016/S0163-7827(03)00050-X

Nordström, J., Aguilera, L., and Matic, A. (2012). Effect of lithium salt on the stability of dispersions of fumed silica in the ionic liquid BMImBF4. *Langmuir* 28, 4080–4085. doi: 10.1021/la204555g

O′Sullivan, C. M., Davidovich-Pinhas, M., Wright, A. J., Barbut, S., and Marangoni, A. G. (2017). Ethylcellulose oleogels for lipophilic bioactive delivery – effect of oleogelation on *in vitro* bioaccessibility and stability of beta-carotene. *Food Funct.* 8, 1438–1451. doi: 10.1039/C6FO01805J

Patel, A. R., Babaahmadi, M., Lesaffer, A., and Dewettinck, K. (2015a). Rheological profiling of organogels prepared at critical gelling concentrations of natural waxes in a triacylglycerol solvent. *J. Agric. Food Chem.* 63, 4862–4869. doi: 10.1021/acs.jafc.5b01548

Patel, A. R., Mankoc, B., Bin Sintang, M. D., Lesaffer, A., and Dewettinck, K. (2015b). Fumed silica-based organogels and 'aqueous-organic' bigels. *RSC Adv.* 5, 9703–9708. doi: 10.1039/C4RA15437A

Pereira Camelo, S. R., Franceschi, S., Perez, E., Girod Fullana, S., and Ré, M. I. (2016). Factors influencing the erosion rate and the drug release kinetics from organogels designed as matrices for oral controlled release of a hydrophobic drug. *Drug Dev. Indus. Pharm.* 42, 985–997. doi: 10.3109/03639045.2015.1103746

Pratsinis, S. E. (1998). Flame aerosol synthesis of ceramic powders. *Prog. Energy Combust. Sci.* 24, 197–219. doi: 10.1016/S0360-1285(97)00028-2

Proctor, A., Adhikari, C., and Blyholder, G. D. (1996). Lipid adsorption on commercial silica hydrogels from hexane and changes in triglyceride complexes with time. *J. Am. Oil Chem. Soc.* 73, 693–698. doi: 10.1007/BF02517942

Pușcaș, A., Mureșan, V., Socaciu, C., and Muste, S. (2020). Oleogels in food: a review of current and potential applications. *Foods* 9:70. doi: 10.3390/foods9010070

Raghavan, S. R., Hou, J., Baker, G. L., and Khan, S. A. (2000a). Colloidal interactions between particles with tethered nonpolar chains dispersed in polar media: direct correlation between dynamic rheology and interaction parameters. *Langmuir* 16, 1066–1077. doi: 10.1021/la9815953

Raghavan, S. R., Walls, H. J., and Khan, S. A. (2000b). Rheology of silica dispersions in organic liquids: new evidence for solvation forces dictated by hydrogen bonding. *Langmuir* 16, 7920–7930. doi: 10.1021/la991548q

Raikos, V., and Ranawana, V. (2017). Designing emulsion droplets of foods and beverages to enhance delivery of lipophilic bioactive components - a review of recent advances. *Int. J. Food Sci. Tech.* 52, 68–80. doi: 10.1111/ijfs.13272

Reis, P., Holmberg, K., Debeche, T., Folmer, B., Fauconnot, L., and Watzke, H. (2006). Lipase-catalyzed reactions at different surfaces. *Langmuir* 22, 8169–8177. doi: 10.1021/la060913s

Reis, P., Holmberg, K., Miller, R., Krägel, J., Grigoriev, D. O., Leser, M. E., et al. (2008). Competition between lipases and monoglycerides at interfaces. *Langmuir* 24, 7400–7407. doi: 10.1021/la800531y

Reis, P., Holmberg, K., Watzke, H., Leser, M. E., and Miller, R. (2009). Lipases at interfaces: A review. *Adv. Colloid Interface Sci.* 147–148, 237–250. doi: 10.1016/j.cis.2008.06.001

Rogers, M. A. (2018). Hansen solubility parameters as a tool in the quest for new edible oleogels. *J. Am. Oil Chem. Soc.* 95, 393–405. doi: 10.1002/aocs.12050

Roke, S., Buitenhuis, J., Miltenburg, J. C., v., Bonn, M., Blaaderen, A., et al. (2005). Interface–solvent effects during colloidal phase transitions. *J. Phys. Condens. Matter* 17, S3469–S3479. doi: 10.1088/0953-8984/17/45/036

Sato, K., and Ueno, S. (2014). "Physical properties of fats in food," in *Fats in Food Technology* (Chichester: John Wiley & Sons), 1–38. doi: 10.1002/9781118788745.ch1

Schmid, R. D., and Verger, R. (1998). Lipases: interfacial enzymes with attractive applications. *Angew. Chem. Int. Ed.* 37, 1608–1633. doi: 10.1002/(SICI)1521-3773(19980703)37:12<1608::AID-ANIE1608>3.0.CO;2-V

Siepmann, J., and Siepmann, F. (2008). Mathematical modeling of drug delivery. *Int. J. Pharma.* 364, 328–343. doi: 10.1016/j.ijpharm.2008.09.004

Simovic, S., Heard, P., Hui, H., Song, Y., Peddie, F., Davey, A. K., et al. (2009). Dry hybrid lipid–silica microcapsules engineered from submicron lipid droplets and nanoparticles as a novel delivery system for poorly soluble drugs. *Mol. Pharm.* 6, 861–872. doi: 10.1021/mp900063t

Singh, H., Ye, A., and Ferrua, M. J. (2015). Aspects of food structures in the digestive tract. *Curr. Opin. Food Sci.* 3, 85–93. doi: 10.1016/j.cofs.2015.06.007

Skelhon, T. S., Grossiord, N., Morgan, A. R., and Bon, S. A. F. (2012). Quiescent water-in-oil Pickering emulsions as a route toward healthier fruit juice infused chocolate confectionary. *J. Mat. Chem.* 22, 19289–19295. doi: 10.1039/c2jm34233b

Smith, W. E., and Zukoski, C. F. (2006a). Aggregation and gelation kinetics of fumed silica-ethanol suspensions. *J. Colloid Interface Sci.* 304, 359–369. doi: 10.1016/j.jcis.2006.09.016

Smith, W. E., and Zukoski, C. F. (2006b). Role of solvation forces in the gelation of fumed silica-alcohol suspensions. *J. Colloid Interface Sci.* 304, 348–358. doi: 10.1016/j.jcis.2006.08.021

Sugino, Y., and Kawaguchi, M. (2017). Fumed and precipitated hydrophilic silica suspension gels in mineral oil: stability and rheological properties. *Gels* 3:32. doi: 10.3390/gels3030032

Tan, A., Martin, A., Nguyen, T.-H., Boyd, B. J., and Prestidge, C. A. (2012). Hybrid nanomaterials that mimic the food effect: controlling enzymatic digestion for enhanced oral drug absorption. *Angew. Chem. Int. Ed.* 51, 5475–5479. doi: 10.1002/anie.201200409

Tan, A., Simovic, S., Davey, A. K., Rades, T., Boyd, B. J., and Prestidge, C. A. (2010). Silica nanoparticles to control the lipase-mediated digestion of lipid-based oral delivery systems. *Mol. Pharm.* 7, 522–532. doi: 10.1021/mp900 2442

Tang, D., and Marangoni, A. G. (2006). Quantitative study on the microstructure of colloidal fat crystal networks and fractal dimensions. *Adv. Colloid Interface Sci.* 128-130, 257–265. doi: 10.1016/j.cis.2006.11.019

Vansant, E. F., van Der Voort, P., and Vrancken, K. C. (1995). *Characterization and Chemical Modification of the Silica Surface*. Amsterdam: Elsevier.

Wang, R., Guo, J., Baran, G., and Wunder, S. L. (2000). Characterization of the State of order of octadecylsilane chains on fumed silica. *Langmuir* 16, 568–576. doi: 10.1021/la9908081

Whitby, C. P., Krebsz, M., and Booty, S. J. (2018). Understanding the role of hydrogen bonding in the aggregation of fumed silica particles in triglyceride solvents. *J. Colloid Interface Sci.* 527, 1–9. doi: 10.1016/j.jcis.2018.05.029

Wilde, P. J., and Chu, B. S. (2011). Interfacial & colloidal aspects of lipid digestion. *Adv. Colloid Interface Sci.* 165, 14–22. doi: 10.1016/j.cis.2011.02.004

Wu, X.-J., Wang, Y., Wang, M., Yang, W., Xie, B.-H., and Yang, M.-B. (2012a). Structure of fumed silica gels in dodecane: enhanced network by oscillatory shear. *Colloid Poly. Sci.* 290, 151–161. doi: 10.1007/s00396-011-2535-4

Wu, X.-J., Wang, Y., Yang, W., Xie, B.-H., Yang, M.-B., and Dan, W. (2012b). A rheological study on temperature dependent microstructural changes of fumed silica gels in dodecane. *Soft Matter* 8, 10457–10463. doi: 10.1039/c2sm25668a

Yziquel, F., Carreau, P. J., and Tanguy, P. A. (1999). Non-linear viscoelastic behavior of fumed silica suspensions. *Rheol. Acta* 38, 14–25. doi: 10.1007/s003970050152

Zaborski, M., Vidal, A., Ligner, G., Balard, H., Papirer, E., and Burneau, A. (1989). Comparative study of the surface hydroxyl groups of fumed and precipitated silicas. I. grafting and chemical characterization. *Langmuir* 5, 447–451. doi: 10.1021/la00086a028

Zetzl, A. K., Gravelle, A. J., Kurylowicz, M., Dutcher, J., Barbut, S., and Marangoni, A. G. (2014). Microstructure of ethylcellulose oleogels and its relationship to mechanical properties. *Food Struc.* 2, 27–40. doi: 10.1016/j.foostr.2014.07.002

Zhuravlev, L. T. (2000). The surface chemistry of amorphous silica. *Zhuravlev Model. Colloids Surf. A* 173, 1–38. doi: 10.1016/S0927-7757(00)00556-2

Conflict of Interest: The author declares that the research was conducted in the absence of any commercial or financial relationships that could be construed as a potential conflict of interest.

frontiers in Sustainable Food Systems

ORIGINAL RESEARCH
published: 30 November 2020
doi: 10.3389/fsufs.2020.559510

Application of Complex Chitosan Hydrogels Added With Canola Oil in Partial Substitution of Cocoa Butter in Dark Chocolate

Andres Silvestre Gallegos Soto[1]*, *Renata Santos Rabelo*[1], *Eliana Marcela Vélez-Erazo*[1], *Paulo Túlio de Souza Silveira*[2], *Priscilla Efraim*[2] and *Miriam Dupas Hubinger*[1]*

[1] Laboratory of Process Engineering, Department of Food Engineering, University of Campinas (UNICAMP), Campinas, Brazil, [2] Laboratory of Fruits, Vegetables, Beverages, and Confectionery, Department of Food Technology, University of Campinas (UNICAMP), Campinas, Brazil

OPEN ACCESS

Edited by:
Stephen Robert Euston, Heriot-Watt University, United Kingdom

Reviewed by:
Guillermo Alfredo Picó, Institute of Biotechnological and Chemical Processes Rosario (IPROBYQ), Argentina
Elena Simone, University of Leeds, United Kingdom

***Correspondence:**
Andres Silvestre Gallegos Soto
andres.silgaso@gmail.com
Miriam Dupas Hubinger
mhub@unicamp.br

Specialty section:
This article was submitted to Sustainable Food Processing, a section of the journal Frontiers in Sustainable Food Systems

Received: 06 May 2020
Accepted: 16 October 2020
Published: 30 November 2020

Citation:
Gallegos Soto AS, Rabelo RS, Vélez-Erazo EM, de Souza Silveira PT, Efraim P and Hubinger MD (2020) Application of Complex Chitosan Hydrogels Added With Canola Oil in Partial Substitution of Cocoa Butter in Dark Chocolate. Front. Sustain. Food Syst. 4:559510. doi: 10.3389/fsufs.2020.559510

The complexation of polymeric materials can be an alternative to trapping oil in a physical network for formulating foods with reduced saturated fat content. In this research, we have evaluated the use of different polymer ratios of Sodium Alginate (ALG), Carrageenan predominance *iota* (CR1) and Carrageenan predominance *kappa* (CR2) complexed with Chitosan (CHI) at a fixed polymer concentration (2% w/v) to formulate complex hydrogels and assess their oil holding capacity. The objective was to determine the polymer ratios of CHI to anionic polysaccharides (75:25, 50:50, and 25:75), determining the oil retention capacity in different ratios, and how this can affect the stability, microstructure and rheology of to produce low saturated chocolate with trapped canola oil. The stability of the hydrogels was characterized, considering the water retention and retention of canola oil in polysaccharides complexes. The more stable system was the hydrogel CHI:CR2 in a polymer ratio of 25:75. This formulation, when added of 20% of canola oil presented an apparent viscosity of 0.631 Pa.s at 300 s^{-1}, and its use as replacer of saturated fat allowed the production of dark chocolate with 16% reduction in fat content and 80% of added cocoa butter. Stability studies showed that polysaccharides complexes network can retain the edible oil in chocolate formulation for 60 days. It has been proven that polysaccharides complexes can be incorporated to partially replace the fatty phase in chocolates without considerable changes in relevant characteristics as consumer acceptance evaluated by sensory tests and rheological properties.

Keywords: canola oil, polymer network, polysaccharide, alginate, carrageenan, structured oil

INTRODUCTION

In the last years, food scientists have made a great effort to obtain fat substitutes with potential applications in foods due to consumers' interest in finding healthier options. Some of these efforts have involved the substitution of trans and saturated fats for polyunsaturated oils using different kinds of structurants. Recently, the use of carbohydrate-based systems as fat substitutes have been studied because hydrocolloids are widely used in the food industry and have demonstrated satisfactory results. For example, the inulin was used as a carbohydrate-based fat replacer, with good

fat imitating properties when combined with water due to the ability to form a gel (O'Brien et al., 2003). In chocolate formulations, Skelhon et al. (2013) reduced the product's fat content replacing 50% cocoa butter content with 2% agar microgels (containing 20% of sunflower oil).

The combined use of different polysaccharides can also be an interesting alternative as fat substitutes. They can provide improved functional properties over individual polymers. Some examples were presented by Rather et al. (2015, 2016) and Alnemr et al. (2016), who made blends of some food-grade polysaccharides, such as guar, xanthan, locust, and kappa-carrageen gum to partially replace saturated fat in different food products. They explored the synergism between polysaccharides as an alternative to formulate new fat substitutes. With the use of chitosan, electrostatic interaction between different polysaccharides could be also explored in this kind of application.

Chitosan (CHI) is a cationic polysaccharide that can function as dietary fiber with hypocholesterolemic effects and reduce lipid absorption and increase cholesterol elimination (Maezaki et al., 1993; Gallaher et al., 2002). The complexation of chitosan with anionic polymers and its interaction with lipid matrices have already been evaluated by Rabelo et al. (2018, 2019). In these works, the optimal conditions for polymeric complexation were obtained, showing that even at low temperatures and in concentrations where pure polymers do not gel, CHI complexes with ALG and CRG could form structured polymeric networks. It has also been observed that CHI, at higher temperatures, exposes hydrophobic groups that entrap the lipids, preventing or at least reducing their expulsion in formulations with lipid particles.

The use of polymeric complexes and complex hydrogels obtained from the complexation of chitosan with alginates and carrageenans were also investigated by other authors (Goycoolea et al., 2000; Espinosa-Andrews et al., 2007, 2010, 2013; Sæther et al., 2008; Volod'ko et al., 2012, 2014, 2016; Kulig et al., 2016, 2017; Afzal et al., 2018). However, none of these works has evaluated the use of these complexes as fat substitutes in dark chocolate formulations, which is the purpose of this study.

The chocolate application was proposed because there is a need to find innovative technological solutions to establish a chocolate formulation with low saturated fat content, keeping adequate fractions of solid volume and flow properties. For this purpose, the influence of the polymer ratio of biopolymers in the reticulation degree of the polymer network, the retention of oil in the polysaccharides complexes without emulsifying properties, the microstructure, stability and rheological properties of the formulated chocolates were studied, leading to interesting to formulate dark chocolate with 80% less cocoa fat added.

MATERIALS AND METHODS

Material

Sodium Alginate (ALG, Grindsted Alginate FD 175) was donated by Danisco Brazil Ltda (Pirapozinho, SP, Brazil), Carrageenans (CR1 predominance *iota* and CR2 predominance *kappa*) were donated by Alibra Ingredientes Ltda (Campinas, SP, Brazil), and Chitosan (CHI, Deacetylation degree of 85%) was purchased from Sigma Aldrich Inc. (USA). Soy Lecithin (Bunge Alimentos S.A., Gaspar-SC, Brazil), Acetic Acid (Dinâmica, Química Contemporânea Ltda, Campinas, SP, Brazil), and Canola oil (CO, Vitaliv®, ADM do Brazil Ltda, Brazil) were purchased from industries located in Brazil. All experiments were performed with Milli-Q water (Milli-Q system, Millipore, USA); other reagents were of analytical grade. The molecular weight and polydispersity of Sodium Alginate (7.83×10^4 g/mol, 1.18) and Chitosan (1.51×10^5 g/mol, 1.44) were obtained from the previous study carried out by Rabelo et al. (2019).

Formulation of Complex Hydrogels and Addition of Canola Oil

Aqueous Dispersion Preparation

Polymeric dispersions were prepared at a polymer concentration of 2.0% (w/v) in water, except for CHI, which was dispersed in acetic acid solution (2% v/v). Then, the dispersions were heated up to 60°C and stirred for 30 min to obtain a clear and homogeneous solution. After preparation, all solutions were stirred overnight (300 rpm) at room temperature for 12 h to ensure complete hydration of the biopolymers. Before use, the pH of all the solutions was adjusted to 3.5, where both polysaccharides are protonated. All experiments were conducted at low ionic strength, to favor the polymer complexation.

Complex Hydrogel Preparation

CHI solutions were prepared and mixed with CR1, CR2, or ALG solutions to obtaining CHI:polysaccharide ratios of 25:75, 50:50, and 75:25 (w/w). All samples were homogenized for 10 min at 18,000 rpm using an UltraTurrax IKA® T18B (IKA-Werke GmbH & Co. KG, Germany) equipped with a dispersing rotor S18N-19G. Then, the drying of the samples was carried out in a heating oven (ORION 515, FANEM, São Paulo, Brazil) at 70°C for 48 h. The drying process was monitored by weight loss along time and stopped when the sample reached a moisture content of 25% (on dry basis).

Addition of Oil

The process of oil addition to hydrogels formulation is presented in **Figure 1**. Initially, the solutions of CHI:ALG, CHI:CR1 and CHI:CR2 complexes were heated at 80°C using a jacketed beaker connected to a bath MA 126/BD (Marconi Ltda, Brazil) to reduce the viscosity and improve mixing with oil (canola oil) to obtain appropriate ratios of 80:20, 50:50, and 20:80 oil/dry hydrogel (w/w). After that, the canola oil with 1% lecithin (final formulation weight) was added gradually and homogenized for 2 min at 18,000 rpm using a UltraTurrax IKA® T18B (IKA-Werke GmbH & Co. KG, Germany). Finally, the samples were stored in a refrigerated chamber at 25°C for further analysis.

Characterization of Complex Hydrogels

Microstructure

The microstructure of complex hydrogels with and without added oil was visualized using an optical microscope Carl Zeiss Axio Scope A1 (Gottingen, Germany), with a 10 and 40x objective. The images were analyzed using software Zen 2.3 (Zeiss, Germany).

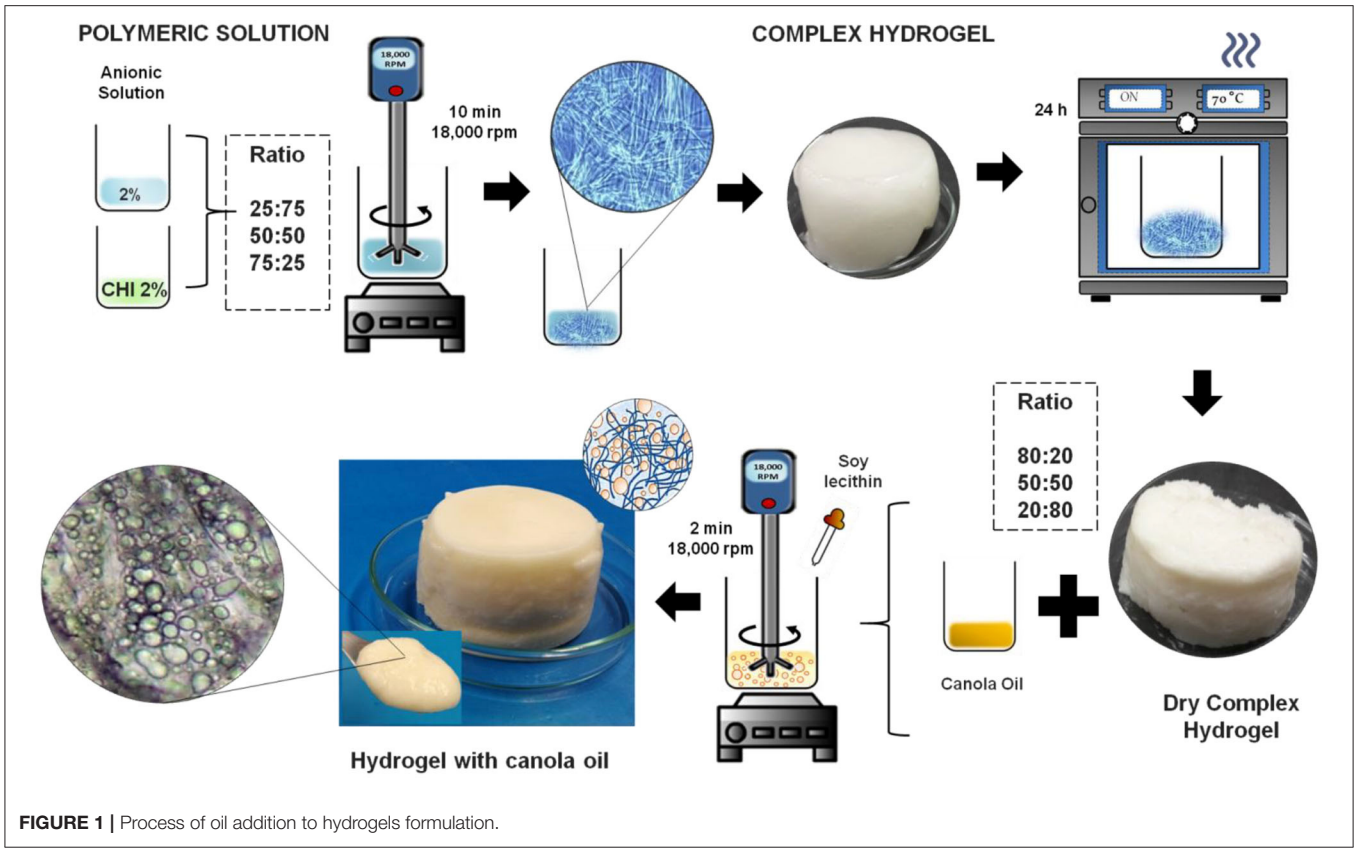

FIGURE 1 | Process of oil addition to hydrogels formulation.

Stability Studies

Stability of formulations was evaluated by measuring the water and oil retention of samples (hydrogels with or without oil added). Measurement was performed in triplicate according to the methodology proposed by Wijaya et al. (2017) and Paglarini et al. (2018) with some modifications. The water or oil retention was measured after 30 days of storage in a refrigerated chamber with controlled temperature (25 ± 1°C). Approximately 2 g of sample were weighed in centrifuge tubes and then centrifuged for 1 h at 2,000 rpm, and 25°C. The total amount of water or oil released was expressed as a percentage of the weight of the sample.

Rheological Measurement

The rheological analysis for the pure polymeric solutions and of hydrogels with or without added oil were carried out on an advanced rheometer AR 1500 ex (TA Instruments, Elstree, UK), with a stainless-steel cone-plate geometry (4 cm diameter, and GAP of 58 μm). Measurements were done in triplicate. Flow curve measurements were performed at 25°C, in three stages (up, down and up) cycles, with a shear rate ranging from 0 to 300 s^{-1}. Viscosity was calculated as the instantaneous ratio of shear stress and shear rate. The third flow curve data were fitted to the models Herschel–Bulkley fluids Equation (3).

$$\sigma = \sigma_0 + K_{HB} \times \left(\gamma^n\right) \quad (1)$$

Where: σ is the shear stress (Pa), σ_0 the initial shear stress, γ the shear rate (1/s), and the consistency index (K_{HB}), as well as the behavior index (n), are model constants.

Chocolate Production

Two formulations of dark chocolate were produced. The control chocolate (CC) was produced with 29.5% refined sugar, 60% natural liquor and 10% deodorized cocoa butter (IBC- Indústria Brasileira de Cacau, SP, Brazil), 0.5% soy lecithin (Bunge Alimentos SA, SC, Brazil). The chocolate containing hydrogel added with canola oil was produced with the same ingredients and quantities of CC, with 80% of the cocoa butter being replaced by hydrogel added with canola oil, allowing a 16% reduction in the total fat content of the formulation (Reduced fat chocolate, RFC). CC was processed following the steps described by Afoakwa et al. (2009) and Biswas et al. (2017). The ingredients (sugar, cocoa liquor and cocoa butter) were mixed, refined and conched using a Melanger Spectra 11 (Spectra, India) equipped with two adjustable cylindrical granite stones and a double scraper arm. The period of the process (7 h) was defined to obtain a maximum particle size < 25 μm monitored by a digital micrometer (Mitutoyo, Japan). During this period the temperature of the chocolate mass was close to 60°C. After particle size has been reached, soy lecithin was added and the chocolate was mixed for 1 more hour. For RFC processing, the hydrogel added with canola oil was added with the soy lecithin after particle size has been reached and the chocolate

was mixed for 1 additional hour. The tempering was performed in an ACMC temper machine (model D45134, United States). The tempering conditions were defined by pre-tests using a ChocoMeter (AastedApS-Farum, Denmark). Temper Index of 5.0 ± 1.0 was accepted. First, the mass was completely melted up to 40°C, and then cooled at a rate of 2°C min^{-1}, until it reached 28°C and was kept in this condition for 10 min. After this period, the temperature has been raised to 31°C and maintained for 5 min to allow unstable crystals melting. The chocolates were molded in rectangular molds (18 g) and cooled in a cooling chamber at 15°C. Then samples were packed in aluminum paper and stored in chambers with controlled temperature (24 ± 1°C) for further characterization at 1, 15, 30, 45, and 60 days of storage (when applied).

Chocolate Characterization

Moisture Content

Evaluated by Karl Fisher method (701 KF Titrino, Metrohm, Herisau Switzerland) (AOAC, 2016). The samples were melted at 40°C and then ∼0.1 g was weighed in chloroform: methanol (1:1) solution for analysis.

Whiteness Index (WI)

A Hunterlab/ColorQuest II (Hunter Association, Inc., USA) colorimeter was used to quantify the changes on the surface of the chocolate samples at storage times 1, 15, 30, 45, and 60 days (11). The equipment measured the L*, a* and b* values for 10 times and the tests were performed in triplicate (totalizing 30 readings for each formulation). The values obtained were converted to whiteness index (WI) values according to Lohman and Hartel (1994), presented in Equation 1:

$$WI = 100 - \left[(100 - L)^2 + a^2 + b^2\right]^{0.5}. \quad (2)$$

Microstructure

The visualization of the surface structure and cross-section of chocolate samples was performed by scanning electron microscopy (SEM), in a table-type microscope, Hitachi High Technologies America, Inc., model TM-3000 (Japan), according to the methodology described by Miyasaki (2013). The samples were sectioned in the dimensions of 20 × 20 mm, to be observed on the surface, as well as in the cross-section, in the *Analy* mode (automatic of the equipment) with an increase of × 500, × 1,500, and × 2,500 times.

Rheological measurements

The measurement procedure was based on the method described by Biswas et al. (2017) with minor modifications. A Rheometer AR 1500ex (TA Instruments, Elstree, United Kingdom) fitted with a stainless steel flat plate geometry (4 cm in diameter) was used. Approximately 2 g of the chocolate sample were melted at 50°C for 1 h and were placed on a pre-heated plate with a height of 1 mm. The bottom plate temperature was adjusted to 40°C to prevent solidification of the fat crystals. A stepped flow procedure was applied, increasing the shear rate logarithmically from 2 to 110 s^{-1}. Yield stress (Pa) and viscosity (Pa.s) were measured at 65 s^{-1} using the Casson's model (Equation 3) (Afoakwa et al., 2008a).

$$\sqrt{\tau} = \sqrt{\tau_{CA}} + \sqrt{\mu_{CA}}.\sqrt{\gamma} \quad (3)$$

where τ is the yield stress; τ_{CA} is the Casson yield stress; μCA is the Casson viscosity; and γ is the shear rate.

Texture Analysis (Snap Test)

The determinations were performed according to the methodology described by Quast et al. (2013) in a TA-XT2i texture analyser (Stable Micro Systems, Surrey, United Kingdom) equipped with an HDP/3PB -probe. Measurements were performed after 1, 15, 30, 45, and 60 days of storage; with 10 replicates per sample in a controlled temperature room (20 ± 0.5°C). The conditions used were: distance between bar supports: 6 cm; pre-test speed: 3 mm s^{-1}; test speed: 1.7 mm s^{-1}; post-test speed: 10 mm s^{-1}. The breaking force applied in the center of the bars, expressed in kgf, was obtained from the force vs. deformation graphs.

Melting Profile

The melting profile of dark chocolate was measured using a differential scanning calorimetry (DSC Modulated 2920, TA Instruments- New Castle, Delaware, USA), following the method of Biswas et al. (2017) with minimal modifications. Two samples of chocolate bars were randomly selected and were comminuted and homogenized, transferring 4 ± 0.5 mg of the samples to an aluminum pan hermetically sealed, using a covered and empty aluminum pan as a reference. When the system reached equilibrium conditions at 20°C, the pan was placed in the DSC cell and the fusion thermograms were recorded by heating from −20 to 70°C at a rate of 5°C/min. Each sample was analyzed in triplicate. The initial melting temperature (T_{onset}), the final temperature (T_{end}) and the maximum peak temperature (T_{max}), the melting enthalpy (ΔH) were calculated from the melting thermogram using the DSC software.

Nutritional Profile Analysis

The gravimetric analyzes to determine the nutritional information of the chocolate samples were carried out in an accredited external laboratory, following the methodologies: Protein by DUMAS (CBAA, 2013: method 45), Total Fat by acid hydrolysis (AOCS, 2017; CBAA, 2017: method 12), Saturated Fat and Fat Trans (AOAC, 2016), Sodium by Atomic Absorption (CBAA, 2013: method 40) and Dietary Fiber by enzymatic-gravimetric method (ADOLFO LUTZ, 2008), the carbohydrate and total energy values were obtained by difference calculation. Each analysis was performed in duplicate.

Sensory Analysis

For the sensory analysis, carried out at the Sensory Analysis Laboratory in the Department of Food and Nutrition (School of Food Engineer- UNICAMP), chocolate samples were labeled with three-digit codes and, along with the questionnaire, were given to 120 untrained evaluators with a minimum age of 18 years. Two samples were evaluated (1) control chocolate (CC) and (2) reduced fat chocolate (RFC). The sensory attributes:

appearance, sweetness, waxiness, general flavor, texture (snap), mouth-feel (melting) and overall acceptability were evaluated using a 9-point hedonic scale (9 = "extremely more intense than I like it" to 1 = "extremely less intense than I like it"). The order of presentation of the plates to each evaluator was different in a random sequence. Bottled drinking water at room temperature was also provided to clean the palate between each sample. At the end of the test, an assessment was also made between CC and RFC to evaluate the purchase intention using a 5-point structured scale (1 = would certainly buy to 5 = certainly would not buy). The assessors recorded their responses on an evaluation sheet designed to indicate the score of the sample of each formula.

Statistical Analysis

The data were statistically analyzed by the Tukey test using Minitab® 18.1 Statistic (Minitab Inc., USA). Differences between means were considered significant at a 95% confidence level ($p \leq 0.05$). Excel Solver Microsoft 2010® was used for the adjustment of the models Herschel–Bulkley Equation (1). The XLSTAT 2017 software (Addinsoft, France 2017) for Microsoft Excel was used for data analysis and statistical solution of the results obtained in the sensory analysis.

RESULTS AND DISCUSSION

Optical Microscopy of Complex Hydrogels

The microstructure of complex hydrogels is shown in **Figure 2**, where each micrograph corresponds to the optical image of samples at 40x magnification. The ability of polysaccharides to form a three-dimensional structure, independent on the polymer ratio (25:75, 50:50, and 75:50) was observed to all hydrogels (CHI:ALG, CHI:CR1, and CHI:CR2). In particular, the increase of the reticulation degree observed in **Figure 2** can be described in the following order: 75:25 < 50:50 < 25:75. This behavior is in agreement with Rabelo et al. (2019), who reported the maximal complexation of CHI with sodium alginate and carrageenan around of 25:75 (in mass proportion) and discussed the contribution of the electrostatic interaction and the hydrogen bonding in the complexation of these polymers.

Still, in **Figure 2**, the hydrogels CHI:ALG show a more organized structure than the other ones (CHI:CR1 and CHI:CR2), which may be associated with the aggregation and gel formation kinetics of these hydrogels. However, the greater compaction of the polymeric network of CHI:CR1, when compared with CHI:CR2 may result from the presence of an additional sulfate group in the molecular structure of CR1 (predominance *iota*) in relation to CR2 (predominance *kappa*), which contributes to the formation of tight binding between CHI and CR1 (Volod'ko et al., 2016).

Water Retention

The hydrogels are materials characterized by their strong water retention capacity, and one of the main factors that contributes to this is the presence of hydrophilic functional groups (i.e., carboxyl, hydroxyl, amide and sulfonic groups) in the molecular structure of their polymer constituents (Peppas and Khare, 1993; Künzler, 2002). The reticulation degree, particle size and ionic osmotic pressure are also important factors that can influence on the water retention capacity of hydrogels (Ahmed, 2015). Here, the water retention for CHI:ALG, CHI:CR1, and CHI:CR2 in three different polymers ratio (75:25, 50:50, and 25:75) are presented in **Figure 3**, where the effect of the composition and reticulation degree of polymers in the hydrogels was observed. In this context, CHI:CR2 formulated at a polymer ratio of 25:75 (more reticulate) presented the highest water retention among the complex hydrogels, while CHI:CR1 presented the lower water retention, independent of the polymer ratio (**Figure 3**). This behavior is attributed to the formation of a tight binding between CHI and CR1, as previously mentioned. These tight junctions are associated with the formation of amorphous precipitated structures with low solvent retention capacity (Comert et al., 2016).

For CHI:ALG, the change in the polymer ratio from 50:50 to 25:75 increases the reticulation degree and the firmness of hydrogel **(Figure 4),** but has no significant effect on the water retention (**Figure 3**).

The greater water retention of both hydrogels obtained at a polymer ratio of 25:75 (**Figure 3**) is in agreement with the more reticulated network structure presented by these formulations (Section Optical microscopy of complex hydrogels, **Figure 2**). Those results are in accordance with the profile presented in **Figure 4,** where the samples were inverted to observe the phase separation of hydrogels before centrifugation. The hydrogels 75:25 and 50:50 flowed into the mouth of the bottle, while the formulations 25:75 remained (totally or partially) in the base of the bottle, indicating the formation of a gel-like state. All these results contributed to the hydrogels obtained at a polymer ratio of 25:75 to be selected to continue this study.

Oil Retention

The oil retention of formulations after 30 days of storage at 25 ± 1°C is shown in **Figure 5**. Samples with 80% of CO (canola oil) showed bigger oil release, while formulations with 50% CO presented oil retention higher than 80% for CHI:ALG and CHI:CR2. The greatest oil retention was observed for CHI:CR2 (99.83%), CHI:ALG (98.63%), and CHI:CR1 (85.58 %), respectively, both with 20% of canola oil. This result is important to exemplify that hydrogels based on polysaccharides without interfacial activity cannot retain large oil amounts in their structure, hampering the formulation of structured oils. On the other hand, the results still reached a good oil trap, which is attributed to the addition of lecithin (1%).

The formulations CHI:ALG and CHI:CR2 promoted oil retention higher than 98%. The best performance of these formulations when compared with the CHI:CR1 can be also attributed to the tight binding between CHI and CR1, which may not be favorable for the oil entrapped into the polysaccharides complexes.

In **Figure 6** the microstructure of the hydrogel with 20% of canola oil is shown. The micrograph corresponds to the optical projection of the sample at 10 and 40 x magnifications. The CHI:ALG presented a more organized 3D structure, allowing more uniform oil droplets trapping. CHI:CR2 shows a large number of oil droplets trapped in its polymeric structure when compared with CHI:CR1, but the way oil was trapped in the polymer network was similar. However, it is known that in

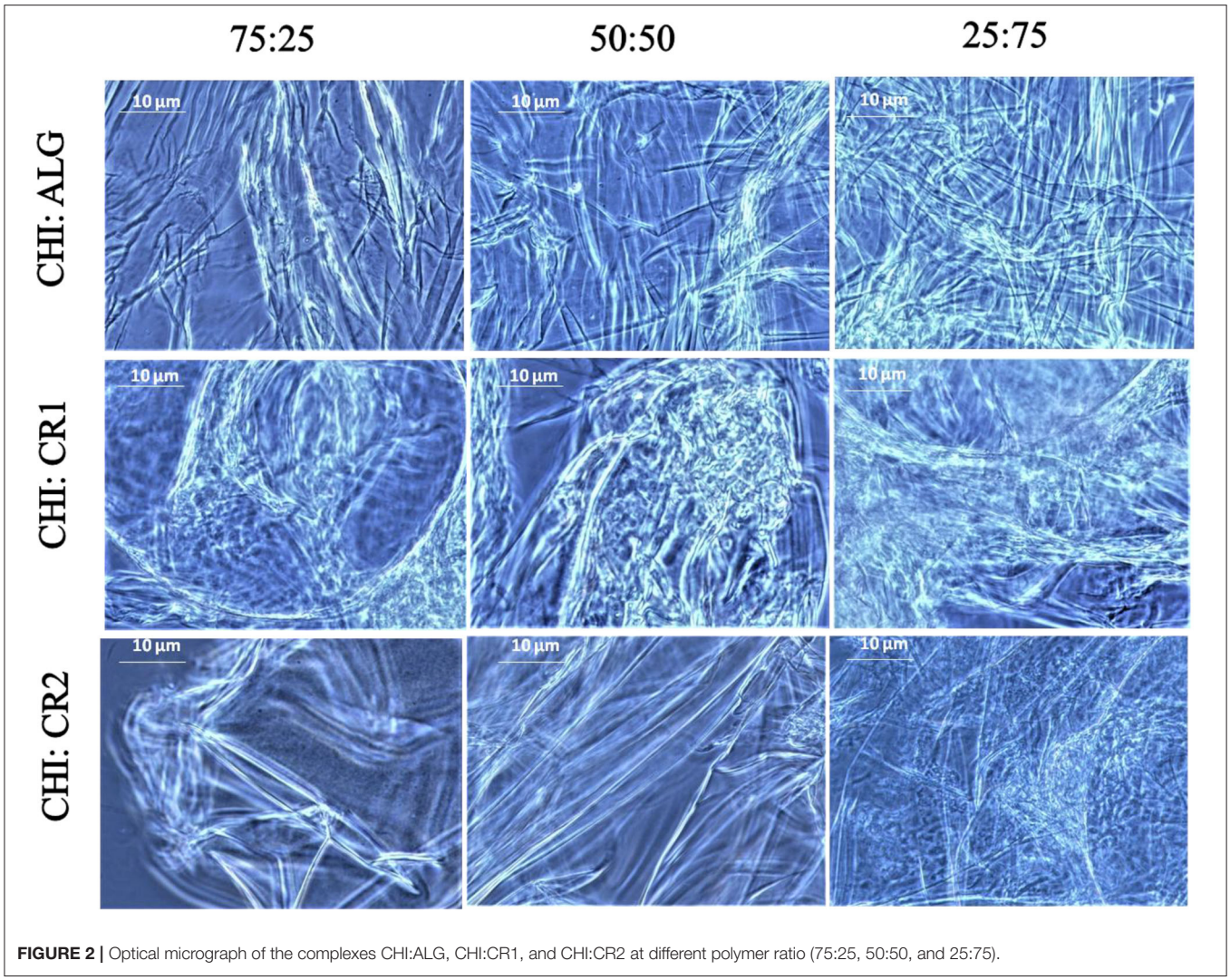

FIGURE 2 | Optical micrograph of the complexes CHI:ALG, CHI:CR1, and CHI:CR2 at different polymer ratio (75:25, 50:50, and 25:75).

order to achieve effective steric stabilization with for good oil entrapment, the size and structure of the carbohydrate play an important role. Small sugar molecules or low molecular weight polysaccharides are not as effective as high molecular weight or branched molecules (Wong et al., 2011). Presumably, the polysaccharides complex' steric properties to produce oil entrapment has an important contribution in preventing the oil release of all these formulations. These polysaccharide molecules could provide an additional steric barrier between the emulsion droplets when the complex is adsorbed at emulsion interfaces.

Rheological Measurement

Steady-state flow analysis was performed to investigate the apparent viscosity of polysaccharides (dispersion), conventional hydrogels and hydrogel with added oil, in which the HB model showed high correlations for all samples ($R^2 > 98\%$).

For polysaccharides dispersions at 2% (w/w), the initial shear stress values (σ_o) were zero for CHI and ALG, but 2.71 for CR1 and 44.45 for CR2, indicating the necessity of an initial force for the CR1 and CR2 dispersions to begin to flow (**Table 1**). The flow behavior index (n) is related to the shear-thinning or elastic behavior. All dispersions presented shear-thinning behavior with a significant difference in the n values between them. CHI with $n = 0.816$ is the closest one to the Newtonian behavior ($n = 1$), coinciding with that reported by Shepherd et al. (1997), and the CR2 is the most shear-thinning system. The consistency index (k) has a relationship with viscosity. It can be observed that the higher the k value, the higher the σ_o and the apparent viscosity, and the lower the n value, characterizing the CR2 dispersion as the more structured dispersion.

Each dispersion's characteristics may have influenced on all hydrogels' behavior stabilized by electrostatic complexes of CHI (cationic) with ALG, CR1, or CR2 (anionic). The increase in CHI concentration in the hydrogel increases the n value, resulting in softer complex hydrogels. In the CHI:CR1 (25:75), it was impossible to perform the test on the parameters determined for this rheological analysis, reminding that it was the hydrogel that showed the least stability (compared with CHI:ALG and

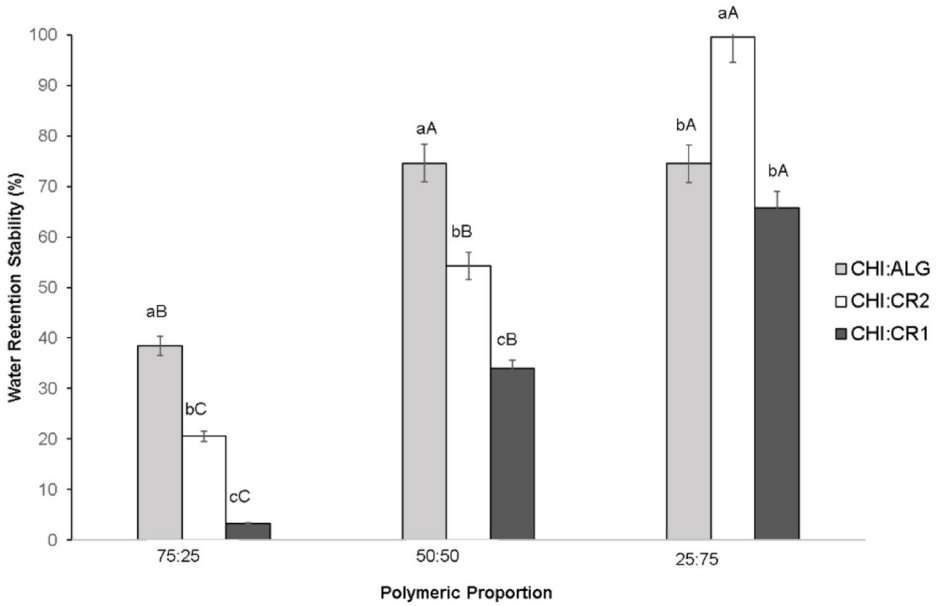

FIGURE 3 | Water retention of the complex hydrogels (CHI:ALG, CHI:CR1, and CHI:CR2) at different polymer ratios (75:25, 50:50, and 25:75). Different uppercase letters indicate a significant difference ($p \leq 0.05$) in the same complex at different polymer ratios. Different lowercase letters indicate a significant difference ($p \leq 0.05$) in the same polymer ratio of different Complexes.

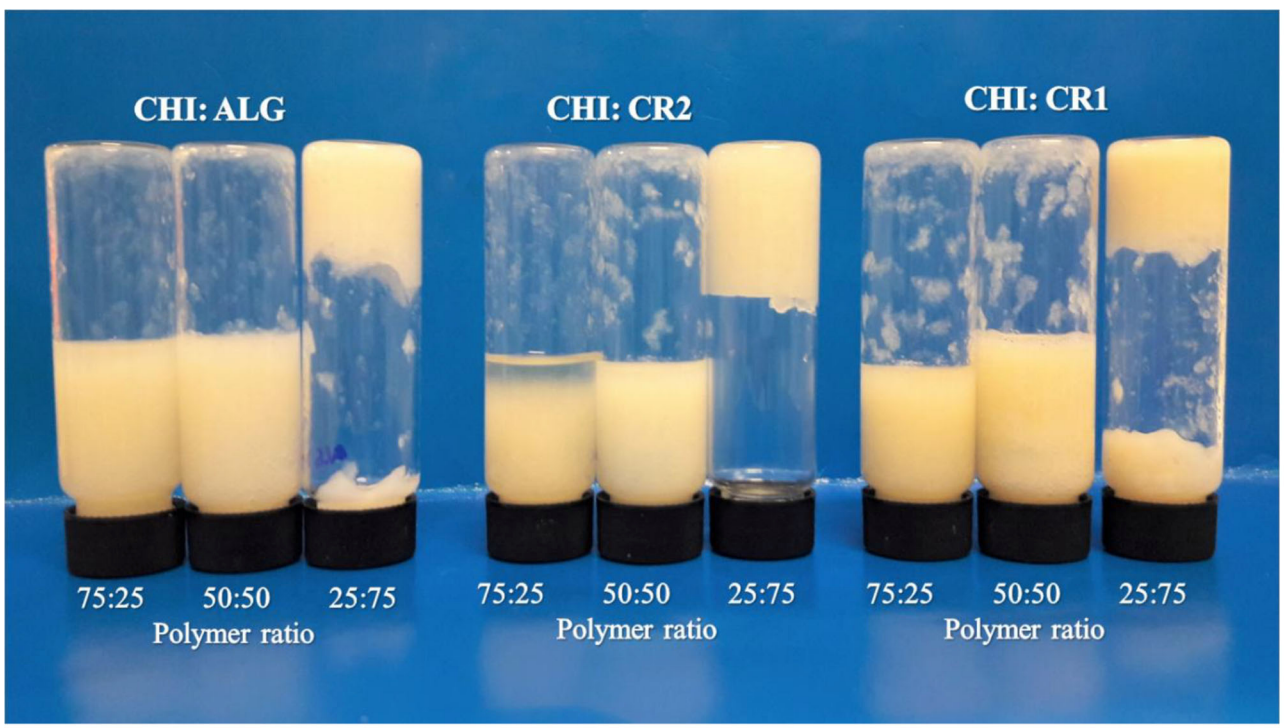

FIGURE 4 | Visual image of complex hydrogels (CHI:ALG, CHI:CR1, and CHI:CR2) at different polymer ratios (75:25, 50:50, and 25:75).

CHI:CR2 at 25:75). Only the hydrogel at CHI:CR2 25:75 showed σ_o (19.55 Pa) and the lower n value, presenting similar characteristics with the CR2 dispersion.

Additionally, both the hydrogel (with or without oil) formulated with CHI:CR2 at 25:75 ratio have the lower n among all formulations and apparent viscosity ($\sim$ 0.240 Pa.s), indicating

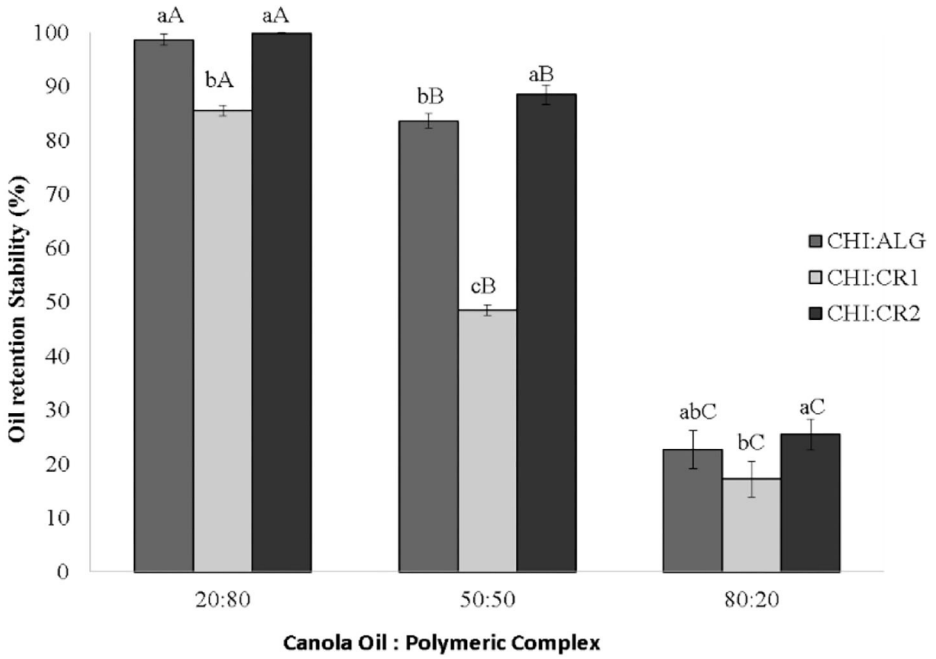

FIGURE 5 | Oil retention of polysaccharides complexes (CHI:ALG, CHI:CR1, and CHI:CR2) at three different percentages of canola oil (80, 50, and 20%) in the formulation. Different uppercase letters indicate a significant difference ($p \leq 0.05$) in the same formulation at different oil ratio. Different lowercase letters indicate a significant difference ($p \leq 0.05$) in the same oil ratio in different formulations.

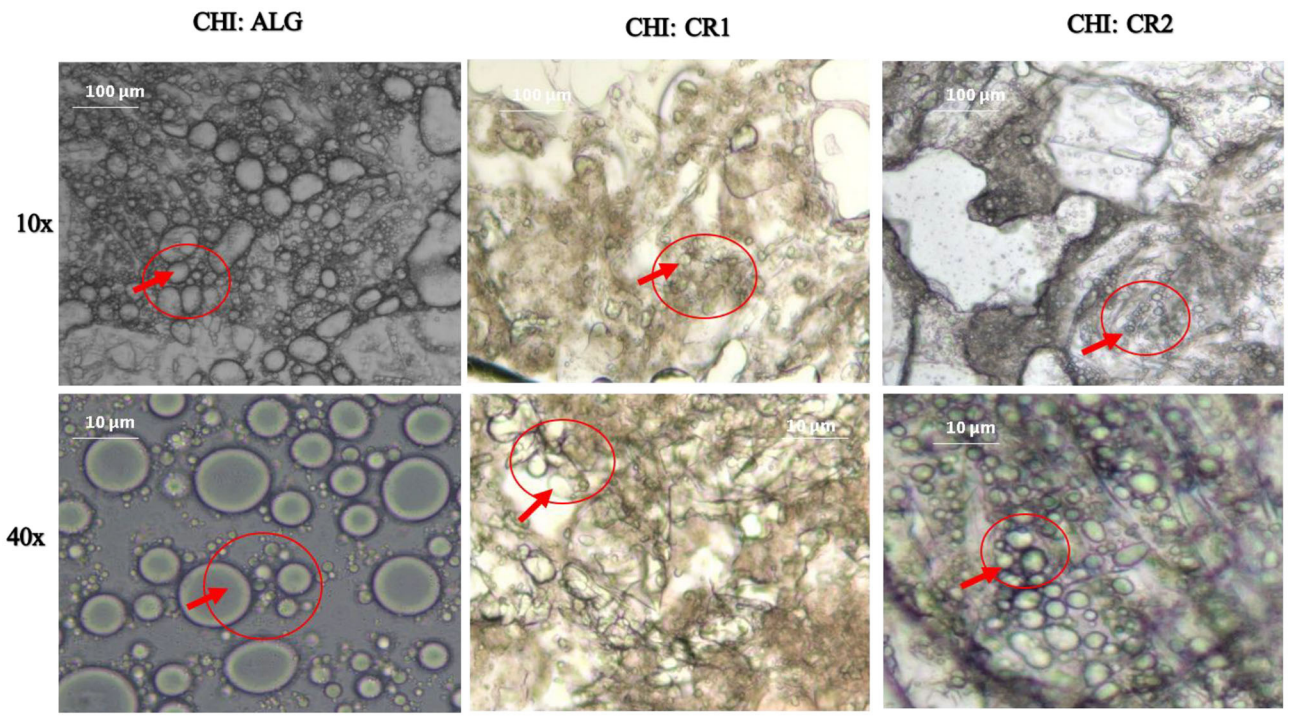

FIGURE 6 | Optical micrograph of CHI:ALG, CHI:CR1, and CHI:CR2 (polymer ratio = 25:75) with 20% w/w of canola oil.

TABLE 1 | Rheological parameters (HB model) and apparent viscosity at a shear rate of 300 s^{-1} ($\eta_{(300)}$) of pure materials (2% w/v), complex hydrogels (CHI:ALG, CHI:CR1, and CHI:CR2) at different polymer ratios (75:25, 50:50, and 25:75), and hydrogels (CHI:ALG 25:75; CHI:CR1 25:75, and CHI:CR2 25:75) with 20% of canola oil.

Pure material	σ_o	***k***	***n***	R^2 **(%)**	$\eta_{(300)}$ **(Pa.s)**
CHI	0.00 ± 0.00^{c}	0.548 ± 0.001^{c}	0.816 ± 0.003^{a}	99.98	0.190 ± 0.014^{c}
ALG	0.00 ± 0.00^{c}	4.959 ± 0.074^{c}	0.593 ± 0.001^{b}	99.83	0.475 ± 0.007^{b}
CR1	2.708 ± 0.252^{b}	15.537 ± 1.874^{b}	0.380 ± 0.021^{d}	99.93	0.452 ± 0.082^{b}
CR2	44.446 ± 5.401^{a}	44.463 ± 5.454^{a}	0.206 ± 0.003^{c}	99.82	0.620 ± 0.068^{a}
Hydrogel	σ_o	***k***	***n***	R^2 **(%)**	$\eta_{(300)}$**(Pa.s)**
CHI:ALG 75:25	0.00 ± 0.00	5.661 ± 0.968^{b}	0.579 ± 0.009^{a}	99.98	0.505 ± 0.062^{b}
CHI:ALG 50:50	0.00 ± 0.00	14.918 ± 1.044^{a}	0.495 ± 0.006^{b}	99.99	0.738 ± 0.040^{ab}
CHI:ALG 25:75	0.00 ± 0.00	18.034 ± 3.831^{a}	0.473 ± 0.003^{c}	99.92	0.993 ± 0.172^{a}
CHI:CR1 75:25	0.00 ± 0.00	0.433 ± 0.195^{b}	0.825 ± 0.102^{a}	99.74	0.151 ± 0.025^{c}
CHI:CR1 50:50	0.00 ± 0.00	0.905 ± 0.101^{b}	0.614 ± 0.021^{b}	99.93	0.099 ± 0.007^{c}
CHI:CR1 25:75	–	–	–	–	–
CHI:CR2 75:25	0.00 ± 0.00	0.723 ± 0.185^{b}	0.776 ± 0.047^{a}	99.92	0.203 ± 0.012^{c}
CHI:CR2 50:50	0.00 ± 0.00	3.915 ± 0.195^{b}	0.434 ± 0.003^{b}	99.86	0.153 ± 0.005^{c}
CHI:CR2 25:75	19.550 ± 3.842	43.753 ± 9.415^{a}	0.240 ± 0.004^{c}	99.67	0.631 ± 0.237^{b}
Hydrogel with 20% of oil	σ_o	***k***	***n***	R^2 **(%)**	$\eta_{(300)}$**(Pa.s)**
CHI:ALG 25:75	9.333 ± 3.214^{b}	4.958 ± 0.073^{c}	0.593 ± 0.001^{a}	99.99	0.537 ± 0.031^{a}
CHI:CR1 25:75	20.584 ± 2.401^{a}	15.946 ± 0.499^{b}	0.287 ± 0.027^{b}	99.96	0.286 ± 0.012^{b}
CHI:CR2 25:75	23.455 ± 3.858^{a}	21.036 ± 0.925^{a}	0.246 ± 0.001^{c}	94.71	0.246 ± 0.034^{b}

Different letters in the same column indicate a significant difference ($p \leq 0.05$) in the same assay. k: consistency index (Pa.s^n). n: flow index.

a greater variation in viscosity with an increasing shear rate. This may be related to the breakdown of structure and reordering of the tangled units through the dynamic shear forces (Patel et al., 2013). Analyzing the hydrogels with added oil, it is possible to observe that when the water concentration decreases, the σo increases significantly and the k decreases compared with the values of their respective hydrogels. For this reason, hydrogels with 20% of canola oil have a more coherent structure, requiring greater force to begin to flow.

Most processes in the food industry use shear rate values between 300 and 500 s^{-1} (Steffe, 1996); for this reason, a shear rate of 300 s^{-1} was considered to measure the apparent viscosity of hydrogels with or without oil (**Table 1**), once the fabrication of a low saturated fat chocolate-based product with similar flow behavior could be feasible under the formulation conditions used in this study. Complex hydrogels with CHI:ALG and CHI:CR2 presented the biggest apparent viscosity values, especially at a polymer ratio of 25:75, with an apparent viscosity of 0.993 Pa.s for CHI:ALG and 0.631 Pa.s for CHI:CR2. These values were significantly higher than the ones observed for the pure polymers or in hydrogels containing canola oil. CHI:CR2 with added oil presented an apparent viscosity of 0.246 Pa.s, lower than respective formulations CHI:ALG (0.537 Pa.s) and CHI:CR1 (0.286 Pa.s), but presenting the biggest σ_o (23.45 Pa), being the formulation with the more coherent structure.

A relationship between the microstructure and the rheological parameters of the hydrogels with oil was observed since the more organized the structure, the higher the viscosity and n value, and the lower the σ_o (CHI:ALG 25:75). It is possible that stronger gelling effects have occurred in CR1 and CR2 than in ALG, resulting in the n and σ_o observed values, and the difference in the apparent viscosity could be related to the possible free oil observed in the CR1 and CR2 micrographs; however, the thickening and gelling properties of these polysaccharides avoided the oil expulsion.

This study considered the values obtained from water retention and oil retention to choose the formulation CHI:CR2 for application in chocolate. Future applications may also be evaluated for the use of alginate-based hydrogels, which also showed excellent performance.

TABLE 2 | Whiteness index of chocolate samples during the stability study (samples stored at 24 ± 1°C).

Time (days)	**Chocolate**	
	CC	**RFC**
1	17.18 ± 0.18^{cA}	16.74 ± 0.43^{bA}
15	18.31 ± 0.99^{cA}	18.94 ± 0.83^{abA}
30	18.84 ± 0.54^{bcA}	19.27 ± 0.45^{abA}
45	20.26 ± 0.54^{abA}	19.36 ± 0.51^{aA}
60	20.67 ± 0.89^{aA}	20.78 ± 0.57^{aA}

Control Chocolate (CC) and Reduced Fat Chocolate (RFC).
Different uppercase letters indicate a significant difference ($p \leq 0.05$) in the same column.
Different lowercase letters indicate a significant difference ($p \leq 0.05$) in the same line.

Chocolate

Particle Size, Tempering Index and Moisture Content of Chocolate

The average particle size obtained for the control chocolate (CC) and reduced fat chocolate (RFC) was 22.7 ± 3.71 and 24.4 ± 5.82 μm, respectively. The temper index was 4.13 ± 0.50 (CC) and 4.57 ± 1.25 (RFC), within the recommended range for

appropriately tempered chocolates. The moisture content was 2.12% ± 0.04 (CC) and 2.07% ± 0.05 (RFC). The results indicate suitable processing conditions, without significant differences ($p \leq 0.05$) between treatments by the Tukey test at 95% confidence level.

Whiteness Index

The whiteness index correlates the variations in the reflected light with the development of fat bloom. The manifestation of white, gray spots and loss of characteristic luster of chocolate, due to the formation of crystals extended to the surface, causes diffusion in the reflection of light, thus interfering in the colorimetry of chocolate (Bricknell and Hartel, 1998).

The values obtained for the Whiteness Index (WI – Whiteness Index) of CC and RFC formulations after 1, 15, 30, 45, and 60 days of storage at 24 ± 1°C under controlled conditions, are shown in **Table 2**, observing that there was a significant difference through the storage time between the samples. If the means and deviations between the formulations were evaluated, it can be noticed that there was no significant difference between the two formulations. There was a change in WI over time, but this change has not been caused necessarily by the presence of canola oil.

Microstructure

The microstructural analysis of the CC and RFC samples (surface and cross-section) at 1st storage day is shown in **Figure 7**. A more irregular surface can be observed for CC, while RFC presented a smoother surface (A3, C3). This suggests a uniform spatial distribution of numerous stable β polymorph crystals in a network with well-defined crystalline connections, characteristic of chocolates with good temper (Afoakwa et al., 2009). The cross-sectional image of chocolate formulated with hydrogels (D1, D2 and D3) also showed apparently encapsulated structures, which may be related to the particles of structured oil drops dispersed in the chocolate, but we assumed that there is no homogeneous distribution throughout the sample. Similar structures were reported by Skelhon et al. (2013) who replaced 50% cocoa butter content with 2% agar microgels (containing 20% of sunflower oil).

Figure 8 shows the presence of small dots or circular white spots that are not homogeneous and without a defined shape (A1, C2) giving the appearance of marble on the surface, and on the other hand, small "needles" can be seen in micrographs E2 and E3, which may be related to the formation of new crystals, referring to 60 days of storage. In RFC samples, small holes were observed on the surface (**Figure 8**; C1, C2, and C3). The encapsulated structures found in micrographs H1 and H2 appear to be rougher compared to the cross-sectional images of **Figure 7** (D1, D2, and D3).

On the other hand, comparing sections A1 and A2 with C1 and C2 in **Figure 7**, we observe that in RFC, there is apparently a "covering" effect at the surface, perhaps due to the presence of fat substitutes. But when we look closer (amplification x2.5K), we do not see much difference between the CC and RFC samples. In **Figure 8**, this "covering" effect provided by fat substitutes is clearer and this probably contributed positively to avoid the unwanted visual changes caused by the polymorphic transition from β5 to β6 that occurs with storage. Furthermore, if we compare **Figure 8**, B3 with D3, we notice that the presence of fat substitutes did not cause considerable changes internally to the chocolate, but only at its surface.

In **Figure 8** (A2, A3) needle-like crystals are observed, according to Rousseau; Smith (2008); crystals already present if the food of triacylglycerols in liquid form forming needle-like crystals that emerge on the chocolate surface, so that changes can be observed with the naked eye on the chocolate surface. On the other hand, in regular chocolate, the existing crystals will feed on the available liquid state triglycerides, leading to large needles that extend outside the surface. Although different in appearance and in the flowering and kinetic path of fat, both solid and filled chocolates will appear flowery to the naked eye.

However, further studies using Scanning Electron Microscopy, for a better visualization and X-Ray Diffraction to understand the polymorphic forms of the lipid phase could contribute to a better understanding of the influence of the substitution of part of the chocolate cocoa butter by the hydrogels with 20% of canola oil.

Rheological Analyses

Yield stress parameters and plastic viscosity are shown in **Table 3**. It can be seen that the plastic viscosity of the RFC formulation was greater than CC for all the evaluated conditions. However, the values found for both formulations remained within the range that covers the vast majority of commercial chocolates, from 2 to 4 Pa.s (Beckett, 2009). The differences between the formulations are possibly related with the reduction of the fat content (16%) for RFC. Industrial-scale processing, as well as the use of emulsifiers, can reduce differences in the rheological properties of the formulations.

The CC yield stress did not show significant variations on day 1 and 45 of storage, but at 60 days of storage, the CC yield stress got a significant increase maintaining a more coherent profile compared with the RFC, always showing higher values than the CC. The flow limit is affected by the particle-particle interaction, the quantity and specific surface area of the particles, emulsifiers and moisture content (Do et al., 2007; Ashrafie et al., 2014). The trend observed for the flow limit between treatments may be the result of changes caused by the increase in total solids content together with the reduction of the fatty phase in chocolate in RFC.

Plastic viscosity is always higher in RFC (values from 2.02 to 3.06 Pa.s) than in CC (between 1.57 and 1.95 Pa.s), and decreases in both treatments through the storage time. The effect of the fat is proportionally bigger for the plastic viscosity than for the yield stress. For example, the extra fat in the CC is added to the free fat molecules and this causes the particles, when they flow, to stick together. This free fat has a great effect on the flow lubrication when it occurs and then the plastic viscosity decreases (Ashrafie et al., 2014). And even with these differences found between treatments, very similar values to those reported in the literature were obtained (Lee et al., 2009; Skelhon et al., 2013).

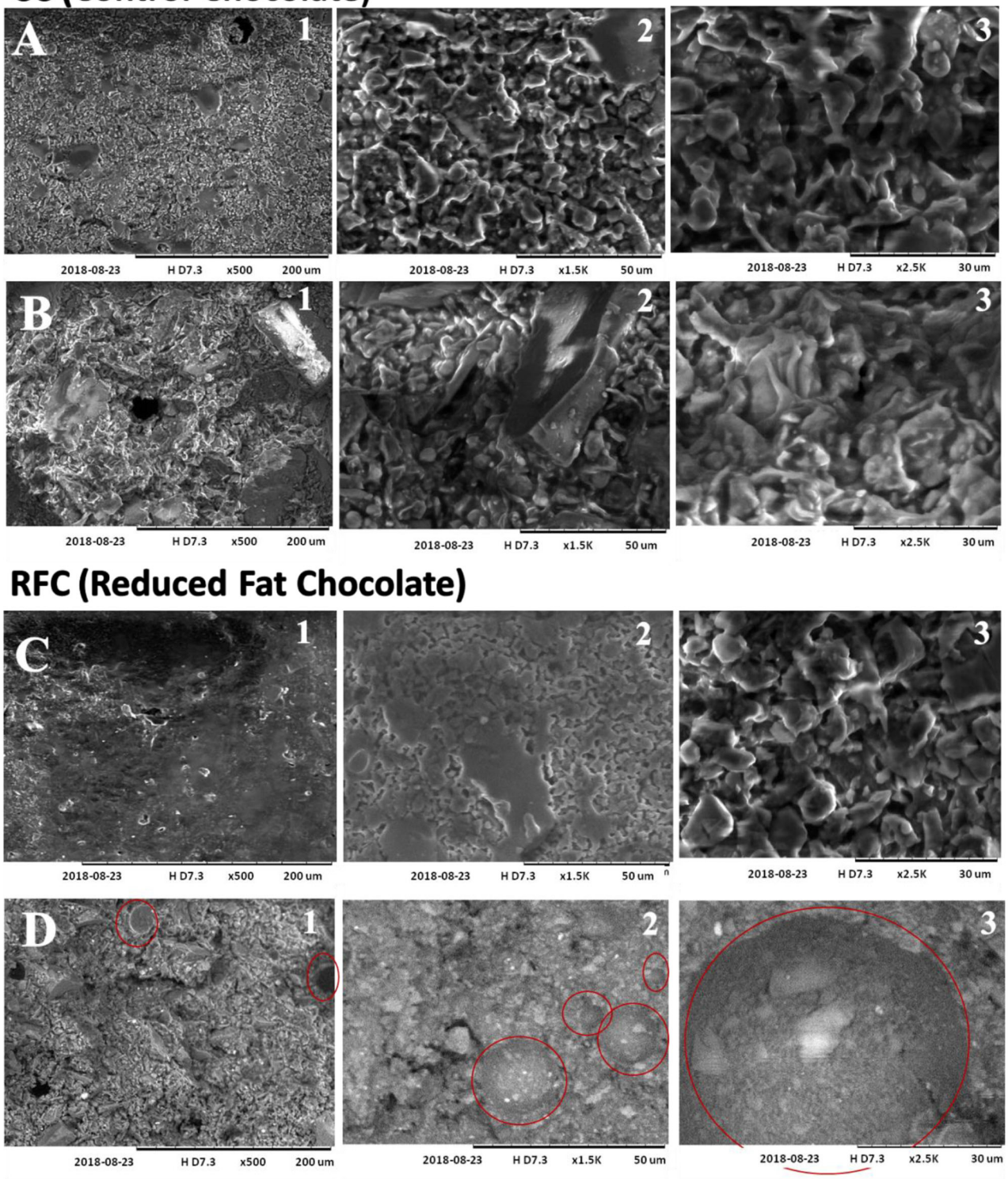

FIGURE 7 | Optical micrograph of control chocolates (CC) and reduced fat chocolate (RFC): Surface **(A,C)**; Cross section **(B,D)** in three different increments 500 × (1), 1,500 × (2), and 2,500 × (3) on day 1 of storage.

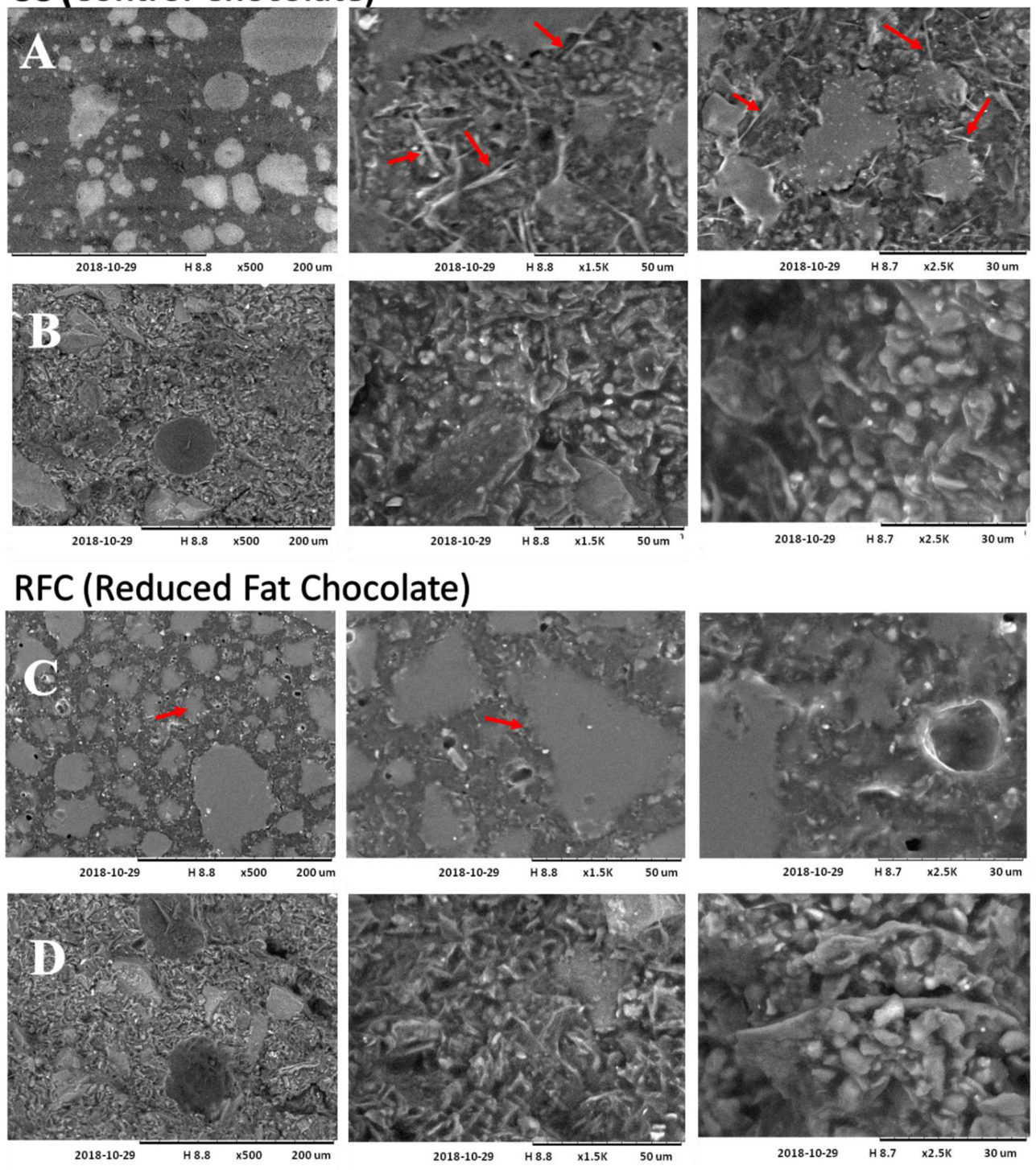

FIGURE 8 | Optical micrograph of control chocolates (CC) and reduced fat chocolate (RFC): Surface **(A,C)**; Cross section **(B,D)** in three different increments 500 × (1), 1,500 × (2), and 2,500 × (3) on day 60 of storage.

Texture (Snap Test)

The tension and breaking strength of the CC and RFC is shown in **Table 4** after 1, 15, 30, 45, and 60 days of storage at 24 ± 1°C. We can observe that the values of tension and force decreased, in both formulations, according to the storage time. After 60 days of monitoring, we can see that the CC had greater variations

TABLE 3 | Yield stress (τCA) and plastic viscosity (μCA) of the control chocolate (CC) and reduced fat chocolate (RFC) obtained by the Casson model.

Times (days)	τ_{CA} Yield stress (Pa)		μ_{CA} Plastic viscosity (Pa.s)	
	CC	RFC	CC	RFC
1	2.246 ± 0.149^{bB}	6.263 ± 0.863^{aA}	1.952 ± 0.007^{aB}	3.064 ± 0.274^{aA}
15	2.130 ± 0.027^{bB}	5.644 ± 0.732^{aA}	$1.838 \pm 0{,}081^{abB}$	2.920 ± 0.093^{aA}
30	2.014 ± 0.026^{bB}	5.075 ± 0.289^{abA}	1.737 ± 0.095^{bcB}	3.096 ± 0.047^{aA}
45	1.927 ± 0.002^{bB}	4.890 ± 0.705^{abA}	1.685 ± 0.007^{bcB}	2.881 ± 0.329^{aA}
60	3.185 ± 0.511^{aA}	3.384 ± 0.053^{bA}	1.578 ± 0.104^{cB}	2.026 ± 0.070^{bA}

Different lowercase letters indicate a significant difference ($p < 0.05$) in the same line at the same storage time (1, 15, 30, 46 e 60 days).
Different capital letters indicate a significant difference ($p < 0.05$) between CC and RFC formulations at the same storage time.

in tension (from 2.17 to 1.17 kgf/cm2) and breaking strength (from 44.32 to 20.87 N) with significant differences in 15–60 days of storage. On the other hand, RFC, even though the values decreased from 1.95 to 1.46 kgf/cm2 and 45.29 to 32.12 did not present significant differences.

The values obtained coincide with those reported for chocolates with partial substitution of cocoa butter by alternative fats such as Cocoa Butter Substitute (CBS) (Biswas et al., 2017), and Cocoa Butter Replacer (CBR) (Quast et al., 2013). The different concentrations of cocoa butter have not been shown to influence the mechanical strength of chocolate in the two formulations, despite the differences found in the treatments. Afoakwa et al. (2009) mention that the force necessary to penetrate the chocolate is dependent on the interaction that exists between the particles; this interaction is a result of the particle size in the chocolate and also the type and quantity of fat.

Melting Point

The study of the melting profile of chocolate allows assume about melting characteristics in the mouth of this product when consumed. According to Clercq et al. (2014), the melting profile of dark chocolate should have a narrow melting peak, leading to a rapid melting at 37°C (body temperature), producing a feeling of freshness and softness in the mouth. This is also related to the type of polymorphic shape of the crystals formed during tempering. **Table 5** shows the thermodynamic data obtained by DSC for the CC and RFC samples, after periodic monitoring for 60 days. The parameters for the evaluation of the melting properties were T_{onset} (temperature at which the corresponding crystalline form starts to melt), T_{end} (temperature at which the sample liquefaction is completed), ΔH_{melt} (amount of energy required for the complete sample fusion) and T_{max} (temperature at which maximum melting occurs) (Afoakwa et al., 2009).

The CC had the highest crystallization temperature on the 30th (30.83°C) and the lowest on the 60th day of storage (27.02°C); this behavior was also observed at the maximum melting temperature (T_{max}) with values between 31.78 and 34.18°C. In RFC, there is a slight variation in the values of T_{onset} and T_{max}, but there is no significant difference with time. At the final sample liquefaction temperatures (Tend), there were significant variations with values between 36.81 and 38.47°C through the storage times. The values obtained are slightly higher than the results presented by Afoakwa et al. (2008b); they carried out tests using DSC for chocolates with different levels of lecithin and fat, but with a total cocoa butter content above 34%, obtaining melting curves for maximum peak temperatures in the range of 32.3–32.5°C. Some authors comment that the specific solid-solid transition to a higher stable crystal structure formation culminates in the development of fat bloom (Lonchampt and Hartel, 2004), and as a consequence, consumers of chocolate need to spend more time for complete melting under the temperature of the mouth (Rousseau, 2007). It can be assumed that this is related to the composition of chocolate. In this case, RFC produced from the CHI:CR2 complex with 20% CO needs a higher temperature to reach the final melting point during storage. It was noted that the enthalpy value increases, with a significant difference, during the storage time from 28.33 J/g on day 1 to 48.65 J/g on day 60, the last one showing the greatest stability due to greater energy adsorbed in the fusion process. Moreover, we observe that the addition of hydrogels with canola oil, in the melting enthalpy values, was initially lower in relation to CC. At the end of the stability evaluation period, it was higher, indicating the polymorphic transition to more stable crystal forms, which coincides with what is displayed in **Figures 7, 8**.

In general, a very similar behavior can be observed between CC and RFC, without a significant difference in the parameters T_{onset}, T_{max}, T_{end}. These three temperatures are related to the type of crystal and the melting properties, which may be the result of the polymorphic stabilization of chocolates. It is interesting to note that the standard deviation of the enthalpy of fusion is higher compared to other parameters. Literature reported that depending on the crystallization technique, a greater distribution of different polymorphic forms in the fat matrix may occur, which would result in less dense and heterogeneous crystalline fat structures. As a result, this variability in polymorphism and heterogeneous crystals would be reflected in the variation found in the fusion parameters (Svanberg et al., 2011). This does not mean that variations observed for RFC reflect a negative effect compared to CC, but possibly CC takes less time to reach stability in the first moment.

Nutritional Profile Analysis

The nutritional information of the two chocolate formulations (control chocolate and modified chocolate) is shown in **Table 6**. The values obtained from the energy value (523.3 Kcal/100 g)

TABLE 4 | Breaking stress (kgf cm-2) and breaking strength (N) of control chocolate bars (CC) and reduced fat chocolate (RFC).

Times (days)	Breaking strength (N)		Breaking stress ($kgfcm^{-2}$)	
	CC	RFC	CC	RFC
1	44.32 ± 12.97^{aA}	45.29 ± 4.24^{aA}	2.17 ± 0.40^{aA}	1.95 ± 0.13^{aA}
15	27.84 ± 6.30^{bcA}	27.46 ± 4.51^{bA}	1.48 ± 0.22^{bcA}	1.22 ± 0.13^{bA}
30	25.54 ± 3.96^{bcB}	31.68 ± 4.60^{bA}	1.40 ± 0.17^{bcB}	1.39 ± 0.13^{bA}
45	36.12 ± 12.71^{abA}	33.67 ± 6.47^{bA}	1.82 ± 0.37^{abA}	1.54 ± 0.20^{bA}
60	20.87 ± 5.10^{cB}	32.12 ± 7.15^{bA}	1.17 ± 0.18^{cB}	1.46 ± 0.25^{bA}

Different lowercase letters indicate a significant difference ($p \leq 0.05$) in the same line in the same storage time (1, 15, 30, 46 e 60 days).
Different uppercase letters indicate a significant difference ($p \leq 0.05$) between CC and RFC formulations in the same storage time.

TABLE 5 | Overview of the melting profile of control chocolate (CC) and modified chocolate (RFC).

Times (days)	T_{onset} (°C)	T_{max} (°C)	T_{end} (°C)	ΔT (°C)	ΔH (J/g)
CC					
1	29.73 ± 0.67^{abA}	32.79 ± 0.35^{bcA}	36.95 ± 0.96^{aA}	7.21 ± 1.03^{bcA}	40.32 ± 5.53^{aA}
15	$29.62 \pm 2.46_{abA}$	32.48 ± 0.81^{bcA}	36.45 ± 0.78^{aA}	6.83 ± 1.69^{cA}	45.76 ± 1.47^{aA}
30	30.83 ± 1.66^{aA}	34.18 ± 0.14^{aA}	38.04 ± 0.37^{aA}	7.22 ± 1.40^{bcA}	37.47 ± 7.22^{aA}
45	28.21 ± 0.56^{abA}	33.50 ± 0.49^{abA}	38.23 ± 0.78^{aA}	10.02 ± 0.65^{abA}	44.64 ± 3.28^{aA}
60	27.02 ± 0.08^{bA}	31.78 ± 0.08^{cA}	37.43 ± 0.28^{aA}	10.41 ± 0.33^{aA}	40.94 ± 4.24^{aB}
Times (days)	**T_{onset} (°C)**	**T_{max} (°C)**	**T_{end} (°C)**	**ΔT (°C)**	**ΔH (J/g)**
RFC					
1	29.83 ± 1.56^{aA}	33.25 ± 0.24^{aA}	36.81 ± 0.59^{bA}	8.12 ± 1.15^{bA}	28.33 ± 2.54^{cB}
15	27.23 ± 0.68^{aA}	31.88 ± 0.64^{aA}	37.95 ± 0.42^{abA}	9.58 ± 0.79^{abA}	37.39 ± 2.71^{bB}
30	29.72 ± 1.40^{aA}	33.08 ± 0.81^{aA}	38.15 ± 0.40^{abA}	8.43 ± 1.20^{bA}	36.17 ± 1.48^{bA}
45	28.82 ± 0.23^{aA}	33.31 ± 0.07^{aA}	38.47 ± 0.46^{aA}	9.65 ± 0.31^{abA}	38.07 ± 2.14^{bB}
60	27.47 ± 0.63^{aA}	33.11 ± 1.03^{aA}	38.47 ± 0.95^{aA}	11.01 ± 0.74^{aA}	48.65 ± 1.31^{aA}

Different lowercase letters indicate a significant difference ($p \leq 0.05$) in the same line in the same storage time (1, 15, 30, 46 e 60 days).
Different uppercase letters indicate a significant difference ($p \leq 0.05$) between CC and RFC formulations in the same storage time.

and total fat value (36.8 g/100 g) of the modified chocolate are slightly lower than the control. This was an expected result, due to the partial substitution of cocoa butter in the final product. On the other hand, modified chocolate is the one that presents a higher value of sodium content (38.0 mg/kg) and carbohydrates (38.2 g/100 g), possibly due to the influence of polysaccharides (included in the carbohydrates group), and the lower saturated fat of RFC than CC. Even with these slight differences, RFC has a caloric and fat reduction advantage in the nutritional profile, and above all the decrease of 4.4 g of saturated fat corresponding to 16% less than the control chocolate. This makes it a final product with an interesting nutritional profile to be explored in the healthier market for the consumer, with a low content of saturated fat.

Sensory Evaluation

Figure 9 presents the results from the sensory evaluation of CC and RFC. There was no significant difference ($p \leq 0.05$) between CC and RFC regarding the appearance and flavor (cocoa and fat aroma). For all of the attributes evaluated, average values between 6.39 and 7.40 were obtained, indicating on the hedonic scale that most tasters defined that they "liked the chocolates a little" and "liked the chocolates a lot" (numerical values between 6 and 8). This result is considered good, indicating that addition of hydrogels with 20% of canola oil did not influence the sensory acceptance of chocolate.

On the other hand, the results show that the attributes of sweetness, and mainly mouthfeel, were the most affected by the partial substitution of cocoa butter proposed in this work. Values for both attributes present significant differences. Among the total number of evaluators, 47% would certainly buy CC and 40% would certainly buy RFC.

However, although there is a significant difference in the general impression of the different treatments, this difference was not very large, considering that RFC is a "new" product, so it is interesting to study attributes that are the most affected in the technological process, such as the melting, and which represent a significantly greater difference for the consumer, compared to CC.

It should be noted that the results presented are only the result of the sensory evaluation of the products attributes (color, aroma,

TABLE 6 | Comparison of the nutritional profile of control chocolate (CC) with reduced fat chocolate (RFC).

Nutritional information	Value/100 g	Dark chocolate 70%	
		CC	RFC
Energetic value**	(kJ)	2,304.3	2,189.5
Calories	(Kcal)	550.7	523.3
Carbohydrates**	(g)	34.8	38.2
Protein	(g)	9.6	9.8
Total fat	(g)	41.5	36.8
Saturated fat	(g)	27.1	22.7
Fat trans	(g)	0.0	0.0
Dietary fiber	(g)	9.5	10.4
Sodium	(mg/kg)	23.0	38.0

*** Values obtained by Calculations.*

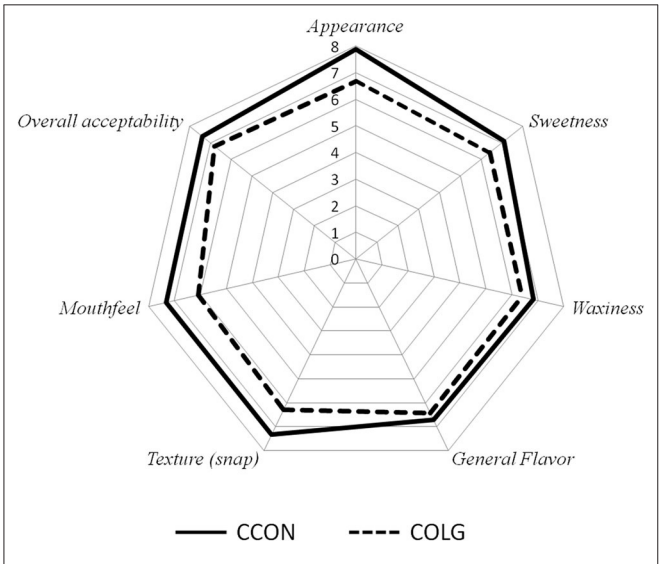

FIGURE 9 | Sensory evaluation of the attributes of — control chocolate (CC) and – – – reduced fat chocolate (RFC).

taste, and texture); therefore, they are not decisive in defining the purchase intention of the product. In addition to the fundamental role of sensory properties, there are other factors, such as type of consumer, packaging, messages on labels (for example: health benefits, absence of additives, traditional and distinct production) and, to a large extent, price (Carneiro et al., 2005; Haddad et al., 2007).

CONCLUSIONS

We demonstrated that polymeric materials such as sodium alginate and carrageenans for the production of complex hydrogels with chitosan allow obtaining cross-linked systems to form a 3D structure with good physical stability, using polysaccharides without emulsifying properties. However, due to the fact that these polymers do not have an active surface, the systems cannot retain large amounts of oil. Nevertheless, the oil retention in hydrogels CHI:ALG (25:75) and CHI:CR2 (25:75) with 20% of canola oil was considered effective. CHI:CR2 hydrogel with 20% of canola oil was used as a partial substitute for cocoa fat in the formulation of 70% dark chocolate with a reduction of 16% of saturated fat in the final product (compared to control). Also, a technical differential for chocolate production was the "covering" effect observed with the reformulation of chocolate, which brings positive contributions to avoid the unwanted visual changes caused by the polymorphic transition of the β5 to β6 crystals that occurs with storage. We hope that these findings generate great interest in the polymeric materials used in this study, due to the natural, non-toxic, and food-grade nature, which guarantees greater exploration, as a strategy for structuring foods with lower fat content.

DATA AVAILABILITY STATEMENT

The raw data supporting the conclusions of this article will be made available by the authors, without undue reservation.

ETHICS STATEMENT

The studies involving human participants were reviewed and approved by Comitê de Ética em Pesquisa da Universidade Estadual de Campinas. The patients/participants provided their written informed consent to participate in this study.

AUTHOR CONTRIBUTIONS

All authors listed have made a substantial, direct and intellectual contribution to the work, and approved it for publication.

FUNDING

The authors gratefully acknowledge the financial support for this research from The National Council for the Support of Research CAPES (Finance Code 001) and CNPq (170289/2017-6, 306461/2017-0) for fellowship and FAPESP for financial support (projects 2018/20466-8, 2009/54137-1).

REFERENCES

Afoakwa, E. O., Paterson, A., and Fowler, M. (2008a). Effects of particle size distribution and composition on rheological properties of dark chocolate. *Eur. Food Res. Technol.* 226, 1259–1268. doi: 10.1007/s00217-007-0652-6

Afoakwa, E. O., Paterson, A., Fowler, M., and Vieira, J. (2008b). Characterization of melting properties in dark chocolates from varying particle size distribution

and composition using differential scanning calorimetry. *Food Res. Int.* 41, 751–757. doi: 10.1016/j.foodres.2008.05.009

Afoakwa, E. O., Paterson, A., Fowler, M., and Vieira, J. (2009). Influence of tempering and fat crystallization behaviours on microstructural and melting properties in dark chocolate systems. *Food Res. Int.* 42, 200–209. doi: 10.1016/j.foodres.2008.10.007

Afzal, S., Maswal, M., and Dar, A. A. (2018). Rheological behavior of pH responsive composite hydrogels of chitosan and alginate: characterization and its use in encapsulation of citral. *Colloids Surfaces B: Biointerf.* 169, 99–106. doi: 10.1016/J.COLSURFB.2018.05.002

Ahmed, E. M. (2015). Hydrogel: preparation, characterization, and applications: a review. *J. Adv. Res,* 6, 105–121. doi: 10.1016/j.jare.2013.07.006

Alnemr, T., Helal, A., Hassan, A., and Elsaadany, K. (2016). Utilizing the functions of hydrocolloids as fat mimetic to enhance the properties of low-fat domiati cheese. *J. Food Proces. Technol.* 7, 105–121. doi: 10.4172/2157-7110.1000637

AOAC (2016). "Cocoa beans and its products," in *International Official Methods of Analysis of AOAC International Guidelines for Standard Method Performance Requirement*, ed P. S. ARIA (Gaithersburg: AOAC International).

Ashrafie, N., T., Azizi, M. H., Taslimi, A., Mohammadi, M., Neyestani, T. R., et al. (2014). Development of reduced-fat and reduced-energy dark chocolate using collagen hydrolysate as cocoa butter replacement agent. *J. Food Nutrit. Res.* 53, 13–21.

Beckett, S. T. (2009). *Industrial Chocolate Manufacture and Use: Fourth Edition*. Oxford: Blackwell Publishing Ltd.

Biswas, N., Cheow, Y. L., Tan, C. P., and Siow, L. F. (2017). Physical, Rheological and sensorial properties, and bloom formation of dark chocolate made with cocoa butter substitute (CBS). *LWT - Food Sci. Technol.* 82, 420–428. doi: 10.1016/j.lwt.2017.04.039

Bricknell, J., and Hartel, R. W. (1998). Relation of fat bloom in chocolate to polymorphic transition of cocoa butter. *J. Am. Oil Chem. Soc.* 75, 1609–1615.

Carneiro, J. D. S., Minim, V. P. R., Deliza, R., Silva, C. H. O., Carneiro, J. C. S., and Leão, F. P. (2005). Labelling effects on consumer intention to purchase for soybean oil. *Food Qual. Prefer.* 16, 275–282. doi: 10.1016/j.foodqual.2004.05.004

Clercq, N., De., Depypere, F., Delbaere, C., Nopens, I., Bernaert, H., et al. (2014). Influence of cocoa butter diacylglycerols on migration induced fat bloom in filled chocolates. *Eur. J. Lipid Sci. Technol.* 116, 1388–1399. doi: 10.1002/ejlt.201300476

Comert, F., Malanowski, A. J., Azarikia, F., and Dubin, P. L. (2016). Coacervation and precipitation in polysaccharide-protein systems. *Soft Matter* 12, 4154–4161. doi: 10.1039/c6sm00044d

Do, T. A. L., Hargreaves, J. M., Wolf, B., Hort, J., and Mitchell, J. R. (2007). Impact of particle size distribution on rheological and textural properties of chocolate models with reduced fat content. *J. Food Sci.* 72, 541–552. doi: 10.1111/j.1750-3841.2007.00572.x

Espinosa-Andrews, H., Báez-González, J. G., Cruz-Sosa, F., and Vernon-Carter, E. J. (2007). Gum Arabic-chitosan complex coacervation. *Biomacromolecules* 8, 1313–1318. doi: 10.1021/bm0611634

Espinosa-Andrews, H., Enríquez-Ramírez, K. E., García-Márquez, E., Ramírez-Santiago, C., Lobato-Calleros, C., and Vernon-Carter, J. (2013). Interrelationship between the zeta potential and viscoelastic properties in coacervates complexes. *Carbohyd. Poly.* 95, 161–66. doi: 10.1016/j.carbpol.2013.02.053

Espinosa-Andrews, H., Sandoval-Castilla, O., Vázquez-Torres, H., Vernon-Carter, E. J., and Lobato-Calleros, C. (2010). Determination of the gum arabic–chitosan interactions by fourier transform infrared spectroscopy and characterization of the microstructure and rheological features of their coacervates. *Carbohyd. Poly.* 79, 541–546. doi: 10.1016/j.carbpol.2009.08.040

Gallaher, D. D., Gallaher, C. M., Mahrt, G. J., Carr, T. P., Hollingshead, C. H., Hesslink, R., et al. (2002). A glucomannan and chitosan fiber supplement decreases plasma cholesterol and increases cholesterol excretion in overweight normocholesterolemic humans. *J. Am. College Nutrit.* 21, 428–433. doi: 10.1080/07315724.2002.10719246

Goycoolea, F. M., Argüelles-Monal, W., Peniche, C., and Higuera-Ciapara, H. (2000). Effect of chitosan on the gelation of K-Carrageenan under various salt conditions. *Hydrocolloids* 2000, 211–216. doi: 10.1016/B978-044450178-3/50087-1

Haddad, Y., Haddad, J., Olabi, A., Shuayto, N., Haddad, T., and Toufeili, I. (2007). Mapping determinants of purchase intent of concentrated yogurt (Labneh) by conjoint analysis. *Food Qual. Preference* 18, 795–802. doi: 10.1016/j.foodqual.2007.01.009

Kulig, D., Zimoch-Korzycka, A., Jarmoluk, A., and Marycz, K. (2016). Study on alginate-chitosan complex formed with different polymers ratio. *Polymers* 8, 1–17. doi: 10.3390/polym8050167

Kulig, D., Zimoch-Korzycka, A., Kr,ó, Z., Oziembłowski, M., and Jarmoluk, A. (2017). Effect of film-forming alginate/chitosan polyelectrolyte complex on the storage quality of pork. *Molecules* 22:98. doi: 10.3390/molecules22010098

Künzler, J. F. (2002). "Hydrogels," in *Encyclopedia of Polymer Science and Technology* (Hoboken, NJ: John Wiley & Sons, Inc.). Available online at: https://onlinelibrary.wiley.com/page/book/10.1002/0471440264/homepage/editorscontributors.html

Lee, S., Biresaw, G., Kinney, M. P., and Inglett, G. E. (2009). Effect of cocoa butter replacement with a β-glucan-rich hydrocolloid (C-Trim30) on the rheological and tribological properties of chocolates. *J. Sci. Food Agri.* 89, 163–167. doi: 10.1002/jsfa.3424

Lohman, M. H., and Hartel, R. W. (1994). Effect of milk fat fractions on fat bloom in dark chocolate. *J. Am. Oil Chem. Soc.* 71, 267–276. doi: 10.1007/BF02638052

Lonchampt, P., and Hartel, R. W. (2004). Fat bloom in chocolate and compound coatings. *Eur. J. Lipid Sci. Technol.* 106, 241–274. doi: 10.1002/ejlt.200400938

Maezaki, Y., Tsuji, K., Nakagawa, Y., Kawai, Y., Akimoto, M., Tsugita, T., et al. (1993). Hypocholesterolemic effect of chitosan in adult males. *Biosci. Biotechnol. Biochem.* 57, 1439–1444. doi: 10.1271/bbb.57.1439

Miyasaki, E. K. (2013). *Avaliação a Adição de Emulsificantes do Tipo Lecitinas Modificadas na Cristalização de Manteiga de Cacau e de Chocolate Amargo*. [master's thesis]. Universidade Estadual de Campinas.

O'Brien, C. M., Muller, A., Scannell, A. G. M., and Arendt, E. (2003). Evaluation of the effects of fat replacers on the quality of wheat bread. *J. Food Eng.* 56, 265–267. doi: 10.1016/S0260-8774(02)00266-2

Paglarini, C., de, S., Furtado, G. de, F., Biachi, J. P., Silva, V. A. V., Martini, S., et al. (2018). Functional emulsion gels with potential application in meat products. *J. Food Eng.* 222, 29–37. doi: 10.1016/j.jfoodeng.2017.10.026

Patel, A. R., Schatteman, D., Lesaffer, A., and Dewettinck, K. (2013). A foam-templated approach for fabricating organogels using a water-soluble polymer. *RSC Adv.* 3, 22900–22903. doi: 10.1039/c3ra44763d

Peppas, N. A., and Khare, A. R. (1993). Preparation, Structure and diffusional behavior of hydrogels in controlled release. *Adv. Drug Delivery Rev.* 11, 1–35. doi: 10.1016/0169-409X(93)90025-Y

Quast, L. B., Luccas, V., Ribeiro, A. P. B., Cardoso, L. P., and GuenterKieckbusch,. T. (2013). Physical properties of tempered mixtures of cocoa butter, CBR and CBS fats. *Int. J. Food Sci. Technol.* 48, 1579–1588. doi: 10.1111/ijfs.12127

Rabelo, R. S., Oliveira, I. F., Da Silva, V. M., Prata, A. S., and and. Hubinger, M. D. (2018). Chitosan coated nanostructured lipid carriers (NLCs) for loading vitamin D: A physical stability study. *Int. J. Biol. Macromol.* 119, 902–912. doi: 10.1016/J.IJBIOMAC.2018.07.174

Rabelo, R. S., Tavares, G. M., Prata, A. S., and and. Hubinger, M. D. (2019). Complexation of chitosan with gum arabic, sodium alginate and κ-carrageenan: effects of pH, polymer ratio and salt concentration. *Carbohyd. Poly.* 223:115120. doi: 10.1016/j.carbpol.2019.115120

Rather, S. A., Masoodi, F. A., Akhter, R., Rather, J. A., Gani, A., Wani, S. M., et al. (2015). Effects of guar-xanthan gum mixture as fat replacer on the physicochemical properties and oxidative stability of goshtaba, a traditional indian meat product. *J. Food Proces. Preserv.* 39, 2935–2946. doi: 10.1111/jfpp.12545

Rather, S. A., Masoodi, F. A., Akhter, R., Rather, J. A., Gani, A., Wani, S. M., et al. (2016). Application of guar–xanthan gum mixture as a partial fat replacer in meat emulsions. *J. Food Sci. Technol.* 53, 2876–2886. doi: 10.1007/s13197-016-2270-4

Rousseau, D. (2007). "The microstructure of chocolate," in *Understanding and Controlling the Microstructure of Complex Foods*. ed Woodhead Publishing. (Ryerson University: Woodhead Publishing).

Sæther, H. V., Holme, H. K., Maurstad, G., Smidsrød, O., and Stokke, B. T. (2008). Polyelectrolyte complex formation using alginate and chitosan. *Carbohyd. Poly.* 74, 813–821. doi: 10.1016/j.carbpol.2008.04.048

Shepherd, R., Reader, S., and Falshaw, A. (1997). Chitosan functional properties. *Glycoconj. J.* 14, 535–542. doi: 10.1023/A:1018524207224

Skelhon, T. S., Olsson, P. K. A., Morgan, A. R., and Bon, S. A. F. (2013). High internal phase agar hydrogel dispersions in cocoa butter and chocolate as a route towards reducing fat content high internal phase agar hydrogel dispersions in cocoa butter and chocolate as a route towards reducing fat content. *Food Funct.* 44, 1279–1422. doi: 10.1039/c3fo60122f

Smith, J. (2008). *Post-Structuralist Discourse Relative to Phenomological Pursuits in the Deconstructivist Arena*. [dissertation/master's thesis]. (Chicago, IL: University of Chicago).

Steffe, J. F. (1996). *Rheological Methods in Food Process Engineering, 2nd edition*. East Lansing, MI: Freeman Press.

Svanberg, L., Ahrn,é, L., Lorén, N., and Windhab, E. (2011). Effect of sugar, cocoa particles and lecithin on cocoa butter crystallisation in seeded and non-seeded chocolate model systems. *J. Food Eng.* 104, 70–80. doi: 10.1016/j.jfoodeng.2010.09.023

Volod'ko, A. V., Davydova, V. N., Barabanova, A. O., Soloveva, T. F., and Ermak, I. M. (2012). Formation of soluble chitosan-carrageenan polyelectrolyte complexes. *Chem. Nat. Comp.* 48, 353–357. doi: 10.1007/s10600-012-0250-0

Volod'ko, A. V., Davydova, V. N., Chusovitin, E., Sorokina, I. V., Dolgikh, M. P., Tolstikova, T. G., et al. (2014). Soluble chitosan–carrageenan polyelectrolyte complexes and their gastroprotective activity. *Carbohydr. Poly.* 101, 1087–1093. doi: 10.1016/j.carbpol.2013.10.049

Volod'ko, A. V., Davydova, V. N., Glazunov, V. P., Likhatskaya, G. N., and Yermak, I. M. (2016). Influence of structural features of carrageenan on the formation of polyelectrolyte complexes with chitosan. *Int. J. Biol. Macromol.* 84, 434–441. doi: 10.1016/j.ijbiomac.2015.12.031

Wijaya, W., Van der Meeren, P., Wijaya, C. H., and Patel, A. R. (2017). High internal phase emulsions stabilized solely by whey protein isolate-low methoxyl pectin complexes: effect of pH and polymer concentration. *Food Funct.* 8, 584–594. doi: 10.1039/c6fo01027j

Wong, B. T., Day, L., and Augustin, M. A. (2011). Deamidated wheat protein–dextran Maillard conjugates: Effect of size and location of polysaccharide conjugated on steric stabilization of emulsions at acidic pH. *Food Hydrocoll.* 25, 1424–1432. doi: 10.1016/j.foodhyd.2011.01.017

Conflict of Interest: The authors declare that the research was conducted in the absence of any commercial or financial relationships that could be construed as a potential conflict of interest.

frontiers in Sustainable Food Systems

MINI REVIEW
published: 14 January 2021
doi: 10.3389/fsufs.2020.566445

Water-in-Oleogel Emulsions—From Structure Design to Functionality

Khakhanang Wijarnprecha[1], *Auke de Vries*[1], *Sopark Sonwai*[2] *and Dérick Rousseau*[1]*

[1] Department of Chemistry and Biology, Ryerson University, Toronto, ON, Canada, [2] Department of Food Technology, Faculty of Engineering and Industrial Technology, Silpakorn University, Bangkok, Thailand

The development of water-in-oleogel (W/Og) emulsions is highlighted, with focus placed on the key properties dictating the structuring ability of both the continuous oleogelled and dispersed phases present. The gelling ability of oleogelators is distinguished by the formation of crystalline structures, polymeric strands, or tubules. Once a dispersed aqueous phase is introduced, droplet stabilization may occur via oleogelator adsorption onto the surface of the dispersed droplets, the formation of a continuous gel network, or a combination of both. Surface-active species (added or endogenous) are also required for effective W/Og aqueous phase dispersion and stabilization. Processing conditions, namely temperature-time-shear regimes, are also discussed given their important role on dispersed droplet and oleogel network formation. The effects of many factors on W/Og emulsion formation, rheology, and stability remain virtually unknown, particularly the role of dispersed droplet size, gelation, and clustering as well as the applicability of the active filler concept to foods. This review explores some of these factors and briefly mentions possible applications of W/Og emulsions.

Keywords: oleogel, water-in-oleogel emulsion, emulsifier, active filler, inactive filler

OPEN ACCESS

Edited by:
Luiz Henrique Fasolin, Campinas State University, Brazil

Reviewed by:
Maya Davidovich-Pinhas, Technion Israel Institute of Technology, Israel
Artur Martins, International Iberian Nanotechnology Laboratory (INL), Portugal
Yong Wang, Jinan University, China

***Correspondence:**
Dérick Rousseau
rousseau@ryerson.ca

Specialty section:
This article was submitted to Sustainable Food Processing, a section of the journal Frontiers in Sustainable Food Systems

Received: *28 May 2020*
Accepted: *30 November 2020*
Published: *14 January 2021*

Citation:
Wijarnprecha K, de Vries A, Sonwai S and Rousseau D (2021) Water-in-Oleogel Emulsions—From Structure Design to Functionality. Front. Sustain. Food Syst. 4:566445. doi: 10.3389/fsufs.2020.566445

INTRODUCTION

Much has been written about emulsion gels and the role of their dispersed and continuous phases on texture and rheology. Research efforts have centered on oil-in-water (O/W) emulsion gels, with far less attention paid to structured water-in-oil (W/O) emulsions (Rafanan and Rousseau, 2019; Wijarnprecha et al., 2019a,b). Many W/O emulsions are stabilized by the presence of a continuous fat crystal network that confers desirable texture, palatability, and functionality. Driven by human health concerns, ingredient sourcing, and consumer acceptability, alternate ways of solidifying the oil phase via oleogelation have come to the forefront (Hughes et al., 2009; Davidovich-Pinhas et al., 2016).

From a food structure design perspective, most processed foods are complex mixtures of building blocks that result in composite materials with distinctly different properties compared to their starting components. This mini-review focuses on the recent progress made in oleogelator-stabilized W/O emulsion gels [water-in-oleogel emulsions (W/Og)], with a focus on the properties of the oleogelators used to create a network in W/Og systems as well as those of the dispersed phase and oil-water interface. An understanding of the contributions of the different phases in W/Og systems offers a pathway to the effective design of these structured emulsions.

DESIGNING W/OG SYSTEMS

Oleogelator Characteristics

The replacement of solid fat in the continuous phase of a W/O emulsion by an oleogel is a novel structuring approach that contributes to lower caloric value and saturated fat content (Scholten, 2017). It is well-known that oleogelators can be used to entrap liquid oil into a self-assembled network of weakly-interacting species (Hu et al., 2015). Upon introduction of a dispersed water phase, however, the oleogelator network must also prevent water droplet coalescence and phase separation, which may be achieved in one of two ways. Via network stabilization, the oleogel matrix encases the dispersed phase and acts as a physical barrier between neighboring droplets. When the oleogelators adsorb to the droplet surface, the resulting interfacial film may limit coalescence, as seen in fat crystal-stabilized W/O emulsions (Ghosh et al., 2011). In this regard, certain emulsifiers may not only affect the kinetics of oleogelator solidification in the bulk, but also interactions between oleogelators and dispersed droplets. Their ability to do so will depend on parameters such as emulsifier concentration, molecular weight, solubility, and molecular compatibility with the oleogelator molecules.

Crystal-Based W/Og Systems

Crystal-based W/Og stabilizers often consist of waxes and, to a lesser extent, emulsifiers, or fatty acids. Sources of wax include rice bran, beeswax, candelilla, shellac, or sunflower. Typically, these consist of long chain fatty acids, or alcohols and wax esters, along with minor compounds such as ketones or aldehydes. Upon cooling, different crystal morphologies may arise, whose shape and size will depend on the inherent wax composition, solvent type, and processing parameters such as cooling and shear regime (Doan et al., 2018).

Certain waxes may also promote formation of kinetically-stable W/O emulsions (Binks and Rocher, 2009; Patel et al., 2013). As little as 2 wt% shellac wax in oil, for example, was shown to stabilize W/Og systems containing a 20 wt% dispersed aqueous phase. Stability arose from the formation of droplets $<5\,\mu m$ in diameter and the presence of small wax crystals at the water droplet surface (Patel et al., 2013). In another study, 10 wt% rice bran wax in oil was used to form and stabilize W/Og systems. Here, stability was conferred by long, needle-like wax crystals present on both the surface of dispersed droplets and in the continuous phase (Wijarnprecha et al., 2019a).

Using waxes as the sole emulsifying agent generally remains challenging as these often lack the necessary surface-active compounds. Efforts to surmount this problem have focused on hybrid systems consisting of wax and an appropriate emulsifier to generate and stabilize kinetically-stable W/Og systems. Toro-Vazquez et al. (2013) found that the use of monoacylglycerols in W/Og systems stabilized by 2 wt% candelilla wax reduced droplet size, but also decreased hardness even though the final solids content with added emulsifier was higher. They ascribed this to weakened crystal-crystal interactions (Toro-Vazquez et al., 2013). In a study on crude oil, Ma et al. (2017) found evidence of synergy between paraffin wax and sorbitan monooleate, which facilitated the adsorption of wax crystals onto the surface of aqueous droplets, resulting in an increased interfacial elastic modulus. Similarly, Haj-shafiei et al. (2013) found that the combination of paraffin wax and glycerol monooleate yielded kinetically-stable W/Og systems with controllable droplet size, as opposed to the use of wax alone.

Besides waxes, other species may be used to stabilize W/Og systems. Using a combination of soy lecithin and stearic acid at up to 30 wt% of the oil phase, Gaudino et al. stabilized W/Og systems containing up to 20 wt% dispersed water. The authors described a mixed system wherein the lecithin formed worm-like micelles that stabilized the stearic acid-covered water droplets (Gaudino et al., 2019). In another study, Hughes et al. found that use of 2 wt% 12-hydroxystearic acid could effectively stabilize W/Og emulsions containing a 10 or 20 wt% dispersed aqueous phase. The resulting system consisted of large, polydisperse water droplets solely stabilized by the surrounding oleogelled network. Addition of an emulsifier decreased droplet size, but also hampered gel formation (Hughes et al., 2009). Such studies demonstrate the need for added emulsifiers or the presence of endogenous surface-active species for effective W/Og system formation and stabilization (Beri et al., 2013).

Fibril-Based W/Og Systems

A number of fibrillar oleogelator networks have been used to stabilize W/Og systems. These either consist of polymers or small molecules that form thin fibers with a high aspect ratio under optimized processing conditions. Using the well-known combination of ß-sitosterol and γ-oryzanol for oleogelation, Bot et al. showed that 30 wt% water could be dispersed within a network of fibers that adsorbed onto the water droplet surface and also structured the continuous phase (Bot et al., 2011). Ethylcellulose (EC) is another oleogelator that forms long crosslinked, fiber-like structures, and whose rheological properties also depend on solvent type and molecular weight (Davidovich-Pinhas et al., 2016). This polymer was shown to form oil-continuous emulsion gels using propylene glycol as the dispersed phase. Although not visualized directly, it was hypothesized that the EC adsorbed onto the surface of the dispersed droplets, as well as providing network stabilization (Ceballos et al., 2014). In a study using 2-octyldodecanol as the oil phase and EC, temperature was found to play a key role on emulsion gel formation. Emulsification at 15°C resulted in a solid-like, oil-continuous structure whereas at 30°C, phase inversion was observed. The authors concluded that the EC formed colloidal particles that adsorbed to the oil-water interface, rather than fibers, and stated that temperature-dependent EC solubility in oil led to the formation of either a water or oil-continuous emulsion (Melzer et al., 2003). Finally, Munk et al. found that EC could be used to stabilize O/W emulsions when emulsification took place at temperatures below the melting point of the oleogel (Munk et al., 2019).

Dispersed Phase Contributions

Aqueous droplet properties to consider in regards to W/Og system functionality include the dispersed phase droplet size

and distribution, volume fraction, extent of interaction with neighboring species, state of aggregation, and rigidity (either of individual droplets or clusters), as studied in O/W emulsion gels (van Vliet, 1988; Scholten, 2017). In such systems, it was found that dispersed droplet size directly contributed to large deformation behavior (Sala et al., 2009). Fuhrmann et al. found that clustering of dispersed oil droplets increased viscosity up to three orders of magnitude due to the increase in effective volume fraction (Fuhrmann et al., 2019). Elsewhere, effective clustering of oil droplets could increase O/W emulsion gel rigidity in a controllable manner (Oliver et al., 2015; Van Aken et al., 2015). In W/Og systems, however, controlling such parameters remains virtually unexplored. Decades ago, Pal showed that a reduction in aqueous droplet size increased the viscosity of concentrated W/O emulsions (Pal, 1996), and he also showed that combining small and large droplet sizes greatly affected emulsion viscosity and small deformation (Pal, 1996). Droplet clustering is likely to be an important factor in W/O emulsion viscosity (Liu et al., 2016), which also warrants its scrutiny in W/Og systems.

Droplet Interactions With the Oleogel Matrix

The structure and rheology of a W/Og system will depend on the type and extent of interactions between the surface of dispersed aqueous droplets and the surrounding oleogel. As active fillers, droplets interact with the oleogel matrix and enhance W/Og rigidity and resistance to deformation, which occurs more readily when the dispersed droplets are stiffer than the gel network. As inactive fillers, aqueous droplets show little or no interaction with the surrounding oleogel, and either have no effect on, or reduce, W/Og rigidity.

Active Fillers

Affinity between droplet-bound emulsifier molecules and the surrounding oleogel matrix can play a significant role in determining whether droplets behave as active or inactive fillers. Effective emulsifier adsorption and molecular alignment on the droplet surface increases the likelihood of the ordering of oleogelator species close to the droplet surface, possibly through heterogeneous nucleation and interfacial templating of surrounding oleogelators present in the continuous phase. In this scenario, the resulting aqueous droplets are active contributors to the texture and rheology of the surrounding volume-spanning oleogel network. For instance, Wijarnprecha et al. showed that droplet-bound monostearin crystals acted as heterogeneous nucleation sites for continuous phase rice bran wax crystals in W/Og systems, resulting in the dispersed aqueous phase acting as an active filler (Wijarnprecha et al., 2019a). Using monoacylglycerols for emulsification and a combination of candelilla wax and fully hydrogenated fats to stabilize W/O emulsions, da Silva et al. showed that adding up to 20 wt% water increased W/Og rigidity, with higher proportions of water having a limited effect on rigidity compared to the control (da Silva et al., 2019). Interestingly, in contrast to Wijarnprecha et al. they also found that addition up to 5 wt% water substantially increased rigidity, which the authors attributed to a reduction in crystal size (Wijarnprecha et al., 2019a).

Inactive Fillers

In many cases, incorporating aqueous droplets within an oleogel will structurally weaken the resulting W/Og, even when there are interfacially-bound oleogelator species or emulsifiers present (Patel et al., 2013). Much of this may be ascribed to poor emulsifier interfacial ordering or lack of molecular compatibility with neighboring oleogelator species in the continuous oil phase. For instance, in a study on lipstick-like wax-stabilized W/O emulsions where the oligomeric emulsifier polyglycerol polyricinoleate (PGPR) was used as the emulsifier, the storage modulus of the matrix alone was higher than that of the composite emulsion (Le Révérend et al., 2011). In this case, the droplets acted as inactive fillers given their lack of interaction with the matrix and low viscosity. In EC-stabilized W/Og systems, increasing the dispersed phase volume fraction decreased the hardness of the emulsion gels obtained, which was attributed to interference of polymer gel structure by the dispersed droplets (Ceballos et al., 2014). Similarly, when PGPR was used to stabilize W/Og systems using rice bran wax as the oleogelator, dispersed droplets did not interact with the gel matrix resulting in a decrease in W/Og rigidity (Wijarnprecha et al., 2019b). In this case, it was shown that wax crystals were indeed the only structuring agent, as replacing water droplets with an equivalent amount of liquid oil did not alter overall gel network strength. Yet another example of inactive fillers used a phytosterol-stabilized emulsion gel, with glycerol as the dispersed phase (Matheson et al., 2018). Glycerol droplets acted as inactive fillers due to a lack of anchoring to the surrounding fibrillar gel network, which weakened the overall structure.

Structuring the Internal Water Phase

The gelation of the dispersed aqueous phase present in W/Og systems is an alternate route to limit the "destructuring" effect of adding water droplets. By gelling the internal water phase, these droplets become stiffer, and limit any weakening effect. Iqbal et al. (2019) explored the gelation of the dispersed aqueous phase of W/O emulsions using different kinds of polysaccharides (high-methoxy pectin, kappa-carrageenan, and starch). Alexa et al. (2010) found that addition of κ-carrageenan to W/O spreads resulted in an altered microstructure with larger aqueous droplets, but did not affect overall rigidity. Recent work has shown that the stability of gel-in-gel W/O high internal phase emulsions (HIPEs) resulted from the combined presence of a highly-packed dispersed aqueous phase stabilized by carrageenan, glycerol monooleate at the oil-water interface, and a surrounding beeswax crystal network (Lee et al., 2019). Ono et al. developed HIPEs that comprised silicone oil and water prepared with low concentrations of a glucose-based gelator that gelled both the dispersed and continuous phases, which resulted in HIPEs with tunable rigidity (Ono et al., 2018). Other work looked at the effect of xanthan gum in the aqueous phase of beeswax-stabilized W/Og systems, but no clear effect on overall properties was established (Öğütcü et al., 2015).

Processing Parameters to Tune W/Og Properties

Emulsion processing parameters such as shear and cooling rate will directly affect the physical properties of W/Og systems. Using a combination of glycerol monooleate and paraffin wax to stabilize W/O emulsions, Ghosh et al. (2015) found that altering cooling rate [slow (1°C/min) vs. fast (5°C/min)], end temperature (25 or 4°C) and the presence/absence of shear during cooling had a marked effect on final W/Og properties. They noted that the presence of wax crystals at the oil-water interface was promoted when cooling at 5°C/min in combination with agitation (Ghosh et al., 2015). When comparing cooling rates of 1 or 10 °C/min, Patel et al. (2013) found that a larger number of smaller shellac wax crystals were formed using a higher cooling rate, which led to stronger crystal–crystal interactions and network formation. Using different wax sources, Binks and Rocher showed that emulsion stability was affected by emulsification and storage temperatures (Binks and Rocher, 2009). Here, wax crystallized at the oil-water interface gave rise to enhanced emulsion resistance against breakdown compared to pre-adsorbed crystals. This was also shown by Rousseau and Hodge, where post-emulsification crystallization of paraffin wax yielded W/O emulsions that were noticeably more stable against physical breakdown than with pre-crystallized wax—a finding attributed to the smaller wax crystal size with post-crystallization (Rousseau and Hodge, 2005). When summarized, these findings show that processing conditions related to temperature-time-shear regimes can be used to not only tune droplet size and stability, but also the location of the oleogelator—either in the continuous phase, at the droplet surface, or both. Results to-date suggest that processing regimes that promote smaller average droplet sizes and narrower size distributions along with the presence of interfacially-bounds species will promote W/Og emulsion stability against coalescence and phase separation.

SUMMARY AND FUTURE PROSPECTS

Figure 1 summarizes many of the key parameters used to tune the rheology and structure of W/Og systems. Gel matrix functional attributes can be controlled by oleogelator type, concentration, crystal/fiber size, and aggregation state. Properties of the dispersed aqueous phase, including volume fraction, clustering, droplet size, and size distribution and possible gelation may alter the final properties of the W/Og system. Structuring the interface into a solid-like film can be responsible for making liquid, spherical inclusions behave as solid particles (Van Aken

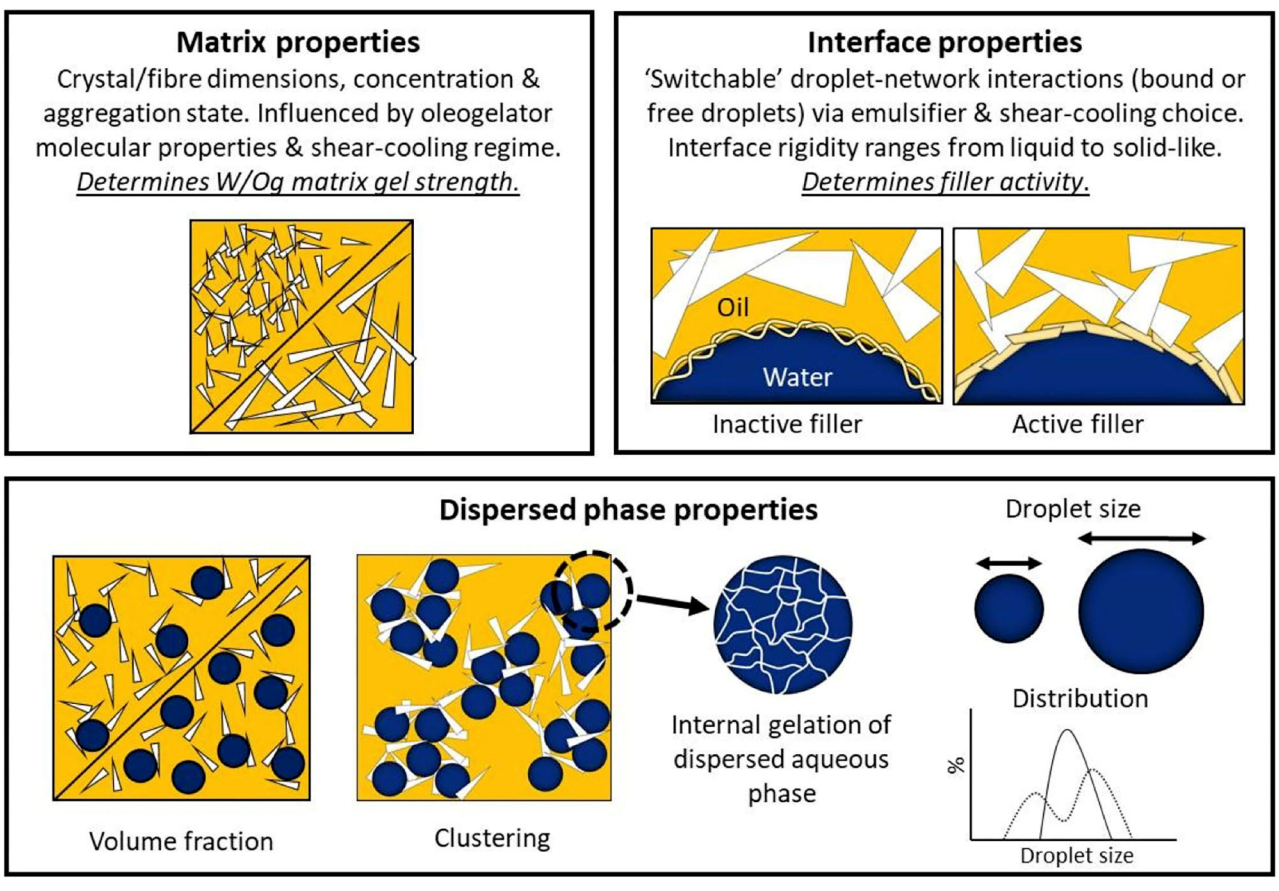

FIGURE 1 | Major factors to consider in the design of water-in-oleogel systems.

et al., 2015). Finally, processing conditions, namely temperature-time-shear regimes, can be used to tune the properties of both the oleogel and aqueous phases.

The surface of aqueous droplets can be selectively tailored toward attractive interactions between the matrix and the surface of the droplet. This is the central tenet of the filler concept, which has been extensively explored in gelled O/W emulsions, but which remains virtually unexplored in W/Og systems. Similar to water-continuous emulsions, it is presumed that dispersed water droplets in an oleogelled matrix will only act as active fillers when the modulus of the dispersed phase is higher than that of the matrix. In practice, this might be difficult, as typically, the elastic modulus of fat-continuous gels is higher than those in water-continuous systems. In most wax-based W/Og systems, for example, there exists a relatively strong crystal network and addition of water droplets would only weaken the composite. Moreover, since the modulus of the dispersed phase is affected by droplet radius, W/Og systems are at a disadvantage since emulsified water droplets are more often larger than oil droplets.

A further complicating factor is that addition of water droplets or emulsifiers to oleogels can alter several W/Og properties at once, e.g., wax crystal size and 3D spatial arrangement, which makes direct identification of the contributions of the dispersed phase to W/Og behavior more difficult. Similarly, processing parameters such as temperature, time and shear that are optimized for effective W/Og formation may differ from those for oleogel formation, resulting in divergent end-product characteristics. Finally, compared to O/W emulsions, the ability to enhance the functionality of W/Og systems is limited by the general lack of available oil-soluble emulsifiers and gelling agents.

Ultimately, the ability to determine the contributions of the oleogel matrix, emulsifier, and dispersed aqueous phase to the structure, rheology, and shelf life of W/Og systems will result in their incorporation into novel food applications. Examples include reduction or removal of solid fat in processed foods such as sausages, pâtés, and chocolate. In such products, while targeting calorie or fat reduction and perhaps costs savings, maintaining textural and sensory attributes similar to their higher solid fat equivalents will be the prime consideration in order to meet consumer expectations. The successful introduction of a W/Og system into a processed food product will very likely hinge on controlling non-specific interactions with other added ingredients, which may affect stability and shelf life. For example, presence of proteins dissolved within the dispersed aqueous phase may hamper the ability of W/Og systems to effectively form whereas added salts may enhance the interfacial modulus of the oil-water interface. Such challenges demonstrate that a holistic approach that takes into consideration an entire product formulation rather than a model formulation is necessary for the successful design and use of W/Og systems in foods.

AUTHOR CONTRIBUTIONS

All authors listed have made a substantial, direct and intellectual contribution to the work, and approved it for publication.

FUNDING

The support from the Natural Sciences and Engineering Research Council of Canada is acknowledged.

REFERENCES

Alexa, R. I., Mounsey, J. S., O'Kennedy, B. T., and Jacquier, J. C. (2010). Effect of k-carrageenan on rheological properties, microstructure, texture and oxidative stability of water-in-oil spreads. *LWT Food Sci. Technol.* 43, 843–848. doi: 10.1016/j.lwt.2009.10.003

Beri, A., Norton, J. E., and Norton, I. T. (2013). Effect of emulsifier type and concentration, aqueous phase volume and wax ratio on physical, material and mechanical properties of water in oil lipsticks. *Int. J. Cosmet. Sci.* 35, 613–621. doi: 10.1111/ics.12085

Binks, B. P., and Rocher, A. (2009). Effects of temperature on water-in-oil emulsions stabilised solely by wax microparticles. *J. Colloid Interface Sci.* 335, 94–104. doi: 10.1016/j.jcis.2009.03.089

Bot, A., den Adel, R., Regkos, C., Sawalha, H., Venema, P., and Flöter, E. (2011). Structuring in β-sitosterol+γ-oryzanol-based emulsion gels during various stages of a temperature cycle. *Food Hydrocoll.* 25, 639–646. doi: 10.1016/j.foodhyd.2010.07.026

Ceballos, M. R., Brailovsky, V., Bierbrauer, K. L., Cuf, S. L., Beltramo, D. M., and Bianco, I. D. (2014). Effect of ethylcellulose on the structure and stability of non-aqueous oil based propylene glycol emulsions. *Food Res. Int.* 62, 416–423. doi: 10.1016/j.foodres.2014.03.040

da Silva, T. L. T., Arellano, D. B., and Martini, S. (2019). Effect of water addition on physical properties of emulsion gels. *Food Biophys.* 14, 30–40doi: 10.1007/s11483-018-9554-3

Davidovich-Pinhas, M., Barbut, S., and Marangoni, A. G. (2016). Development, characterization, and utilization of food-grade polymer oleogels. *Annu. Rev. Food Sci. Technol.* 7, 65–91. doi: 10.1146/annurev-food-041715-033225

Doan, C. D., Tavernier, I., Kiyomi, P., and Dewettinck, K. (2018). Internal and external factors affecting the crystallization, gelation and applicability of wax-based oleogels in food industry. *Innov. Food Sci. Emerg. Technol.* 45, 42–52. doi: 10.1016/j.ifset.2017.09.023

Fuhrmann, P. L., Sala, G., Stieger, M., and Scholten, E. (2019). Clustering of oil droplets in o / w emulsions: controlling cluster size and interaction strength. *Food Res. Int.* 122, 537–547. doi: 10.1016/j.foodres.2019.04.027

Gaudino, N., Ghazani, S. M., Clark, S., Marangoni, A. G., and Acevedo, N. C. (2019). Development of lecithin and stearic acid based oleogels and oleogel emulsions for edible semisolid applications. *Food Res. Int.* 116, 79–89. doi: 10.1016/j.foodres.2018.12.021

Ghosh, S., Pradhan, M., Patel, T., Haj-shafiei, S., and Rousseau, D. (2015). Long-term stability of crystal-stabilized water-in-oil emulsions. *J. Colloid Interface Sci.* 460, 247–257. doi: 10.1016/j.jcis.2015.08.074

Ghosh, S., Tran, T., and Rousseau, D. (2011). Comparison of pickering and network stabilization in water-in-oil emulsions. *Langmuir* 27, 6589–6597. doi: 10.1021/la200065y

Haj-shafiei, S., Ghosh, S., and Rousseau, D. (2013). Kinetic stability and rheology of wax-stabilized water-in-oil emulsions at different water cuts. *J. Colloid Interface Sci.* 410, 11–20. doi: 10.1016/j.jcis.2013.06.047

Hu, L., Zhang, Y., and Ramström, O. (2015). Gelation-driven dynamic systemic resolution: *in situ* generation and self-selection of an organogelator. *Sci. Rep.* 5, 1–7. doi: 10.1038/srep11065

Hughes, N. E., Marangoni, A. G., Wright, A. J., Rogers, M. A., and Rush, J. W. E. (2009). Potential food applications of edible oil organogels. *Trends Food Sci. Technol.* 20, 470–480. doi: 10.1016/j.tifs.2009.06.002

Iqbal, S., Xu, Z., Huang, H., and Dong, X. (2019). Structuring of water-in-oil emulsions using controlled aggregation of polysaccharide in aqueous phases. *J. Food Eng.* 258, 34–44. doi: 10.1016/j.jfoodeng.2019.04.008

Le Révérend, B. J. D., Taylor, M. S., and Norton, I. T. (2011). Design and application of water-in-oil emulsions for use in lipstick formulations.

Int. J. Cosmet. Sci. 33, 263–268. doi: 10.1111/j.1468-2494.2010.00624.x

Lee, M. C., Tan, C., Ravanfar, R., and Abbaspourrad, A. (2019). Ultrastable water-in-oil high internal phase emulsions featuring interfacial and biphasic network stabilization. *ACS Appl. Mater. Interfaces* 11, 26433–26441. doi: 10.1021/acsami.9b05089

Liu, C., Li, M., Han, R., Li, J., and Liu, C. (2016). Rheology of water-in-oil emulsions with different drop sizes. *J. Dispers. Sci. Technol.* 37, 333–344. doi: 10.1080/01932691.2015.1010729

Ma, Q., Wang, W., Liu, Y., Yang, J., Shi, B., and Gong, J. (2017). Wax adsorption at paraffin oil-water interface stabilized by Span 80. *Colloids Surf. A Physicochem. Eng. Asp*. 513, 168–177. doi: 10.1016/j.colsurfa.2017.01.023

Matheson, A., Dalkas, G., Mears, R., Euston, S. R., and Clegg, P. S. (2018). Stable emulsions of droplets in a solid edible organogel matrix. *Soft Matter.* 14, 2044–2051. doi: 10.1039/C8SM00169C

Melzer, E., Kreuter, J., and Daniels, R. (2003). Ethylcellulose: a new type of emulsion stabilizer. *Eur. J. Pharm. Biopharm*. 56, 23–27. doi: 10.1016/S0939-6411(03)00025-0

Munk, M. B., Utoft, A., Larsen, F. H., Needham, D., and Risbo, J. (2019). Oleogelating properties of ethylcellulose in oil-in-water emulsions: the impact of emulsification methods studied by 13C MAS NMR, surface tension and micropipette manipulation studies. *Food Hydrocoll.* 89, 700–706. doi: 10.1016/j.foodhyd.2018.11.019

Öğütcü, M., Arifoğlu, N., and Yilmaz, E. (2015). Preparation and characterization of virgin olive oil-beeswax oleogel emulsion products. *J. Am. Oil Chem. Soc.* 92, 459–471. doi: 10.1007/s11746-015-2615-6

Oliver, L., Berndsen, L., van Aken, G. A., and Scholten, E. (2015). Influence of droplet clustering on the rheological properties ofemulsion-filled gels. *Food Hydrocoll.* 50, 74–83. doi: 10.1016/j.foodhyd.2015.04.001

Ono, F., Shinkai, S., and Watanabe, H. (2018). High internal phase water/oil and oil/water gel emulsions formed using a glucose-based low-molecular-weight gelator. *New J. Chem*. 42, 6601–6603. doi: 10.1039/C7NJ04508E

Pal, R. (1996). Effect of droplet size on the rheology of emulsions. *AIChE J.* 42, 3181–3190. doi: 10.1002/aic.690421119

Patel, A. R., Schatteman, D., De Vos, W. H., L.esaffer, A., and Dewettinck, K. (2013). Preparation and rheological characterization of shellac oleogels and oleogel-based emulsions. *J. Colloid Interface Sci.* 411, 114–121. doi: 10.1016/j.jcis.2013.08.039

Rafanan, R., and Rousseau, D. (2019). Dispersed droplets as tunable fillers in water-in-oil emulsions stabilized with fat crystals. *J. Food Eng.* 244, 192–201. doi: 10.1016/j.jfoodeng.2018.09.001

Rousseau, D., and Hodge, S. M. (2005). Stabilization of water-in-oil emulsions with continuous phase crystals. *Colloids Surf. A Physicochem. Eng. Asp*. 260, 229–237. doi: 10.1016/j.colsurfa.2005.02.035

Sala, G., van Vliet, T., Stuart, M. C., van de Velde, F., and van Aken, G. A. (2009). Deformation and fracture of emulsion-filled gels: effect of gelling agent concentration and oil droplet size. *Food Hydrocoll.* 23, 1853–1863. doi: 10.1016/j.foodhyd.2009.03.002

Scholten, E. (2017). Composite foods: from structure to sensory perception. *Food Funct*. 8, 481–497. doi: 10.1039/C6FO01099G

Toro-Vazquez, J. F., Mauricio-Pérez, R., González-Chávez, M. M., Sánchez-Becerril, M., Ornelas-Paz, J., de, J., et al. (2013). Physical properties of organogels and water in oil emulsions structured by mixtures of candelilla wax and monoglycerides. *Food Res. Int*. 54, 1360–1368. doi: 10.1016/j.foodres.2013.09.046

Van Aken, G. A., Oliver, L., and Scholten, E. (2015). Rheological effect of particle clustering in gelled dispersions. *Food Hydrocoll.* 48, 102–109. doi: 10.1016/j.foodhyd.2015.02.001

van Vliet, T. (1988). Rheological properties of filled gels. Influence of filler matrix interaction. *Colloid Polym. Sci.* 266, 518–524. doi: 10.1007/BF01420762

Wijarnprecha, K., de Vries, A., Santiwattana, P., Sonwai, S., and Rousseau, D. (2019a). Microstructure and rheology of oleogel-stabilized water-in-oil emulsions containing crystal-stabilized droplets as active fillers. *LWT Food Sci. Technol*. 115:108058. doi: 10.1016/j.lwt.2019.04.059

Wijarnprecha, K., de Vries, A., Santiwattana, P., Sonwai, S., and Rousseau, D. (2019b). Rheology and structure of oleogelled water-in-oil emulsions containing dispersed aqueous droplets as inactive fillers. *LWT Food. Sci. Technol*. 115:108067. doi: 10.1016/j.lwt.2019.04.068

Conflict of Interest: The authors declare that the research was conducted in the absence of any commercial or financial relationships that could be construed as a potential conflict of interest.

Advantages of publishing in Frontiers

OPEN ACCESS
Articles are free to read for greatest visibility and readership

FAST PUBLICATION
Around 90 days from submission to decision

HIGH QUALITY PEER-REVIEW
Rigorous, collaborative, and constructive peer-review

TRANSPARENT PEER-REVIEW
Editors and reviewers acknowledged by name on published articles

Frontiers
Avenue du Tribunal-Fédéral 34
1005 Lausanne | Switzerland

Visit us: www.frontiersin.org
Contact us: frontiersin.org/about/contact

REPRODUCIBILITY OF RESEARCH
Support open data and methods to enhance research reproducibility

DIGITAL PUBLISHING
Articles designed for optimal readership across devices

FOLLOW US
@frontiersin

IMPACT METRICS
Advanced article metrics track visibility across digital media

EXTENSIVE PROMOTION
Marketing and promotion of impactful research

LOOP RESEARCH NETWORK
Our network increases your article's readership